Theoretical and Experimental Determination of Key Operating Parameters for Composting Systems

Thesis submitted for the degree of Doctor of Philosophy

By

David Notton M.Eng.(Hons.)(Wales)

May 2005

Centre for Research in Energy, Waste and the Environment
Institute of Sustainability, Energy and Environmental Management
Cardiff School of Engineering
Cardiff University

ProQuest LLC
789 East Eisenhower Parkway
P.O. Box 1346
Ann Arbor, MI 48106-1346

Abstract

The combination of increasing quantities of Municipal Solid Waste (MSW) and increased legislation for the disposal of this type of waste have created a need to develop different disposal or treatment routes for waste. Approximately 60% of MSW by mass is biodegradable and many disposal routes for this waste allow energy recovery. However the waste hierarchy presented in the National Waste Strategy for Wales emphasises the importance of materials recovery over energy recovery. It has been shown that the only way to achieve these targets is through the recovery of catering waste, which requires an in-vessel composting facility.

In order to gain an insight into the aeration requirements for in-vessel composting, calculations were performed to ascertain the required airflow for the supply of oxygen, the removal of excess moisture and the removal of excess heat. It was found that approximately 450kJ are released for each mole of oxygen utilised whilst 500kJ are released per mole of carbon dioxide evolved. It was found that the air requirement for removal of heat from the process was approximately 100 times greater than the air required to supply oxygen to the system. In order to determine the power of aeration equipment required for composting facilities a static pressure test rig was constructed. From the results gained a model relating the static pressure to the bulk density of compost was developed.

Initially a windrow composting system processing green waste at the Carmarthenshire Environmental Resources Trust (CERT) composting facility was studied. A canopy system was developed to monitor the respiration rate of this system and allow comparison between different feedstocks and control strategies. For a green waste only windrow the highest recorded respiration rate was $38gCO_2kgVS^{-1}day^{-1}$. The respiration rate was observed to reduce with temperature above 55°C. In addition to the green waste windrows a temperature managed windrow and a windrow constructed from a mixture of green waste and chicken litter were also tested.

The final series of trials involved the testing of the ability of a containerised composting system to meet the Animal By-Products Regulations. The vessel was fed various mixtures of green waste and factory waste. Airflow and insulation within the vessel were analysed and a composting rate of over $45gCO_2kgVS^{-1}day^{-1}$ was achieved. If this had been sustained then the vessel may have met the Animal By-Products Regulations.

Acknowledgements

There have been so many great people who have really helped me get through this. I would like to start by thanking the staff and students of the waste research team at Cardiff: Prof. Keith Williams, Prof. Tony Griffiths, Guy Hewings, Dr Sian Myrddin and Muhammad Ali. I am also grateful to the board of Carmarthenshire Environmental Resources Trust and to EB Nationwide for the funding of this work through the Landfill Tax Credit Scheme.

I would also like to thank my parents, Robin and Anne, for giving me their support and understanding throughout. I would also like to thank all the members of the Alston clan, but particularly to the Borley part, Helen, Julian, Jimmy and Tom.

I would also like to thank my friends-without whom life would be less interesting. Little Will has, despite his relentless taunting been a good friend throughout this period. Thanks to Chris and Lowri for being such good friends. Also Carrie and Mitch, Sean and Christelle, Chris (Tool), Tony Giles, Clare, Pix, Sophie, Emma, Sharky, Mr Tucker and apologies to anyone I have not mentioned but otherwise I will be going on for pages.

I would like to dedicate this to Ann. There is no way I could have done any of this without you.

Lisa: Wow. Um ... I started an organic compost pile at home.
Jesse: Only at home? You mean you don't pocket-mulch? [takes out pocket stuff for Lisa to feel]
Lisa: Oh, it's so decomposed! Do you think I could join Dirt First?

Lisa the Treehugger
The Simpsons

Table of Contents

List of Figures

List of Tables

Nomenclature

Symbol	Definition	Units
a	Number of moles of microbial cell	-
A	Cross sectional area	m^2
b	Number of moles of carbon dioxide	-
c	Number of moles of water	-
C	Percentage by mass of carbon in substrate	%
d	Number of moles of ammonia	-
D	Equivalent spherical diameter of particle	m
e	Void ratio	-
E_{CO2}	Concentration of carbon dioxide	%
f	Number of moles of methane	-
F	Composting rate	gCO_2/kg VS-day
g	Number of atoms of carbon per mole of microbial cell	-
h	Number of atoms of hydrogen per mole of microbial cell	-
H	Percentage by mass of hydrogen in substrate	%
H_{in}	Inlet enthalpy of air	kJ/kg
H_{out}	Exhaust enthalpy of air	kJ/kg
HR_{in}	Humidity ratio of inlet air	kg/kg
HR_{out}	Humidity ratio of exhaust air	kg/kg
i	Number of atoms of oxygen per mole of microbial cell	-
j	Number of atoms of nitrogen per mole of microbial cell	-
k	width of composting vessel	m
l	Length of composting vessel	m
L	Depth of packed bed	m
m	Height of composting vessel	m
m_l	Fill height of composting vessel	m
M	Moisture content on a wet basis	%
M_{air}	Molecular mass of air	g/mole
M_{CO2}	Molecular mass of carbon dioxide	g/mole
M_{H2O}	Molecular mass of water	g/mole
M_{O2}	Molecular mass of oxygen	g/mole
MC	Moisture content on a wet basis	-
N	Number of seconds per day (86,400)	s/day

O	Percentage by mass of oxygen in substrate	%
P	Pressure	Pa
Q	Calorific value	kJ/kg
Q_{con}	Heat lost through convection from surfaces	kW
Q_{gen}	Heat released by composting process	kW
R_{CO2}	Specific Gas Constant for carbon dioxide	Nm/kg K
R_o	Universal gas constant	Nm/kmol K
T	Temperature	K
T_g	Gas Temperature	K
ΔT	Temperature difference	K
u	Number of atoms of carbon per mole of substrate	-
U	Superficial velocity of air	m/s
$\overline{U}$	Average velocity	m/s
v	Number of atoms of hydrogen per mole of substrate	-
V_{air}	Volumetric flow rate of air per cubic metre of compost	$m^3/s\text{-}m^3$
V_g	Volume of gas in compost	m^3
V_s	Volume of solids in compost	m^3
V_t	Total volume of compost	m^3
V_w	Volume of water in compost	m^3
VS	Proportion of volatile solids on dry basis	-
w	Number of atoms of oxygen per mole of substrate	-
W_g	Mass of gas in compost	kg
W_s	Mass of solid in compost	kg
W_t	Total mass of compost	kg
W_w	Mass of water in compost	kg
x	Number of atoms of nitrogen per mole of substrate	-
Y	Yield coefficient	-
z	Number of moles of oxygen	-

Greek Letters

μ_x	Mean of data set x	-
μ_y	Mean of data set y	-
μ_{air}	Dynamic viscosity of air	Pa s
ρ_{air}	Density of air	kg/m^3
ρ_{ash}	Density of ash	kg/m^3
$\rho_{compost}$	Density of compost	kg/m^3
ρ_s	Density of solids	kg/m^3
ρ_t	Total density	kg/m^3
ρ_{vs}	Density of volatile solids	kg/m^3
ρ_w	Density of water	kg/m^3
ρ_{xy}	Correlation coefficient between data set x and data set y	-
σ_x	Standard deviation of data set x	-
σ_y	Standard deviation of data set y	-

1 Introduction

1.1 The Waste Problem

430 million tonnes of waste were generated in the UK during 2002 (Defra, 2002), of this household waste accounted for 30 million tonnes and commercial waste 28 million tonnes. The quantity of waste produced increases annually at a rate of between 3 and 4% whilst population is growing at approximately 0.3% per annum.

Figure 1.1 shows that most of the waste that is generated is not recycled which generally means that it is sent to landfill. Whilst an increasing quantity of waste is recycled each year the rate of growth of total waste outstrips this and leads to increased quantities of waste not being recycled each year. In order to impact on the quantity of waste that is being landfilled each year more recycling and reprocessing plants and collection schemes will be required.

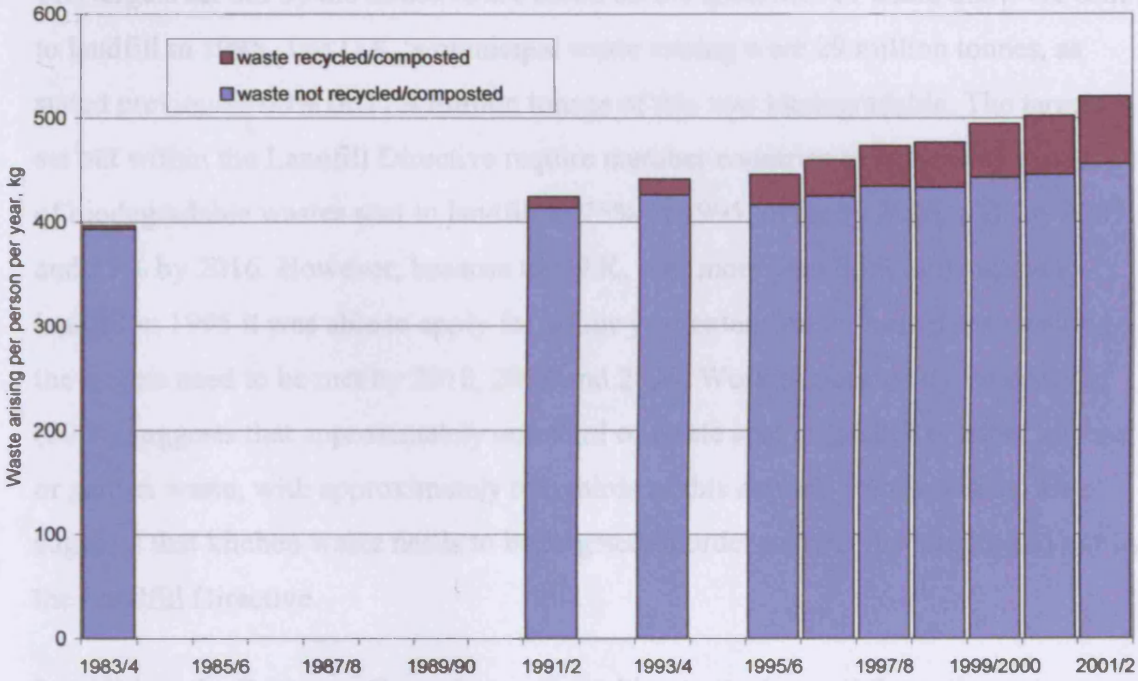

Figure 1.1. Chart showing total household waste produced and the proportion of waste recycled per person in England and Wales. (Data from Defra, 2002; 2003)

Of the waste that is generated annually a large portion is biodegradable. The Environment Agency estimate that 60% of municipal solid waste (MSW) is biodegradable whilst the Welsh Assembly Government puts the figure at 64% (WAG,

2002). By targeting biodegradable waste a large reduction in the quantity of waste that is sent to landfill could be achieved.

1.2 Drivers for Recycling

There are a variety of legislative drivers to encourage a sustainable approach to waste management. In order to reduce the quantity of methane released by landfill sites The European Landfill Directive (European Commission, 1999) has set limits on the quantity of biodegradable waste that is allowed to be sent to landfill. Methane is a greenhouse gas with a global warming potential 21 times greater than carbon dioxide over 100 years (AESA, 2001). Methane is generated by the anaerobic decay of biodegradable wastes, such as in the conditions that can be found within landfill sites.

The targets set out by the directive are based on the quantities of waste that were sent to landfill in 1995. The U.K.'s municipal waste arising were 29 million tonnes, as stated previously 60% or 17.4 million tonnes of this was biodegradable. The targets set out within the Landfill Directive require member countries to reduce the quantity of biodegradable wastes sent to landfill to 75% of 1995 levels by 2006, 50% by 2009 and 35% by 2016. However, because the U.K. sent more than 80% of its waste to landfill in 1995 it was able to apply for a four year extension to these dates meaning the targets need to be met by 2010, 2013 and 2020. Work performed by Emery *et al.* (2000) suggests that approximately one third of waste sent to landfill is either kitchen or garden waste, with approximately two thirds of this coming from kitchens. This suggests that kitchen waste needs to be targeted in order to meet the targets laid out by the Landfill Directive.

In addition, the European Commission is working towards a soil thematic strategy which recognises soil as an important yet endangered resource. A Directive on the Biological Treatment of Biological Waste (European Commission, 2001), the aims of which are to encourage the treatment of biological waste by biological methods, such as composting and anaerobic digestion has been presented for consultation. This directive would require member states to set up separate collection systems for

biodegradable wastes to maximise the quantity of material that can be treated and hence diverted from landfill. The European Commission had been committed to the preparation of a directive on biowastes by the end of the year 2004 (European Commission, 2004). However, the merger of the Directive on Sewage Sludge and of the initiative on Biological Treatment of Biodegradable Wastes under the Thematic Strategy on Soil was still being discussed in January 2005.

Wales, like all other countries of the U.K. has produced a national waste strategy published as Wise About Waste (WAG, 2002), within this are specific recycling targets that need to be achieved. Unlike other countries` waste strategies, Wise About Waste includes specific composting targets. By 2003/4 Wales was hoping to achieve a recycling figure of 15% of MSW of which 5% must have been due to composting. In 2006/7 the recycling target increases to 25% with 10% composting and the final target is for 2009/10 by when 40% of MSW should be recycled with at least 15% being composted.

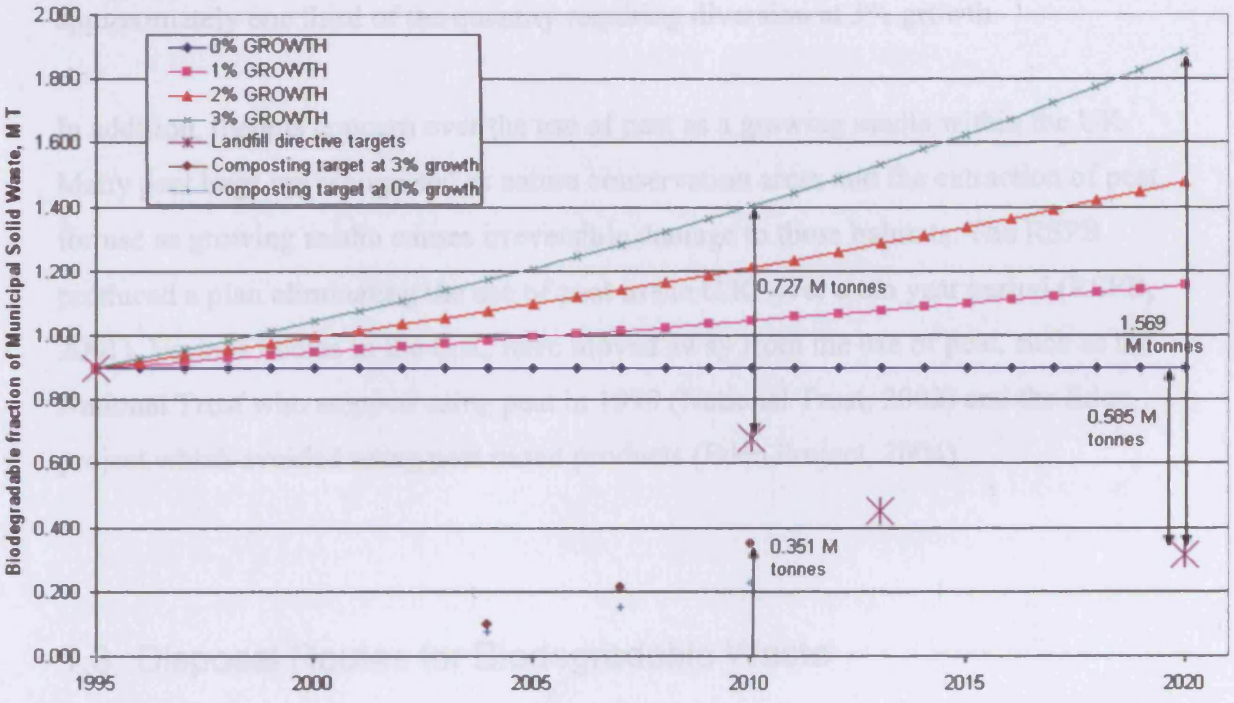

Figure 1.2. Comparison of growth of biodegradable waste in Wales and Landfill Directive and Wise About Waste targets

To put all of the targets into perspective they are shown in Figure 1.2. In 1995 Wales sent 0.9 million tonnes of biodegradable waste to landfill. If this grows at a rate of 3% per annum then by 2010 Wales will have to deal with 1.402 million tonnes of

biodegradable waste. But under the landfill directive Wales will only be able to send 0.675 million tonnes to landfill, at the 3% level of waste growth the National waste strategy will require the composting of 0.351 million tonnes of waste. In order to meet the landfill directive another 0.376 million tonnes will need to be diverted from landfill. If waste were to remain at 1995 levels then by 2010 Wales would need to be diverting 0.225 million tonnes of biodegradable waste from landfill, this can be met exactly by achieving the composting target set out in the National Waste Strategy (WAG, 2002).

Slowing the growth of waste down is of critical importance since if waste continues to grow at 3% per year by 2020 Wales will need to divert 1.569 million tonnes of biodegradable waste from landfill to other processes to meet its obligations under the Landfill Directive. This reinforces the problem highlighted in Figure 1.1 which shows growth in recycling being outstripped by growth in total waste. Without the annual growth in waste the quantity to be diverted is only 0.585 million tonnes; approximately one third of the quantity requiring diversion at 3% growth.

In addition, there is concern over the use of peat as a growing media within the UK. Many peat bogs are recognised as nature conservation areas and the extraction of peat for use as growing media causes irreversible damage to these habitats. The RSPB produced a plan eliminating the use of peat in the U.K. over a ten year period (RSPB, 2001). Various bodies in the U.K. have moved away from the use of peat, such as the National Trust who stopped using peat in 1999 (National Trust, 2002) and the Eden project which avoided using peat based products (Eden Project, 2004).

1.3 Disposal Routes for Biodegradable Waste

There are a variety of different disposal routes for the biodegradable stream of municipal solid wastes (MSW). Currently most of this waste is sent to landfill but other options for the disposal of MSW include:

- Anaerobic digestion,
- Gasification,

- Pyrolysis,
- Incineration,
- Composting.

The waste hierarchy that is set out in the waste strategy for Wales (WAG, 2002) places the recovery of materials above the recovery of energy. This means that composting for the recovery of a growth medium is above the recovery of energy through anaerobic digestion, gasification, pyrolysis or incineration. Therefore composting is the preferred disposal route for biodegradable waste within Wales.

Anaerobic digestion can, however, be used to produce a biogas similar in composition to landfill gas which can be burnt to recover energy, it also leaves a residue which can be matured and used as a soil improver or growing medium. The heat released during the composting process is all lost and is of a low grade and is therefore unrecoverable.

1.4 Regulatory Framework–Mandatory and Voluntary

Over the last few years in the U.K. there have been numerous animal health scares such as BSE, swine fever and foot and mouth disease. It is important that any material containing any of the pathogens associated with animal disease is treated in an appropriate manner so that it causes no further risk to health. This has lead to a certain level of turmoil within the composting industry over the last 5 years. The Animal By-Products Order (1999) controlled the disposal of waste containing animal by-products and did not allow composting or biogas production as disposal routes for this material. However only catering waste that had been in contact with or contained animal carcases, parts of animal carcases or products of animal origin (other than those which have been incorporated into another product) was controlled by the Animal By-Products Order (1999). A guidance note was released by MAFF in 2001 that helped to clarify the situation with regards to disposal of animal by-products, the only exceptions which allowed composting were:

- catering waste which does not contain, and has not been in contact with, any meat or products of animal origin

- catering waste to which ruminant animals, pigs or poultry (including wild birds) will not gain access

The outbreak of Foot and Mouth disease during 2001 lead to the production of the Animal By-Products (Amendments)(Wales) Order 2001 and legislation was also passed for Scotland and England. The principal effect of this order was the ban on the use of swill produced from catering waste containing meat.

During 2002, the European Union introduced regulation 1774/2002 which came into force on the 1st of May 2003. This regulation sets out the conditions under which animal by-products can be composted or treated by anaerobic digestion. The regulations split animal by-products into three categories based on risk to animal health. Category 1 material is the highest risk and includes all body parts of animals that could be infected with Transmissible Spongiform Encephalopathies or environmental contaminants as well as catering wastes from international transport. Category 2 material includes manure and digestive tract content as well as waste water from plants treating such material. Finally, Category 3 animal by-products are those parts of an animal that are fit for human consumption but for commercial reasons are not intended for human consumption, parts of an animal not fit for human consumption but unaffected by disease and former foodstuffs of or containing products of an animal origin such as shells, hatchery by-products and catering waste.

Unsurprisingly, the composting of Category 1 material is not allowed and the only approved disposal routes for this material are: incineration, rendering followed by incineration, rendering to the pressure cooking standard followed by landfill, and finally, landfill but only for catering wastes from international transport. The composting of Category 2 material is allowed provided that it has first been rendered to the pressure cooking standard of 133°C, 3 bar for 20 minutes, however manure, digestive tract content, milk and colostrum can be composted without pre-treatment. Category 3 material is allowed to be composted, however if the only Category 3 waste present is catering waste then this can be composted under national guidelines.

A risk assessment was performed on behalf of Defra (Gale, 2002) to investigate treatment regimes other than the one laid out by the European legislation for the treatment of catering wastes. The results of this are shown in Figure 1.3 and the details for each barrier are shown in Table 1-1.

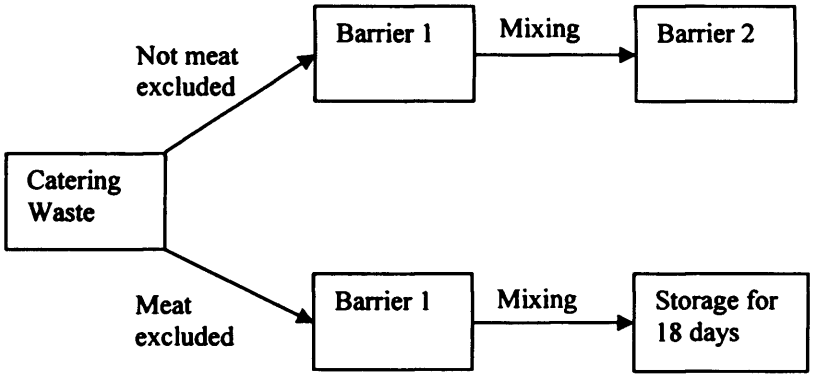

Figure 1.3. Schematic of the multi barrier approach to the treatment of catering wastes

Table 1-1. Details for the barriers for the treatment of catering wastes

System / Parameter	Composting in a closed reactor	Composting in a closed reactor	Composting in housed windrows
Maximum Particle Size	40 cm	6 cm	40 cm
Minimum temperature	60°C	70°C	60°C
Minimum time at minimum temperature	2 days	1 hour	8 days, with 3 turnings at intervals greater than 2 days

The introduction of these regulations means that to meet the targets set out by the Landfill Directive (European Commission, 1999) composting systems will have to incorporate an in-vessel stage for sanitisation of the material.

The guidance note on the Animal By-Products Regulations that was published on the 7th of July 2003 (Defra, 2003a) required that all of the composting material achieved the required time temperature profiles and that all of the heat to achieve this came from the composting process. Material that was to be treated through anaerobic

digestion was allowed to undergo a pre-treatment pasteurisation phase where it could be heated to 70°C for one hour, however at this stage no such allowances were made for the composting process.

The Composting Association (2000) produced a set of standards for compost to introduce a level of quality assurance into the compost production. These require regular testing of the finished product for heavy metals, physical contaminants, weed contaminants, phytotoxins and human pathogens. The scheme was run entirely by the Composting Association. The standards were used as a basis for WRAP (The Waste and Resources Action Program) in the production of BSI PAS 100, a publicly available standard for the quality assurance of composted material which includes all of the testing and limits set out in the Compost Association's standards. Its main benefit lies in the fact that products meeting the standard can be sold as conforming to BSI PAS 100, providing a sense of security for members of the public who may be sceptical about recycled compost.

1.5 The Composting Process

At present there are a myriad of different techniques available to the investor or practitioner. Examples of many in-vessel composting processes can be found in the Composting Association's guide to in-vessel composting (Edwards *et al.*, 1998), many of these in-vessel systems are very technical in their approach to materials handling, aeration and control systems. However, the composting process is one which can and does occur naturally and simple systems such as windrows have been used successfully for many years.

The composting process was defined by Haug (1993) as the biological decomposition and stabilisation of organic substrates, under circumstances that allow development of thermophillic temperatures as a result of biologically produced heat. Golueke (1972) defines composting as the biological decomposition of the organic constituents of wastes under controlled conditions. This allows for a large number of descriptions to be applied to a composting system, including technological basis, management

regimes and temperatures. In terms of this thesis the composting process is aerobic with the substrate being decomposed to produce carbon dioxide, water and other trace compounds.

In order to meet the legislation on the sanitisation of catering wastes, high temperatures and an in-vessel approach are required. The composting process normally consists of a stabilisation phase, followed by a maturation phase once the material no longer requires management. To cope with these difficult wastes a sanitisation phase needs to be included, either as part of the initial stabilisation phase or as a pre treatment to composting.

1.6 The CERT Composting Project

The Carmarthenshire Environmental Resources Trust (CERT) was set up as a not for profit company to distribute the Landfill tax credits of the Carmarthenshire Waste Management (CWM) landfill site at Nantycaws near Carmarthen, West Wales. The composting facility is detailed in Chapter 5. There are several aspects of composting that require addressing if the U.K. is to meet the targets set by the Landfill Directive and perhaps even become a profitable process. Many of these areas are highlighted by the Animal By-Products Regulations and create an engineering challenge.

The research work presented in this thesis, funded by CERT and EB Nationwide through the Landfill Tax Credit Scheme, will look at developing some of the data that will be required to design composting systems to allow the U.K. to meet its Landfill Directive obligations.

During this project initial quantification of the composting process was undertaken on windrows to allow comparison between the level of composting within a technologically simple system and any highly complicated system.

As an enclosed area will now be required for the composting of material it is unlikely that the passive aeration, such as with windrows, will be enough to allow for rapid

composting. It is therefore likely that aeration will be required, this presents several problems, such as direction of aeration, quantity of aeration and the static pressures required in order to get varying quantities of air through the compost bed. A theoretical analysis of the composting process was undertaken in order to gain an understanding of the aeration requirements of the composting process. The static pressures required to provide appropriate aeration were determined experimentally using a bespoke static pressure test rig.

A containerised in-vessel composting system has been monitored in order to see if this technology could be applied to meet the Animal By-Products Regulations in a simple manner. The system was monitored using both green waste and two substitutes for catering waste.

2 Literature Review

2.1 Background and Optimisation

As discussed in Chapter 1, the composting process involves the breakdown of organic matter to a stabilised product in the presence of oxygen. Although composting is a biological process that occurs naturally, it can be dependant on various parameters which can affect how rapidly that degradation can occur. Although many composting facilities will be required to process a mixture of green and kitchen wastes, the properties and quantities of this mixture are likely to vary throughout the year. So although certain mixture ratios and moisture contents may be optimal it may not be possible to operate at those levels for the majority of the year.

2.1.1 Micro Organisms

The two main types of micro organism involved in the composting process are bacteria and fungi. Fungi have a eukaryotic cell type-like plants and animals whilst bacteria have a prokaryotic cell type, meaning that the nuclear substance is not enclosed within a distinct membrane. There are currently about 5000 known types of bacteria and 70,000 types of fungi (Bryson, 2003). The sheer number of different micro organisms involved combined with difficulties in isolation of species of micro organism make it unlikely that the exact make up of a composting system will ever be known. However there are various species which are known to cause illness in humans such as *E. Coli* and *A. Fumigatus*.

Inoculations have often been added to composting material to optimise the rate at which the composting activity occurs. Velikonja Bolta *et al.* (2003) compared compost inoculated with material from the active composting phase with non-inoculated compost. The viable microbial biomass in the inoculated compost was 6 times that of the non-inoculated compost, this caused the inoculated compost to heat up quicker initially and after turnings than the non inoculated compost. However by

day 18 of the trial the viable microbial biomass for both the inoculated and non-inoculated composts had reached the same level, implying that any lag due to non-inoculation had been made up and both systems were now at their optimal population levels. There were small differences between the quantities of fungi, non-thermophiles, thermophiles and bacteria in the non-inoculated and the inoculated piles after the 18th day of the trial, this implies that the system will move to an appropriate microbial population for composting of the particular feedstock.

Singh and Sharma (2003) investigated the effect of three different inoculants; each of these three inoculants was a pure culture of a particular fungus. It was found that use of inoculate reduced the quantities of cellulose, hemicellulose and lignin within the compost after the composting process.

2.1.2 Moisture Content

The moisture content has been shown to affect other properties of the composting material, for instance Mears *et al.* (1975) showed that both the thermal conductivity and specific heat capacity of a compost are linearly proportional to its moisture content. The specific heat capacity appeared to be most strongly related to the overall weight of water that was present within the compost, whilst the solid part of the compost made a very small contribution to the overall specific heat capacity.

Jeris and Regan (1973a) observed that at moisture contents below 20% wet basis (w.b.) there was very little biological activity. The activity, as measured by oxygen uptake rate then increases linearly until a maximum is reached in the range of 50-70%. At moisture contents above this level the level of aerobic biological activity begins to decrease, although no observations or quantifications of anaerobic activity were made.

Suler and Finstein (1977) investigated the effect of moisture content on CO_2 production. Three different moisture contents were used: 50%, 60% and 70% (w.b.), all maintained at a temperature of 56°C. By monitoring the quantity of CO_2 produced

in a 96 hour period it was shown that 60% was the optimum moisture content for the composting of waste. The material with a 50% moisture content produced almost as much CO_2 as that at 60% moisture content. The higher moisture content of 70% generally produced about half as much CO_2 as the compost with a moisture content of 60%.

Cathcart *et al.* (1986) showed that for unshredded blue crab scrap mixed with straw the optimum moisture content was 67%, whilst for shredded blue crab scrap the optimum moisture content was 55%.

Hamoda *et al.* (1998) used bench scale tests to determine the optimum conditions for composting material. Half kilogram samples were tested at room temperature. It was found that at a moisture content of 60% approximately 12.5% of the total organic carbon was lost in a period of 15 days. The samples at moisture contents of 45% and 75% only lost approximately 8.5% of the organic carbon in the same time period.

It seems likely that the optimum moisture conditions may well vary with the different materials being investigated. Cathcart *et al.* (1986) show this with the difference between shredded and unshredded material. However, the range of 50% to 70%(w.b.) does appear to contain the optimum point for the majority of materials. It would therefore be beneficial to use this range in later composting trials.

2.1.3 Volatile Solids

The volatile solids content is found using BS EN 13039:2000 (BSI, 2000), this involves determination of the loss on ignition at 450°C. The organic matter is the part of the compost that is being stabilised by the composting process. As CO_2 is produced during the composting process the quantity of volatile solids reduces in relation to the quantity of ash present in the material. The Composting Association (2004) recommend a volatile solids content of at least 40% dry basis (d.b.) for the material to be suitable for composting.

2.1.4 Nutrient Availability

The main indicator of nutrient availability in composting is the ratio of the mass of carbon to the mass of nitrogen (C:N). The Composting Association (2004) suggests a range of between 25:1 and 40:1 to be optimal for rapid composting. If there is a lack of nitrogen, giving a high C:N ratio the composting process may be slow, if there is too much nitrogen it may be lost as odorous ammonia. Various tables of carbon to nitrogen ratios are available within the literature, allowing estimation of mixtures to be found.

Cathcart *et al.* (1986) investigated the variables affecting composting of blue crab scrap mixed with straw. Where the crab scrap had been shredded the C:N ratio did not appear to affect the rate of composting. If the scrap was left un-shredded the C:N ratio did affect the composting rate. C:N ratios in the range of 12-28 were tested and the highest rates were found at these extremes with the lowest rate being at a C:N ratio of 19. It is quite possible that a higher rate might have been achieved using a higher C:N ratio than 28.

Hamoda *et al.* (1998) found that the optimum C:N ratio for municipal solid waste was 30:1 as 11% of the total organic carbon (TOC) was degraded over a 15 day period at this level. At a C:N ratio of 20:1 only 8.7% of TOC was degraded and 8% at a C:N ratio of 15:1. However no C:N ratios of greater than 30 were trialled and if the results had been taken after only 6 days, rather than 15 then the C:N ratio of 15:1 would have been the best whilst the 30:1 ratio was the worst performing. The cooked rice residue that was used to adjust the C:N ratio of the samples would have had different physical properties to the municipal solid waste being used which may also have affected the results.

Sadaka and El-Taweel (2003) studied the composting process on Egyptian household waste using a laboratory scale composting unit. Three different C:N ratios were studied: 11, 26 and 39. At different aeration rates the mixture with a C:N ratio of 26 consistently heated up faster and reached higher temperatures than the other

composts. This implies that it was composting at a greater rate than the other mixtures.

As with moisture content it is likely that different materials may have different optimum levels due to the availability of either nitrogen or carbon to the composting micro organisms. If a difficult feedstock is to be composted this may well have an affect upon the nutrient availability. Several have been used to augment the composting of green waste or MSW, for example poultry litter (Lhadi *et al.* 2004; Tiquia & Tam, 2002). Because of the importance of nitrogen to the composting process various methods have been trialled in order to preserve it within the system, for example, Jeong and Kim (2001) used magnesium and phosphorus salts to precipitate ammonia produced during the composting process and conserve the nitrogen within the finished compost.

Although for municipal solid wastes the range of 26:1 to 30:1 appears optimum, a different ratio will not inhibit activity altogether but it is likely to affect the overall composting rate. There is no guarantee that material being delivered to a site will be in the optimum range of C:N ratio, meaning that either another material needs to be found to mix with the waste in order to augment the waste or that the waste delivered to site will simply have to be composted as it comes. If the first option is chosen, a suitable waste with security of supply needs to be sourced, shredded and mixed. All of this will add cost to the process which may be greater than simply accepting the cost associated with a reduction in capacity caused by a reduced composting rate.

2.1.5 Oxygen Supply

As the composting process should be kept aerobic in order to reduce offensive odours it is necessary to ensure that oxygen is supplied to the material. Suler and Finstein (1977) used several bench top composting chambers to investigate the effects of moisture, temperature and aeration. The residual oxygen concentration in the exhaust gas was measured and compared with the total CO_2 evolved over a 96 hour period. Small amounts of CO_2 were formed with an oxygen residual of 2%, whilst at oxygen

residuals of 10% and above significantly more CO_2 was evolved. This implies that the greater quantity of oxygen supplied to a composting system the better it will perform.

Beck-Friis *et al.* (2003) used a compost reactor to monitor the emissions from composting. Three oxygen levels in the compost gas were trialled: 1%, 2.5% and 16%. The cumulative carbon emissions at the 16% oxygen concentration were greater than for either the 1% or 2.5 % concentrations. This indicates higher levels of composting activity occurring at higher oxygen supply rates. At the 16% oxygen concentration the composting activity begins at the start of the trial whilst at the lower concentrations there is a lag period; 4 days for the 2.5% oxygen concentration and 9 days at the 1% oxygen concentration.

2.1.6 Emissions from Composting

As mentioned previously the main emission from the composting process is CO_2. A comparison of emissions from waste treatment processes was performed by the national society for clean air and environmental protection (NSCA, 2002). But there was insufficient data available from the composting process to allow a comparison of emissions with other waste disposal technologies such as pyrolysis, anaerobic digestion and landfill.

If there is an excess of nitrogen present within the mixture the elevated temperatures and pH may lead to a volatilisation of ammonia. Witter and Lopez-Real (1988) reported that up to 50% of the total nitrogen present could be lost during the composting process whilst Eklind and Kirchmann (2000) recorded losses of up to 70% of total nitrogen. This could be reduced using a variety of different compost mixtures or additives, such as the magnesium and phosphorus salts used by Jeong and Kim (2001).

Hellebrand (1998) observed the release of a variety of gases including ammonia, nitrous oxide, carbon monoxide and methane during field scale composting trials of grass and green wastes. It was observed that of the original 4300kg of carbon present

1.7 kg was lost as carbon monoxide, 75 kg as methane and 3500 kg as CO_2. Of the 158 kg of initial nitrogen 0.8 kg was lost as nitrous oxide and 1.9 kg as ammonia. The methanogens which produce the methane are strictly anaerobic therefore any methane produced must be coming from anaerobic pockets within the composting mass. These results show that the majority of the carbon is lost as CO_2 with only 2% of the carbon lost being in a different form, showing that the process was highly aerobic, a very small portion, 1.7%, of the nitrogen was lost. It was thought that the quantity of nitrogen lost by the system varied with the aeration regime and that lower nitrogen losses were recorded at higher air flow rates. Schmidt (2000) used a mixture of sunflower hulls and manure to assess the odour and gas emissions from composting and used two separate methods for assessing the nitrogen loss from the compost. The first method, which assumed that the quantity of ash present was constant throughout the whole process, recorded losses of 37%, 32% and 58% for volumetric mixtures of 1:1, 2:1 and 3:1 of sunflower hulls to manure. The second method, which assumed that the quantity of phosphorus present was constant throughout the whole process, recorded losses of 50%, 35% and 42% for the same mixtures. Although the losses were high the disparities between the two sets of results also suggest that there may have been a problem with the methods used.

The other major emission from the composting process is bio aerosols; these can be a serious health concern. Various sampling protocols have been used to monitor the release of bio aerosols including one published by the UK Composting Association (1999). This method details a standardised approach to the sampling and enumeration of Bacteria and Aspergillus fumigatus. Hibbard and Strong (1996) stated that centralised composting systems do not introduce a significant risk of *Aspergillus Fumigatus* induced disease, though certain specific design measures for the avoidance of potential health aspects in both workers and the general public can be taken such as the inclusion of bio filters in plant design and the provision of air filters to machinery.

Work by Fischer *et al.* (1998) showed that both the turning frequency and C:N ratio affect the release of *Aspergillus fumigatus* in windrow composting. It was found that for the less frequently turned windrows counts of *Aspergillus fumigatus* within the compost remained elevated whilst in composts turned daily the level of *Aspergillus fumigatus* within the compost were reduced. This may imply that *Aspergillus*

fumigatus is released to the air during the frequent turnings, causing lower levels to be contained within the windrows. However, no atmospheric monitoring of *Aspergillus fumigatus* was performed during the study and it may be the case that both improved oxygen levels within the windrow and moisture removal by the turning process resulted in the reduced *Aspergillus fumigatus* levels.

2.1.7 Temperature

Temperature within the composting process is of great importance for two reasons: the inactivation of pathogens and the affect that temperature has on the rate of composting. However, it is often used as the only control parameter for a composting system. Polprasert (1989) explains that the succession is due to a series of events: initially the compost releases more heat than it can disburse, this leads to an increase in the compost's temperature, but this is followed by a decrease in the temperature once the compost is generating less heat that it can disburse. This succession is shown in Figure 2.1.

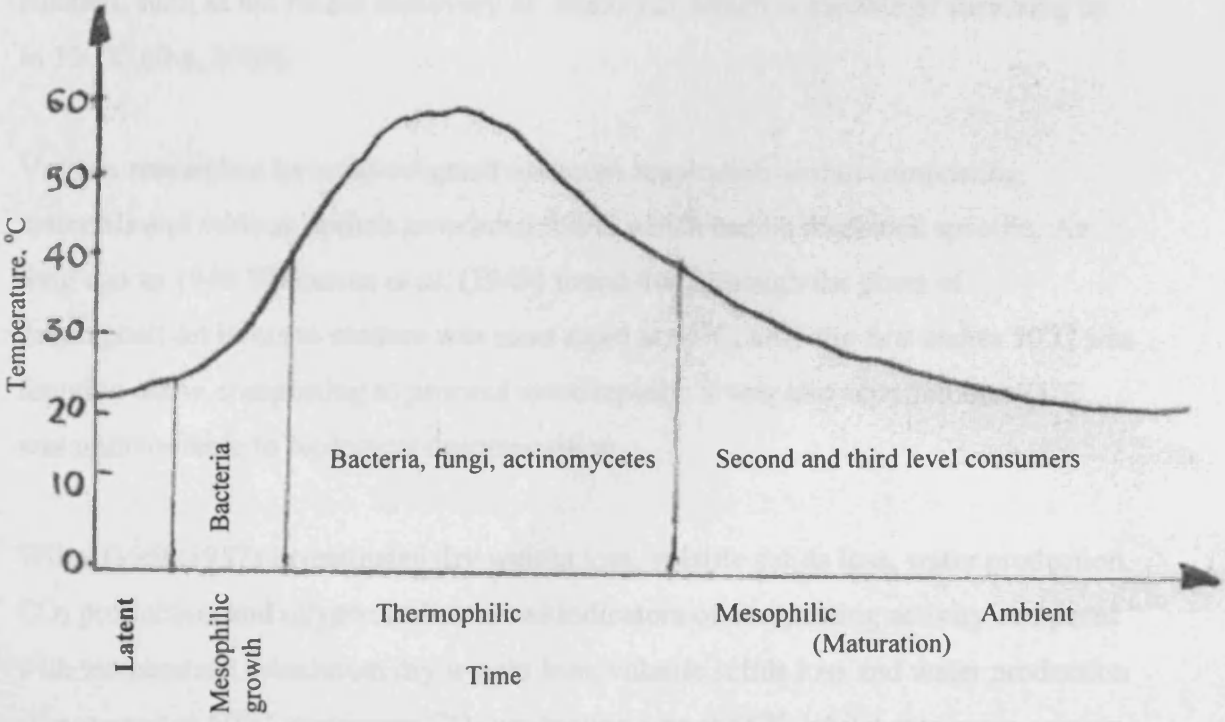

Figure 2.1. Patterns of temperature development within a compost pile (Redrawn from Polpraset, 1989)

The temperature is dependant on several factors including the rate of heat released by the composting process, the rate at which heat is lost to the surroundings and the thermodynamic properties of the composting material. The heat released by the composting process will be discussed in more detail in Section 2.4 and Chapter 3. Mears *et al.* (1975) showed that both the thermal conductivity and the specific heat capacity were both linearly proportional to the moisture content of the compost. This means that the heat stored within the pile is dependant on the quantity of water present. The heat lost will be through the mechanisms of mass transfer, convection, conduction and radiation.

The higher temperatures required for the sanitisation of the compost are not necessarily beneficial to the organisms that are carrying out the process. Strom (1985) investigated the effect of temperature on species diversity within a composting system and concluded that temperatures above 60°C have a marked detrimental effect upon species diversity. Droffener *et al.* (1995) showed that even in composts sampled at above 60°C bacteria strains that had been classed as mesophiles were isolated implying that they have survival and possibly replication mechanisms at elevated temperatures. Bacteria capable of withstanding extreme temperatures have also been isolated, such as the recent discovery of strain 121 which is capable of surviving up to 130°C (Jha, 2003).

Various researches have investigated optimum respiration within composting materials and various optima have been found which can be feedstock specific. As long ago as 1949 Waksman *et al.* (1949) found that although the onset of decomposition in horse manure was most rapid at 65°C, after the first stages 50°C was found to allow composting to proceed more rapidly. It was also reported that 75°C was unfavourable to biological decomposition.

Wiley (1956;1957) investigated dry weight loss, volatile solids loss, water production, CO_2 production and oxygen utilisation as indicators of composting activity compared with temperature. Maximum dry weight loss, volatile solids loss and water production all occurred at 60°C, maximum CO_2 production was at 56°C whilst maximum oxygen utilisation occurred at 64°C.

Rothbaum (1961) showed the optimum rate of CO_2 production on thermophiles occurring on wool occurred at 60°C, but at 70°C 94% of the optimum activity was still being recorded. The activity dropped readily at temperatures higher than this; at 74°C the level of CO_2 production had dropped to 53% of the optimum and only 5% at 78°C.

Jeris and Regan (1973) investigated a variety of feedstocks using bench scale reactors with a volume of 1.5 cubic feet ($0.042m^3$). The reactors were kept at a constant temperature using a rheostat and heater this meant that the temperature experienced by the compost was not a result of biological activity. The feedstocks used included newsprint, municipal refuse, synthetically prepared refuse and composted mixed refuse. The newspaper reached its peak CO_2 production rate at a temperature of 48°C and the stabilised mixed refuse peaked at 40°C. The lower temperatures were explained by the predominance of micro organisms capable of utilising cellulose to be mesophiles. The mixed refuse gave an optimum CO_2 production rate close to 60°C, decreasing at higher temperatures.

Suler and Finstein (1977) investigated various parameters using a bench scale, continuously thermophillic reactor, which was held at temperature by a water bath. The optimum temperature for composting was determined to be in the range of 56°C to 60°C similar to several other results that have been recorded.

Cathcart *et al.* (1986) compared variables affecting the composting of blue crab scrap, both shredded and unshredded, these data were then used to create a predictive model of the CO_2 generated by the composting process based on the properties of the initial scrap. The crab scrap was investigated both in shredded and un-shredded forms using $0.2m^3$ reactors. For the shredded scrap the maximum CO_2 production was recorded at a temperature of 55-56°C and a moisture content of 55%, the rate was also found to be independent of the carbon to nitrogen ratio in the range 10.4:1 to 28.5:1. The un-shredded scrap was found to give the greatest output of CO_2 at 63°C and 67% moisture content. Unlike the shredded crab scrap the CO_2 evolution depended upon the carbon to nitrogen ratio, giving peaks at 26:1 and 12:1.

Myrddin (2003) investigated the composting of difficult wastes in order to meet the Animal By-Products Order using a vertical composting unit. The maximum CO_2 production corresponded with a peak temperature of approximately 60°C.

Many of these results are from relatively small composting vessels and an open windrow system or a large vessel may have its hottest point at the core with contours of lower temperature (perhaps even ambient temperatures) towards the edges of the system. If the temperature is of sole interest in relation to the composting rate then several different respiration rates will occur throughout the pile, with the contour at 60°C providing CO_2 at the maximum rate and the other regions operating at a proportion of this maximum.

2.1.8 Physical Properties

The physical properties of the compost can affect the design and running of a compost plant. Something as simple as the bulk density will be used in the design of a site and the selection of equipment. The Composting Association (2004) recommends a range of 500 to 750 kgm^{-3}, whilst Hewings *et al.* (2002) showed that green waste shredded in a Seko shredder had a density of approximately 370 kgm^{-3} which increased as the material underwent the composting process. Both Michel *et al.* (1996) and Larney *et al.* (2000) observed an increase in compost density over processing time. Hannon and Mason (2003) compared the effect of two different shredders on the composting process. It was found that both the crush cut roller and low speed counter rotating shredder provided a suitable material for large scale windrow composting in remote areas. The crush cut roller was constructed from a second hand road compactor drum of diameter 750mm and length 1250mm. This was filled with concrete and helical steel blades were welded to the surface of the roller. This was then mounted on a tracked excavator. The low speed counter rotating shredder was rather more conventional and was a Brentwood TM 40.

Particle size and distribution present a variety of problems. The particle size gives an indication of the total available surface area within the compost, so may affect static

pressures (Ergun, 1952) as well as area available for microbial growth (Nakasaki *et al.*, 1986). With uniformly sized particles filling a volume, for example metal spheres, there is a limit on the proportion of the volume that will be filled. However with a variety of particle sizes the smaller particles are capable of fitting into the interstitial gaps between the larger particles, increasing the bulk density of the material. The distribution is also affected by high moisture content which causes agglomeration of particles. This agglomeration can cause difficulty in measurement of the particle size distribution. Agnew and Leonard (2003) conclude that further research is required to determine the most suitable method to provide reliable results of particle size distribution for composts.

Van Grinkel *et al.* (2001) showed that various physical properties of composting material, such as gas permeability, oxygen diffusion coefficients and thermal conductivity were dependant upon other more simply measured characteristics. For example the oxygen diffusion coefficient varied with the gas filled volume of the compost whilst the thermal conductivity depended upon the moisture content of the material.

2.1.9 Stability and Maturity

The terms stability and maturity are used widely in the field of composting and it is important to understand what is meant by these terms. Haug (1993) defines compost as being sufficiently stable when the rate of oxygen consumption was reduced to the point that anaerobic or odorous conditions were not produced to such an extent that they interfered with the storage, marketing and use of the end product. A differentiation needs to be made between the terms stability and maturity. Lasaridi (1997) uses the terms interchangeably but with the caveat that where agronomic quality is considered the term maturity is preferred whilst in reference to the rate and extent of decomposition the term stability is favoured.

The most simple test for stability is that mentioned previously in Section 2.1.7 and shown in Figure 2.1 where a drop in temperature indicates a reduction in composting activity. Other approaches include:

- reheating potential (Dewar vessel),
- organic content,
- chemical oxygen demand,
- carbon content,
- oxygen uptake rate (SOUR, DSOUR and ASTM d-5975-96) and
- CO_2 evolution rate (Solvita).

Richard and Zimmerman (1995) compared volatile solids lost, internal windrow temperature and a laboratory recorded respiration rate for a variety of feedstocks. The results showed that peak respiration rates diminished with time and that the temperatures were not a significantly accurate or sensitive measure of this.

Brewer and Sullivan (2003) used the definition that stability refers exclusively to the resistance of compost organic mater to further degradation (Sullivan and Miller, 2001). Brewer and Sullivan (2003) compared the Solivita test, alkaline trapping of CO_2 and the self-heating potential (Dewar flask). When results from these tests are plotted against time it can be seen that all three diminish as time increases. However, the alkaline trapping of CO_2 provided greater sensitivity than either the reheating potential or the Solvita tests.

Many of the stability tests available create an ideal environment for bacteria to survive, such as the SOUR test (Lasaridi, 1997). This means that they cannot necessarily be related to the actual level of composting activity. This idealised environment can include the addition of nutrient solutions or holding the compost at a fixed temperature similarly to many of the laboratory scale trials discussed in Section 2.1.7. Both of these changes can affect the respiration rate of the compost. Whilst the approach of creating an ideal growth environment for bacteria will circumvent any limiting factors it cannot inform the user of whether or not the decay of the rest of the composting material in a large scale system is actually being limited by the lack of a nutrient or inappropriate temperatures.

2.2 Composting Systems

The composting process is relatively simple and can be observed occuring in nature as oxygen is used by micro organisms to break down and stabilise organic material, this causes the release of moisture, heat and CO_2. There are, however, a variety of technologies available for the composting of organic wastes and these can be categorised in the manner shown in Figure 2.2. There are several distinctions which can be made, the first of which is whether or not the system is within a reactor or not, and how the material is treated in terms of turning. The systems that are within a reactor are the in-vessel technologies.

Prior to the Animal By Products Regulations (2003) there was no real requirement for in-vessel composting technology. It has been known for some time, and was discussed in Chapter 1, that to meet the European Landfill Directive (European Commission, 1999) targets catering waste would need to be diverted from landfill. As previously discussed apart from energy recovery (which includes anaerobic digestion), which rates lower on the waste hierarchy than composting, there is no other suitable disposal route apart form composting.

Prior to 2003 there were a number of in-vessel composting systems available and some data were available for choosing an appropriate system (Walker *et al.*, 1986). Various claims were made as to their advantages over windrow composting, such as; reduction in odour potential, reduced treatment space and reduced composing time. Now that the composting of catering wastes is allowed there should be a relatively high demand for in-vessel systems that meet the Animal By-Products Regulations (2003). As shown in Figure 2.2 there are a variety of in-vessel technologies. The Composting Association divide all in vessel composters into 6 types (Anonymous, 2002):

- Containers,
- Tunnels,
- Agitated bays,
- Rotating drums,
- Silos or Towers and
- Enclosed halls.

Containers are generally batch type reactors of low capacity where air is often forced in through a perforated floor. One of the main advantages of containerised composting is the relative ease with which the system can be expanded by adding further units. Using the hierarchy shown in Figure 2.2 Grüneklee (1998) compared a no reactor, static, non encapsulated, triangular windrow with a reactor, static, box composting system. Coincidentally these are similar to the systems investigated in Chapters 5 and 6 of this thesis. The conclusions were drawn that the containerised system was superior to the windrow system due to its uniform aeration and even temperature profiles combined with emission, moisture and odour control. Faster composting speeds, due to advanced aeration systems and accelerated initial mass loss, is one further reason given for the superiority of the in-vessel systems, though no data are given to confirm this. It may merely mean that the compost experiences a shorter residence time within the vessel than within the windrow, requiring the material from the vessel to be further matured before use. When estimating the required area for the composting of 60,000 tonnes per year the windrow plant is approximately three times the size of the in-vessel composting plant.

In order to meet the multi barrier approach to sanitisation of catering wastes described in the Defra risk assessment (Gale, 2002) the whole of a container system would need to reach the target temperature, otherwise the vessel would need to be emptied, the material mixed, the vessel cleaned and reloaded all of which would add further expense to the process.

Tunnels are normally capable of taking more material than a containerised composting system. Air is fed into the system and some systems use mechanical agitation. Various bagged tunnel systems are available which load the compost into a high tensile polythene skin-specialist machinery is required to do this and an aeration tube is also fed in at the time of loading. Hoitink and Keener (1995) described the operation of a tunnel system which had a 7 day residence period followed by a 28 day maturation period in windrows. Control of the system was through monitoring of oxygen and temperature levels within the compost. As with the container type systems the entirety of the material needs to reach the target temperatures in order to meet the Animal By-Products Regulations (2003). Some of the bagged systems are achieving this through use of an insulative quilt (Roberts *et al.*, 2004).

Agitated bays are similar to tunnels; containing walls are constructed either side of the bay thus allowing a turner to straddle the bay and move the material along. Because of the containing walls the floor area can be used more efficiently than a windrow. Several bays can be constructed next to each other and the turning machine moved between them. Because they are contained they can not benefit from natural ventilation like windrows so they also need to be artificially aerated. There is the possibility of by-pass within this type of system due to the material being thrown by an overhead compost turner. This would need to be addressed in order to meet the Animal By-Products Regulations (2003).

Rotating drums are large drums, horizontally mounted that rotate as the material is treated. Ali (2004) compared several commercially available rotating drum composting systems. Throughputs of the systems were calculated using data available from manufacturers as well as an addition of extra space for curing of the material. Ali (2004) concluded that although these systems do offer very short processing times it is uncertain as to whether or not they are capable of meeting the Animal By-Products Regulations. Because the process may be continuous there may be the risk of by-pass without treatment for material being processed in such a system.

Silos or towers are vertical units that normally operate on a continual basis, feedstocks are loaded at the top of the vessel and finished compost removed at the bottom. The loading and unloading of vessels can use some quite complex and heavy machinery such as augers. Because of the small footprint and height this type of system can achieve large throughputs. Myrddin (2003) compared a variety of in-vessel composting systems using manufacturers' data for capacity, footprint and residence time within the composter. It was found that the highest throughput in kilograms per square metre per week was achieved by a vertical composting unit. However the area required for maturation of the compost post treatment was not included in this calculation.

Enclosed halls hold all of the material being processed at once, materials handling equipment such as large buckets or even specialist machines are used to move the material through the building as it undergoes composting. These are often aerated to ensure that the process remains aerobic. One of the key problems with this type of

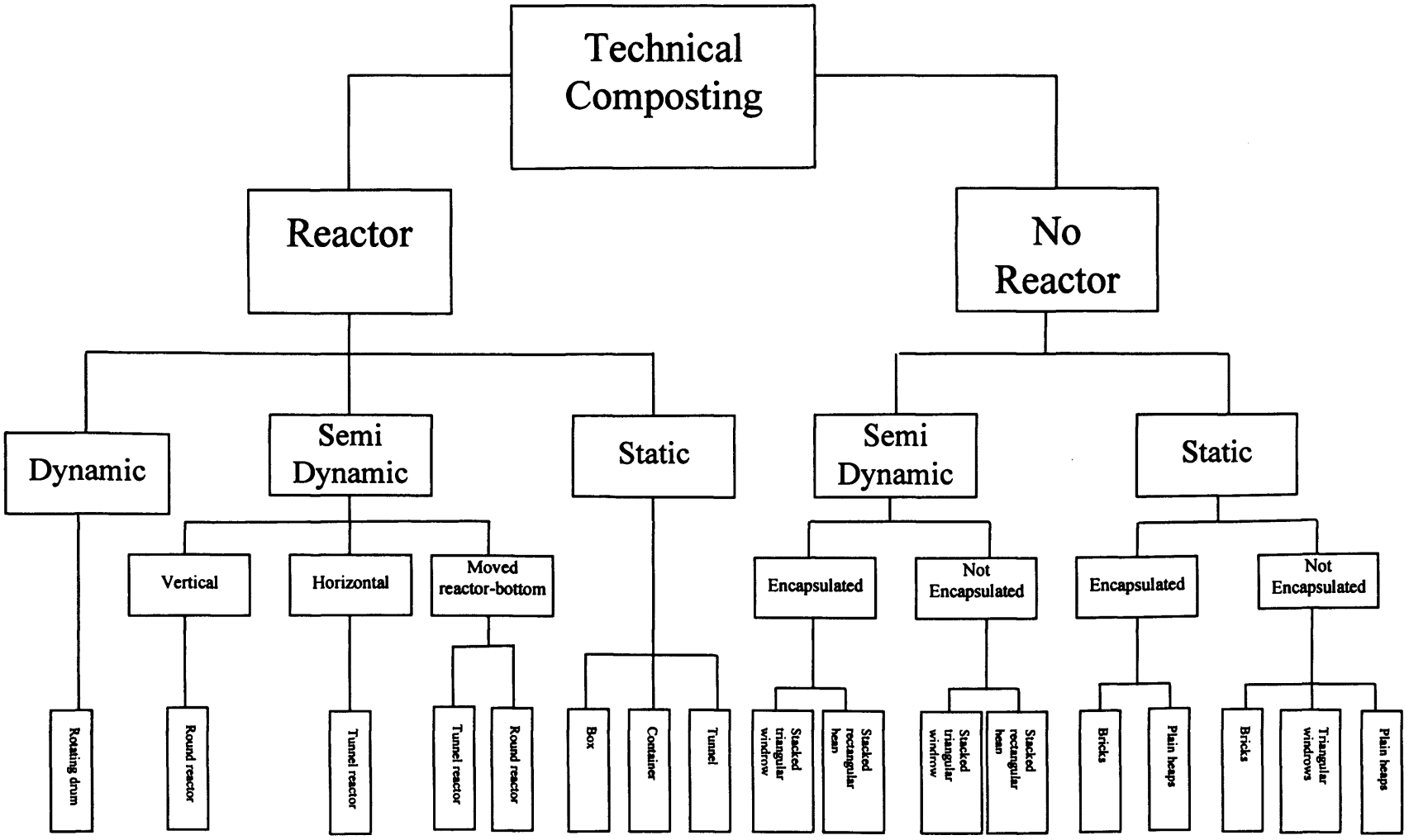

Figure 2.2. Hierachy of composting systems (Redrawn from Grüneklee, 1998)

system is that there is material of a variety of different ages within the vessel, because of this it is unlikely that these can be used to compost within the Animal By-Products Regulations.

Li *et al.* (1991) presents comparative capital and operational costs for tunnels, silos and agitated bins. For capital costs it was noted that the tunnel systems do not benefit from an economy of scale with increasing throughput because more tunnels are needed for greater capacity. With many of the analyses and with much of the commercial data the area required for the maturation of the finished product is not taken into account which as Ali (2004) shows can have a dramatic effect upon the total space required.

2.3 Respiration Rate

Haug (1993) states that the oxygen uptake rate is proportional to the rate of organic decomposition. By measuring the respiration rate of the compost the performance of the feedstock or material can be assessed. Normally the respiration rate is measured using a form of standardised stability test, there are many tests such a SOUR (Lasaridi, 1997), AT4 (Bidlingmaie *et al.*, 2002), Solvita, BOD_5, COD as well as the self heating test performed using a Dewar vessel. Adani *et al.* (2002) demonstrated that there are correlations between many of the test methods used by various researchers and that some tests are more sensitive than others.

Many results for the respiration rate of composts are present in the literature, these are generally based on small samples placed in idealised conditions. For example Cronje *et al.* (2004) assessed the respiration rate of pig manure using 3 litre jars in a water bath. Mari *et al.* (2003) used two 145 litre drums to monitor the composting of olive press cake and olive mill water. Samples of 20 grams were taken to assess the respiration rate of the compost. The results are expressed on a dry weight (dw) basis rather than a volatile solids basis. A maximum rate of 0.013 ml O_2 $min^{-1}g\ dw^{-1}$ (approximately 25 gO_2 kg dw^{-1} day^{-1}) was recorded by Mari *et al.* These results do

show that the respiration rate decreased as the material aged. This is likely to be due to the decreasing volatile solids content.

Myrddin (2003) investigated the respiration rate of compost in a vertical composting unit. This work showed a relationship between the peak temperature of the vessel and the respiration rate of the compost, with the optimum temperature being approximately 60°C. As discussed in Section 2.1.7 similar results have been shown in small scale laboratory tests. The implication of this is that the respiration rate of the whole volume of the compost within a system can be measured, rather than using just a small sample. With the move to in-vessel units required by the ABPR these data could be fed directly into a vessel control system for optimisation of the process.

Some of the tests used to measure respiration rates of compost require the addition of nutrient solutions and also control of temperature. The temperature control may be provided by an incubator or a water bath. These changes bring the compost into previously recorded optimum conditions for degradation and also ensure that the degradation is not limited by lack of any nutrients. This means that the test is measuring the material's potential to degrade rather than the actual degradation that the material still within the system is undergoing. The potential to degrade should decrease with time and this is shown in the results of all of the stability tests.

2.4 Heat release

Although the self-heating of aerobically degrading biomass is well documented, the quantification of the energy that is released during this process has received limited interest. However, heat release is an indicator of the compost's respiration rate and quantification of the heat released from composting material could give an indication of its level of stability. It is normally less expensive to use thermocouples than to buy gas detection equipment, so the usage of heat release could allow for control strategies based on the rate of composting to be utilised.

Because of its relative simplicity to measure and the effect that it has on microbial activity, temperature is often used to evaluate the performance of a compost system. The temperature of a composting system is not only related to activity within the system but other factors such as heat losses are just as important to the overall temperature. This is shown by McCartney *et al.* (2003) who showed the effect that different particle sizes (and hence different airflow rates) have on the temperatures within windrows.

Efforts have been made to quantify the heat released by the composting process. Haug (1980) used value of 104.2 kcal/mole O_2 or 436kJ/mol O_2. The basis for this being that a methane type bond gives 26.05 kcal per electron transferred and oxygen is capable of accepting four electrons. For example if a mole of glucose, $C_6H_{12}O_6$, reacts with 6 moles of oxygen it will produce six moles of both CO_2 and water and it will also release 2808.04 kJ. If all of that heat released went into heating the products of the reaction the temperature increase would be approximately 3,500°C . The energy release from glucose is equivalent to 468 kJ per mole of either oxygen used or CO_2 evolved.

Cooney *et al.* (1969) measured the heat evolution during microbial growth and correlated it with the oxygen consumption and CO_2 evolution. The method involved monitoring the heat production within a nine litre fermenting vessel and the analysis of the air leaving the vessel in order to calculate oxygen usage and CO_2 production. Different substrates such as glucose, molasses and soy bean meal were used to grow four different microbes, *Escherichia coli*, *Bacillus subtilis*, *Candida intermedia* and *Aspergillus niger*. *Escherichia coli* and *Bacillus subtilis* are both bacteria whereas *Candida intermedia* and *Aspergillus niger* are fungi. Figures 2.3 and 2.4 show the results for the organisms as the total heat produced against the total rate of oxygen consumption and CO_2 evolution respectively.

The gradients of the best-fit lines in Figures 2.3 and 2.4 give quantity of energy released per mole of gas. Although originally expressed in units of kcal $mmole^{-1}$, these can be easily converted into SI units, giving 460±41.8 kJ/mol O_2 consumed and 460±83.7 kJ/mol CO_2 evolved. Overall the measurement error is ±9.1% when

comparing heat release to oxygen consumption and ±18.2% when comparing the heat release to CO_2 evolution.

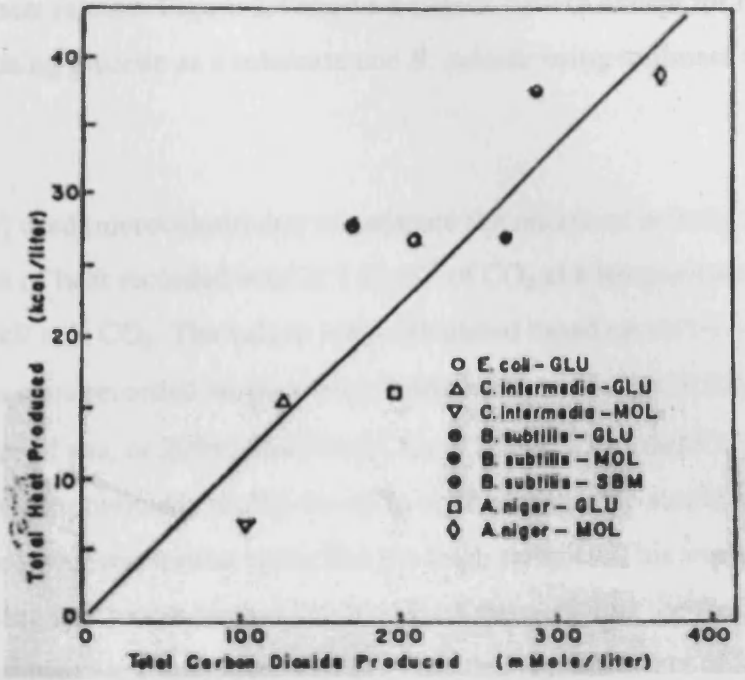

Figure 2.3. Total heat produced versus total carbon dioxide evolved (From Measurement of Heat Evolution and Correlation with Oxygen Consumption during Microbial Growth, Cooney *et al.*, 1969, Biotechnology and Bioengineering Vol 11, Copyright © 1969 Wiley-Liss, Inc., a subsidiary of John Wiley & Sons, Inc. Reprinted with permission of John Wiley & Sons, Inc.)

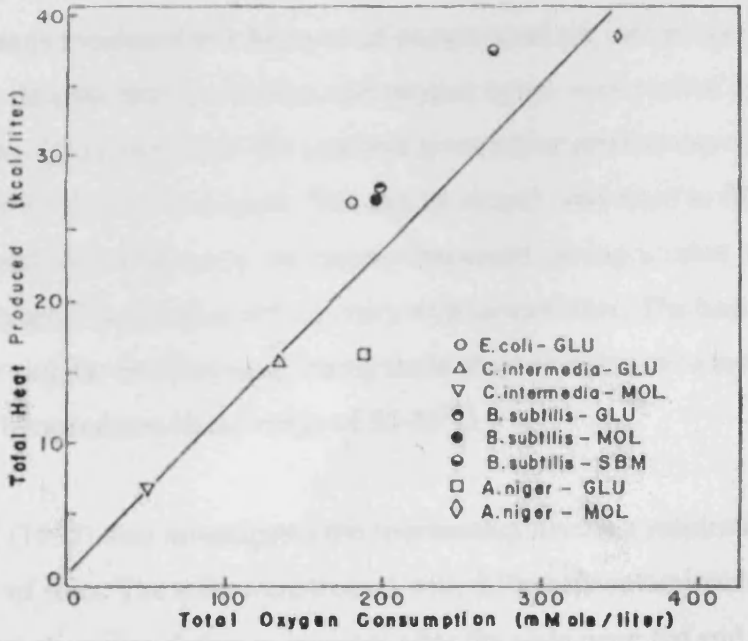

Figure 2.4. Total heat produced versus total oxygen consumed (From Measurement of Heat Evolution and Correlation with Oxygen Consumption during Microbial Growth, Cooney *et al.*, 1969, Biotechnology and Bioengineering Vol 11, Copyright © 1969 Wiley-Liss, Inc., a subsidiary of John Wiley & Sons, Inc. Reprinted with permission of John Wiley & Sons, Inc.)

In Figure 2.3 the points that represent *E. coli* and *B. subtilis*, the two bacteria tested all lie above the best fit line. Points represented by *C. intermedia* and *A. niger*, the two fungi under test all lie beneath or on the line. This suggests that bacteria may have a lower level of heat release. Figure 2.4 shows a similar pattern except for two points: *C. intermedia* using glucose as a substrate and *B. subtilis* using molasses as a substrate.

Sparling (1983) used microcalorimetry to estimate the microbial activity in soils. The average amount of heat recorded was 21.1 J cm^{-3} of CO_2 at a temperature of 22°C, this equates to 510kJ/ mol CO_2. The values were calculated based on active biomass. A range of values were recorded ranging from 8.66±0.645 to 37.63±0.952 joules per cubic centimetre of gas, or 209±15.6kJ/mol CO_2 to 909.5±23 kJ/mol CO_2. Some of these samples were previously stored for up to eight months, the stored samples tending to have lower respiration rates than the fresh samples. This was thought to be due to there being less active biomass in the stored samples than the fresh samples. Some of the samples were amended with glucose; this had the effect of increasing the respiration rate.

Harper *et al.* (1992) used a tunnel reactor for mushroom composting and showed strong correlation between the heat production in Watts per kilogram of compost and the oxygen usage measured in kilograms of oxygen used per second per kilogram of compost. The data for heat production and oxygen usage were plotted against each other and using linear regression the gradient gives a heat production of 9760 kJ for each kilogram of oxygen consumed. This can be simply converted to SI units to allow comparison with the other results previously discussed, giving a value of 312 kJ mol^{-1}. This value of heat output did not vary with temperature. The heat production, and therefore oxygen consumption, during these trials was shown to reach a maximum at temperatures in the range of 55-63°C.

Tancho *et al.* (1995) also investigated the relationship between respiration and heat for a number of soils. The soils were treated with different contaminants and fed with glucose. Respiration was shown to increase after the soils were fed and this correlated with an increase in CO_2 production rates. The comparison of CO_2 evolution and heat

production is shown in Figure 2.5. As opposed to some of the other data discussed where all of the data points on graphs of heat production against oxygen consumption lie on the best fit lines, the data shown in Figure 2.5 show a lot of scatter. It was also observed by Cooney (1969) that the results for energy release per mole of oxygen utilised were closer to the line of best fit than those for CO_2 evolution. The best-fit line in Figure 2.5 gives an average result equivalent to 383kJ/mol CO_2 evolved.

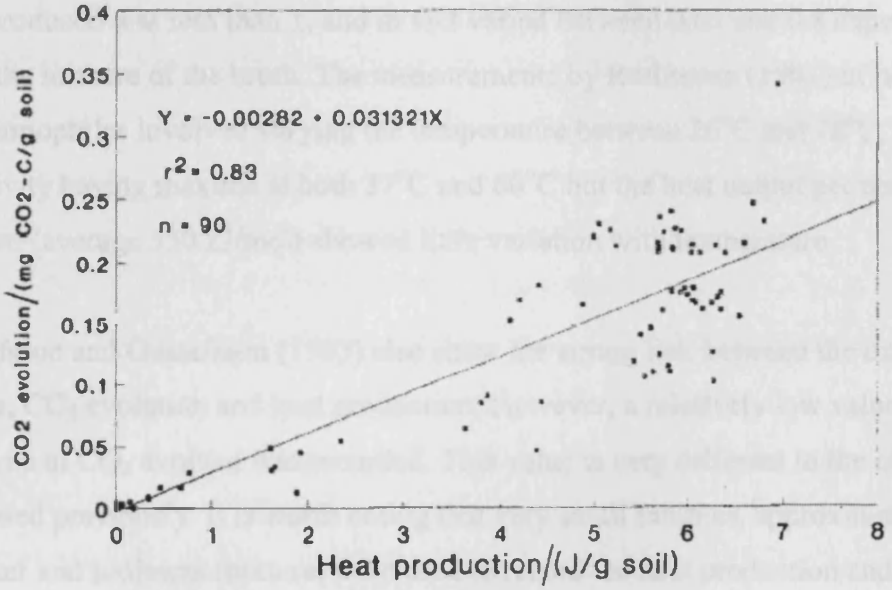

Figure 2.5. CO_2 evolution versus Heat production (Reprinted from Thermochinica Acta 251, Tancho *et al.* Relationship between substrate-induced respiration and heat loss from soil samples treated with various contaminants, pp. 21-28 Copyright (1995), with permission from Elsevier)

Weppen (2001) used a bench scale calorimeter to investigate the relationship between heat generation and gas production. The calorimeters measured both oxygen uptake and CO_2 evolution as well as the heat losses by conduction, evaporation, heating of air and heating of the compost and vessel. Comparing the data given for oxygen utilisation and CO_2 evolution shows more moles of oxygen being used than moles of CO_2 utilised. A control gave a CO_2:O_2 ratio of 0.95 whilst an experiment amended with fat gave a ratio of 0.87, implying that higher fat content will give a lower quantity of CO_2 and hence a larger content of heat released per mole of CO_2. A total of 37 experiments were performed by Weppen (2001) which gave an overall average heat release of 452±29 kJ/mole O_2.

Work by Rothbaum (1961) on the heat output of thermophiles and by Rothbaum and Stone (1961) on the Heat output of *E. Coli* also indicate the strong link between CO_2 evolution and heat production. *E. Coli* was grown by Rothbaum and Stone in a series of broths made from different mixtures of glucose and beef extract, these were kept at a constant temperature of 37°C. The heat output was measured through the temperature differential between the water bath and the centre of the flask. The heat output by E. Coli was recorded as approximately 700 kJ per mole of CO_2 evolved. The data presented also show that the ratio of moles of oxygen utilised to moles of CO_2 produced was less than 1, and in fact varied between 0.65 and 0.8 depending upon the mixture of the broth. The measurements by Rothbaum (1961) of heat output by thermophiles involved varying the temperature between 26°C and 78°C, the level of activity having maxima at both 37°C and 60°C but the heat output per mole of CO_2 evolved (average 530 kJ/mol) showed little variation with temperature.

Gustafsson and Gustafsson (1983) also show the strong link between the oxygen uptake, CO_2 evolution and heat production. However, a relatively low value of 161 kJ per mole of CO_2 evolved was recorded. This value is very different to the others discussed previously. It is worth noting that very small samples, approximately 2 ml of water and sediment mixture, were used to record the heat production and respiratory activity. Zanoni and Mueller related the calorific value of sewage sludge to the chemical oxygen demand (COD) of the sludge. The relationship found states that 1 mol of oxygen utilised would cause 512kJ to be released.

2.5 Aeration

As previously discussed in Chapter 1, the Animal By-Products Regulations (2003) require that composting of catering wastes is performed where animals cannot gain access to the waste. Metcalf & Eddy (2002) state that the composting process can be inhibited at oxygen levels below 10% and in order to ensure that the material is composting it may be necessary to supply air to the system. When supplying air to a system it is important to have an understanding of both the volumetric flow rate of air

that is required and the static pressure that it needs to be supplied at in order to allow the flow.

2.5.1 Air requirements

Air is required for the composting process for a variety of reasons: to dissipate excess heat, to supply oxygen to the micro-organisms and to remove excess moisture. Monitoring of the respiration rate would allow the quantity of oxygen required to be calculated. But as we have previously seen the respiration rate appears to be affected by temperature so greater quantities of air may be required to remove the excess heat. It is often assumed that the molar ratio of oxygen utilised to CO_2 is 1, however Harper *et al.* (1992) whilst mushroom composting found that the ratio of CO_2:O_2 was in some cases greater than 1, though Harper *et al.* state that this may have been due to some anaerobic activity.

Rynk (1992) suggests a figure of $5\times10^{-5}m^3s^{-1}$ per kilo of dry solids of compost for the temperature control of an aerated static pile. Mu and Leonard (1999) use airflows in the range of $3\times10^{-5}m^3s^{-1}$ to $19\times10^{-5}m^3s^{-1}$ per kilogram of dry matter in order to assess the pressure drop through compost.

There are a variety of methods for controlling the aeration through compost and several of these are mentioned by Haug (1993) and they include timer control, feedback based on temperature, CO_2 or O_2, or constant feed of the correct rate. A figure of 1660 m^3hour^{-1} per dry metric ton or $4.6\times10^{-4}m^3s^{-1}$ per kilogram of dry matter is suggested by Haug, This is an order of magnitude greater than the supply rate suggested by Rynk (1992).

Keener *et al.* (1997) in their analysis of aeration upon cost used the fixed figure of 2.68 $m^3kg^{-1}day^{-1}$, which equates to $3.1\times10^{-5}m^3s^{-1}$ per kilogram of compost. This is approximately the same as the figure suggested by Rynk once the compost's moisture content is taken into account. This figure is also comparable with that used by Bari and Koenig (2001) in their laboratory scale trials. Whatever the quantity of air that is

to be supplied to a system it will have an affect on both the production costs and installation costs of the composting facility.

2.5.2 Static Pressure

There are various models for describing the flow through packed beds; the most simple of these is Darcy's law (Massey, 1989) which gives a linear relationship between the steady mean velocity and the pressure gradient. However, under turbulent or transitional flow conditions the relationship ceases to be linear. A good description of this behaviour is given by Coulson *et al.* (1978). Various empirical models, such as the Ergun (1952) equation have been developed to describe the behaviour of turbulent fluid flow through packed beds and these are split into two terms reflecting the losses due to viscous drag and the loss of energy due to turbulent eddies.

$$\frac{-\Delta P}{L} = 150\frac{(1-e)^2 \mu_{air} U}{e^3 D^2} + 1.75\frac{(1-e)\rho_{air} U^2}{e^3 D} \qquad (2.1)$$

where ΔP is the static pressure in Pa,

L is the depth of the bed in m,

e is the proportion of void space,

μ_{air} is the dynamic viscosity in Pa S,

U is the mean velocity in ms^{-1} and

D is a representative particle size in m.

The Ergun equation, given as Equation 2.1, shows the static pressure as being dependant upon factors such as the void ratio of the bed, e, the particle size, D, and the properties of the fluid passing through the bed.

The idea of driving air through organic material is not a new one. Grains are dried for storage by blowing air through the bed of grain although this is performed to avoid microbial growth. Much work has been performed in this field to investigate different

grains (Shedd, 1953; Gunasekaran, 1987; Giner, 1996; Dairo, 1994; ASAE, 2000). These results generally show that the static pressure is related to the velocity, but not linearly.

Gunasekaran (1987) investigated pressure drops through grain sorghum at a range of superficial velocities between 0.05 and 0.3 ms^{-1} with a range of different moisture contents and bed depths. The observed pressure drop was found to increase with the bed depth and the superficial velocity but decreased with increasing moisture content. However the bulk density of the material was found to decrease as the moisture content increased, meaning that the pressure drop increased with increasing bulk density.

Giner (1996) also shows that as the moisture content increased the overall bulk density decreases, higher static pressures were required for the drier grains than the moist grains again suggesting that the density of the grain affects the static pressure required. Also investigated in this study was the affect of fine material on static pressure. It was found that as the proportion of fine material increased so did the static pressure required to drive the airflow. The increase in fines would have caused a decrease in the average particle size and as suggested by Equation 2.1 the static pressure would increase.

Dairo's (1994) results from investigating sesame seed show a similar pattern, as the moisture content is increased, the required static pressure decreases. It is of note that the moisture contents are much lower than those on compost, being in the range of zero to 22.3% (w.b.). It is therefore unlikely that the pore spaces between particles are filled with water. The inclusion of fine material also increases the static pressure. A plot of static pressure against bed depth also shows that the grains are incompressible.

The results from relatively dry grains all show that the bulk density of the material in the bed affects the required static pressure to aerate the bed. McGuckin *et al.* (1999) investigated the pressure drop through food waste compost with a variety of synthetic bulking agents added in varying ratios. The results from the investigations were compared with three different models in order to assess how well the airflow models fitted the data. The models were of the forms

$$\Delta P = A_1 U^{B_1} \tag{2.2}$$

$$\Delta P = \frac{A_2 U^2}{\ln(1 + B_2 U)} \tag{2.3}$$

$$\Delta P = A_3 U + B_3 U^2 \tag{2.4}$$

where ΔP is the static pressure in Pa,

A_1, A_2 A_3, B_2 and B_3 are experimentally derived constants and

U is the superficial velocity in ms^{-1}.

Equation 2.4 is of a similar form to Equation 2.1, it has both U and U^2 terms that would be associated with viscous and kinetic energy losses from laminar and turbulent flow regimes. The bulking agents were added in different quantities varying the volume of bulking agent per kilogram of compost. The addition of bulking agent should affect both the void space within the mixture and the average particle size both of which, according to Equation 2.1, should cause a variation in static pressure. Some of the data recorded by McGurkin *et al.*(1999) are shown in Figure 2.6.

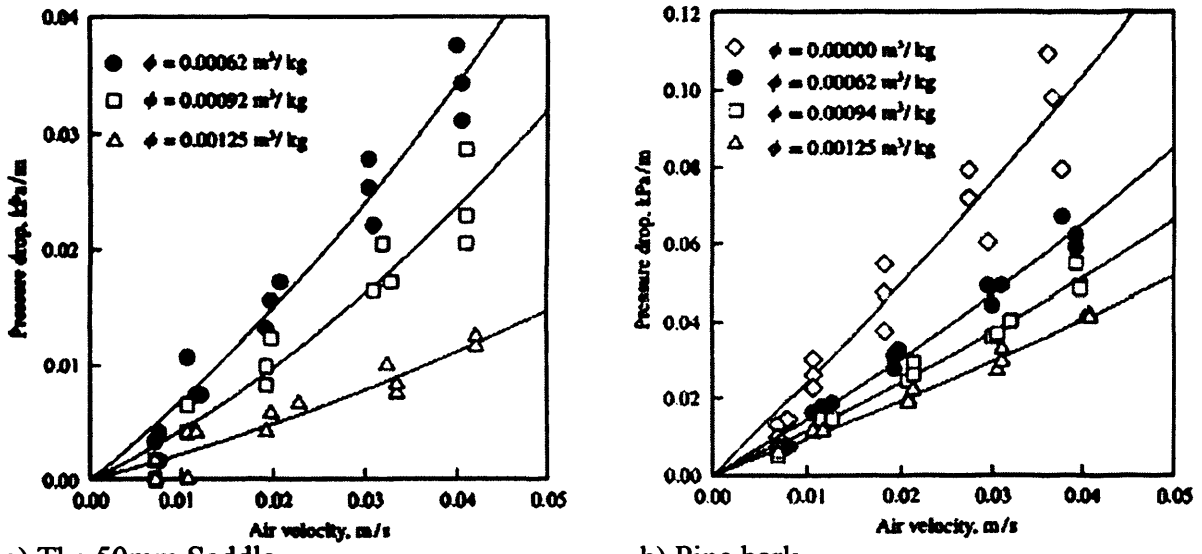

a) The 50mm Saddle b) Pine bark

Figure 2.6. Static pressure per unit depth against superficial air velocity for different bulking agents (Reprinted from Journal of Agricultural Engineering Research 72, McGuckin *et al.* Pressure Drop Through Raw Food Waste Compost Containing Synthetic Bulking Agents., pp. 375-384 Copyright (1999), with permission from Elsevier)

Figure 2.6 shows that as the quantity of bulking agent is increased the static pressure decreases, the required static pressure for the pine bark as a bulking agent was higher than for any of the plastic bulking agents being tested. As the volume of bulking agent used increases, the bulk density of the material decreases due to an increase in the

void space. The increase in void space caused the static pressure required to decrease, this would also be expected from Equation 2.1.

Keener *et al.* (1997) present the implication upon cost and design that is caused by aerating compost. They use a constant static pressure of 203 mmH_2O (2.03 kPa) as a basis for the assumptions, which is very high in comparison to the values observed by McGuckin *et al.* (1999), Dairo (1994) and is at the top end of the ranges presented by most of the researchers already mentioned. As the sizing of aeration equipment could be critical to the commercial viability of a composting plant it is vitally important that the figures used in the design process are accurate.

Mu and Leonard (1999) investigated the relationship between flowrate and static pressure using a column of 600 mm diameter and 2280 mm high. Volumetric flowrates of between 0.004 m^3/s and 0.018m^3/s were tested for a variety of composts at 3 different depths of compost (680 mm, 1450 mm and 2200 mm). Once filled to 2200m the column was left to settle for two weeks which allowed the compost to settle giving a reduction in height of 230mm (approximately 10% of the original height). The relationship between static pressure and flowrate for the material on filling was found to be non linear. The data was fitted to a curve of the form shown as Equation 2.5. The R^2 values for this equation were shown to be greater than 0.999.

$$\Delta P = (101637H + 173473)Q^{(0.0126H + 1.1998)} \qquad (2.5)$$

where ΔP is the static pressure in Pa,

H is the height of the compost column in metres and

Q is the volumetric flow rate of air in m^3s^{-1}.

Equation 2.5 shows that the height of the compost pile, H, is very important in determining the static pressure required to provide a particular flow rate. Using Equation 2.5 and the three heights of compost trialled the trend lines obtained from the experiments are shown in Figure 2.7. There are, however, two modifications; firstly the values obtained from Equation 2.5 have been divided by the depth of

compost, *H*, to give the static pressure per metre depth and secondly the superficial velocity rather than volumetric flow rate has been used.

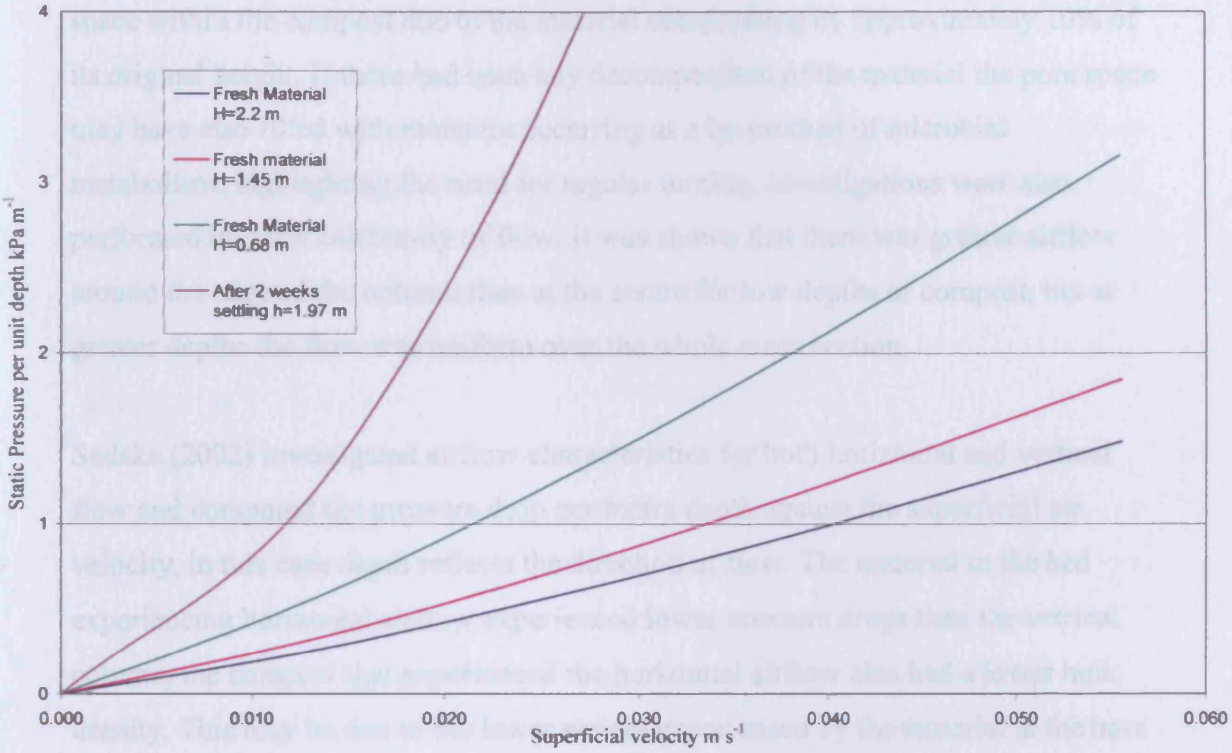

Figure 2.7. Static pressures for airflow through compost (adapted from Mu and Leonard, 1999)

It might be expected that the curves shown in Figure 2.7 for the fresh compost filled to different heights (when expressed as a pressure drop per unit depth) should all show the same pressure drop per unit depth. However, this is not the case and it is the tallest pile which gives the lowest static pressure per unit depth-but the highest total pressure. The only material property of the material given by the authors is the bulk density. When filled to 2.2m the bulk density was 720 kg m^{-3} whereas at a depth of 0.68 metres the density was 870 kg m^{-3}. The increased bulk density implies lower air space within the compost, in accordance with the Ergun equation (Equation 2.1) the reduced pore space would cause an increase in static pressure. The densities are relatively high this is probably due to the material being screened through diamond shaped holes which were 25mm by 13mm. This reduced particle size would also have lead to an increase in the static pressures required for aeration according to Equation 2.1.

Mu and Leonard (1999) then allowed the compost to settle for two weeks. As can be seen in Figure 2.7 the settled material required much higher static pressures for aeration than the fresh material. It is likely that the settled material had a decreased air space within the compost due to the material compressing by approximately 10% of its original height. If there had been any decomposition of the material the pore space may have also filled with moisture occurring as a by-product of microbial metabolism; highlighting the need for regular turning. Investigations were also performed into the uniformity of flow. It was shown that there was greater airflow around the edge of the column than at the centre for low depths of compost, but at greater depths the flow was uniform over the whole cross section.

Sadaka (2002) investigated airflow characteristics for both horizontal and vertical flow and compared the pressure drop per metre depth against the superficial air velocity, in this case depth reflects the direction of flow. The material in the bed experiencing horizontal airflow experienced lower pressure drops than the vertical column, the compost that experienced the horizontal airflow also had a lower bulk density. This may be due to the lower weight experienced by the material at the base of the reactor which is only 1 metre deep rather than 2.4 metres for the vertical flow reactor.

Barrington *et al.* (2002) investigated compost airflow resistance with a variety of bulking agents including pine shavings, chopped hay and straw mixed with pig slurry and tap water. The experiments were performed in a 105 litre capacity vessel with a depth of 0.95 metres. The highest recorded pressure drop was 268 Pa. Superficial velocities of up to $0.002 ms^{-1}$ were used and it was found that these fitted to laminar airflow equations based on the porosity, particle size distribution and depth of the compost bed.

A range of static pressures are given, many of these have been modelled using empirical formulae of the form

$$\Delta P = J H^a U^b \tag{2.6}$$

where J, a and b are empirical coefficients,

H is the height of the pile and

U is the superficial velocity.

Although this does take into account the compressibility of the compost the main problem is that the results cannot simply be compared with each other. Generally the coefficients are all empirically derived and are not related to other properties such as free air space, particle size or even something as simple as bulk density. This makes them very specific. The result of this is that it is difficult to calculate the required pressure for a new feedstock, meaning that testing of the feedstock is required in the development or design stage of a composting facility to allow appropriate aeration equipment to be specified.

Many of the coefficients derived during these tests are only valid for the material on test that day, they do not take the properties of the material into account. This may be workable in a situation where a system is fed with the same waste continuously over its entire operational lifespan. For instance although Mu and Leonard (1999) imply that the increased moisture content and decreased particle size cause the increased static pressure after a two week settling period no mention is made of these and other material properties at any other point, neither do these properties feature in the equation that was developed (2.5). The material that was left to settle for two weeks does not follow equation 2.5 and required a separate power law where the height of the pile is not a factor. The compaction of the material is also important, Mu and Leonard (1999) show that the static pressure for material that had been settling for two weeks was significantly higher than for material that was freshly shredded, this can also be observed in Figure 2.7.

The bulk density of the compost appears to be an important factor in determining the static pressure, it is most likely that the compaction mentioned by Mu and Leonard (1999) which causes the large increase in static pressure also increased the bulk density. Das and Keener (1997) demonstrated the effect of compression on bulk density by applying different compressive stresses to compost using a hydraulic cylinder. This had the effect of increasing the bulk density of the compost as the force applied was increased. The larger the compressive stress applied to the compost the larger the static pressure required to drive air through the compost. This is not

surprising as only the air filled volume of the compost can be crushed, so it is the void ratio that decreases as the bulk density increases. This also agrees with the work preformed by Nicolai and Janni (2001) who show the pressure drop through a bed of compost increasing as the void space within the compost decreases.

The Ergun Equation (2.1) does not use the density of the compost as a variable, it is however highly dependent on the void ratio or free air space. Results from Agnew *et al.* (2003) and those from Baker (1998) are shown in Figure 2.8. These data show that for a constant moisture content the relationship between bulk density and free air space within the compost is linear. This may well explain why so much of the data recorded varies with bulk density, as it is a measure of free air space.

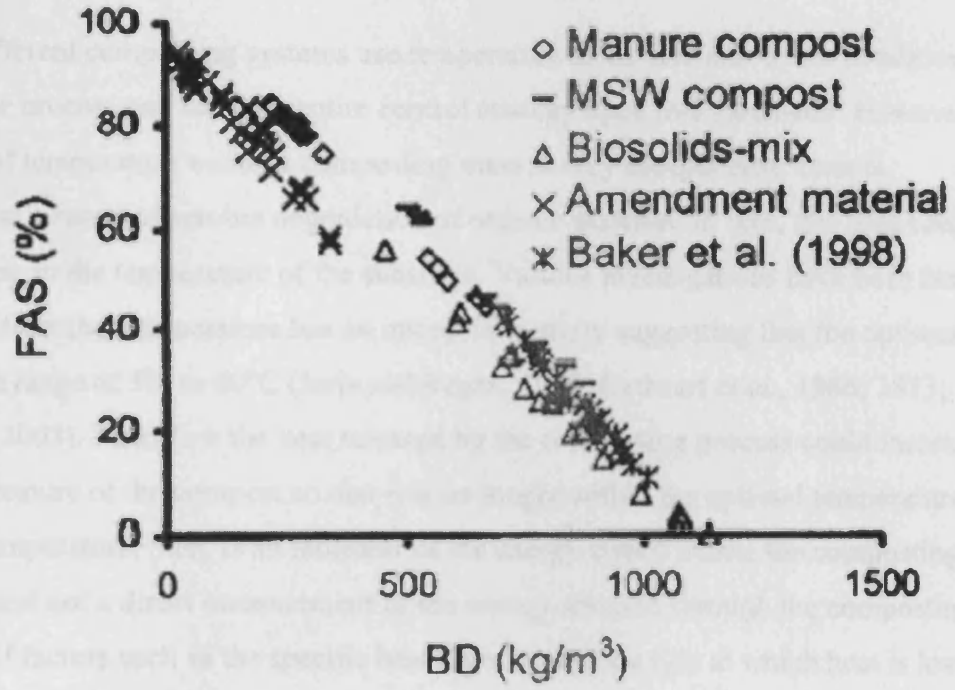

Figure 2.8. Free air space against Bulk Density at a moisture content of 60 % (w.b.) (after Agnew *et al.*, 2003)

It has been shown that the bulk density of compost in a pile or vessel varies with the depth of the bed (Schaub-Szabo, 1999; Agnew, 2003), this is a problem not included in many of the equations relating to packed beds as the measurements are often made on uniformly sized spheres or cubes. However the compressibility of compost needs to be taken into account, equation 2.6 does this by using the coefficient *a*.

3 Calculations for Energy Release and Aeration Requirements and Implication Upon Design

3.1 Introduction

As discussed in Chapter 2 the composting process is aerobic; microbes utilise oxygen to digest biomass. The main products of this process are stabilised biomass, CO_2 and water as well as a variety of other compounds such as ammonia. During the process a quantity of heat is released which can be observed in the elevated temperatures recorded within composting systems. The parameters of oxygen utilisation, CO_2 evolution and heat release, which are the main indicators of composting activity, should all correspond.

Many different composting systems use temperature as an indicator of the conditions within the process and base the entire control strategy upon this parameter. However the role of temperature within a composting mass is very complicated. Heat is released as a result of aerobic degradation of organic material. In turn, this heat causes an increase in the temperature of the substrate. Various investigations have been made into the effect that temperature has on microbial activity suggesting that the optimum lies in the range of 55° to 60°C (Jeris and Regan, 1973; Cathcart *et al.*, 1986; 1973; Myrddin 2003). Therefore the heat released by the composting process could increase the temperature of the compost so that it is no longer within the optimal temperature range. Temperature, then, is an indicator of the energy stored within the composting material and not a direct measurement of the energy released through the composting process. If factors such as the specific heat capacity and the rate at which heat is lost to the surroundings are known then the rate at which energy is released by the composting mass can be calculated.

For the design of composting vessels to meet the relevant legislation as well as to achieve an optimised composting process it is important to know the quantity of air that would be required to replace depleted oxygen and to cool the vessel. This would allow the required air handling capability of blowers and filters to be found. However, the mass flow rate of air is not the only parameter required in order to calculate the

power of blower as the static pressure also needs to be determined (see Section 2.5 and Chapter 4).

The calculations presented in this chapter use simple relationships to investigate the release of energy by the composting process from a variety of organic wastes. Once the stoichiometry of the reactions is known and the relationship between either CO_2 evolution or oxygen utilisation and heat production is understood, this information can be fed into the design process for a variety of composting vessels.

3.2 Stoichiometric Calculation of Energy Release

Shown in Table 3-1 are representative chemical formulae for the volatile component of a variety of feedstocks (Haug, 1980). If the organic matter breaks down in the presence of oxygen to form water and CO_2 then all that will be left is the ash content of the original feedstock. The number of moles of oxygen required for the complete breakdown is given in Table 3-1 as the theoretical molar oxygen demand.

Table 3-1. Substrates, with a representative formula and the quantities of oxygen and carbon dioxide involved in their complete degradation

Waste Component	Typical chemical composition	Moles CO_2 evolved with digestion of one mole of waste	Theoretical molar oxygen demand for one mole of waste	CO_2:O_2 ratio
Carbohydrate	$C_6H_{12}O_6$	6	6	1
Protein	$C_{16}H_{24}O_5N_4$	16	16.5	0.97
Fat and Oil	$C_{50}H_{90}O_6$	50	69.5	0.72
Primary Sludge	$C_{22}H_{39}O_{10}N$	22	26	0.85
Combined sludge	$C_{10}H_{19}O_3N$	10	12.5	0.80
Refuse-total organic fraction* 1	$C_{64}H_{104}O_{37}N$	64	70.75	0.90
2	$C_{99}H_{148}O_{59}N$	99	105.75	0.94
Wood	$C_{295}H_{420}O_{186}N$	295	306.25	0.96
Grass	$C_{23}H_{38}O_{17}N$	23	23.25	0.99
Garbage	$C_{16}H_{27}O_8N$	16	18	0.89
Bacteria	$C_5H_7O_2N$	5	5	1
Fungi	$C_{10}H_{17}O_6N$	10	10.5	0.95

* Two values are quoted by Haug (1980).

The molar quantity of CO_2 that would be released from the complete breakdown of the organic content is also expressed in Table 3-1. For many of these feedstocks, the ratio of CO_2 evolved to O_2 utilised is less than one, implying that fewer moles of CO_2 are released than moles of oxygen consumed.

It is not desirable that all of the organic content be lost as this would leave only the ash content of the initial waste. One of the main benefits of the composting process is that organic material can be returned to the soil in order to assist with moisture and nutrient retention as well as the structure of the soil. It is therefore useful to consider the creation of new biomass as a product of the process as well as the release of CO_2 and moisture during the composting process. This can be represented as:

Substrate + oxygen ⟶ new biomass+carbon dioxide +water+ammonia

or

$$1\ (C_uH_vO_wN_x) + z\ O_2 \longrightarrow a(C_gH_hO_iN_j) + b\ CO_2 + c\ H_2O + d\ NH_3 \quad (3.1)$$

The weight of the new biomass formed is governed by the yield coefficient, this is used to calculate coefficient *a*. The yield coefficient, *Y*, is equal to the weight of new biomass formed divided by the weight of substrate used. The yield coefficient is dictated by the conditions within the biological system. Values for the yield coefficient of between 0.1 and 0.2 are thought to be appropriate for the composting process (Haug, 1993). The value of coefficient a can be found using Equation 3.2 for different yield coefficients.

$$a = \frac{Y \times (12u + 1v + 16w + 14x)}{(12g + 1h + 16i + 14j)} \quad (3.2)$$

By comparing coefficients for carbon, hydrogen, oxygen and nitrogen in Equation 3.1 the relationships given by Equations 3.3, 3.4, 3.5 and 3.6 can be developed. Equations 3.3, 3.4, 3.5 and 3.6 can be solved for different feedstocks by using the appropriate values from Table 3-1 for *u*, *v*, *w* and *x*. Values for either bacteria or fungi can be used to give the values of *g*, *h*, *i* and *j* which can also be found in Table 3-1. The value of a can be found at different yield coefficients.

Because Equation 3.1 is generic to suit all feedstocks no matter what their original carbon to nitrogen ratio, the coefficient d can take negative or positive values

depending on whether nitrogen was added to the original feedstock or not. For feedstocks initially low in nitrogen, coefficient d will be equal to or less than zero. For feedstocks that have excess nitrogen the value of d will be positive implying that the excess nitrogen is lost as ammonia.

$$b = u - ag \tag{3.3}$$

$$c = \frac{v - ah - 3d}{2} \tag{3.4}$$

$$d = x - aj \tag{3.5}$$

$$z = \frac{ai + 2b + c - w}{2} \tag{3.6}$$

This allows calculation of the stoichiometric quantities of oxygen, water, ammonia and CO_2 at different yield coefficients for the substrates presented in Table 3-1 for breakdown by either bacteria or fungi. The complete results for each substrate at each yield coefficient for each type of degradation can be found in Appendix A.

Because the exact composition of most organic wastes is unknown, it is not possible to use enthalpies of reaction to find the heat released during the composting process. There are, however, various methods of calculating the calorific value or stored energy of fuels and these methods can be applied to the substrate, allowing the initial stored energy within the substrate to be found. The stored energy within the new biomass can also be found at each of the different yield coefficients. The difference between the initial stored energy and the final stored energy can be regarded as the energy released during the process. Two methods for calculating the calorific value of fuels are shown in equations 3.7 and 3.8 where *C*, *H* and *O* represent the percentage by mass of carbon, hydrogen and oxygen in the feedstock. The units used can be simply converted in to S.I. units and the calorific values of each feedstock on a molar basis are expressed in Table 3-2. The calorific values presented in Table 3-2 are on a dry, ash free basis and they can also be conveniently converted to a mass basis. For the two values for refuse and the value for garbage these are 21, 20.3 and 23 MJ/kg which is comparable with the figure of 22.6 MJ/kg volatile solids presented by Patumsawad and Cliffe (2002).

The formula from Spoehr and Miller (1949) is

$$Q(cal/g) = \frac{12700[2.66(C)+7.94(H)-(O)]}{398.9} + 400 \quad (3.7)$$

The formula presented by Fowler (1967) is

$$Q(B.T.U./lb) = 145(C) + 615\left(H - \frac{1}{8}O\right) \quad (3.8)$$

This allows the change in the stored energy to be calculated for various different yield coefficients. As the quantity of oxygen utilised or CO_2 evolved has already been found for each of these yield ratios, then the energy release per mole of either gas can be calculated.

Table 3-2. Calorific values of substrates

Substrate	Typical chemical composition	Carbon content (% m/m)	Hydrogen content (% m/m)	Oxygen content (% m/m)	Calorific value by Fowler (kJ/mole substrate)	Calorific value by Spoehr and Miller (kJ/mole substrate)	Average calorific value (kJ/mole substrate)
Carbohydrate	$C_6H_{12}O_6$	40.00	6.67	53.33	2426	2843	2635
Protein	$C_{16}H_{24}O_5N_4$	54.55	6.82	22.73	8471	8865	8668
Fat + Oil	$C_{50}H_{90}O_6$	76.34	11.45	12.21	31366	30816	31091
Primary sludge	$C_{22}H_{39}O_{10}N$	55.35	8.18	33.54	11611	12146	11879
Combined sludge	$C_{10}H_{19}O_3N$	59.70	9.45	23.88	5902	5959	5930
Refuse (TOF)	$C_{64}H_{104}O_{37}N$	51.96	7.04	40.05	30167	32800	31484
Refuse (TOF)	$C_{99}H_{148}O_{59}N$	51.79	6.45	41.15	44319	49013	46666
Wood	$C_{295}H_{420}O_{186}N$	50.94	6.04	42.82	126147	141845	133996
Grass	$C_{23}H_{38}O_{17}N$	46.00	6.33	45.33	9872	11180	10526
Garbage	$C_{16}H_{27}O_8N$	53.19	7.48	35.46	8042	8558	8300
Bacteria	$C_5H_7O_2N$	53.10	6.19	28.32	2451	2629	2540
Fungi	$C_{10}H_{17}O_6N$	48.58	6.88	38.87	4758	5185	4971

3.3 Results

Calculations for both bacterial and fungal degradation of each feedstock at each yield coefficient using equations 3.1 to 3.8 have been performed. The results of these gave the quantity of heat, CO_2 and water produced as well as oxygen utilised.

Four ratios were calculated in order to analyse the results:

- CO_2 evolved to oxygen utilised,
- CO_2 evolved to water evolved,
- energy released per mole of CO_2,
- energy released per mole of oxygen.

The results for breakdown by bacteria are shown in Figures 3.1, 3.2, 3.3 and 3.4. Figures 3.5, 3.6, 3.7 and 3.8 show the data for fungal degradation of the material.

Figure 3.1 shows the CO_2:O_2 ratio for each feedstock plotted against the yield coefficient for degradation by bacteria. Only carbohydrate, represented by glucose, has a value of 1 all of the other series decrease as the yield ratio increases, showing that less carbon is released as more biomass is produced. If no new biomass is generated, then the yield coefficient will be zero, the curves would show the values given for CO_2:O_2 ratio in Table 3-1. The average value for all data points is 0.872 ± 0.023 at a 95% confidence level, with wastes such as refuse and garbage being in the middle of the group, showing that they are a conglomerate of other waste types.

Figure 3.2 shows the ratio of CO_2 evolved to water produced on a molar basis during bacterial degradation plotted against the yield coefficient. For all series except protein the values are closely grouped, the value for protein is approximately 2 to 3 times greater than for the other feedstocks, reflecting a low level of moisture production when composting proteins. The average value for this ratio is 1.21 ± 0.12. All of the series, except protein, decrease in value as the yield coefficient increases this suggests either an increase in water production or a decrease in CO_2 production at higher yield coefficients.

Presented in Figure 3.3 are the quantities of energy released per mole of CO_2 evolved for each feedstock during bacterial degradation plotted against the yield coefficient. The average value of all points is 509.1 ± 19.0 kJ/mole. The fat series has the highest values for the energy released and carbohydrate the lowest. For each individual series the quantity of heat released per mole is reasonably constant over the range of yield coefficients.

Figure 3.4 shows the energy release per mole of oxygen utilised by bacterial degradation against the yield coefficient. These values are very closely grouped together, except for the protein series which has a slightly higher value. The average energy release per mole of oxygen consumed was found to be 436.3±9.5 kJ/mole. The values for each series again remain relatively constant over the range of yield coefficients.

The results of the CO_2:O_2 ratio for fungal degradation are shown in Figure 3.5. Unlike bacterial degradation where all the values remain below 1 both carbohydrate and grass have values greater than 1 across a range of the yield coefficients. This high value of the CO_2:O_2 ratio show that for these two feedstocks more moles of CO_2 are produced than moles of oxygen used. The average value for these points is 0.892±0.024, slightly higher than the value for bacterial degradation.

The ratio of CO_2 evolved to water evolved for fungal degradation is shown in Figure 3.6. As with the bacterial degradation the protein series lies apart from all the other series. The CO_2:H_2O ratio for protein increases in value as the yield increases, whereas for all the other series it falls. This suggests low amounts of water being produced during the composting of substrates high in protein. The average value of the CO_2:H_2O ratio for all data points is 1.53±0.26.

The release of energy per mole of CO_2 evolved is shown in Figure 3.7. The energy release for each feedstock does not vary greatly with yield coefficient. However the values are again spread out and lie between 350 and 700 kJ/mole, with an average of 514.4±17.8 kJ/mole. This value of heat release per mole of CO_2 is slightly higher than the value calculated for breakdown by bacteria. As with the bacteria the highest release was given by fat and the lowest by carbohydrate.

Figure 3.8 shows the energy release per mole of oxygen consumed for degradation by fungi. As with the bacterial breakdown the protein series is the only one that lies outside of a closely packed group. These data points give an average value of 451.3±8.1 kJ/mole of oxygen consumed. This value is also slightly higher than the

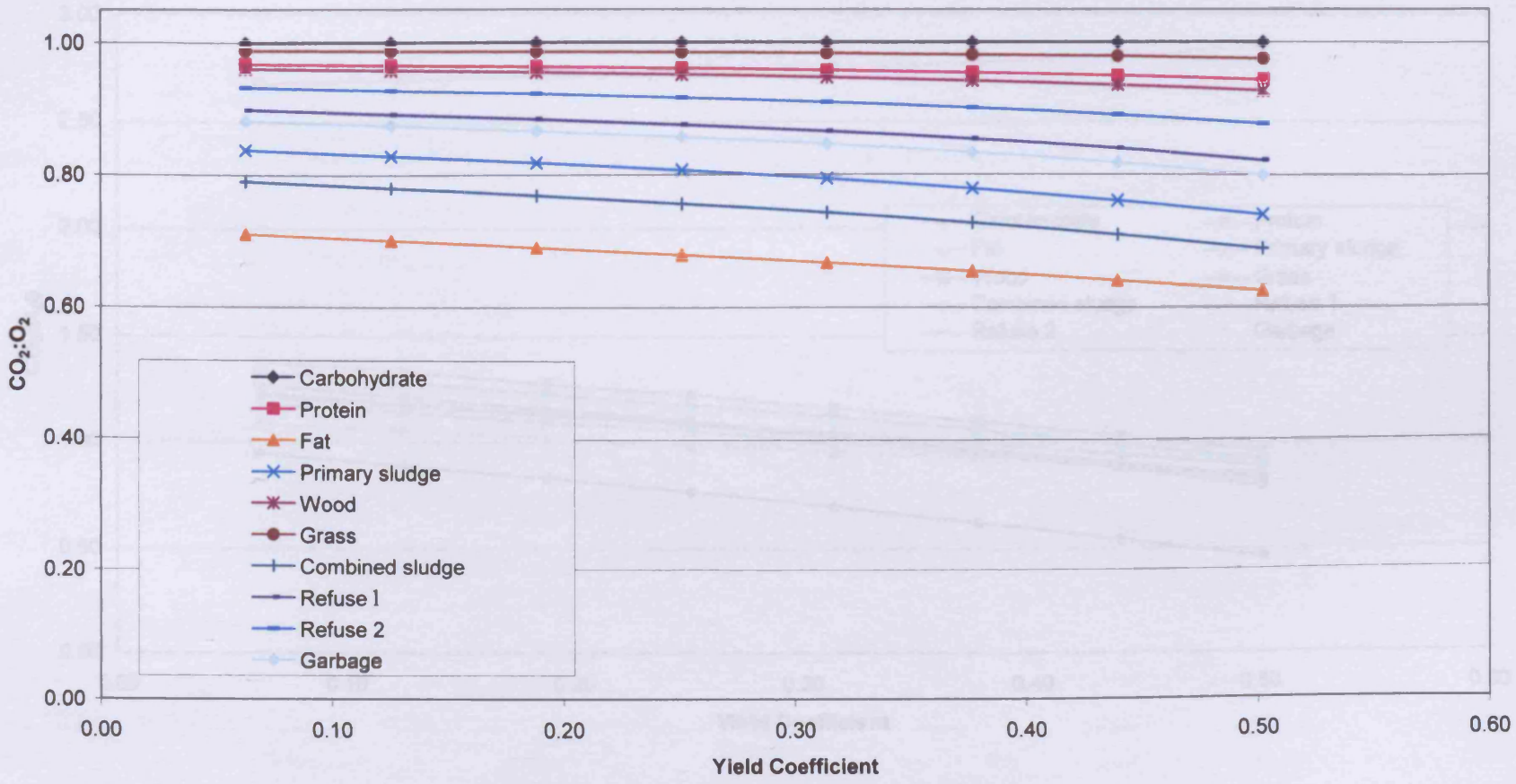

Figure 3.1. CO_2:O_2 ratio against Yield Coefficient for composting by bacteria

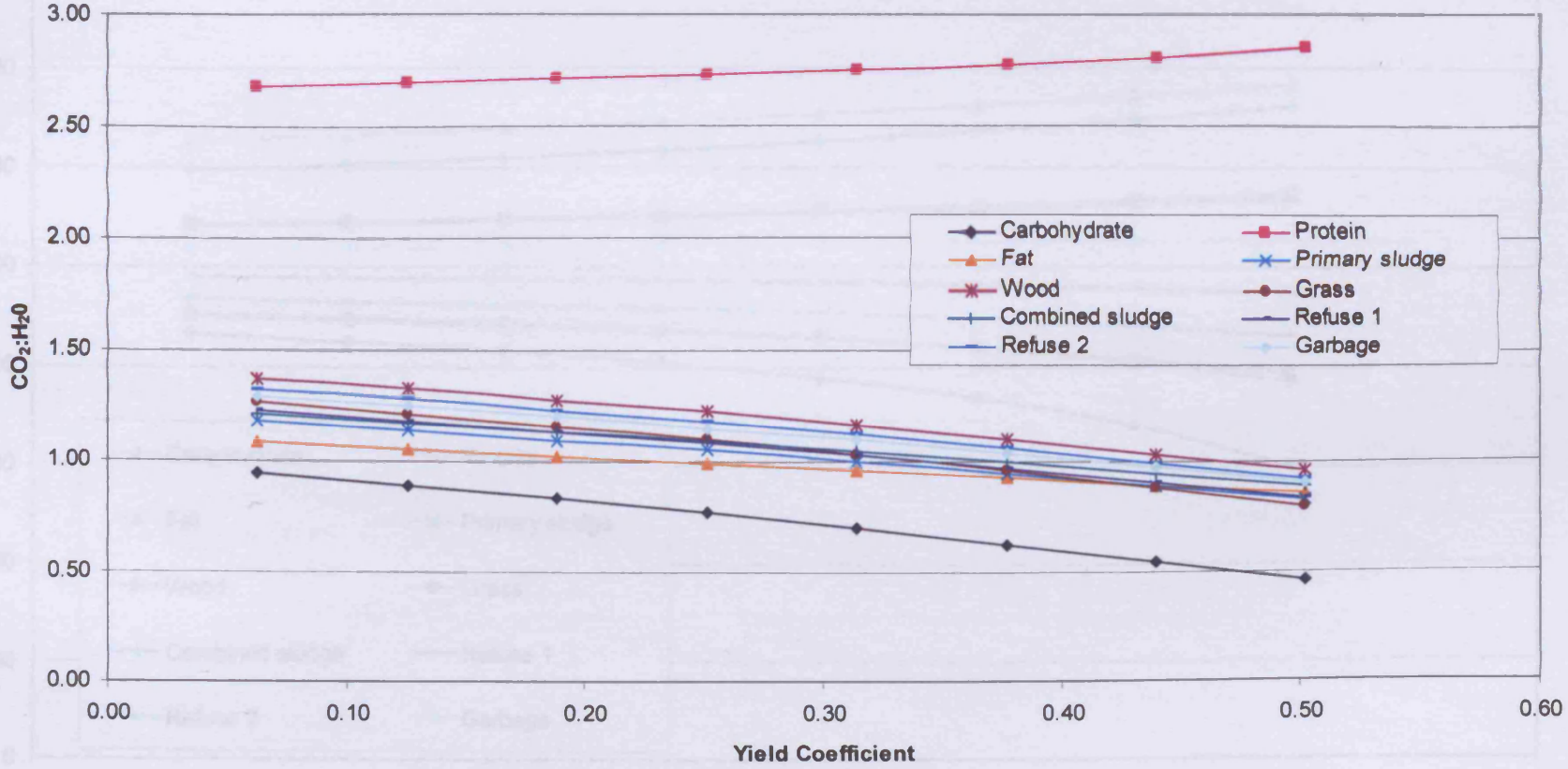

Figure 3.2. CO_2:H_2O ratio against Yield Coefficient for composting by bacteria

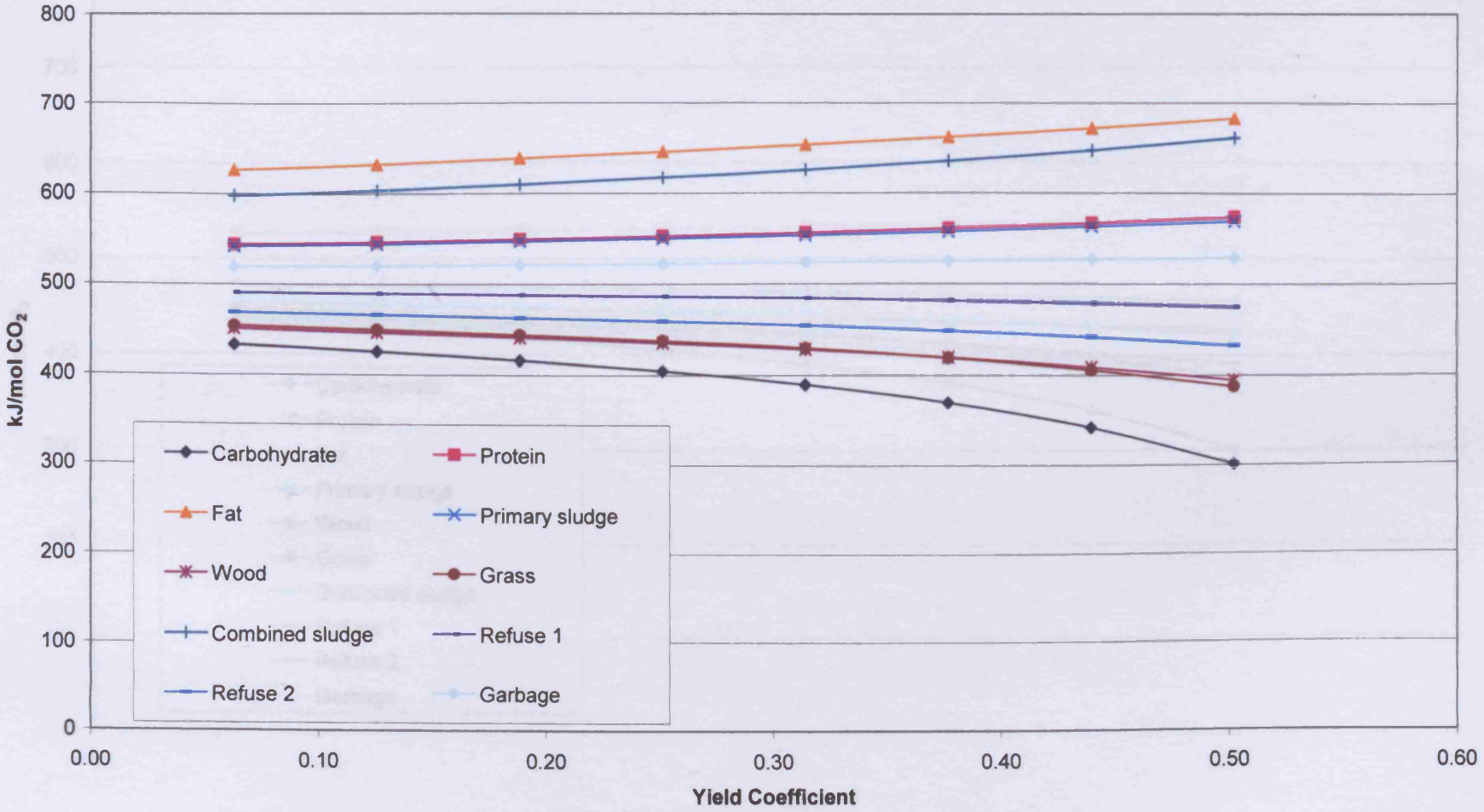

Figure 3.3. Energy release per mole of CO_2 released against Yield Coefficient for composting by bacteria

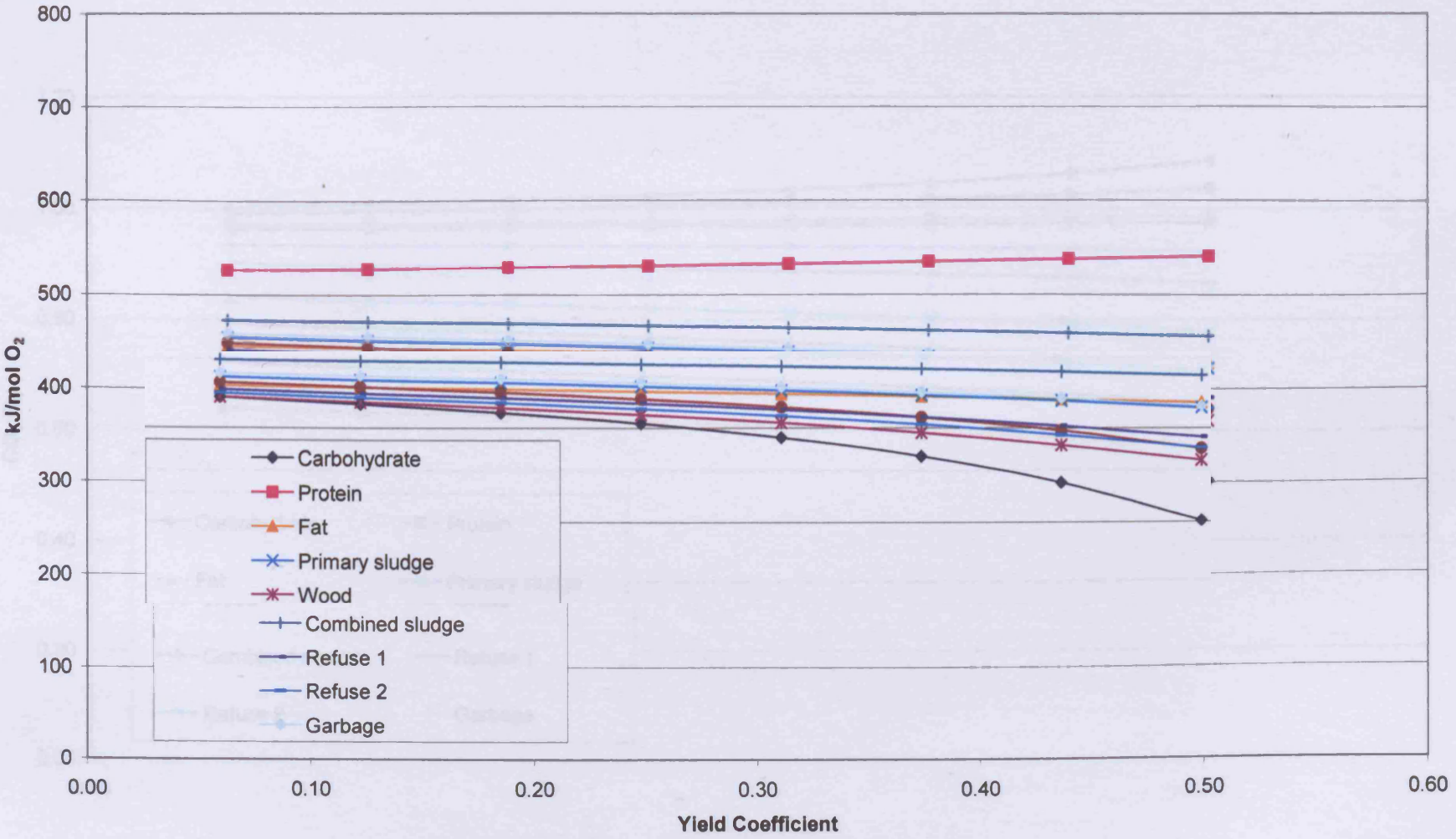

Figure 3.4. Energy release per mole of O_2 released against Yield Coefficient for composting by bacteria

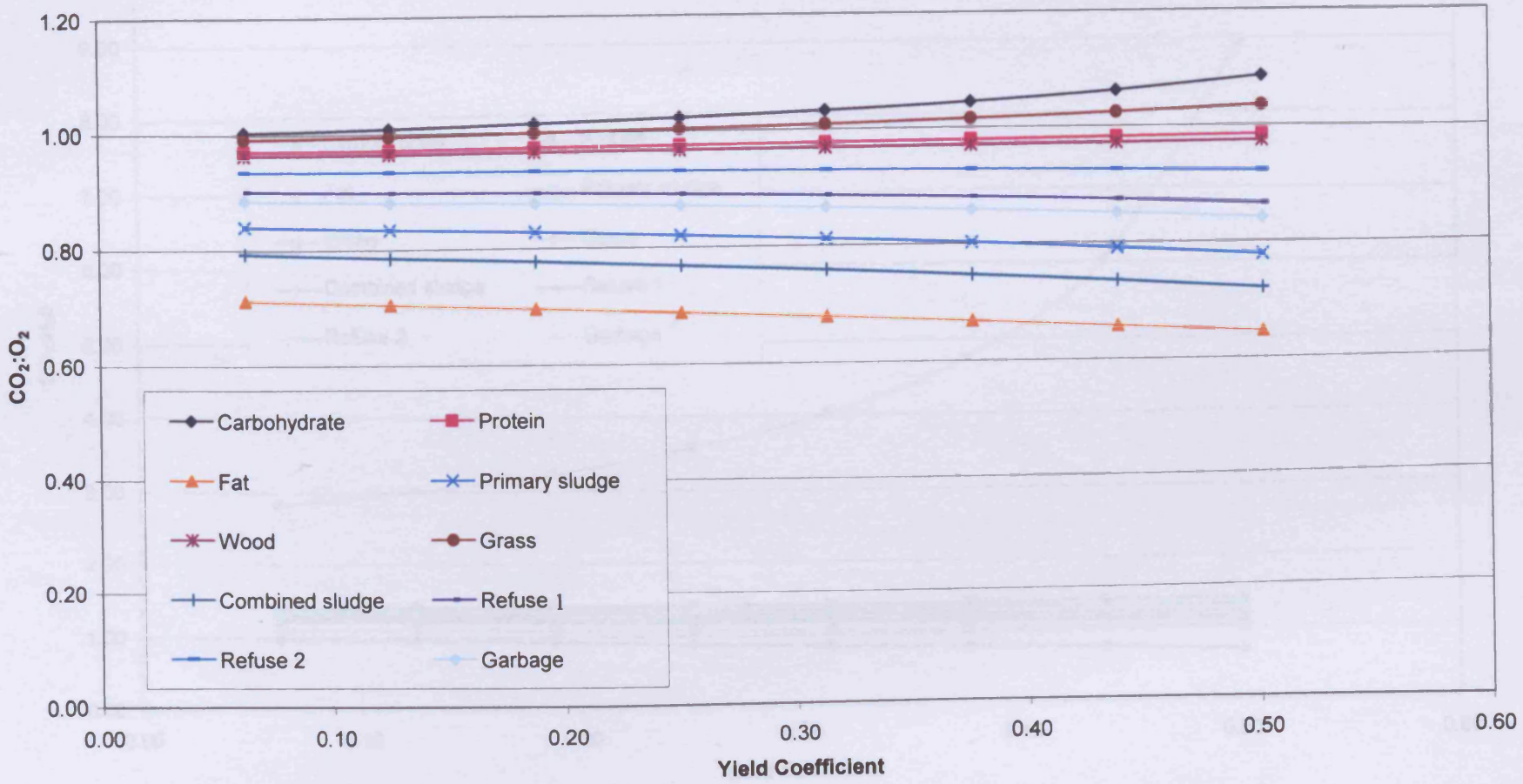

Figure 3.5. CO_2:O_2 ratio against Yield Coefficient for composting by fungi

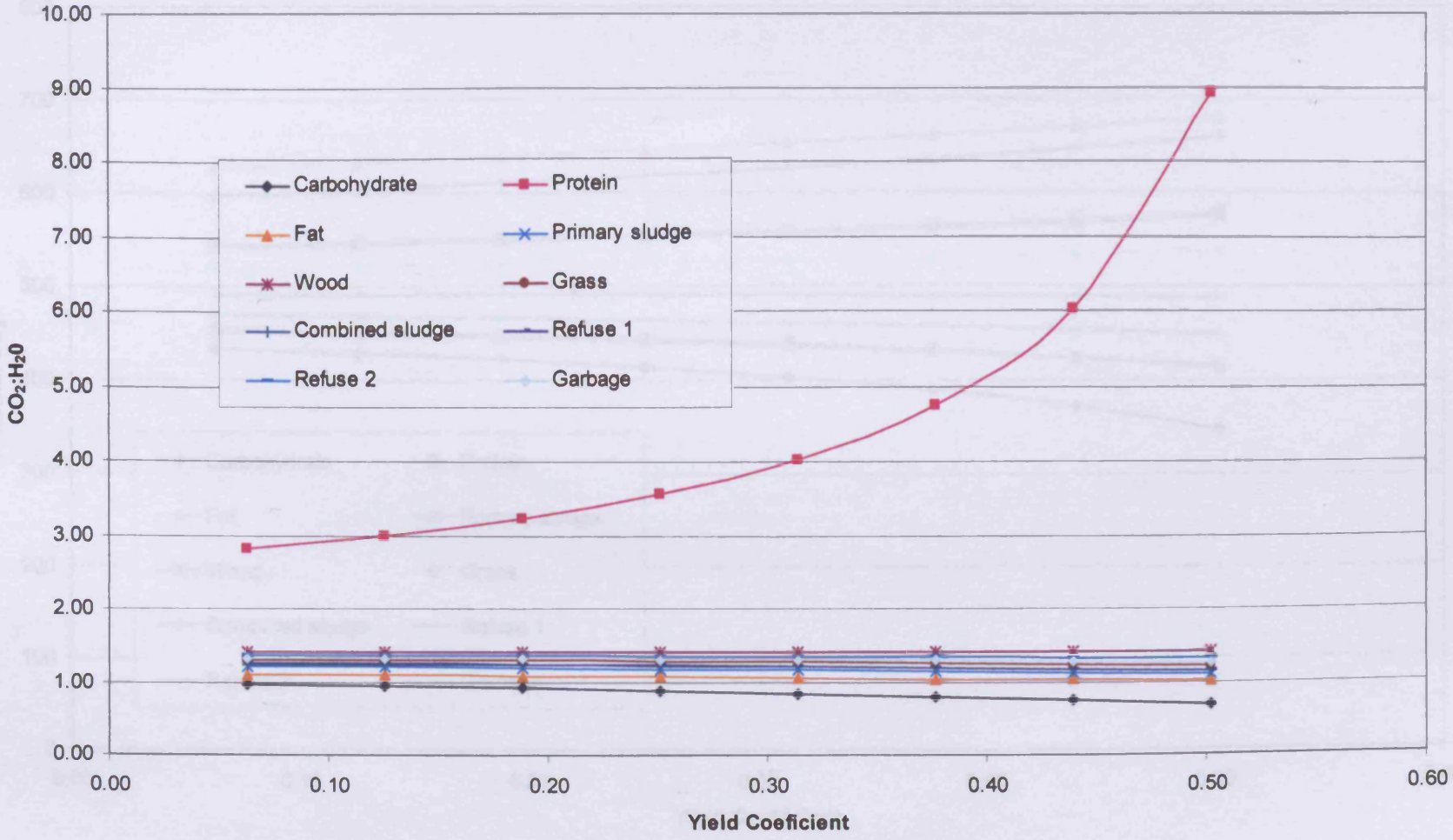

Figure 3.6. CO_2:H_2O ratio against Yield Coefficient for composting by fungi

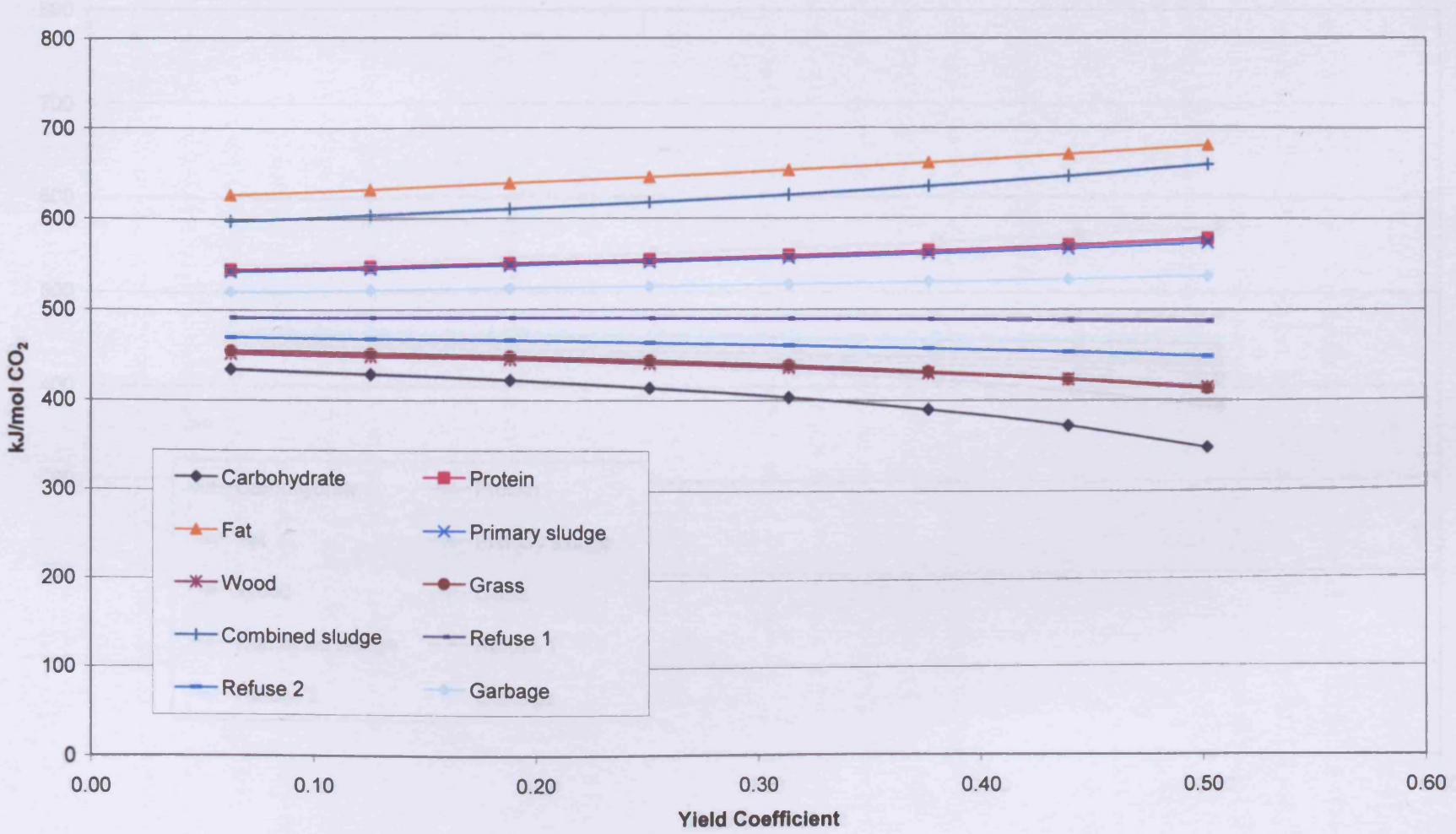

Figure 3.7. Energy release per mole of CO_2 released against Yield Coefficient for composting by fungi

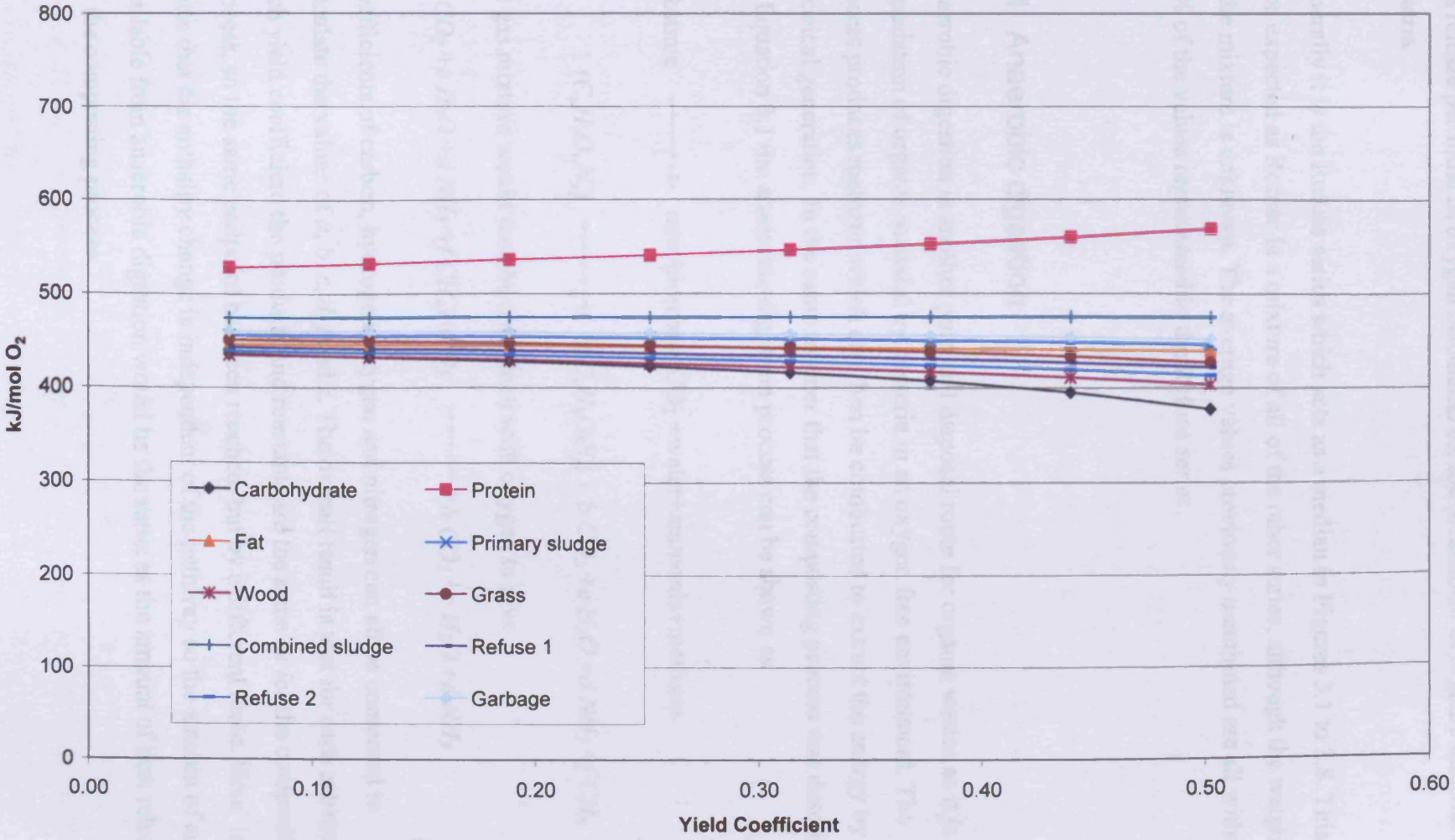

Figure 3.8. Energy release per mole of O_2 released against Yield Coefficient for composting by fungi

heat release per mole of oxygen calculated for the breakdown of organic material by bacteria.

Generally it is the Refuse series which acts as a median in Figures 3.1 to 3.8. This is to be expected as Refuse is a mixture of all of the other series, although the weighting of the mixture is unknown. The average values previously mentioned are all within 10% of the values represented in the Refuse series.

3.4 Anaerobic digestion

Anaerobic digestion is another potential disposal route for organic wastes as it is the degradation of organic material by bacteria in an oxygen free environment. The process produces methane which can then be combusted to extract the energy by electrical generation. In the same manner that the composting process was described by Equation 3.1 the anaerobic digestion process can be shown as

Substrate $\longrightarrow$ new biomass+CO_2 +water+ammonia+methane

Or

$$1\ (C_uH_vO_wN_x) \longrightarrow a(C_gH_hO_iN_j) + b\ CO_2 + c\ H_2O + d\ NH_3 + f\ CH_4 \tag{3.9}$$

the gas mixture would then be combined with oxygen to give

$$(b\ CO_2 + c\ H_2O + d\ NH_3 + f\ CH_4) + z\ O_2 \longrightarrow b\ CO_2 + c\ H_2O + d\ NH_3 \tag{3.10}$$

Coefficients of carbon, hydrogen, oxygen and nitrogen can all be compared to calculate the values of *a*, *b*, *c*, *d*, *f* and *z*. The overall result is that for each substrate at each yield coefficient the products and reactants are the same as for the composting process, so the same endpoint has been reached, but by a different route. Hess' law states that the enthalpy change is independent of the pathway so the amount of energy available from anaerobic digestion would be the same as the amount of heat released by the composting process.

3.5 Discussion

The data presented in Figures 3.1 to 3.8 give a large quantity of information about the composting process. Figures 3.1 and 3.5 show the molar ratio of CO_2 evolved to oxygen used for bacteria and fungi respectively. For bacteria this ratio is lower than for fungi, meaning that fungi release more CO_2 per mole of oxygen utilised than bacteria. Table 3-2 lists the percentages of carbon, hydrogen and oxygen present in the make up of each cell type. Bacterial cell is 53.10% by mass carbon whereas fungi is 48.58% carbon by mass. If a yield coefficient of 0.2 is considered then 200 grams of microbial biomass needs to be created for every kilogram of waste. If the waste underwent decomposition by bacteria then the 200 grams of biomass would contain 106.2 grams of carbon whilst if fungal degradation occurred only 97.14 grams of carbon would be contained in the new biomass. The difference between these two values of 9.04 grams would be lost as CO_2. This loss is reflected in the higher average CO_2:O_2 ratios for fungal degradation.

The highest CO_2:O_2 ratio is given by carbohydrate followed by grass, protein, wood, refuse 2, refuse 1, garbage, primary sludge, combined sludge and finally fat. The order is the same for both bacterial and fungal degradation. If the ratio of hydrogen atoms to oxygen atoms in the feedstock is calculated the order is very similar: carbohydrate, grass, wood, refuse 2, refuse 1, garbage, primary sludge, protein, combined sludge and fat. Only the protein series changes position, this may be due to the extra hydrogen required to react with the relatively high nitrogen content of the protein.

If the CO_2:O_2 ratio for all feedstocks were 1 then there would be no difference between the heat released per mole of either CO_2 evolved or oxygen utilised, meaning there would be no differences between Figures 3.3 and 3.4 or 3.7 and 3.8. However this is not the case and the CO_2:O_2 ratio is rarely 1 even in the theoretical values for complete breakdown shown in Table 3-1. The CO_2:O_2 ratio also varies with yield coefficient. For each substrate at each yield coefficient for each type of degradation the heat released was calculated. By dividing that heat release by the molar quantity of CO_2 evolved or oxygen utilised the heat release per mole of gas was found. Carbohydrate experiencing bacterial degradation does have a CO_2:O_2 ratio of 1 and

the energy released per mole of CO_2 is the same as that released per mole of oxygen used, this is shown in Figures 3.3 and 3.4. The fat series has the lowest CO_2:O_2 ratio and although it is in with the main group in Figure 3.4 the low quantity of CO_2 gives it the highest energy release per mole of CO_2 in Figure 3.3.

With fungal degradation the ratio of CO_2:O_2 can be greater than 1 as shown by both the carbohydrate and grass series. This causes the energy release per mole of CO_2 evolved to be lower than the energy release per mole of oxygen utilised, as shown in Figures 3.7 and 3.8.

MacGregor *et al.* (1981) suggest that the total combined volume of CO_2 and oxygen is constant and equal to 20.78% of air by volume, the implication of this is that the for each mole of oxygen utilised one mole of CO_2 is evolved. The majority of results presented in Figures 3.1 and 3.5 disagree with this and only carbohydrate gives a result of one for bacterial degradation, carbohydrate and grass give results of one or greater for fungal degradation whilst in all other cases the ratio is less than 1. Macgregor *et al.* (1981) only recommended using this relationship for CO_2 concentrations up to 6.5%. Given the limited range and the equipment that was used this may be an acceptable approximation. Weppen (2001) observed a CO_2:O_2 ratio of less than one. A value of 0.870 for a compost amended with fat was observed whilst a mixture of organic garbage and wheat straw had a CO_2:O_2 ratio of 0.960. This agrees with the low values of the CO_2:O_2 ratio for fat shown in Figures 3.1 and 3.5. Both garbage and straw have high levels of carbohydrates and therefore produce high values for this ratio. Cronje *et al.* (2004) also showed respiration quotients (CO_2:O_2 ratios) of between 0.5 and 1 for the composting of pig manure.

Figure 3.2 and 3.6 present the molar ratio of CO_2 evolved to water evolved. Most of the series are grouped closely at a value of around 1 for both bacterial and fungal degradation with averages of 1.21 and 1.53 respectively. The protein series has a much greater value than that of the other substrates. This is likely to be due to the relatively high amount of nitrogen present in the makeup of protein compared to the other feedstocks. Equation 3.1 shows that excess nitrogen is lost as ammonia. This will cause a lot of the hydrogen to be utilised resulting in less water being produced and this will in turn cause the molar ratio of CO_2 to water to be higher.

Figures 3.3 and 3.4 show the quantity of heat released divided by the number of moles of CO_2 evolved and the quantity of heat released divided by the number of moles of oxygen consumed for bacterial degradation. Figures 3.7 and 3.8 show the energy release for fungal degradation, as with the bacterial degradation, the differences between the two figures are due to the ratio of CO_2 evolved to oxygen consumed. The average values for heat release are shown in Table 3-3.

The results in Table 3-3 show a slightly greater release of heat for fungal degradation than for bacterial degradation. The results from Table 3-3 are shown in comparison to measured values from Haug (1993), Cooney *et al.* (1969), Tancho *et al.* (1995), Sparling (1983) and Weppen (2001) in Figure 3.9. The measured values are shown in Figure 3.9 with an average and an upper and lower boundary. The calculated values of energy release lie within the ranges that have been measured experimentally, indicating a good level of accuracy in these theoretical results as well as validating this method of assessing energy release. Weppen (2001) did not give an overall average for the heat released per mole of CO_2 evolved, however in the sample of data given for five of the test runs the ratio of CO_2:O_2 is in the range 0.870 to 0.960. Applying this to the energy release per mole of O_2 gives a range of 470.8 to 519.5 kJ per mole of CO_2.

Table 3-3. Average energy releases for microbial degradation

Type of Microbe	Heat release per mole of oxygen consumed	Heat release per mole of CO_2 evolved
Bacteria	436±9.5 kJ/mole	509.1±19.0 kJ/mole
Fungi	451±8.1 kJ/mole	514.4±17.8 kJ/mole

The estimates for energy release are higher than the enthalpy of formation of CO_2 of 393.5 kJ/mole. This is because it is not simply the enthalpy of formation of CO_2 that is being considered, for each mole of CO_2 evolved there is approximately 1 mole of water created, as shown in Figures 3.2 and 3.6. The enthalpy of formation of water is 241.8 kJ/mole in gaseous form or 285.8 kJ/mole if it has condensed. There is then an unknown quantity of energy that is needed to form the new biomass. It is because of

this unknown quantity of energy that an approach using calorific values was employed.

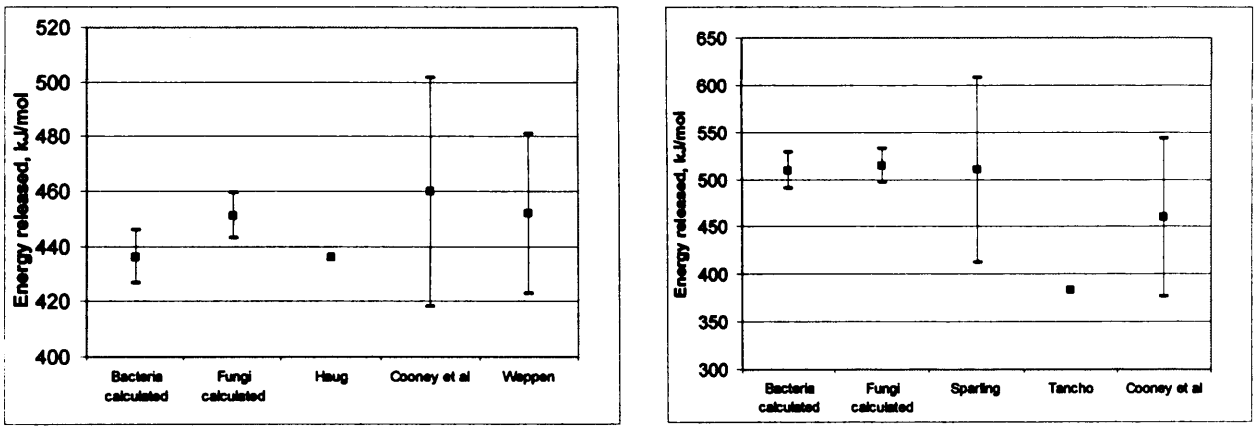

a) oxygen consumption b) carbon dioxide evolution

Figure 3.9. Comparison of calculated energy release with measured values

3.6 Design implications

3.6.1 Heat Release

Relating the quantity of heat released to the quantity of CO_2 evolved allows the calculation of the quantities of air required for cooling as well as a structured approach to the design of composters. As discussed in Chapter 1 the Animal By-Products Regulations (2003) require that for in-vessel composting the entire contents reach either 60°C or 70°C depending on the treatment regime chosen. These are high temperatures and involve a large increase above the ambient temperatures in the UK as well as being higher than the suggested optimum temperatures for composting (Waksman *et al.*, 1939; Wiley, 1956; Wiley, 1957; Rothbaum, 1961; Jeris and Regan, 1973; Suler and Finstein, 1977; MacGregor *et al.*, 1981, Cathcart *et al.*, 1986). For the compost to reach these elevated temperatures a large quantity of heat is required and at these elevated temperatures the compost will be loosing heat at a rate that is proportional to its temperature difference compared to its surroundings.

Mears *et al.* (1975) showed that the specific heat capacity is proportional to the moisture content of the compost and is equal to,

$$C_p(\text{kJ kg}^{-1}\text{K}^{-1})=4.184(0.1551+0.00813M) \tag{3.11}$$

where M is the moisture content of the compost on a wet basis expressed as a mass percentage. As the compost heats up it needs to store the heat that is released whilst losses due to conduction and convection from the vessel, mass transfer and evaporation from airflow need to be minimised in order to achieve the treatment temperatures.

As previously shown the heat generated by the composting process and the CO_2 evolution are closely linked. The respiration rate, measured in grams of CO_2 per kilogram of volatile solids per day, can be converted to a rate of heat output of the compost. It is therefore important to know the density, moisture content and volatile solids content of the material to be composted to allow the weight of volatile solids to be calculated. Much of the green waste arriving at the CERT composting facility (described in Section 5.1) has a moisture content of approximately 50% (w.b.) and a volatile solids content of 60% (d.b.). Once shredded the density is approximately 370 kg m^{-3}. The heat released by the composting process, Q_{gen}, per cubic metre is,

$$Q_{gen} = \frac{509.1 \times F \times \rho_{compost} \times (1-MC) \times VS}{44 \times 86400} \tag{3.12}$$

where 509.1 kJ is the heat released per mole of CO_2,
F is the composting rate in gCO_2 kgVS^{-1} day^{-1},
$\rho_{compost}$ is the bulk density of the compost in kg m^{-3},
MC is the moisture content on a wet basis as a proportion,
VS is the proportion of volatile solids on a dry basis,
44 is the molar mass of CO_2 and
86400 is the number of seconds in a day.

The heat loss from the vessel can be calculated using empirical equations for turbulent convection from vertical and horizontal surfaces (Holman, 1976). The heat released can be quantified using the above relationship between heat and CO_2 release. Assuming that the compost stays at a constant temperature then the heat released by composting can be compared with the heat lost from the vessel allowing a minimum composting rate to be found. Figure 3.10 shows a schematic of a composting vessel where the width, length and height of the vessel are represented by k, l and m, the dimension m_l represents the fill height of the compost inside the vessel.
The heat that is released by the vessel through turbulent convection, Q_{con}, is

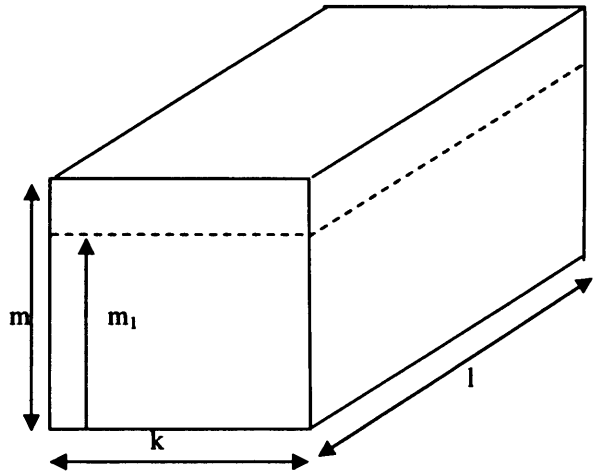

Figure 3.10. Schematic of containerised composting reactor, dashed line represents compost fill height

dependant upon the exposed surface area and the difference in temperature between the surface and the surrounding air, ΔT,

$$Q_{con} = \Delta T\left(\left[m\left((2k+2l)\times 0.95\Delta T^{\frac{1}{3}}\right)\right]+\left[kl\times 1.43\Delta T^{\frac{1}{3}}\right]+\left[kl\times 0.61\left(\frac{\Delta T}{k^2}\right)^{\frac{1}{5}}\right]\right)$$

(3.13 after Holman, 1976)

For equation 3.13 the heat transfer coefficient is a function of the temperature difference, T, and a principle dimension. Assuming that the vessel is at a steady state of either 60 or 70°C depending upon the chosen treatment regime, there will be no change in internal energy or stored heat. The equations 3.12 and 3.13 can be solved for various different shapes at different temperatures to find a rate at which composting needs to occur in order to produce enough heat to meet the Animal By-Products Regulations (2003).

Three different vessel designs are considered: i) the vessel used by Myrddin (2003) to investigate the composting of household waste, ii) the vessel designed by Wormtech which is used in trials detailed in Chapter 6 of this thesis and iii) a cuboid vessel similar to many available of dimensions 3 m wide 3 m high and 5 m long, the total compost fill height being 2.4 m.

The vessel used by Myrddin (2003) to investigate the composting of household wastes was a cylinder 3 metres high with a 1 metre diameter, because of the vessel's shape Equation 3.13 needs to be modified. For a cylinder of height m and radius r Equation 3.13 modifies to Equation 3.14 allowing Figure 3.11 to be generated.

$$Q_{con} = \Delta T\left(\left[2\pi rm \times 0.95\Delta T^{\frac{1}{3}}\right] + \left[\pi r^2 \times 1.43\Delta T^{\frac{1}{3}}\right] + \left[\pi r^r \times 0.61\left(\frac{\Delta T}{r^2}\right)^{\frac{1}{5}}\right]\right)$$

(3.14 after Holman, 1978)

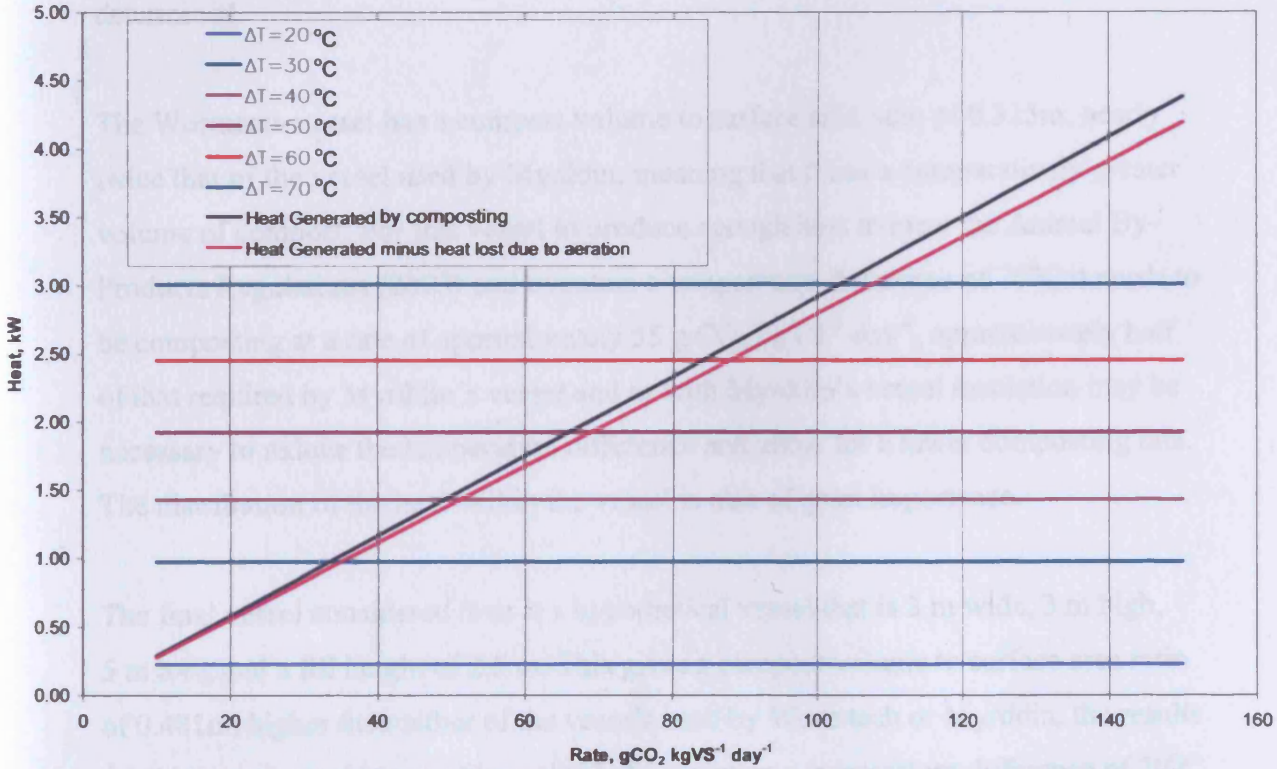

Figure 3.11. Heat lost and heat generated as a function of temperature for the vessel used by Myrddin (2003)

In winter conditions the external air temperature may be 0°C or less, meaning that the temperature difference to meet the Animal By-Products Order (2003) would be at

least 60°C or 70°C, requiring a composting rate of approximately 110 gCO_2kgVS^{-1} day^{-1}, which is exceptionally high. The maximum rate achieved by Myrddin (2003) using this vessel was approximately 60 $gCO_2kgVS^{-1}day^{-1}$. It would seem that without insulation or addition of extra heat this vessel would have little chance of meeting the Animal By-Products Regulations. The rate achieved of 60 $gCO_2kgVS^{-1}day^{-1}$ would be suitable for a temperature difference of approximately 45°C between the vessel and the ambient air and would probably meet the Animal By-Products Regulations in summer with warmer ambient temperatures or could be achieved in winter through use of insulation to lower the rate of heat loss through the walls giving a lower outer wall temperature. This vessel has a compost volume to surface area ratio of 0.179m.

The second vessel is that designed by Wormtech, drawings of which are shown in Appendix D. It is a containerised system 2.25 m wide, 2.37 m high, 5.8 m long with a fill height of approximately 1.6 m. Using the same assumptions for the fill material as before Figure 3.12 can be created, allowing the "break even" composting rate to be determined.

The Wormtech vessel has a compost volume to surface area ratio of 0.325m, nearly twice that of the vessel used by Myrddin, meaning that it has a comparatively greater volume of compost. For this vessel to produce enough heat to meet the Animal By-Products Regulations (2003) and maintain a temperature difference of 70°C it needs to be composting at a rate of approximately 55 g CO_2 $kgVS^{-1}$ day^{-1}, approximately half of that required by Myrddin's vessel and as with Myrddin's vessel insulation may be necessary to reduce the temperature difference and allow for a lower composting rate. The distribution of the heat within the vessel is also of great importance.

The final vessel considered here is a hypothetical vessel that is 3 m wide, 3 m high, 5 m long and a fill height of 2.5 m. This gives a compost volume to surface area ratio of 0.481m, higher than either of the vessels used by Wormtech or Myrddin, the results for this vessel are shown in Figure 3.13. To maintain a temperature difference of 70°C the hypothetical vessel needs to achieve a composting rate of approximately 38 g CO_2 $kgVS^{-1}$ day^{-1} less than for either of the previous two vessels.

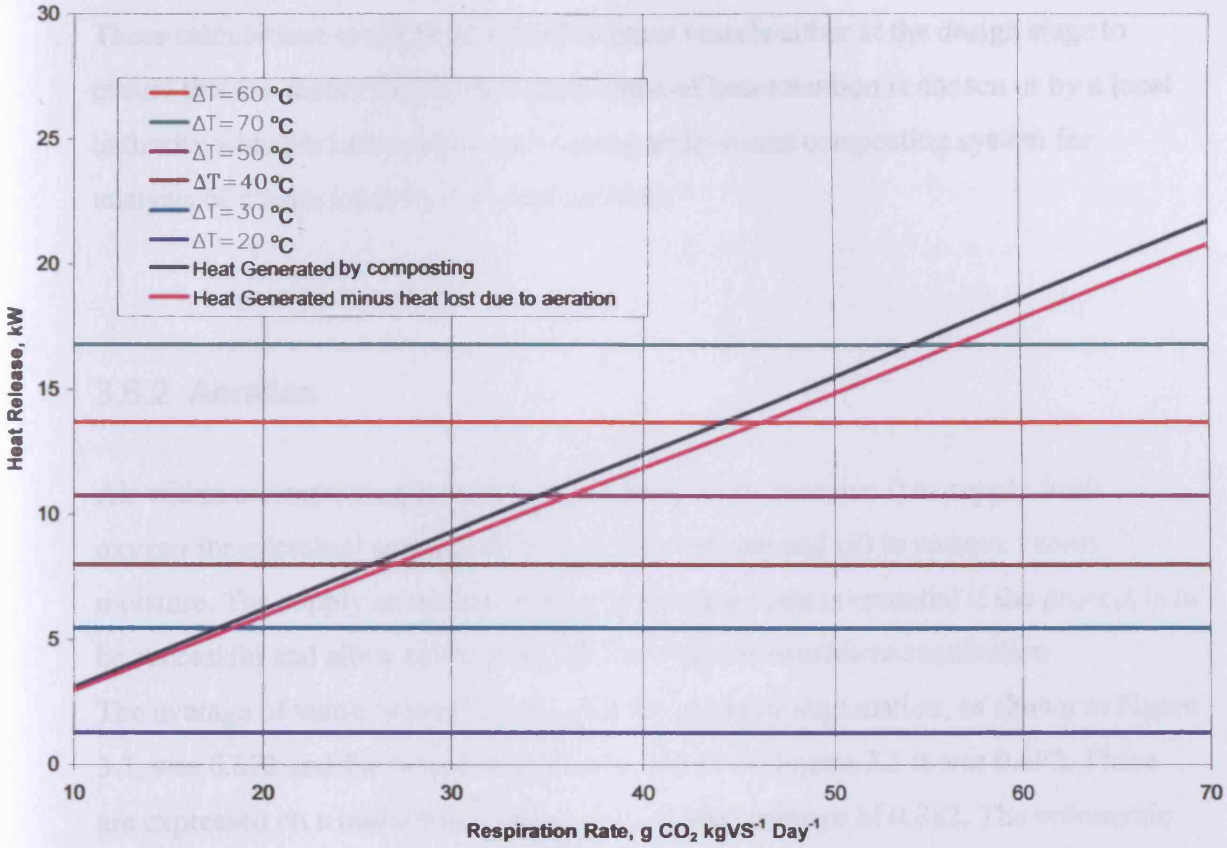

Figure 3.12. Heat lost and heat generated as a function of temperature for the Wormtech vessel

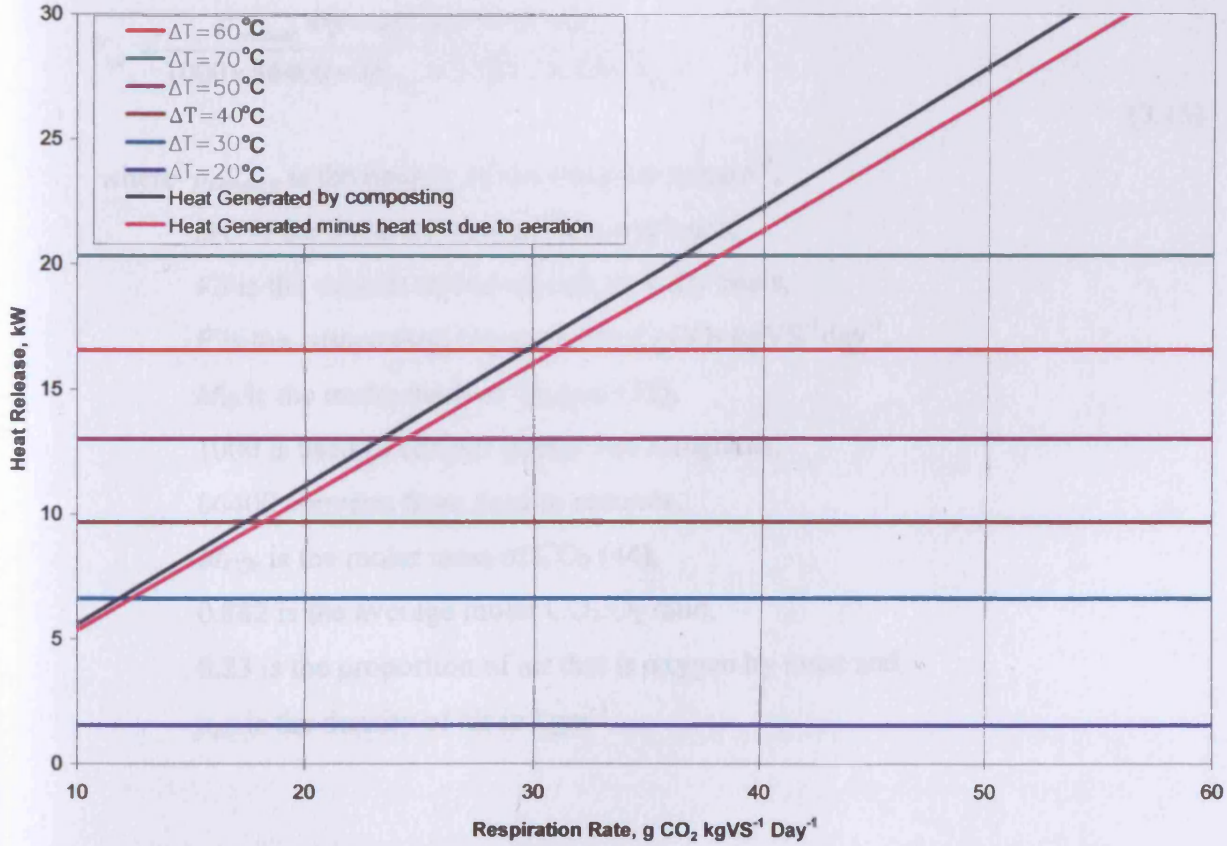

Figure 3.13. Heat lost and heat generated as a function of temperature for the 45 cubic metre vessel

These calculations could be extended to other vessels either at the design stage to ensure that the most efficient design in terms of heat retention is chosen or by a local authority which is interested in purchasing an in-vessel composting system for analysis of claims made by the manufacturer.

3.6.2 Aeration

Air within a composting system is required for three reasons: i) to supply fresh oxygen for microbial activity, ii) to cool the compost and iii) to remove excess moisture. The supply of oxygen to the composting mass is essential if the process is to be successful and allow self-heating of the compost to achieve sanitisation.
The average of value of the CO_2:O_2 ratio for bacterial degradation, as shown in Figure 3.1, was 0.872 and for fungal degradation, shown in Figure 3.5 it was 0.892. These are expressed on a molar basis and give an overall average of 0.882. The volumetric flow rate of air in cubic metres of air per cubic metre of compost per second to provide a stoichiometric supply of oxygen can be found using equation 3.15.

$$V_{air} = \frac{\rho_{compost} \times (1 - MC) \times VS \times F \times M_{O_2}}{1000 \times 86400 \times M_{CO_2} \times 0.882 \times 0.23 \times \rho_{air}} \qquad (3.15)$$

where $\rho_{compost}$ is the density of the compost in kgm^{-3},
MC is the moisture content on a wet basis,
VS is the volatile solids content on a dry basis,
F is the composting rate in units of $gCO_2\ kgVS^{-1}day^{-1}$,
M_{O_2} is the molar mass of oxygen (32),
1000 is used to convert grams into kilograms,
86400 converts from days to seconds,
M_{CO_2} is the molar mass of CO_2 (44),
0.882 is the average molar CO_2:O_2 ratio,
0.23 is the proportion of air that is oxygen by mass and
ρ_{air} is the density of air in kgm^{-3}.

It is important to note that Equation 3.15 gives a stoichiometric value for the aeration and thus assumes that all of the oxygen in the supply air is used by the composting process. However, it is recommended to have an oxygen content of 10% in the exhaust air, as oxygen makes up approximately 21% of air by volume so the value calculated using Equation 3.15 and shown in Figure 3.14 would need to be doubled in order to meet this. Flow rates for other concentrations of oxygen in the exhaust air can be calculated in a similar manner.

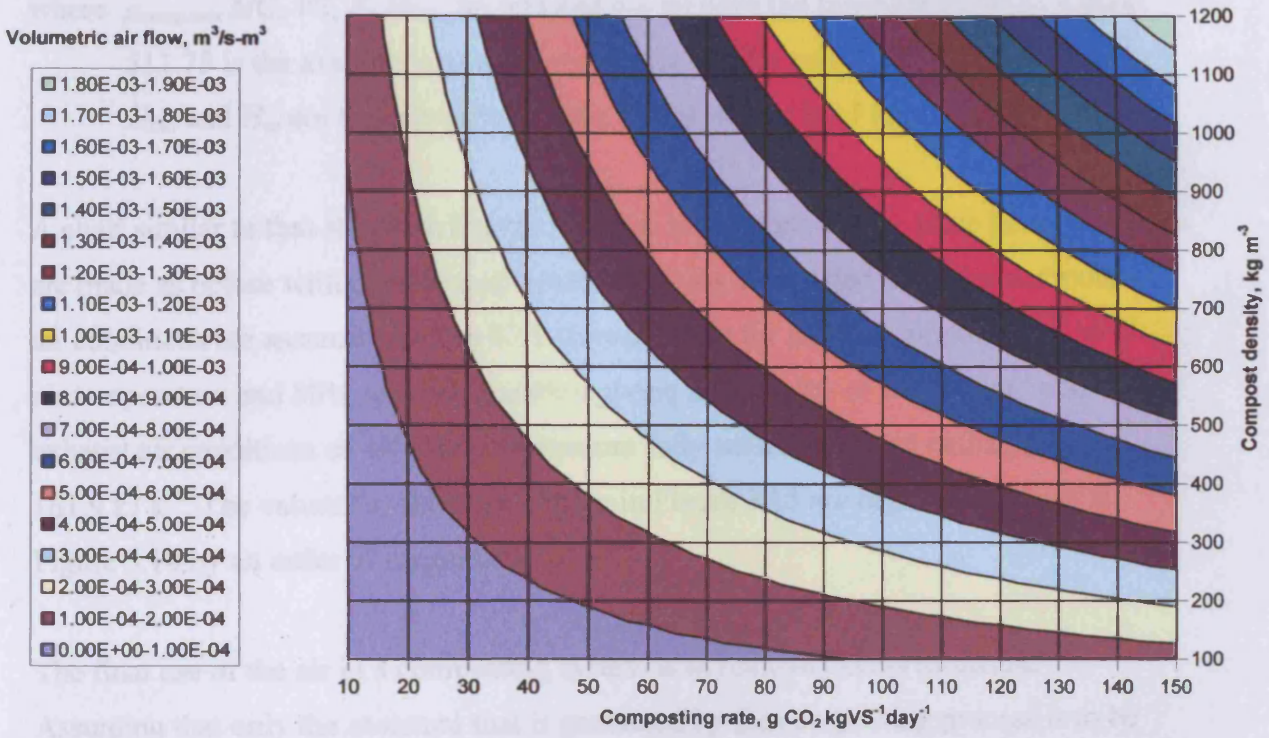

Figure 3.14. Aeration requirements per cubic metre of compost for oxygen supply as a function of composting rate and compost density

If the same assumptions are made about the composting material as before, that it has a 50% moisture content on a wet basis and a 60% volatile solids content on a dry basis and at an air temperature of 23°C, Equation 3.15 is a function of the compost density and the composting rate. Figure 3.14 shows a range of compost densities and composting rates and can be used to determine the stoichiometric air supply for compost.

With the introduction of the Animal By-Products Regulations (2003) the need to remove excess heat from compost is somewhat compromised. Although optimum composting temperatures have been reported by many, these are often below the

temperatures required to meet the required levels of sanitisation. If further stabilisation or maturing of the compost were being carried out under controlled conditions then the quantity of air that need to be supplied to keep one cubic metre of compost at a constant temperature could be calculated by,

$$V_{air} = \frac{\rho_{compost} \times (1 - MC) \times VS \times F \times 511.75}{M_{CO_2} \times 86400 \times (H_{out} - H_{in}) \rho_{air}} \tag{3.16}$$

where $\rho_{compost}$, MC, VS, F, M_{co2}, 86,400 and ρ_{air} all have the same meanings as before,

511.75 is the average heat output per mole of CO_2 and

H_{out} and H_{in} are the exhaust and inlet air enthalpies in kJ kg^{-1}.

A chart similar to that shown in Figure 3.14 can be generated if the same assumptions are made as before with regards to the material being composted and inlet and exhaust air conditions are assumed. Figure 3.15 shows a chart for inlet air conditions of 10°C air temperature and 80% relative humidity giving an enthalpy of 25.3 kJ kg^{-1} and exhaust air conditions of 40°C air temperature fully saturated air, an enthalpy of 161.9 kJ k^{-1}. The values for flow rate shown in Figure 3.15 are higher than those in Figure 3.14 by an order of magnitude.

The final use of the air in a composting system is to remove excess moisture. Assuming that only the moisture that is generated by the composting process is to be removed the volumetric airflow per cubic metre of compost can be calculated by using the average CO_2 to water ratio from Figures 3.2 and 3.6.

$$V_{air} = \frac{\rho_{compost} \times (1 - MC) \times VS \times F \times M_{H_2O}}{1000 \times 86400 \times M_{CO_2} \times 1.37 \times (HR_{out} - HR_{in}) \times \rho_{air}} \tag{3.17}$$

where $\rho_{compost}$, MC, VS, F, 1000, 86400, M_{CO2}, and ρ_{air} represent the same uses as previously described,

M_{H2O} is the molar mass of water (18),

1.37 is the average CO_2:H_2O ratio and

HR_{out} and HR_{in} are the exhaust and inlet air humidity ratios in kilograms of water per kilogram of dry air.

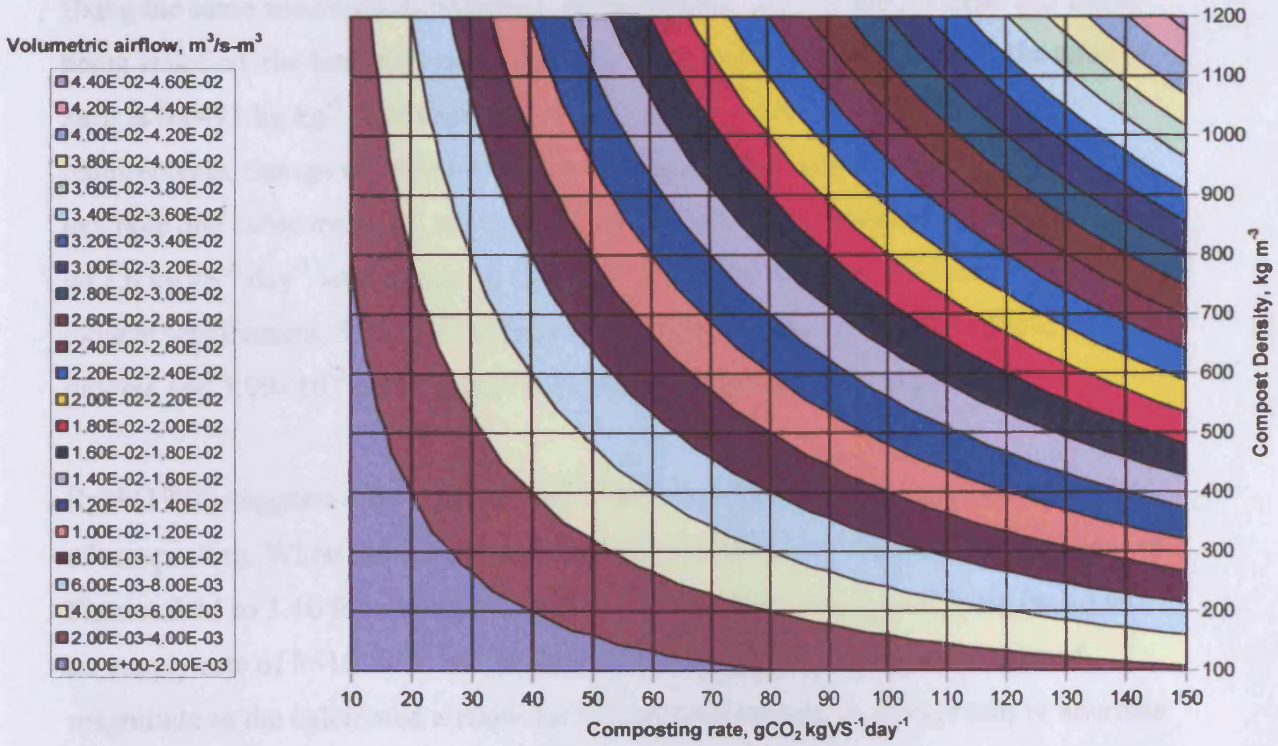

Figure 3.15. Aeration requirements per cubic metre of compost for removal of heat as a function of composting rate and compost density

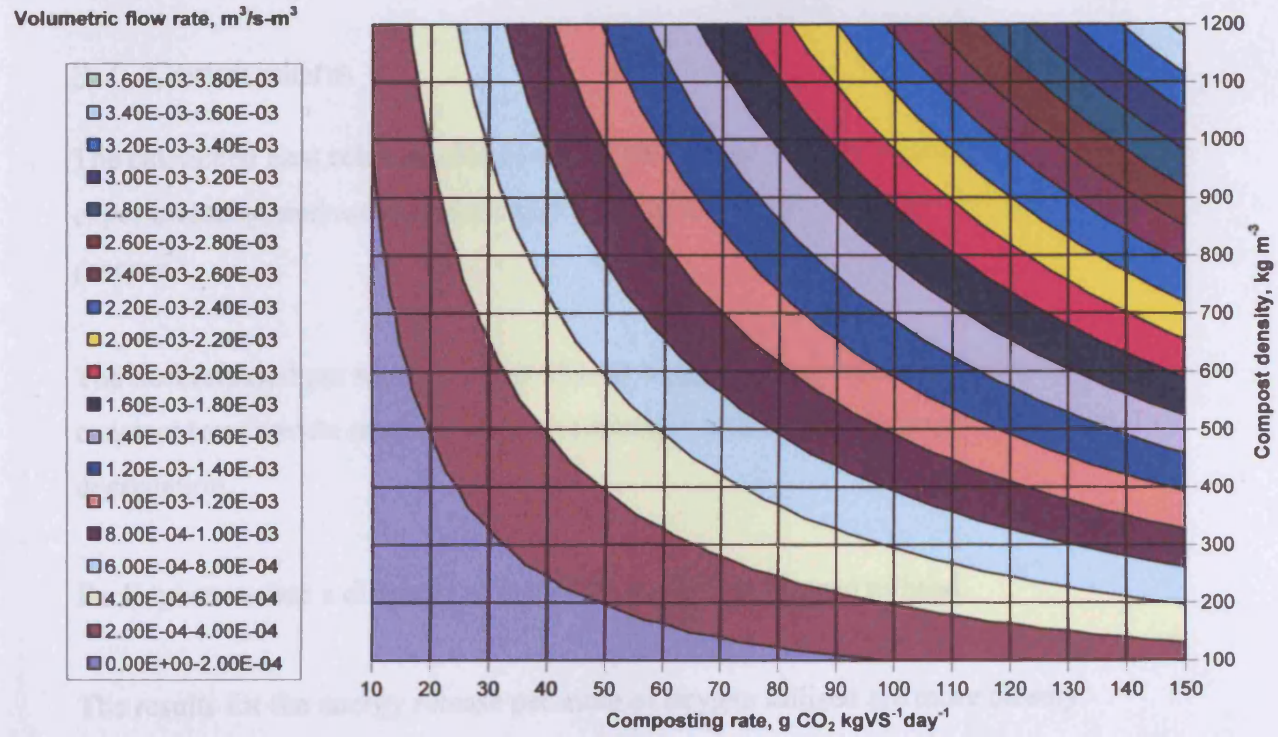

Figure 3.16. Aeration requirements per cubic metre of compost for removal of moisture produced during composting as a function of composting rate and compost density

Using the same assumptions as before about both the composting material and the air being supplied, the humidity ratio of the inlet air is 0.0061 kg kg^{-1} and for the exhaust air it is 0.0491 kg kg^{-1}. The requirement for cooling gives the highest airflow requirements, though all of these are dependant upon various assumptions. For example one cubic metre of compost of density 400 kg m^{-3} composting at a rate of 40 g CO_2 $kgVS^{-1}$ day^{-1} would require 1.68×10^{-4} cubic metres of air per second for its oxygen requirement, 3.25×10^{-4} cubic metres to remove the moisture produced by the process and 3.99×10^{-3} cubic metres per second to remove the heat generated.

Rynk(1992) suggests a flow rate of 5×10^{-5} m^3/s-kg dry matter for temperature control of composting. When the value from Rynk is converted in to the same units as used in Figures 3.14 to 3.16 for a compost of 400kgm^{-3} and 60% moisture content (w.b.) an air supply rate of $8\times10^{-3}m^3s^{-1}m^{-3}$ is determined. This is within the same order of magnitude as the calculated airflow for temperature control. A greater rate or alternate assumptions regarding moisture content would achieve exactly the rate quoted by Rynk (1992).

3.7 Conclusions

The calculated heat releases closely match values that have been recorded experimentally, and are therefore useful for the design of systems in the composting process.

The heat released per mole of either CO_2 or oxygen appears to remain relatively constant over a wide range of carbon to nitrogen ratios for both fungal and bacterial degradation.

Each substrate has a different ratio of CO_2 evolved to oxygen utilised.

The results for the energy release per mole of oxygen utilised are more closely grouped that those for the energy released per mole of CO_2 evolved.

The heat release for CO_2 of 500 kJ/mol is significantly higher than the enthalpy of formation of 393.51 kJ/mole. This shows that it would not be possible to use reaction enthalpies to calculate energy released, as the makeup of the substrates is unknown.

To minimise the heat losses from the vessel system attention should be applied to the compost volume to surface area ratio to ensure that it is as high as possible in order to minimise heat losses from the system.

If recovery of energy is required then it would be worth considering anaerobic digestion as the temperatures involved in the composting process are low. Anaerobic digestion produces methane that can be combusted in a gas turbine or other such technology allowing for energy recovery.

When supplying enough air to cool compost it is important to note that this may supply a large quantity of oxygen which may encourage a greater level of composting activity leading to a greater quantity of heat being released.

If air is being supplied to meet the cooling load of the compost a drying effect may occur, so that extra moisture may need to be added, this may also affect the level of composting activity.

4 Static Pressure Requirements

4.1 Introduction

In order to meet the European Landfill Directive (European Commission, 1999) waste arising from kitchens will need to be diverted from landfill. For catering waste to meet the Animal By-Products Order (2003) it needs to be composted in an in-vessel composting system. Many types of in-vessel system exist and the general types are discussed in Chapter 2. Unlike an open windrow composting system in-vessel technologies have to be fully contained and therefore cannot rely on the passive airflow to supply oxygen to the composting material. It is therefore necessary to supply air to the composting process through an aeration system.

Chapter 3 investigated the heat release from the composting process. This allowed the development of aeration requirements based on oxygen supply, moisture removal and cooling. Although this allows a total flow rate for the system to be calculated it does not give a complete picture of the required aeration system. The static pressure required to drive the air through the compost is unknown. Without knowledge of the static pressure requirements the design decisions on air handling equipment cannot be accurately assessed. As was discussed in Chapter 2 the static pressure required is likely to vary with the moisture content, volatile solids content, particle size distribution, bulk density and free air space of the composting material. During the composting process several of these parameters are likely to change. As volatile solids react with oxygen in the presence of micro-organisms they will release moisture possibly increasing the moisture content whilst decreasing the volatile solids content. The process will also cause a reduction in particle size which may further affect on the available free air space. These changes will all affect the bulk density of the material.

The heat given off and any aeration applied will tend to dry the compost, again affecting the density. The bulk density will reflect how much free air space there is within the compost, the lighter and fluffier the compost is the larger the proportion of air within the pile. The particle size distribution is likely to be reflected in the figures

for the bulk density, for example if all of the particles are similarly sized i.e. steel balls then there is a limit to the quantity of space that can be filled. However, if smaller particles are then introduced then these will fit between the larger particles. If the particle size distribution is fairly broad then the bulk density will be increased. Many of these properties may also have an affect upon the static pressures required to aerate a compost pile.

The information presented in this chapter covers design data on the calculation of the static pressure. This allows the correct specification of compressors or fans to correctly aerate the composting process. By the careful use of such data, correct machinery and equipment can be incorporated into the design of a composting facility in the early stages and by doing this, expensive upgrades to air handling equipment are not required and the installation of overly expensive and powerful equipment can be avoided.

4.2 Methods of Measurement

4.2.1 Moisture content

The moisture content of the compost was determined in accordance with BS EN 13040:2000. After sampling in accordance with BS EN 12579:2000, three sub samples were dried in a ventilated oven. The samples were weighed before and afterwards allowing the mass of water lost to be calculated and expressed either as a proportion or a percentage of the total mass.

4.2.2 Volatile solids content

The volatile solids content of the dry matter was determined in accordance with BS EN 13039:2000. The dried sample was ground to approximately 2mm particle size. This was then ashed in an oven at 450°C. The sample weights before and after ashing were recorded allowing the volatile solids content to be calculated and expressed either as a proportion or percentage of the dry mass.

4.2.3 Particle size distribution

The particle size distribution was determined by placing a sample into a set of sieves and shaking mechanically for 1 hour. The sieves used were 16, 8, 5.6, 2.8, 1.4, 1 and 0.5mm. This allows investigation of smaller particle sizes. The quantity of material retained in each sieve was weighed and these figures were presented both as percentages retained in each sieve and cumulatively, allowing a median particle size to be found.

4.2.4 Bulk density

The bulk density is the mass divided by the total volume, which includes the void space within the material. The experiments were carried out using the pressure drop rig detailed in Appendix B and described in Section 4.5. The volume of the pressure drop rig is calculated from the internal diameter and the depth of the compost bed. The pressure drop rig was stood on a set of scales manufactured by Loadscales Ltd. These scales were used to determine the mass of compost within the rig. This allowed calculation of the compost's bulk density. The scales were 1200mm×1200mm and certified for weighing in commercial operations. The range of the scales was 0-1500kg with a resolution of 0.5 kg. The weight of compost involved in each test was generally over 150 kilograms of compost meaning that the resolution of the scale caused a measurement error of less than 0.3%.

4.2.5 Free air space

The free air space within compost is the volume that is occupied by gas rather than solids or water. A method for measuring this space is detailed in BS EN 13041:2000. This measuring process is very complex and involves specialised equipment. However, it is also possible to calculate the free air space as a function of other variables and this method is discussed in section 4.3.1.

4.2.6 Static pressure

This was measured in a three metre high column of 450mm diameter; drawings for this are given in Appendix B. A plenum at the base receives air from a blower. There is a throttle valve to give control over the flow rate of the air and hence the superficial velocity through the column of compost. Static pressure taps are located at 500mm intervals, allowing the static pressure to be measured relative to atmospheric pressure using a U-tube manometer. The results can then be plotted either as a function of the depth or the velocity.

4.2.7 Superficial velocity

The velocity of air in the inlet pipe was measured initially using a hot wire anemometer (Testo 425) and the superficial velocity calculated. This was later replaced with a Rotameter which measured the volumetric flow rate. The superficial velocity through the column can be found by dividing by the cross sectional area of the column.

4.3 Theory

4.3.1 Free Air Space

The free air space is an important parameter when calculating pressure drops using the Ergun model (Ergun, 1952) for static pressures through packed beds as discussed in Chapter 2. This is because it is the free air space within a composting pile which allows the flow of fresh air through the compost pile. Although permeability and porosity are never the same as each other Das and Keener (1997) demonstrated that these two parameters are related for compost. The flow of air through the compost allows for the CO_2 and moisture produced during the composting process to be removed and the provision of oxygen to allow the process to continue. The air

flowing through a compost bed can also be used for cooling of the material to bring it back to an optimum temperature.

As compost is a compressible material with a density greater than that of air it is intuitive that as it is compressed the density of the compost will increase through a reduction in the proportion of free air space. This of course assumes that the compost particles themselves do not compress. An expression relating the bulk density of compost and the proportion of free air space can be developed. The composting material is made up of a mixture of solids, liquids and gas. The solid component contains volatile solids and mineral ash, the liquid is mainly water and the gas component is air. Figure 4.1 helps to imagine this, where V_g, V_w and V_s represent the volumes of gas, water and solid and W_g, W_w and W_s represent the corresponding masses. In reality of course the compost is a mixture of these three components.

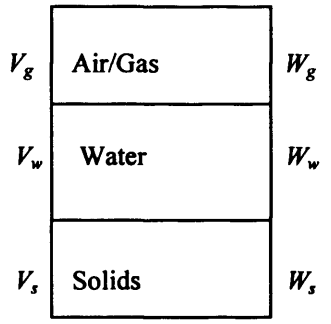

Figure 4.1 Schematic of components of the composting pile

$$Density = \frac{Mass}{Volume} = \frac{W_g + W_W + W_s}{V_g + V_W + V_s} \tag{4.1}$$

$$W_t = W_g + W_W + W_s \tag{4.2}$$

V_tCombining equations 4.1, 4.2 and 4.3 gives

$$\rho_t(V_g + V_W + V_s) = W_g + W_W + W_s \tag{4.3}$$

Combining equations 4.1, 4.2 and 4.3 gives

$$\rho_t(V_g + V_W + V_s) = W_g + W_W + W_s \tag{4.4}$$

$$V_g = \frac{W_g + W_w + W_s - \rho_t V_w - \rho_t V_s}{\rho_t} \tag{4.5}$$

The volume of gas divided by the total volume is the proportion of free air space within the compost. The weight of the gas is very small in comparison to the weights of the water and the solids and this term can be removed so that Equation 4.2 becomes Equation 4.6.

$$W_t = W_w + W_s \tag{4.6}$$

Also defining the moisture content, *MC*, as,

$$MC = \frac{W_w}{W_t} \tag{4.7}$$

gives

$$W_w = W_t MC \tag{4.8}$$

and

$$W_s = W_t(1 - MC) \tag{4.9}$$

This allows simplification to

$$\frac{V_g}{V_t} = 1 - \left[\left(\frac{MC}{\rho_w}\right) + \left(\frac{1 - MC}{\rho_s}\right)\right]\rho_t \tag{4.10}$$

Equation 4.10 allows calculation of the volume of free air space as a function of the total density, the moisture content and the densities of water and solids. The moisture content and compost density can be found using the methods previously described in Sections 4.2.1 and 4.2.4. The density of the solid material can be found in terms of the densities of ash and volatile solids as

$$\rho_s = \frac{\rho_{ash}\rho_{vs}}{(1 - VS)\rho_{vs} + VS\rho_{ash}} \tag{4.11}$$

where *VS* is the volatile solids content on a dry basis. British standard BS EN 13041:2000 gives values for the densities of ash and organic matter as 2650 kg m^{-3} and 1550 kg m^{-3} respectively. Although these values may sound rather high in comparison to compost it is important to realise that they do not include any void space and refer solely to the actual material.

Equations 4.10 and 4.11 can be used to create a series of curves for varying moisture and volatile solids contents such as those shown in Figure 4.2. for a material with a volatile solids content of 0.7 (d.b.). The values shown in Figure 4.2 are very similar to those presented by Agnew *et al.* (2003) which were discussed in Chapter 2.

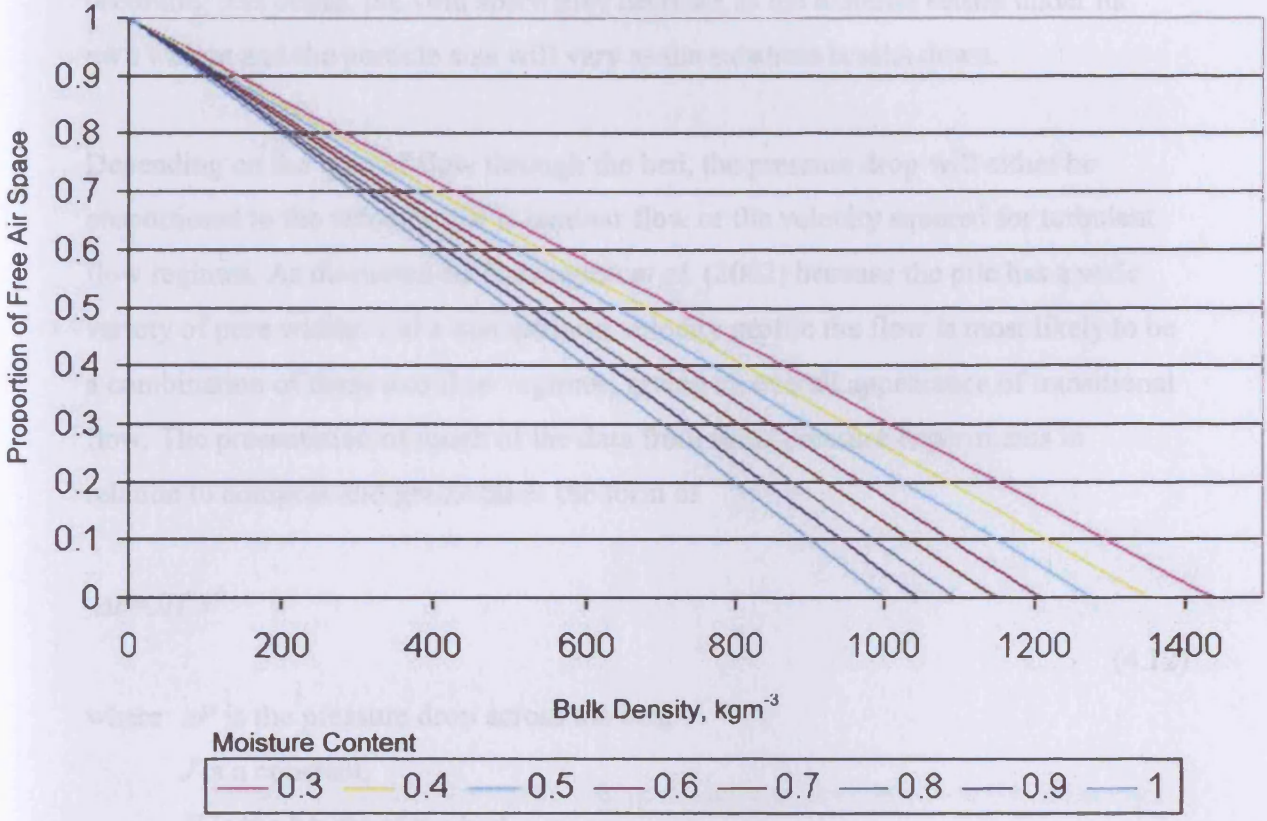

Figure 4.2. Free Air Space as a function of compost bulk density and moisture content for a volatile solids content of 0.7 (d.b.)

4.3.2 Static Pressure

While the proportion of free air space is a measure of the porosity of the material, the static pressure required to drive air through the material is a measure of its permeability. As shown by Das and Keener (1997) these two factors are related, though not linearly. The relationship follows the cubic relationship which is outlined in the Ergun (Ergun, 1952) equation given in Chapter 2.

As was discussed in Chapter 2 the pressure drop through a packed bed is dependant on a variety of factors including the height of the bed, the properties of the fluid flowing through the bed, the proportion of the bed that is void and a representative size of the particles within the bed. Many of the properties will change as the air is passed through the bed. For instance, the air will pick up moisture and heat up becoming less dense, the void space may decrease as the material settles under its own weight and the particle size will vary as the substrate breaks down.

Depending on the type of flow through the bed, the pressure drop will either be proportional to the velocity if it is laminar flow or the velocity squared for turbulent flow regimes. As discussed by Barrington *et al.* (2002) because the pile has a wide variety of pore widths and a non uniform velocity profile the flow is most likely to be a combination of these two flow regimes, giving an overall appearance of transitional flow. The presentation of much of the data from static pressure experiments in relation to compost and grains takes the form of

$$\Delta P = J H^a V^b \tag{4.12}$$

where ΔP is the pressure drop across the bed,

J is a constant,

H is the height of the bed,

a is a compressibility exponent,

V is the superficial velocity and

b is the velocity exponent.

The constant J was shown by Higgins *et al.* (1982) to be affected by the mixing regime, degradation of the compost and ageing. In comparison to the Ergun equation presented in Chapter 2, coefficient J represents free air space, particle size, air density and air viscosity.

Exponent a gives an indication of the compressibility of the compost. When this is equal to 1 the material was either incompressible or the bed depth used in the experiment was of insufficient depth to cause compression. The pressure drop per unit

depth will also be constant through the height of the pile. This exponent was shown by Keener *et al.* (1997) to have a value of 1 for a compost with more than 40% dry matter and to be greater than 1 if the proportion of dry matter was less than 40%.

If b is equal to 1 then the flow would be laminar, as predicted by the Darcy equation discussed in Chapter 2. If the flow becomes turbulent then the value of b will approach 2. Generally, due to the small size of some of the passages through the bed, there will always be a laminar element to the flow. Saint-Joly *et al.* (1989) observed that the value of b varied with the porosity of the compost material. The porosity gives the total free space for air flow so the size of channels available may depend upon it. The Reynolds number is used as an indicator of flow regime and requires a representative dimension-such as pore size-for its calculation. As the pore size and particle sizes changes so will the type of flow, depending upon the amount of viscous drag and inertial forces. This will be reflected by exponent b varying from 1 to 2 and an increase in the Reynolds number.

4.4 Aeration Quantities

The main thrust of this work is to develop accurate design data that can be used in the development of composting sites. It is therefore sensible to use appropriate superficial velocities in the experimental test rig. The quantities of air required for cooling, moisture removal and oxygen supply as a function of both compost bulk density and composting rate were calculated in Chapter 3. The quantities of aeration required for the composting process were also discussed in Chapter 2. The values presented by Rynk (1992), Haug (1993) and Keener *et al.* (1997) have been used to calculate appropriate superficial velocities for the pressure test rig, as have the data developed in Chapter 3.

For a compost of bulk density 370 kgm^{-3} the test rig would contain 176.5 kg of material. This is an appropriate figure for the density of the green waste shredded by the Seko shredder at the CERT composting facility (Hewings *et al.*, 2002). The volumetric airflow rates can then be calculated and the superficial velocities for the

test rig determined. The calculated velocities are shown in Table 4-1. The value derived from the values presented in Chapter 3 is the quantity of air to cool a compost of density 370kgm^{-3} composting at a rate of 40 $gCO_2kgVS^{-1}day^{-1}$. This is a relatively high rate but the quantity of air required is still the lowest given. It should be noted that these velocities would apply to any system as they are the result of dividing a volumetric flow rate by an area.

Table 4-1. Superficial velocities calculated for the pressure test rig

Source	Suggested Airflow rate	Total airflow rate, m^3s^{-1}	Superficial velocity through test rig, ms^{-1}
Rynk (1992)	$5\times10^{-5}m^3s^{-1}kg\ dry^{-1}$	4.4×10^{-3}	0.028
Haug (1993)	$4.6\times10^{-4}m^3s^{-1}kg\ dry^{-1}$	4.1×10^{-2}	0.255
Keener *et al.* (1997)	$3.1\times10^{-5}m^3s^{-1}kg^{-1}$	5.5×10^{-3}	0.034
Chapter 3	$1.85\times10^{-3}m^3s^{-1}m^{-3}$	8.8×10^{-4}	0.006

4.5 Method

To allow measurement of the static pressure required to blow air through the compost a pressure test rig was constructed. The column was constructed from ground drainage pipe with an internal diameter of 450mm. The test rig was 3 metres high with static taps at 500mm intervals. Photographs of the rig are shown in Figure 4.3, whilst full drawings are in Appendix B. At the base a plenum received the air from a fan and the compost was supported on a mesh surface above the plenum. Initially a sliding control valve was used to regulate the airflow through the compost by releasing some of the air from the system. The velocity in the feed pipe was initially recorded using a hot wire anemometer (Testo 425). Both the hot wire anemometer and sliding control valve were later replaced with a Rotameter and a gate valve allowing direct recording of volumetric flow rate and finer flow control.

The compost was manually loaded into the column and the plenum was connected to the fan. The plenum pressurised due to the resistance of the compost. The static

pressure was recorded at half metre intervals using a U-tube manometer. The airflow rate was then adjusted to give a different superficial velocity and the static pressure readings were repeated for the new flow rate once the flow had settled.

Measurements were also taken for compost that had been allowed to settle in the vessel. The distance through which it had settled from the top of the column was measured at 4 points and an average taken. This was then combined with the weight from the scales to give a new density for the material. The vessel was emptied by hoisting the column upwards from the plenum and allowing the compost to slide out of the bottom of the column.

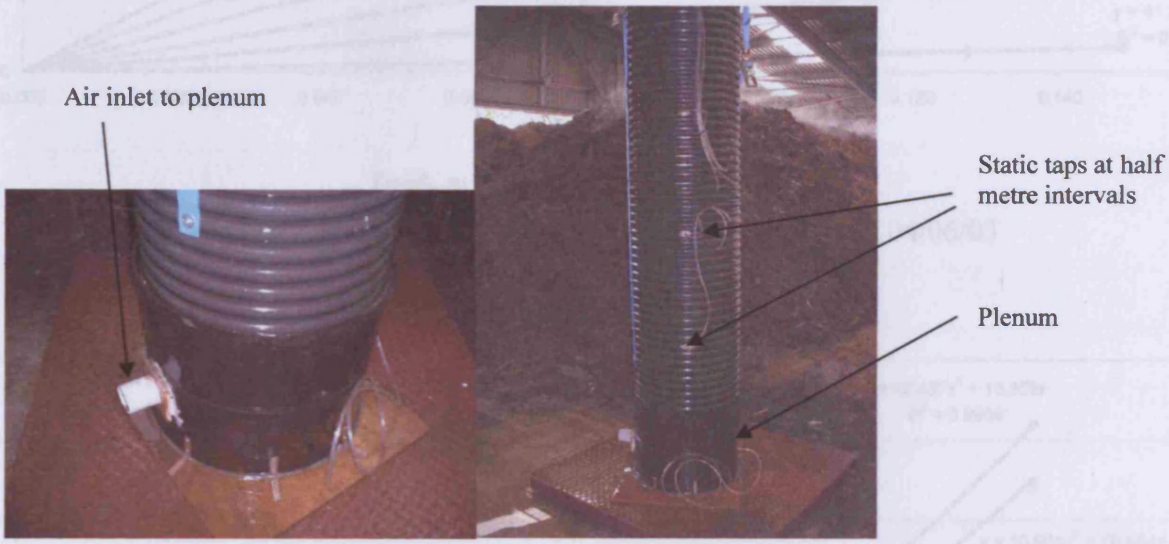

Figure 4.3. Photographs of the static pressure test rig on top of the weigh platform

4.6 Results

The first test using the rig was performed on the 4th of June 2003. The rig was filled with freshly shredded material which appeared to be very fibrous. The particle size distribution for this material is given in Table 4-2. The moisture content of the material was analysed and found to be 51% (w.b.) whilst the density of the material was found to be 370kgm^{-3}. Using the method described in Section 4.3.1 the proportion of free air space can be calculated as approximately 72%. The static pressure plotted against both superficial velocity and the depth of the compost bed are shown in

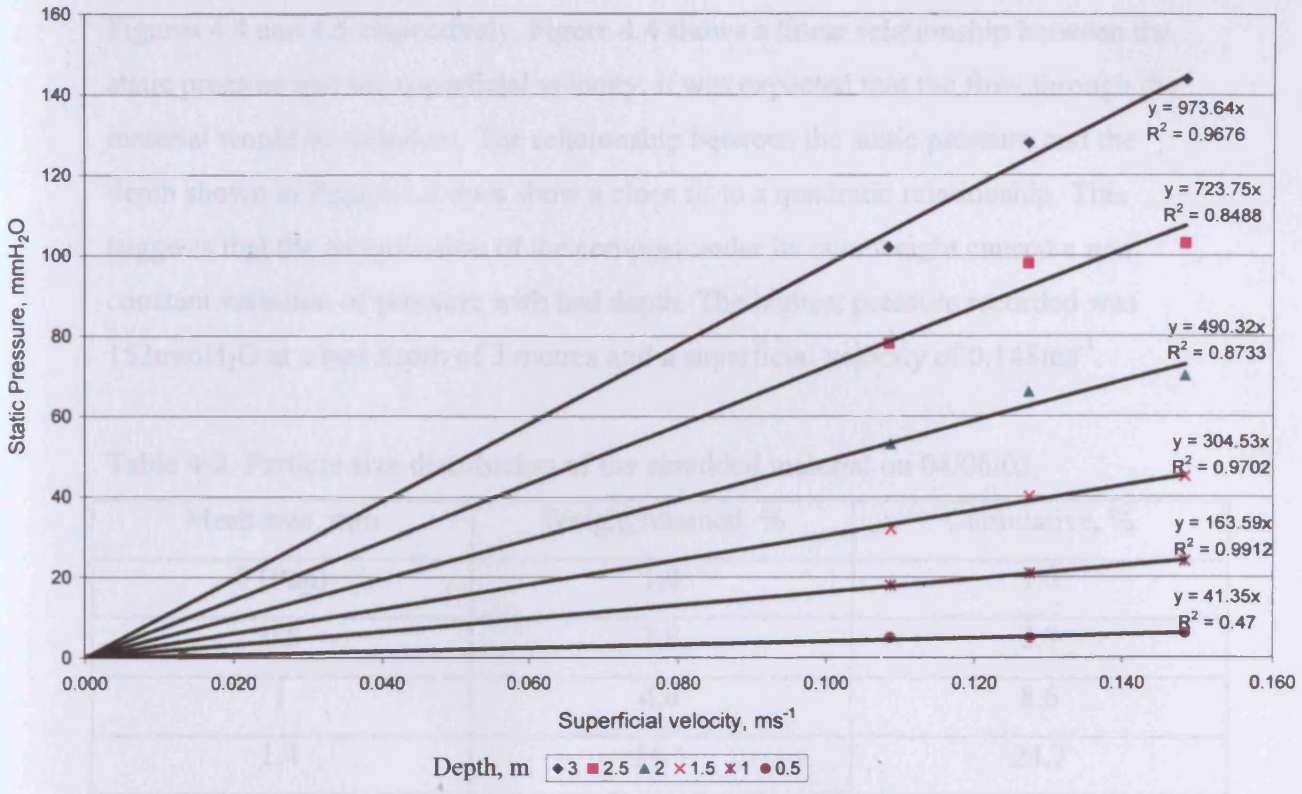

Figure 4.4. Static pressure against superficial velocity for the test on 04/06/03

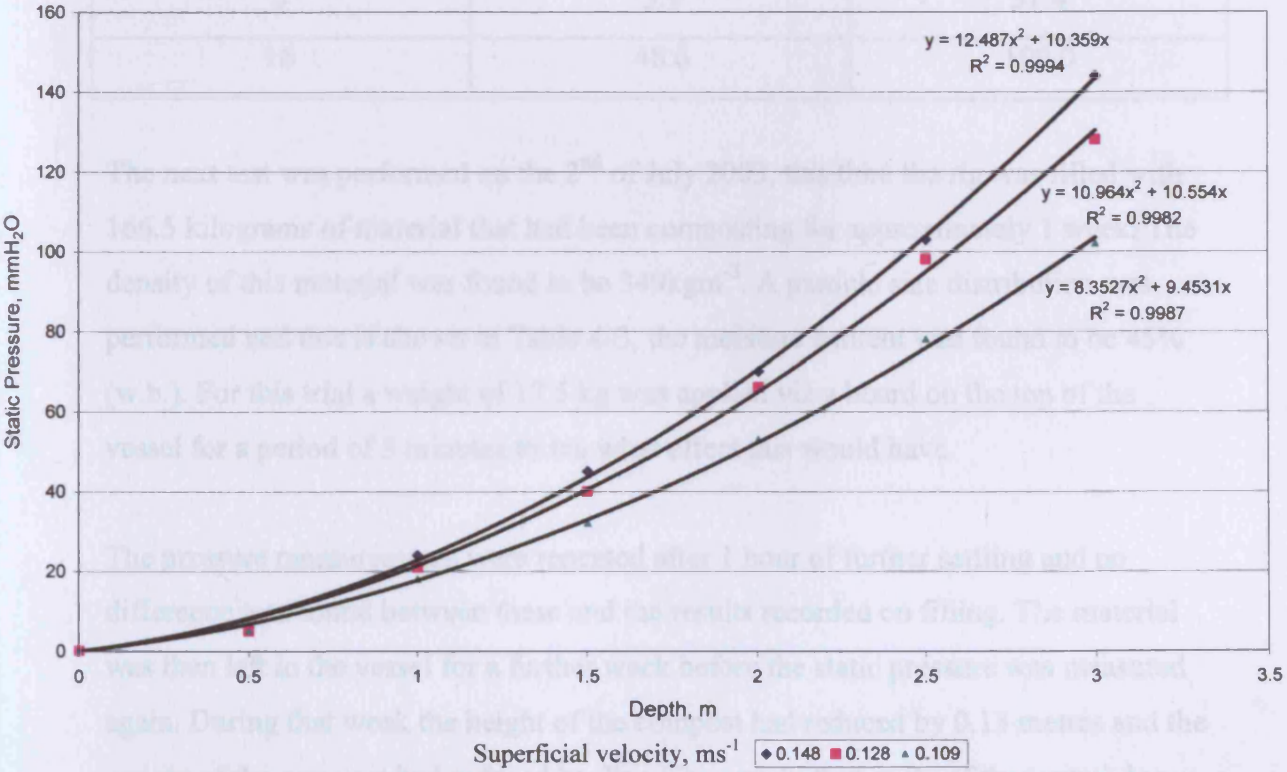

Figure 4.5. Static pressure against depth for the test on 04/06/03

Figures 4.4 and 4.5 respectively. Figure 4.4 shows a linear relationship between the static pressure and the superficial velocity, it was expected that the flow through the material would be turbulent. The relationship between the static pressure and the depth shown in Figure 4.5 does show a close fit to a quadratic relationship. This suggests that the compression of the compost under its own weight caused a non constant variation of pressure with bed depth. The highest pressure recorded was 152mmH_2O at a bed depth of 3 metres and a superficial velocity of 0.148ms^{-1}.

Table 4-2. Particle size distribution of the shredded material on 04/06/03

Mesh size, mm	Weight retained, %	Cumulative, %
0 (Pan)	1.0	1.0
0.5	2.9	3.9
1	4.8	8.6
1.4	16.1	24.7
2.8	13.6	38.3
5.6	7.1	45.4
8	5.9	51.4
16	48.6	100.0

The next test was performed on the 2nd of July 2003, this time the rig was filled with 166.5 kilograms of material that had been composting for approximately 1 week. The density of this material was found to be 349kgm^{-3}. A particle size distribution was performed and this is shown in Table 4-3, the moisture content was found to be 45% (w.b.). For this trial a weight of 17.5 kg was applied via a board on the top of the vessel for a period of 3 minutes to see what effect this would have.

The pressure measurements were repeated after 1 hour of further settling and no difference was found between these and the results recorded on filling. The material was then left in the vessel for a further week before the static pressure was measured again. During that week the height of the compost had reduced by 0.13 metres and the weight of the compost had reduced by 3kg. The new bulk density of the material was 362 kgm^{-3}. The graphs of static pressure against superficial velocity and depth for the filling material are shown in Figures 4.6 and 4.7 whilst Figure 4.8 shows the data after

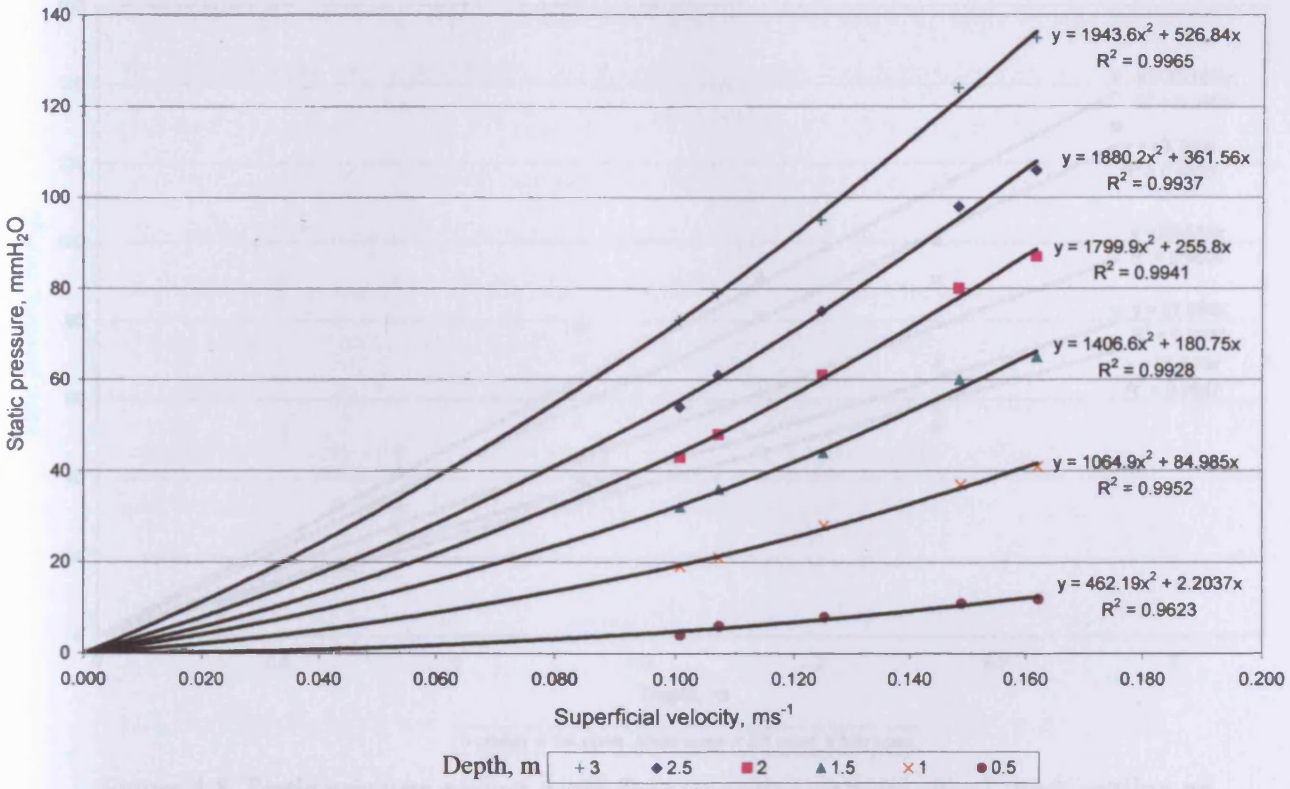

Figure 4.6. Static pressure against superficial velocity for composted material on 02/07/03

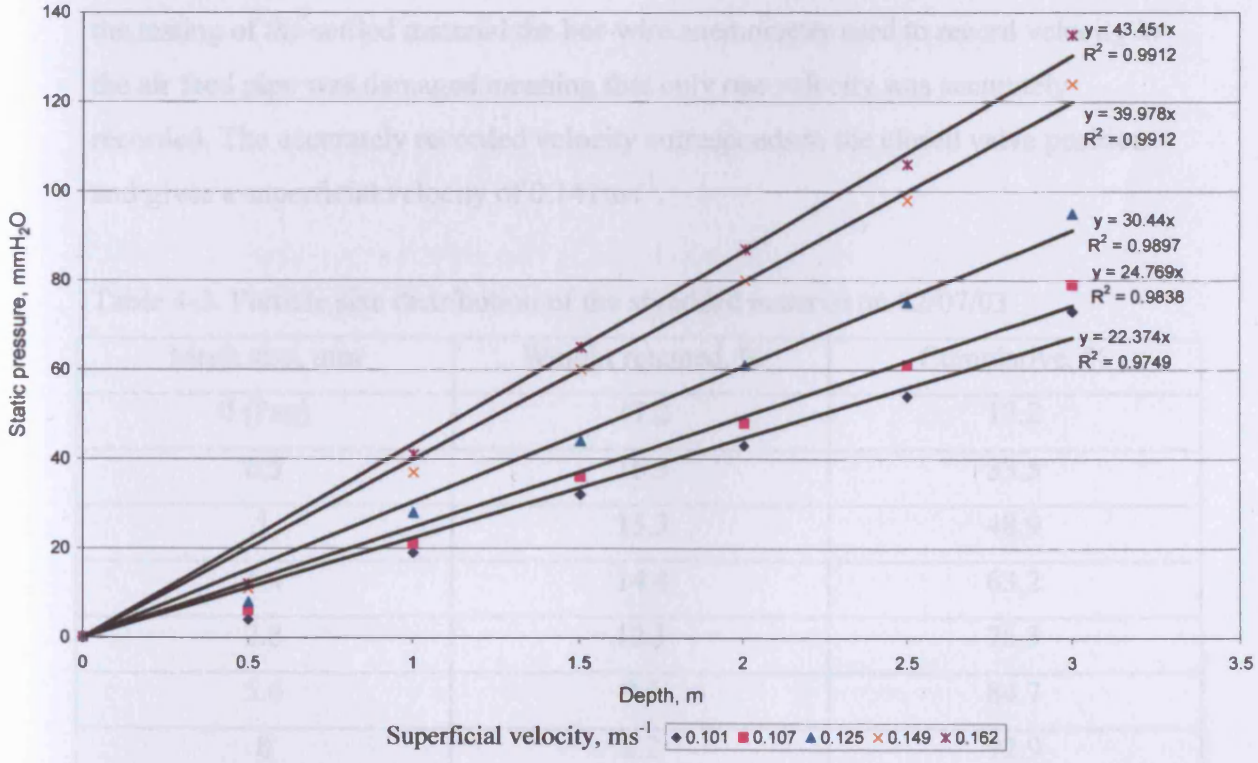

Figure 4.7. Static pressure against depth for composted material on 02/07/03

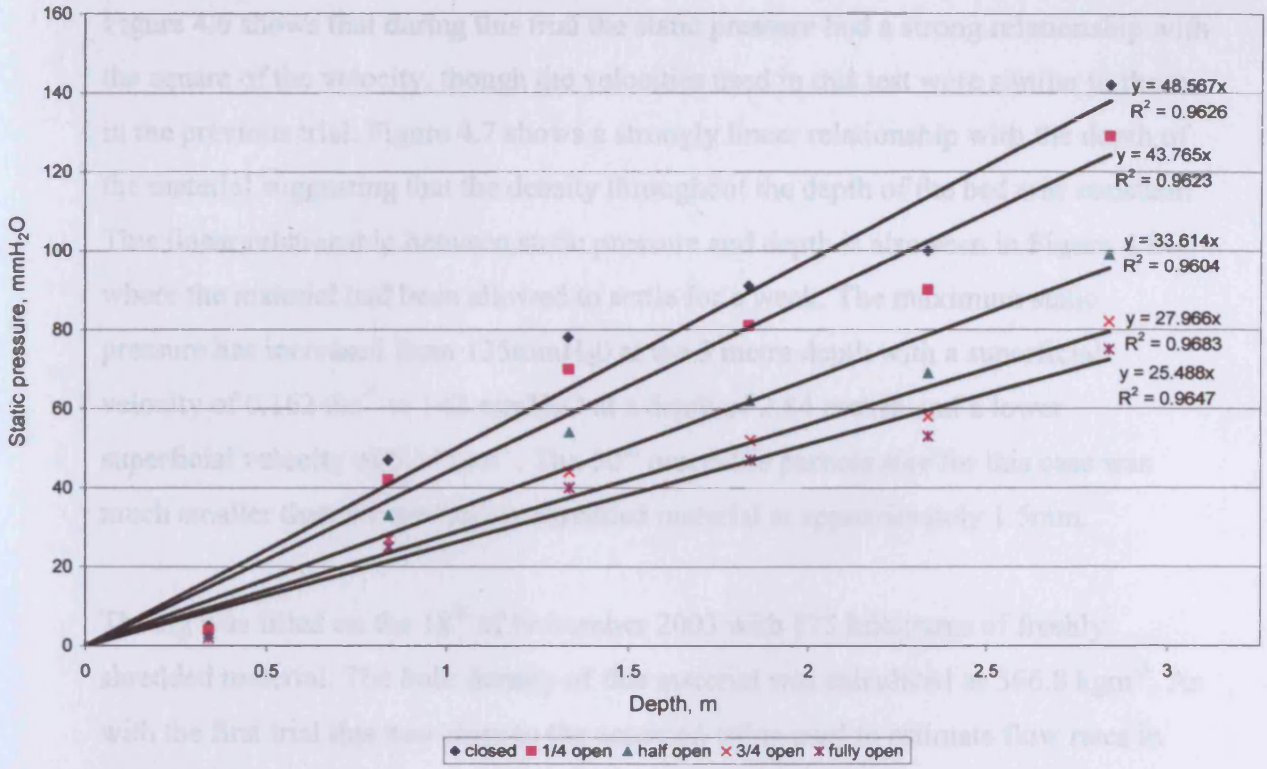

Figure 4.8. Static pressure against depth for composted material after 1 week settling on 09/07/03

the one week settling period plotted as static pressure against depth. However, during the testing of the settled material the hot-wire anemometer used to record velocity in the air feed pipe was damaged meaning that only one velocity was accurately recorded. The accurately recorded velocity corresponds to the closed valve position and gives a superficial velocity of $0.141 ms^{-1}$.

Table 4-3. Particle size distribution of the shredded material on 02/07/03

Mesh size, mm	Weight retained, %	Cumulative, %
0 (Pan)	17.2	17.2
0.5	16.3	33.5
1	15.3	48.9
1.4	14.4	63.2
2.8	12.1	75.3
5.6	9.4	84.7
8	8.2	92.9
16	7.1	100.0

Figure 4.6 shows that during this trial the static pressure had a strong relationship with the square of the velocity, though the velocities used in this test were similar to those in the previous trial. Figure 4.7 shows a strongly linear relationship with the depth of the material suggesting that the density throughout the depth of the bed was constant. This linear relationship between static pressure and depth is also seen in Figure 4.8 where the material had been allowed to settle for a week. The maximum static pressure has increased from 135mmH_2O at the 3 metre depth with a superficial velocity of 0.162 ms^{-1} to 142 mmH_2O at a depth of 2.84 metres and a lower superficial velocity of 0.141ms^{-1}. The 50th percentile particle size for this case was much smaller than for the freshly shredded material at approximately 1.5mm.

The rig was filled on the 18th of November 2003 with 175 kilograms of freshly shredded material. The bulk density of this material was calculated as 366.8 kgm^{-3}. As with the first trial this was close to the assumed value used to estimate flow rates in Section 4.4. A particle size distribution of the material was taken and is shown in Table 4-4. The results for the static pressures plotted against superficial velocity and bed depth for the fresh material are shown in Figures 4.9 and 4.10. The compost was then allowed to settle for 6 days. After the settling period the depth of the compost bed had decreased by 0.43 metres and 1 kilogram of mass had been lost. The post settling density of the material had increased to 428kgm^{-1}. Pressure measurements were taken for the settled material and these are shown in Figures 4.11 and 4.12.

Table 4-4. Particle size distribution of the freshly shredded material on the 18/11/03

Mesh size, mm	Weight retained, %	Cumulative, %
0 (Pan)	0.2	0.2
0.5	0.7	0.9
1	2.2	3.1
1.4	15.1	18.2
2.8	22.6	40.8
5.6	11.5	52.3
8	15.3	67.6
16	32.4	100.0

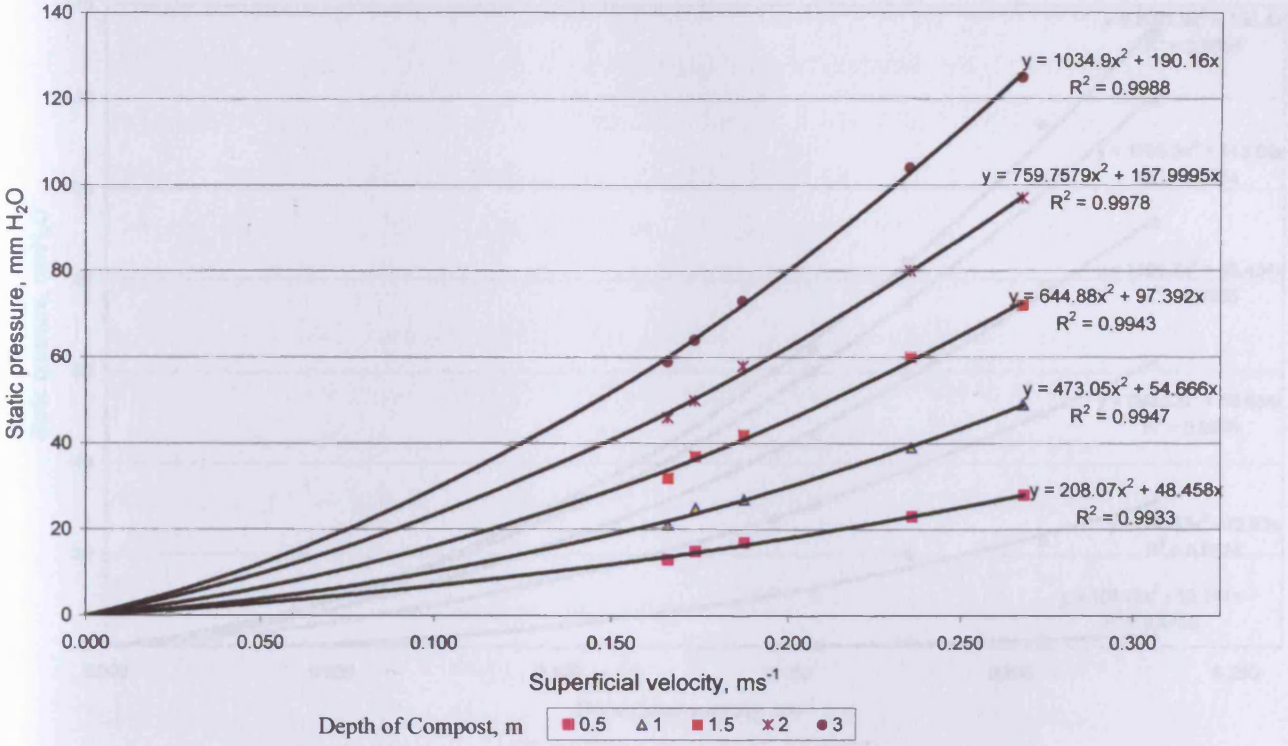

Figure 4.9. Static pressure against superficial velocity for the freshly shredded material on 18/11/03

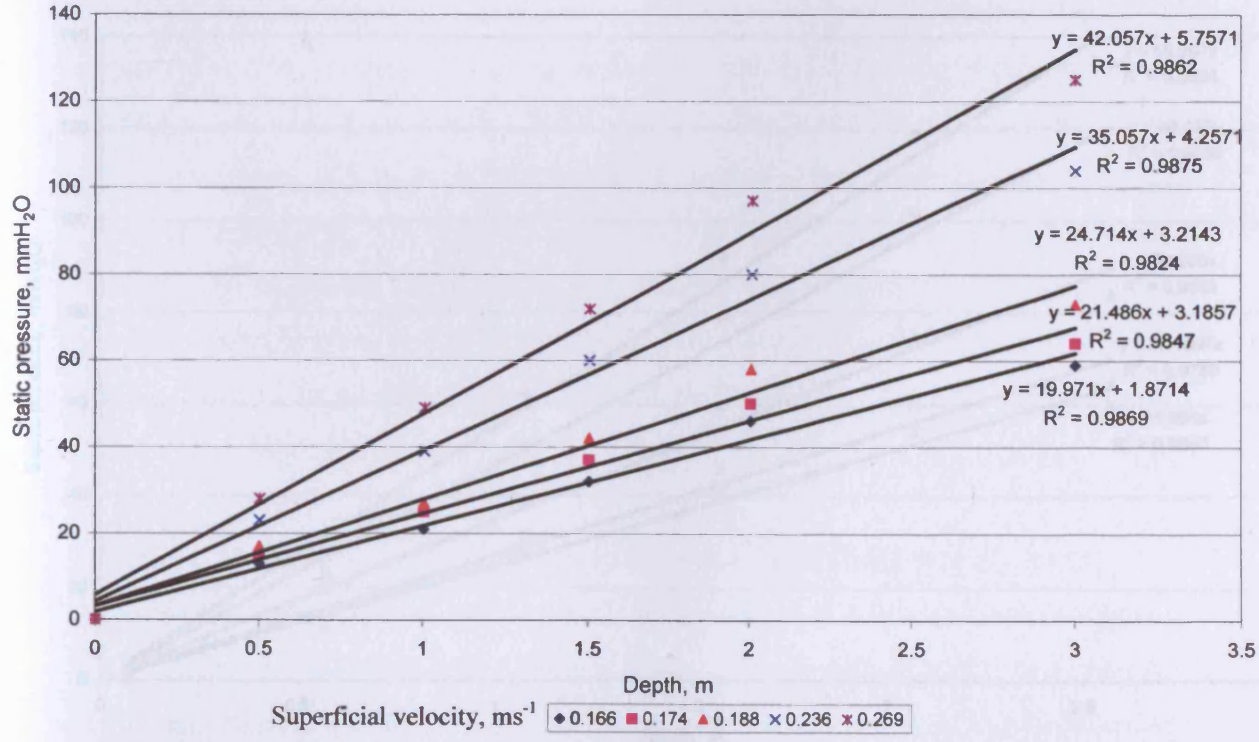

Figure 4.10. Static pressure against depth for the freshly shredded material on 18/11/03

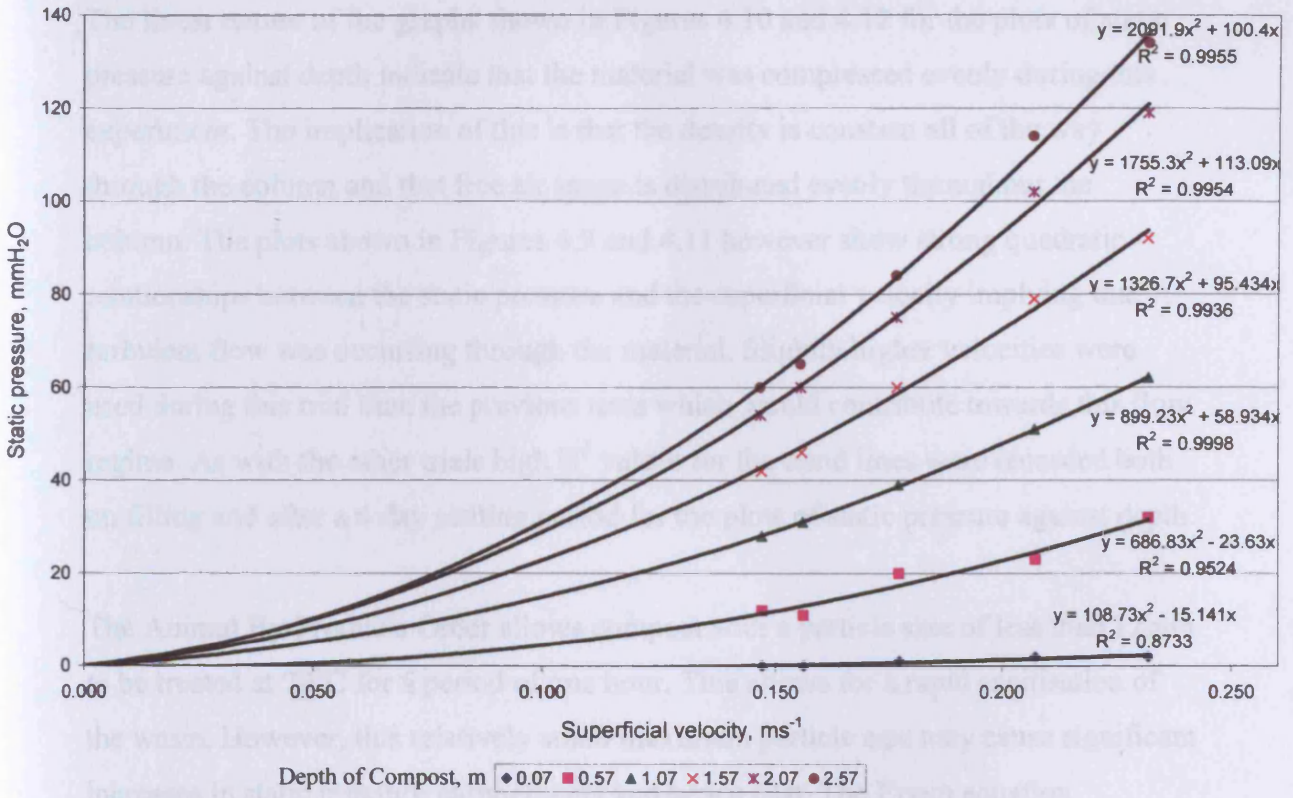

Figure 4.11. Static pressure against superficial velocity after 6 days settling

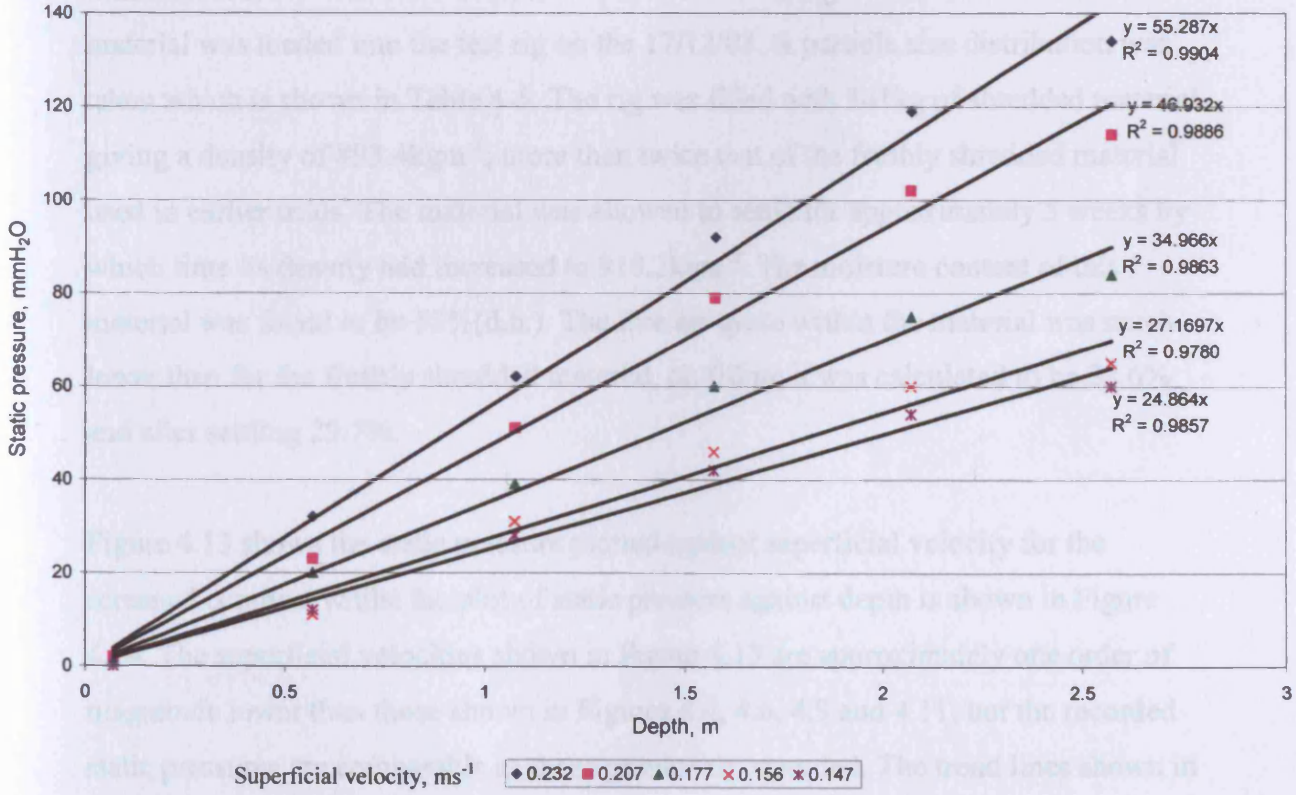

Figure 4.12. Static pressure against depth after 6 days settling

The linear nature of the graphs shown in Figures 4.10 and 4.12 for the plots of static pressure against depth indicate that the material was compressed evenly during this experiment. The implication of this is that the density is constant all of the way through the column and that free air space is distributed evenly throughout the column. The plots shown in Figures 4.9 and 4.11 however show strong quadratic relationships between the static pressure and the superficial velocity implying that turbulent flow was occurring through the material. Slightly higher velocities were used during this trial than the previous tests which would contribute towards this flow regime. As with the other trials high R^2 values for the trend lines were recorded both on filling and after a 6 day settling period for the plots of static pressure against depth.

The Animal By-Products Order allows compost with a particle size of less than 12mm to be treated at 70°C for a period of one hour. This allows for a rapid sanitisation of the waste. However, this relatively small maximum particle size may cause significant increases in static pressure requirements and hence cost. The Ergun equation presented in Chapter 2 suggests that the required static pressure will increase as the nominal particle size decreases. Because of this the next trial was performed using finished compost which had been screened to 10mm using a Seko screen. The material was loaded into the test rig on the 17/12/03. A particle size distribution was taken which is shown in Table 4-5. The rig was filled with 341kg of shredded material giving a density of 893.4kgm^{-3}; more than twice that of the freshly shredded material used in earlier trials. The material was allowed to settle for approximately 5 weeks by which time its density had increased to 918.2kgm^{-3}. The moisture content of this material was found to be 52%(d.b.). The free air space within the material was much lower than for the freshly shredded material, on filling it was calculated to be 32.6% and after settling 29.7%.

Figure 4.13 shows the static pressure plotted against superficial velocity for the screened compost whilst the plot of static pressure against depth is shown in Figure 4.14. The superficial velocities shown in Figure 4.13 are approximately one order of magnitude lower than those shown in Figures 4.4, 4.6, 4.9 and 4.11, but the recorded static pressures are comparable as those previously recorded. The trend lines shown in Figure 4.13 are also strongly quadratic, as are those in Figure 4.14 implying an uneven distribution of resistance with depth. The post settling data are shown in

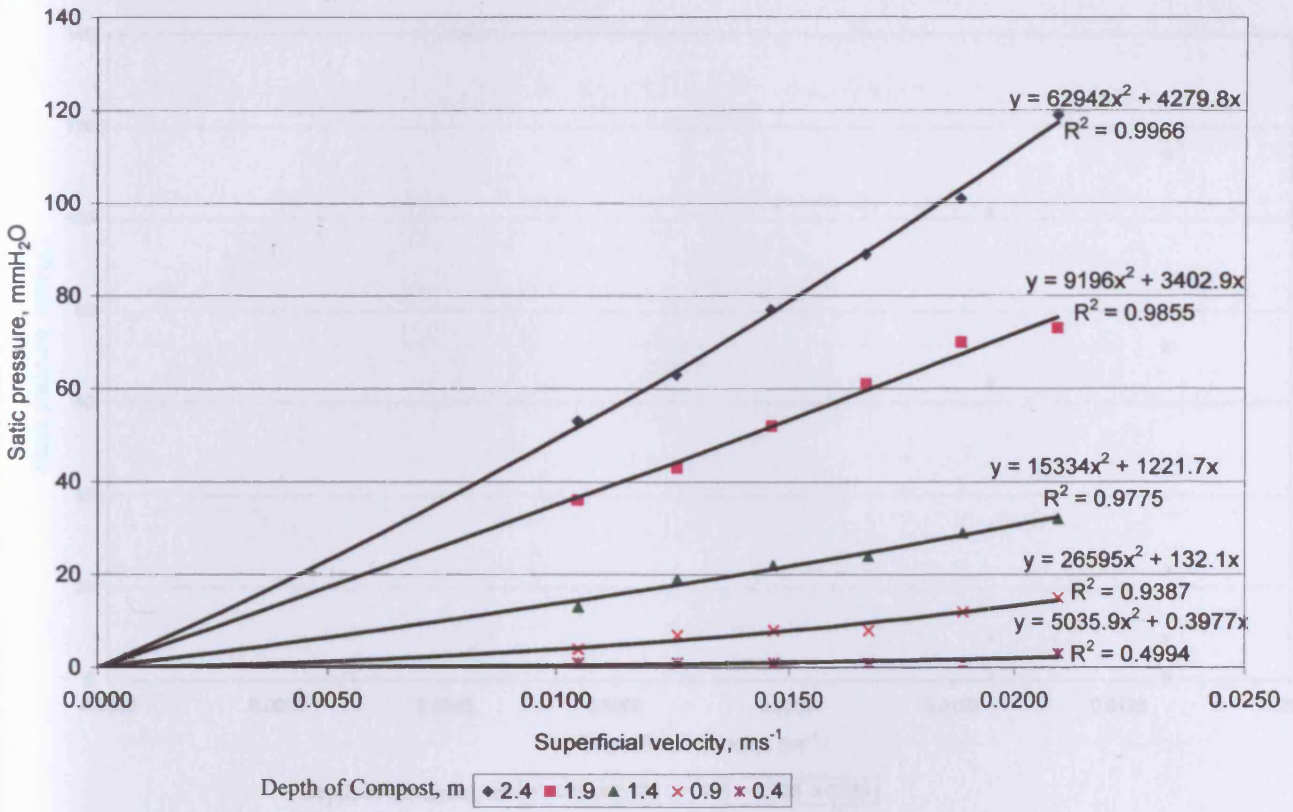

Figure 4.13. Static pressure against superficial velocity for the screened compost

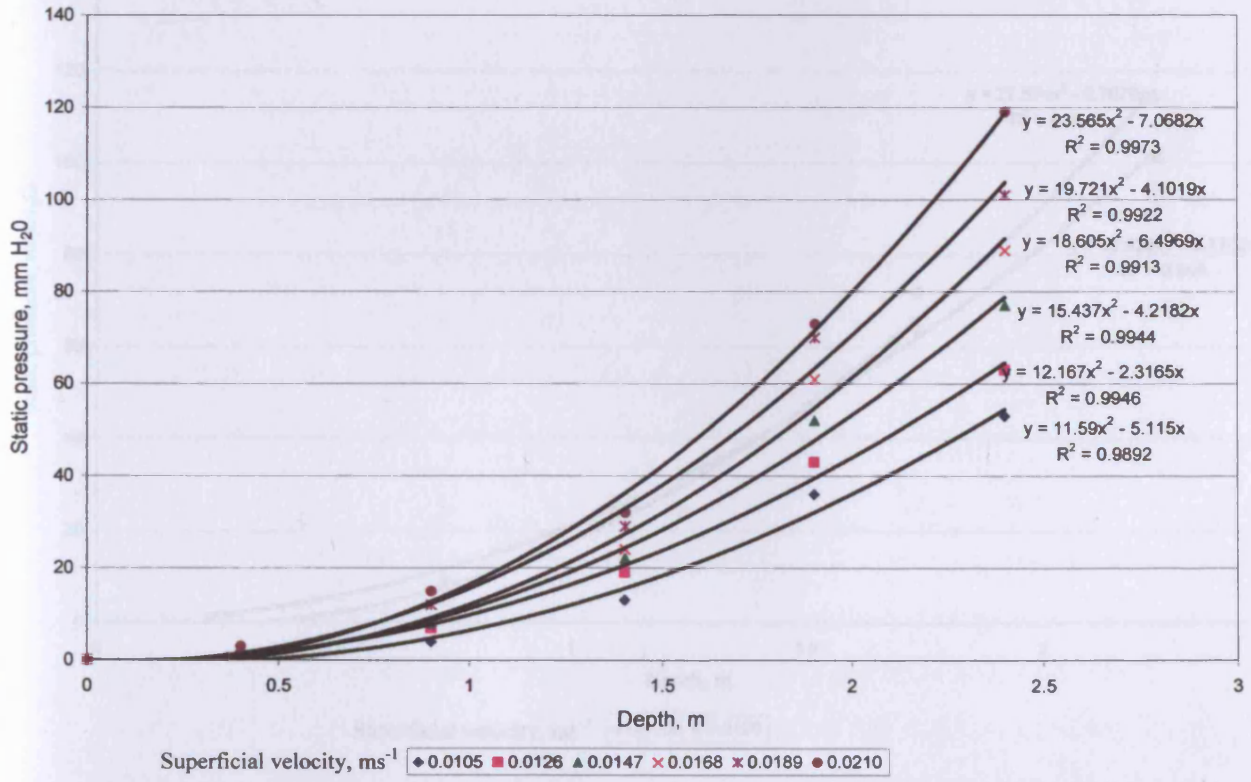

Figure 4.14. Static pressure against depth for the screened compost

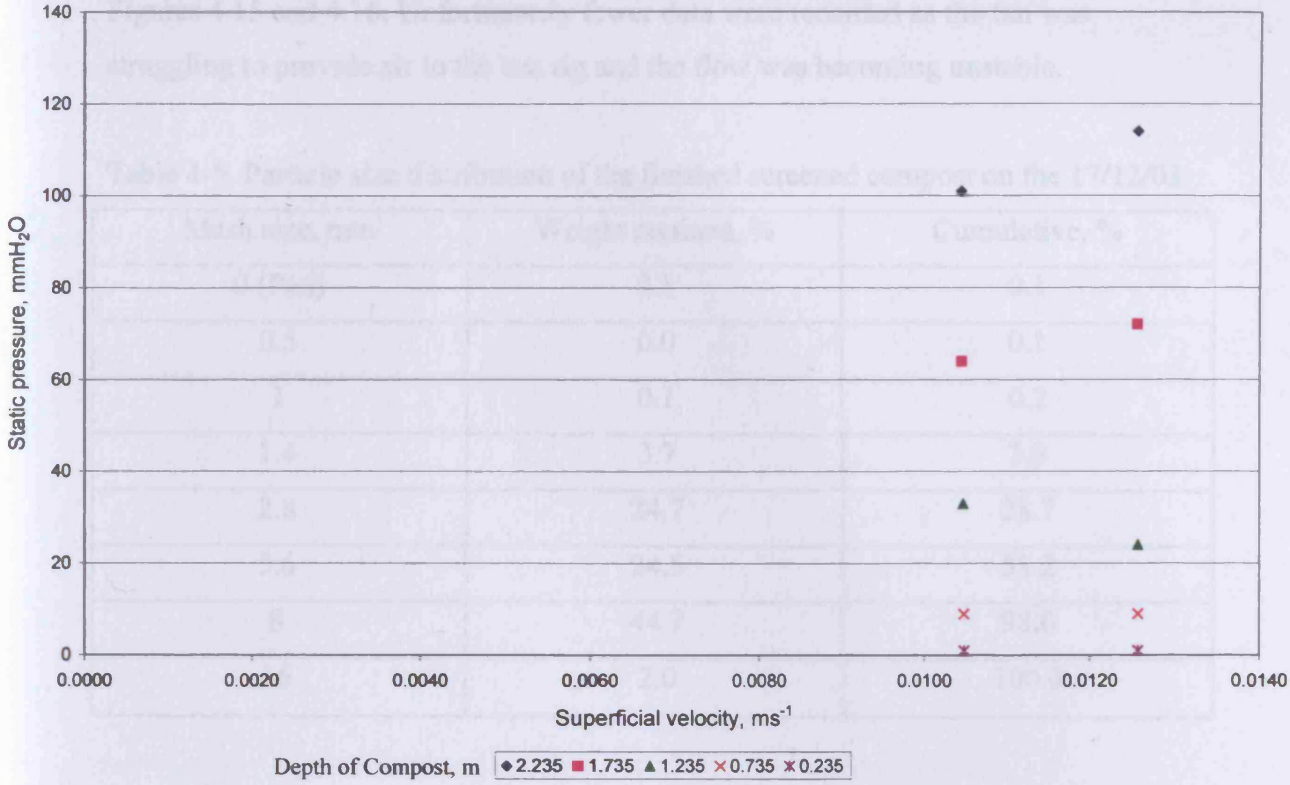

Figure 4.15. Static pressure against superficial velocity for the screened compost after settling

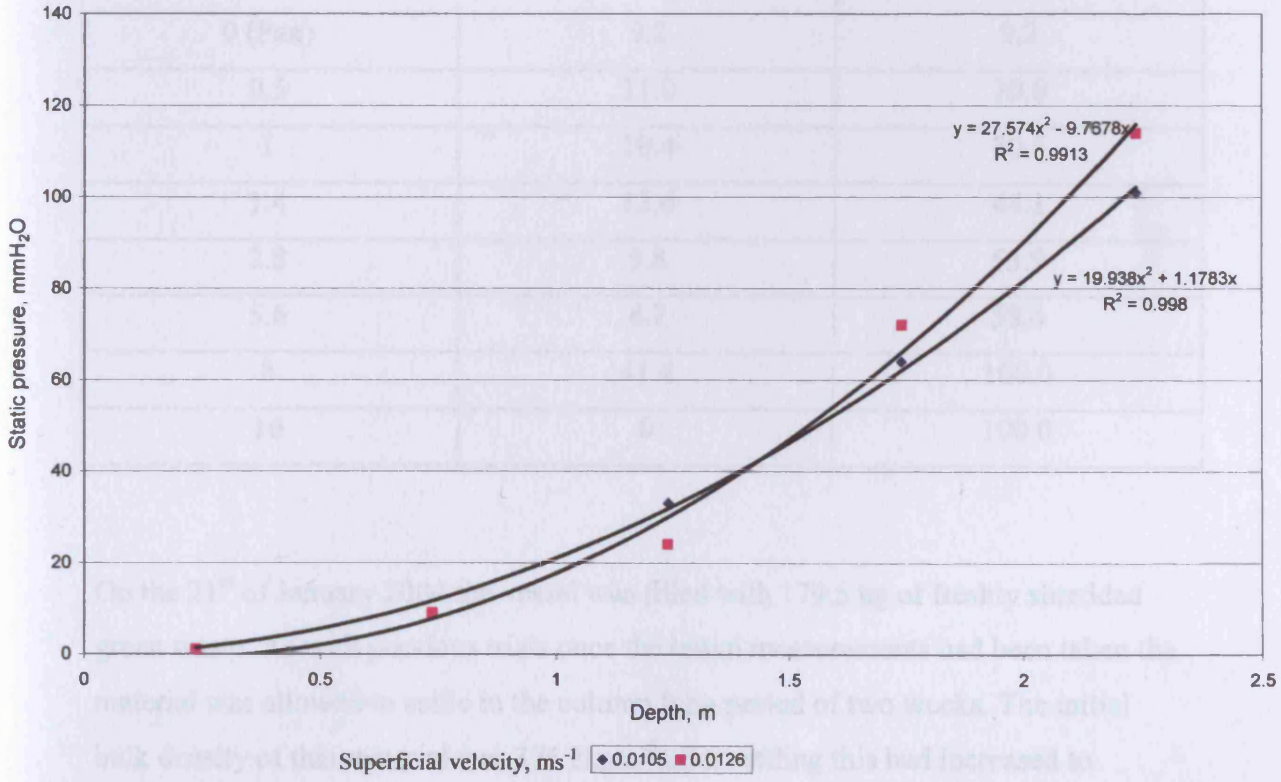

Figure 4.16. Static pressure against depth for the screened compost after settling

Figures 4.15 and 4.16. Unfortunately fewer data were recorded as the fan was struggling to provide air to the test rig and the flow was becoming unstable.

Table 4-5. Particle size distribution of the finished screened compost on the 17/12/03

Mesh size, mm	Weight retained, %	Cumulative, %
0 (Pan)	0.1	0.1
0.5	0.0	0.1
1	0.1	0.2
1.4	3.7	3.9
2.8	24.7	28.7
5.6	24.5	53.2
8	44.7	98.0
16	2.0	100.0

Table 4-6. Particle size distribution of the freshly shredded compost on the 21/01/04

Mesh size, mm	Weight retained, %	Cumulative, %
0 (Pan)	9.2	9.2
0.5	11.0	20.0
1	10.4	30.5
1.4	13.6	44.1
2.8	9.8	53.9
5.6	4.7	58.6
8	41.4	100.0
16	0	100.0

On the 21st of January 2004 the vessel was filled with 179.5 kg of freshly shredded green waste. As with previous trials once the initial measurements had been taken the material was allowed to settle in the column for a period of two weeks. The initial bulk density of this material was 376.2kgm^{-3} after settling this had increased to 393.9kgm^{-3}. A particle size distribution of the material was taken and this is shown in Table 4-6, the 50th percentile particle size was approximately 4.2 mm.

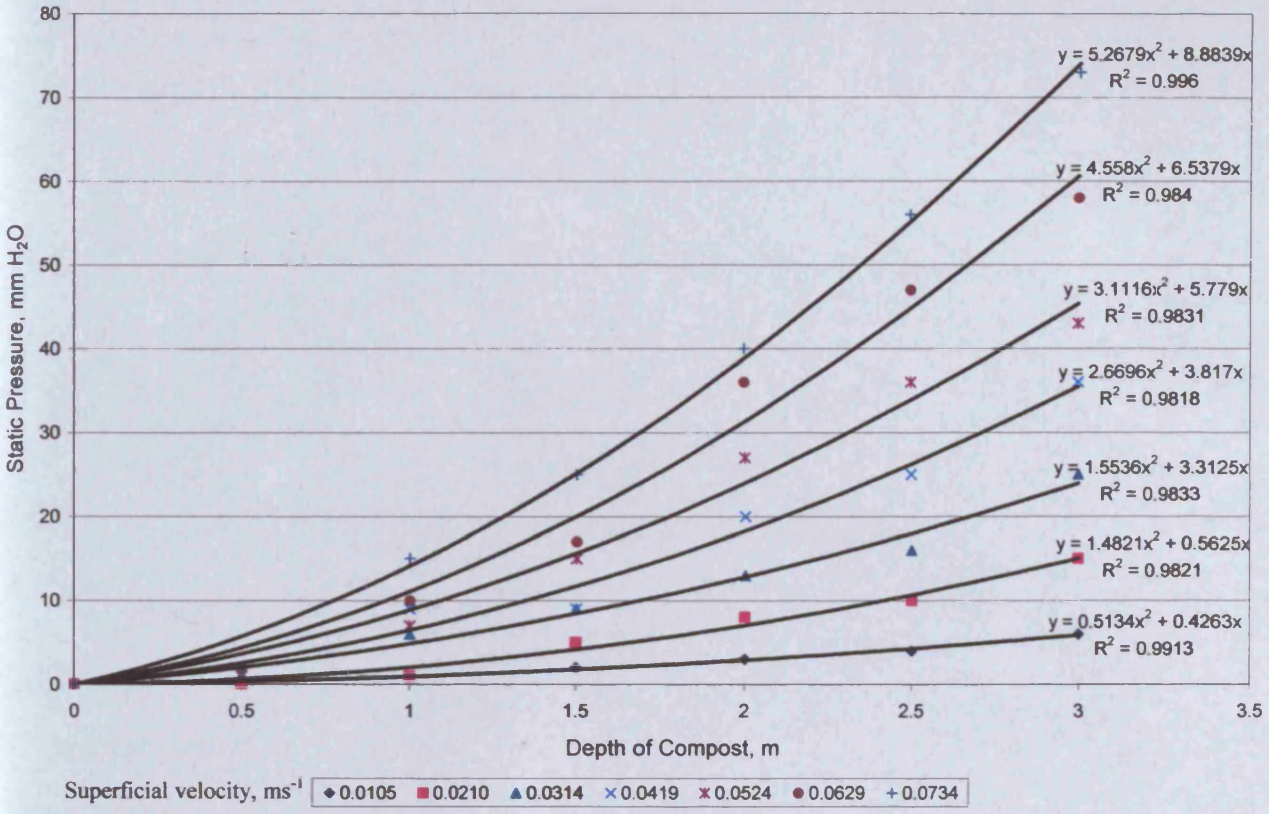

Figure 4.17. Static pressure against depth for the material shredded on 21/01/04

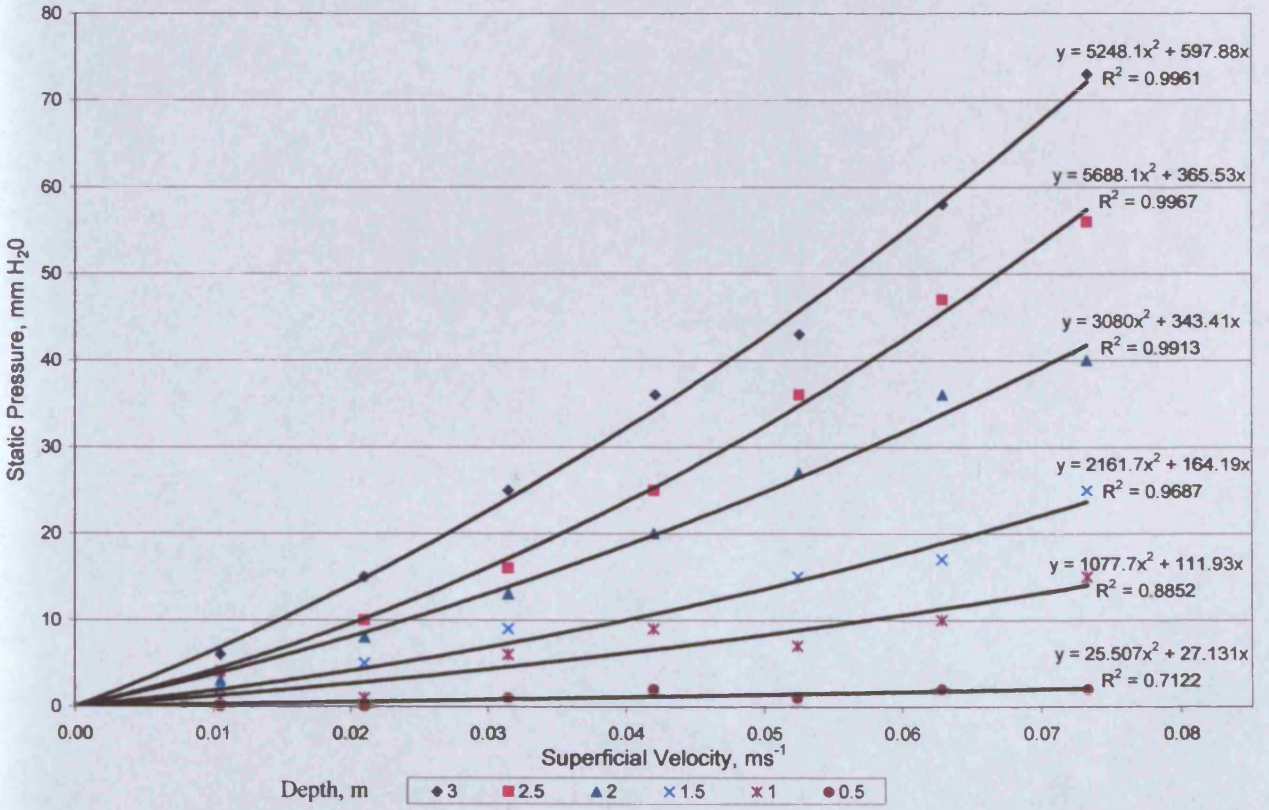

Figure 4.18. Static pressure against superficial velocity for the material shredded on 21/01/04

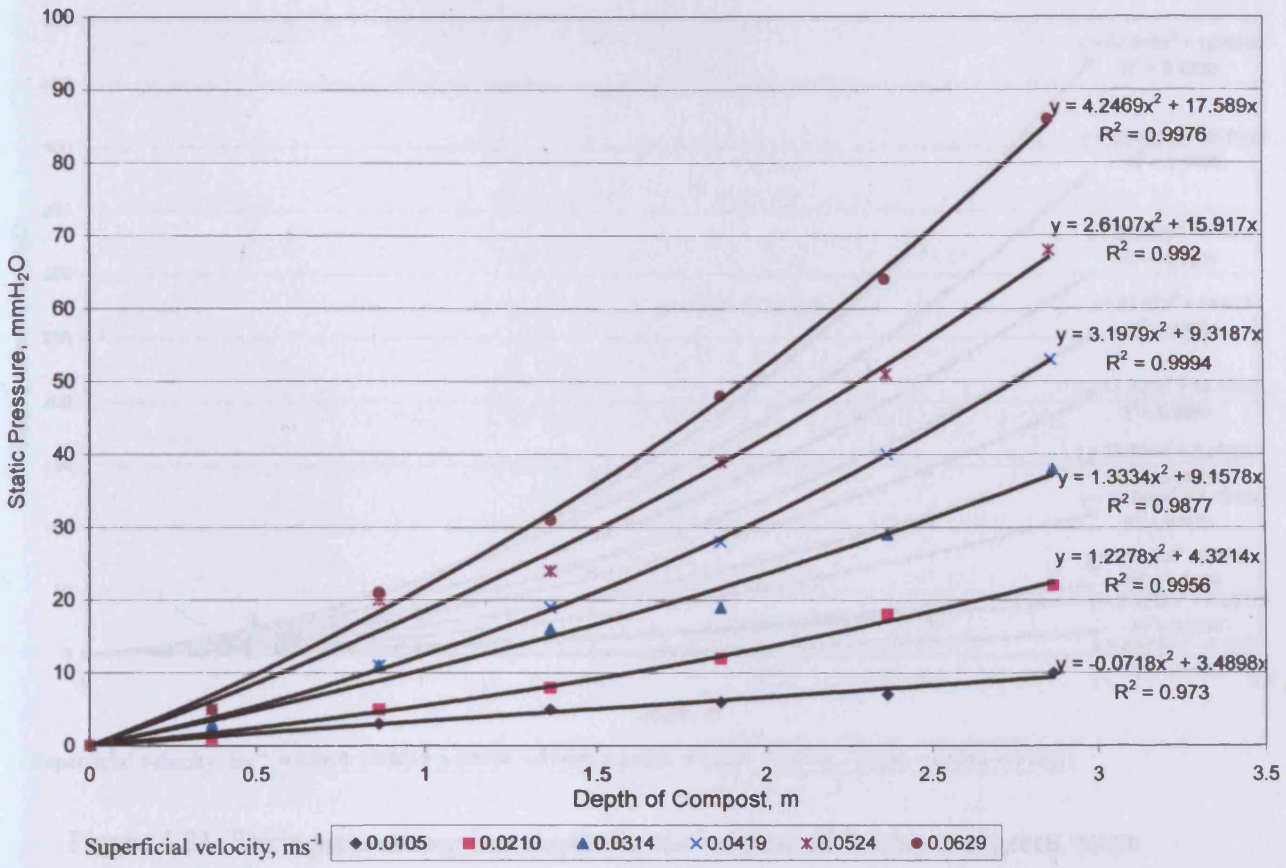

Figure 4.19. Static pressure against depth for the material shredded on 21/01/04 after 2 weeks settling

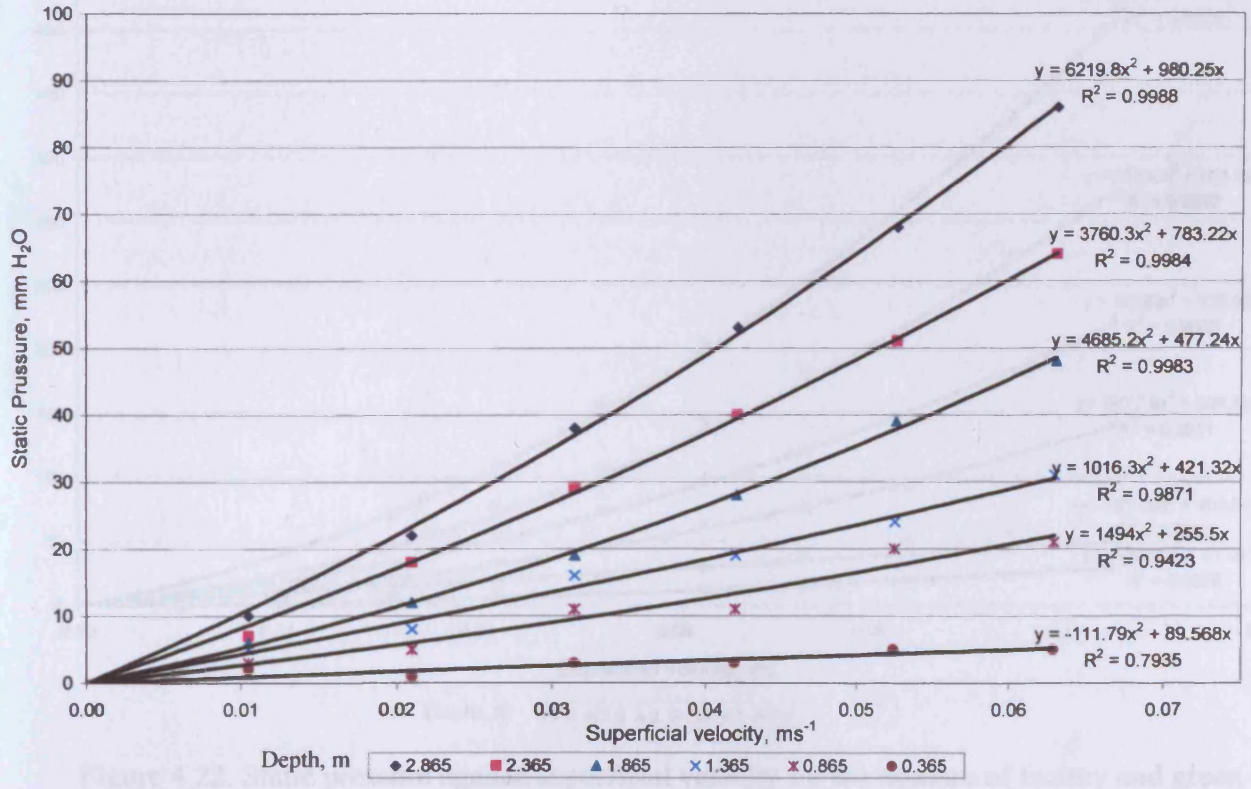

Figure 4.20. Static pressure against superficial velocity for the material shredded on 21/01/04 after 2 weeks settling

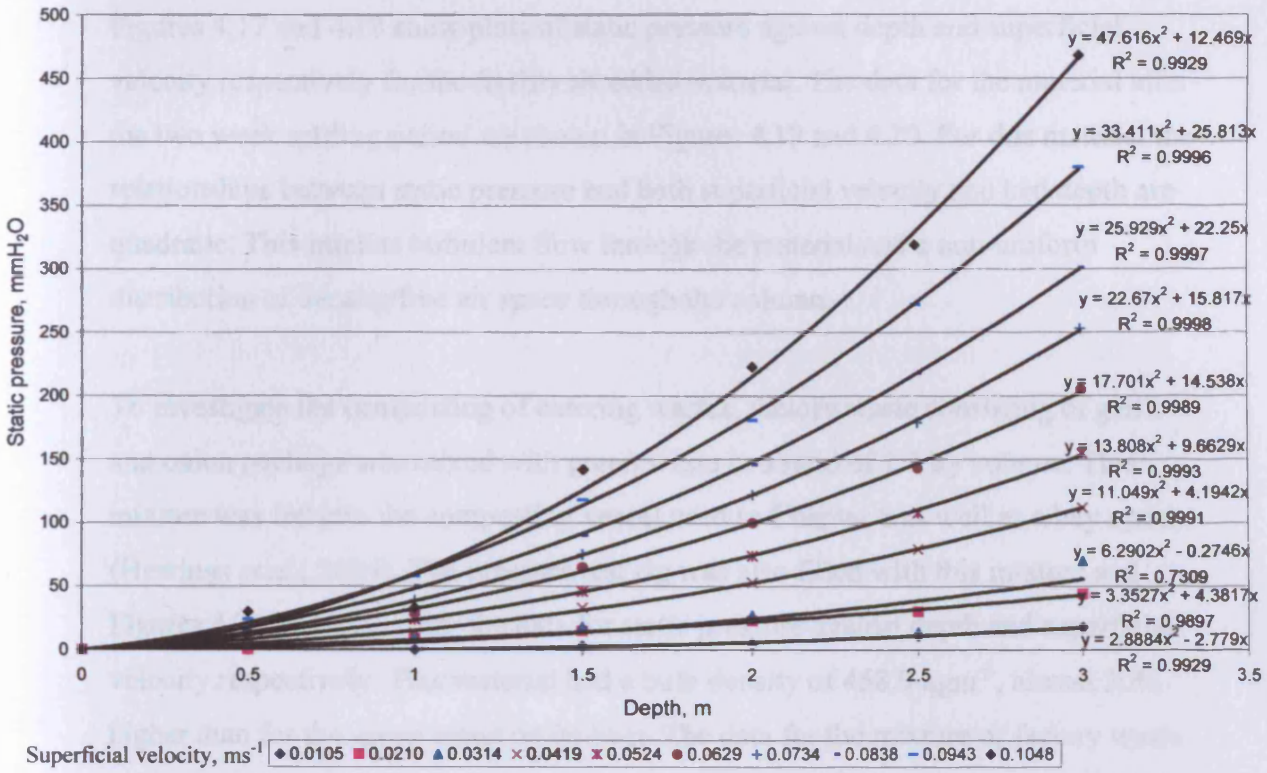

Figure 4.21. Static pressure against depth for the mixture of factory and green waste

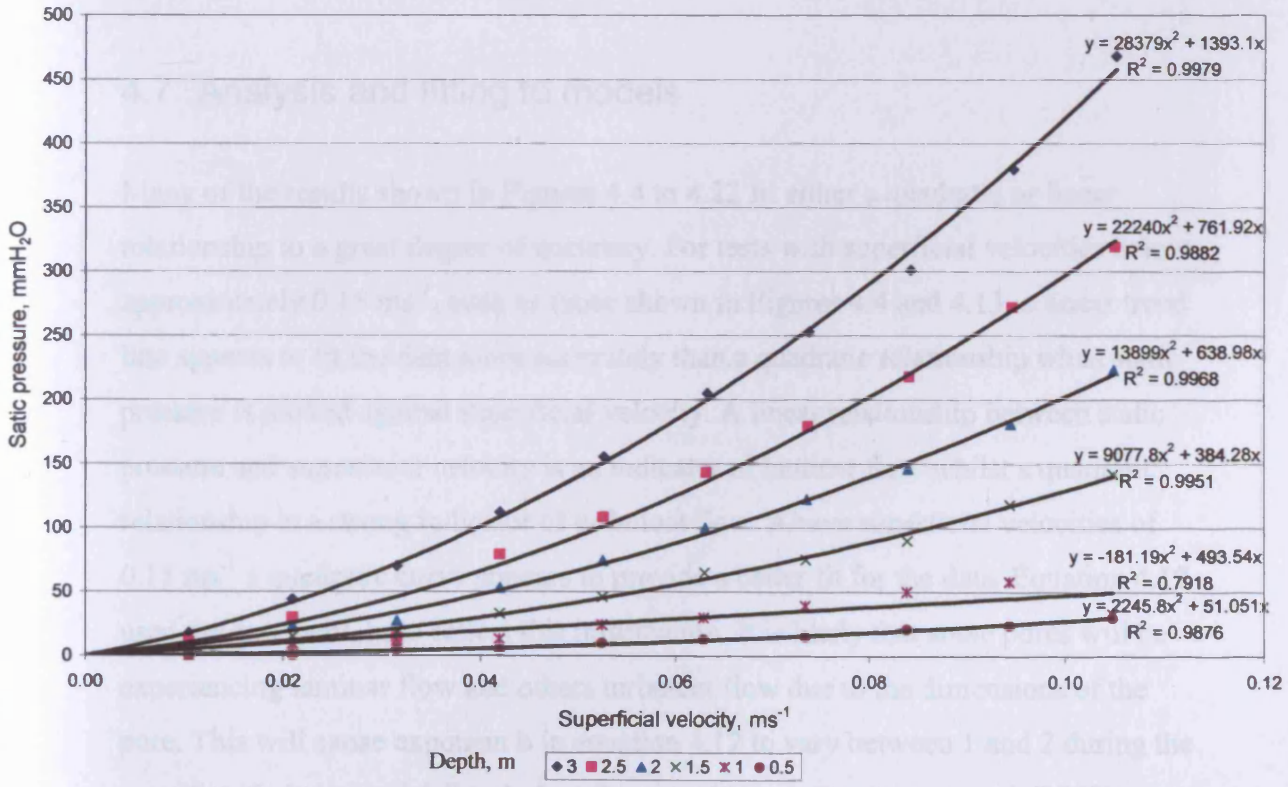

Figure 4.22. Static pressure against superficial velocity for the mixture of factory and green waste

Figures 4.17 and 4.18 show plots of static pressure against depth and superficial velocity respectively for the freshly shredded material. The data for the material after the two week settling period are shown in Figures 4.19 and 4.20. For this material the relationships between static pressure and both superficial velocity and bed depth are quadratic. This implies turbulent flow through the material and a non-uniform distribution of density/free air space through the column.

To investigate the composting of catering wastes, factory waste consisting of garlic and onion peelings was mixed with green waste in a ratio of 1:2 by volume. This mixture was fed into the composting vessel used in Chapter 6 as well as a bay system (Hewings *et al.*, 2004). The pressure test rig was also filled with this mixture and Figures 4.21 and 4.22 show the data for static pressure against depth and superficial velocity respectively. This material had a bulk density of 458.9 kgm^{-3}, almost 50% higher than for the green waste on its own. The data for the mixture of factory waste and green waste also shows quadratic relationships between static pressure and both the bed depth and superficial velocity.

4.7 Analysis and fitting to models

Many of the results shown in Figures 4.4 to 4.22 fit either a quadratic or linear relationship to a great degree of accuracy. For tests with superficial velocities below approximately 0.15 ms^{-1}, such as those shown in Figures 4.4 and 4.13, a linear trend line appears to fit the data more accurately than a quadratic relationship when static pressure is plotted against superficial velocity. A linear relationship between static pressure and superficial velocity is an indicator of laminar flow whilst a quadratic relationship is a strong indicator of turbulent flow. Above superficial velocities of 0.15 ms^{-1} a quadratic curve appears to provide a better fit for the data. Equation 4.12 used the exponent, b, to reflect this information. It is likely that some pores will be experiencing laminar flow and others turbulent flow due to the dimensions of the pore. This will cause exponent b in equation 4.12 to vary between 1 and 2 during the transitional phase until full turbulent flow is achieved. Barrington *et al.* (2002) reports

laminar flow through grains for superficial velocities of up to 0.02 ms^{-1} with fully turbulent flow occurring at superficial velocities of over 1 ms^{-1}.

In the data shown in Figures 4.5, 4.14, 4.17, 4.19 and 4.21 the plots of static pressure against depth give quadratic relationships whilst the other tests give linear relationships. Where the relationship between static pressure and depth is linear this suggests that the material compresses uniformly implying a uniform distribution of free air space throughout the column. In Equation 4.12 this is represented by exponent, a. If a is equal to 1 then the material has not been compressed, whilst if values of greater than 1 are recorded then compression has occured. This is essentially an indication of the bulk modulus of the material. Keener *et al.* (1993) demonstrated that exponent a, has a value of 1 for composts with a moisture content of up to 60%(w.b.), whilst Das and Keener (1997) showed that free air space through the pile decreased with pile depth for moisture contents as low as 42.8%(w.b.).

The screened material, shown in Figures 4.14 and 4.16, was considerably denser than the shredded green waste used for the majority of the other tests. Figure 4.14 and 4.16 show that the static pressure increased quadratically with increasing depth. This implies that the material compressed non uniformly under its own weight meaning that the compost at the base of the column had less free air space, as observed by Das and Keener (1997). To show this increased resistance to aeration in the screened waste a comparison with freshly shredded waste is presented in Figure 4.23. The density of the freshly shredded waste was 366.8 kgm^{-3} whilst the screened waste had a density of 893.4 kgm^{-3}.

Both curves shown in Figure 4.23 are quadratic-indicating turbulent flow for both cases. However, the denser screened material gives far greater static pressures even though the column is slightly less deep than for the shredded material. In addition the denser material may well have greater quantities of volatile solids per cubic metre than the less dense material. The aeration requirements presented in Chapter 3 are a function of both composting rate and density. Because of this the increased density would require a higher superficial velocity which would cause an increase in the required static pressure. This would have a significant effect on both the equipment used to supply the air and the running costs of the equipment.

As discussed in Chapter 2 the particle size distribution has an effect on the bulk density. The European treatment regime for sanitisation of Animal By-Products requires a maximum particle size of 12mm, although this is slightly larger than the screened size of 10mm it will have a significant effect on the bulk density and the available surface area dramatically increasing the power requirement for any fans on site. The effect of reduced particle size is also seen in Chapter 5 where the addition of chicken litter significantly increases the density of shredded green waste and reduces the airflow within the windrow. Figure 4.2 shows the relationship between free air space and bulk density for changing moisture content and this is reinforced by Agnew and Leonard (2003). The Ergun equation, Equation 2.1, shows static pressure as being a function of both the particle size and the free air space. As both affect the bulk density it is reasonable to attempt to plot the static pressure as a function of the composts` bulk density.

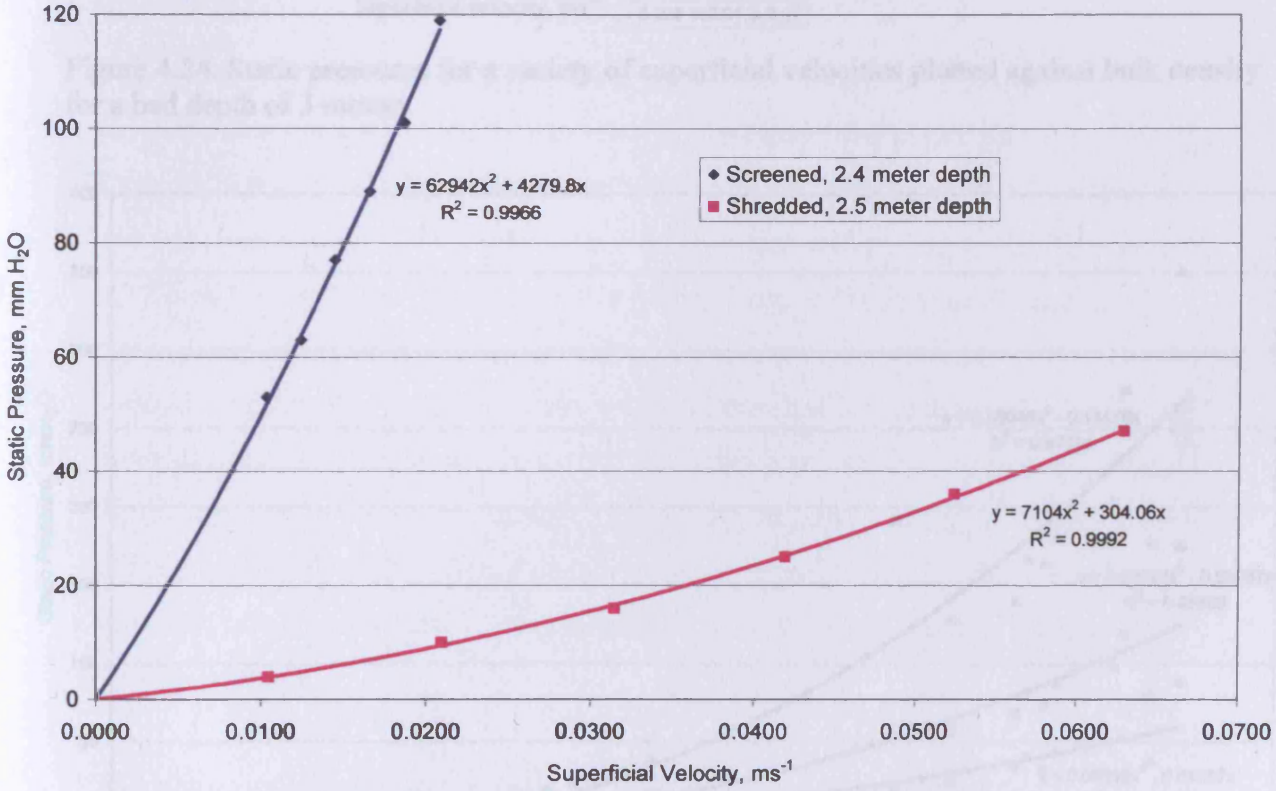

Figure 4.23. Comparison of static pressure required to aerate freshly shredded material and compost screened to a 10mm particle size

Microsoft Excel was used to both create and analyse the trend lines shown in Figures 4.4 to 4.22. Initially the equations relating static pressure and superficial velocity for a depth of 3 metres were found. The calculations from Chapter 3 allow reasonable flow

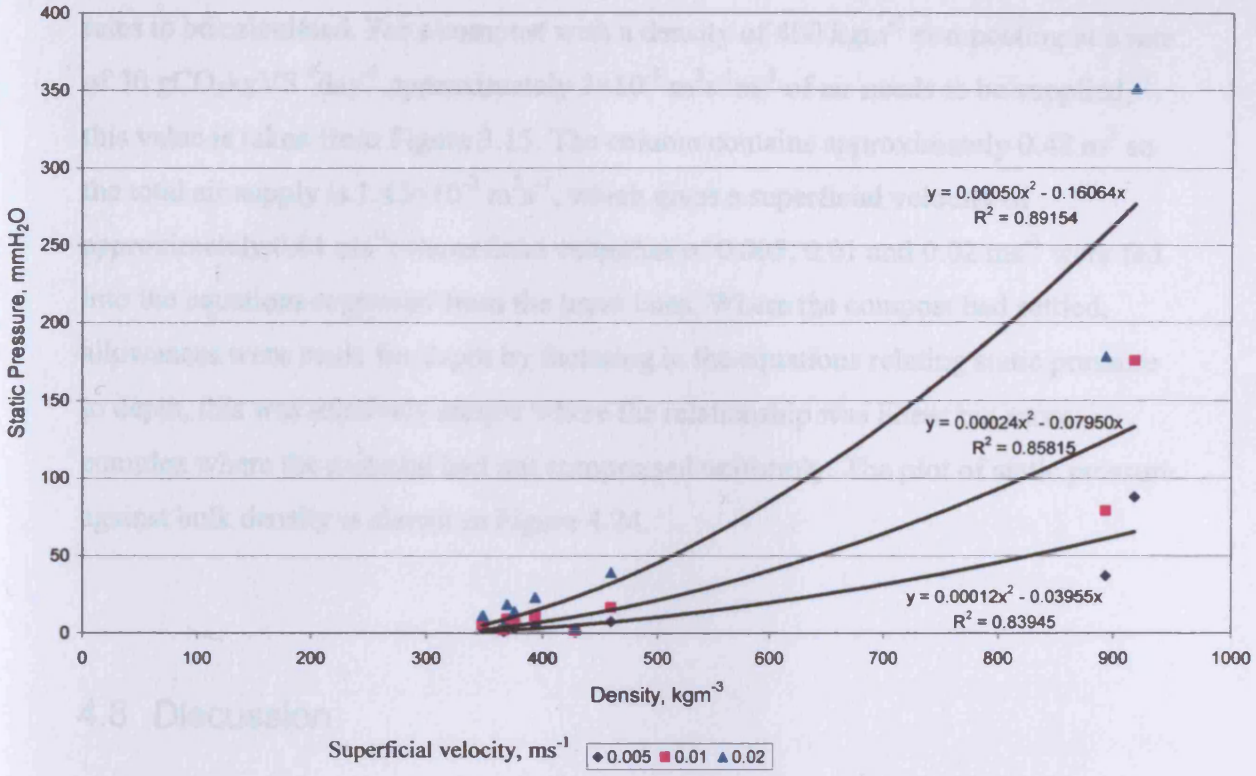

Figure 4.24. Static pressures for a variety of superficial velocities plotted against bulk density for a bed depth of 3 metres

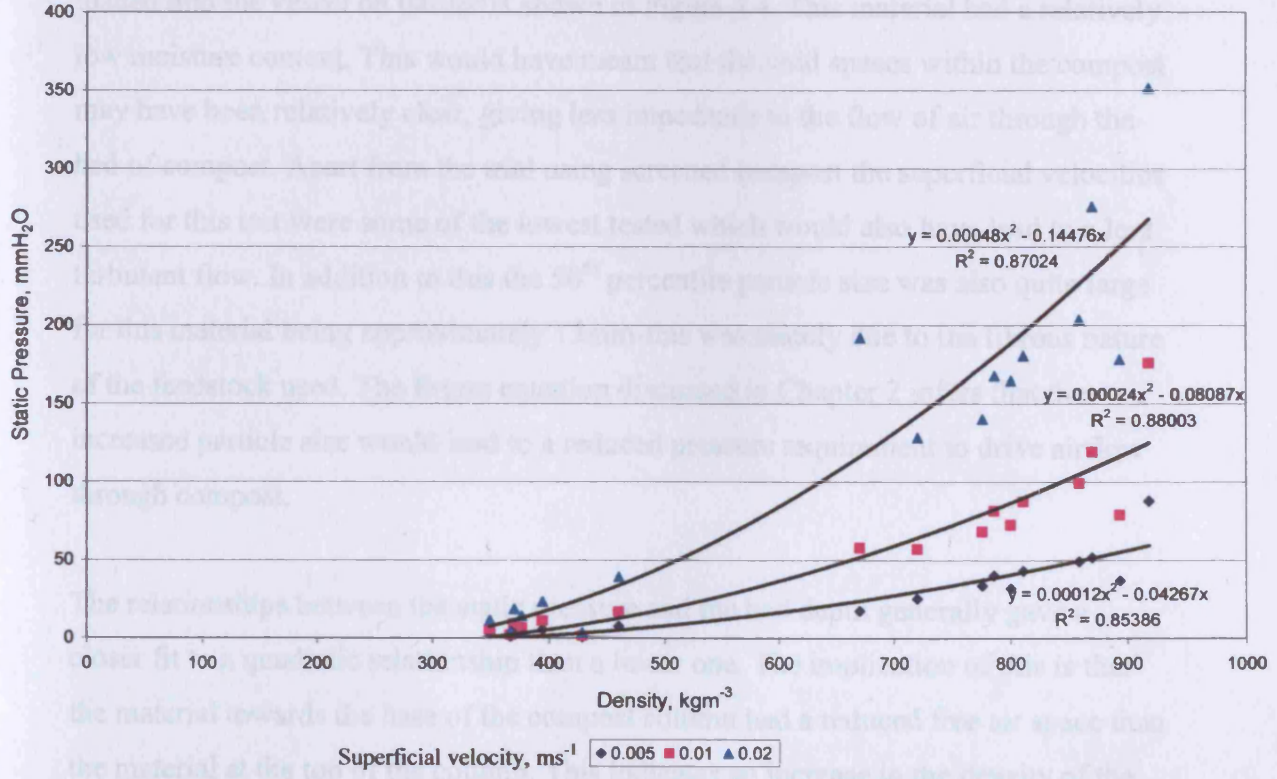

Figure 4.25. Static pressures for a variety of superficial velocities plotted against bulk density for a bed depth of 3 meters including data from Mu and Leonard (1999) and Giner and Denisienia (1996)

rates to be calculated. For a compost with a density of 400 kgm^{-3} composting at a rate of 30 $gCO_2kgVS^{-1}day^{-1}$ approximately 3×10^{-3} $m^3s^{-1}m^{-3}$ of air needs to be supplied, this value is taken from Figure 3.15. The column contains approximately 0.48 m^3 so the total air supply is 1.43×10^{-3} m^3s^{-1}, which gives a superficial velocity of approximately 0.01 ms^{-1}. Superficial velocities of 0.005, 0.01 and 0.02 ms^{-1} were fed into the equations regressed from the trend lines. Where the compost had settled, allowances were made for depth by factoring in the equations relating static pressure to depth, this was relatively simple where the relationship was linear but more complex where the material had not compressed uniformly. The plot of static pressure against bulk density is shown in Figure 4.24.

4.8 Discussion

The majority of the relationships between the static pressure and the superficial velocity fitted a quadratic model very closely. One exception to this was the material loaded into the vessel on 04/06/03 shown in Figure 4.4. This material had a relatively low moisture content. This would have meant that the void spaces within the compost may have been relatively clear, giving less impedance to the flow of air through the bed of compost. Apart from the trial using screened compost the superficial velocities used for this test were some of the lowest tested which would also have lead to a less turbulent flow. In addition to this the 50^{th} percentile particle size was also quite large for this material being approximately 15mm-this was mainly due to the fibrous nature of the feedstock used. The Ergun equation discussed in Chapter 2 infers that the increased particle size would lead to a reduced pressure requirement to drive airflow through compost.

The relationships between the static pressure and the bed depth generally gave a closer fit to a quadratic relationship than a linear one. The implication of this is that the material towards the base of the compost column had a reduced free air space than the material at the top of the column. This indicates an increase in the density of the compost at the base as the material settles under its own weight.

A smaller particle size within the compost gives a larger total surface area within the bed. The larger surface area causes increased levels of friction. The freshly shredded material used to fill the vessel on the 18th of November, shown in Figures 4.9 and 4.10, gave relatively low static pressures in comparison to the freshly shredded material used on the 4th of June 2003 (Figures 4.4 and 4.5). For example the static pressure induced by a 3 metre column of compost at a superficial velocity of approximately $0.15ms^{-1}$ was $142mmH_2O$ in Figure 4.4 and $50mmH_2O$ in Figure 4.9. The densities of these materials are very similar at $370kgm^{-3}$ and $366.8kgm^{-3}$. The significant difference in the static pressures could be due to the reduced proportion of fine material in this batch. Approximately 3.1% of the material used on the 18th of November was retained in the 1mm sieve or smaller in size whilst the material shredded on 04/06/03 had 8.6% retained in the 1 mm sieve or smaller. The results shown in Figures 4.17 and 4.18 further reinforce the importance of particle size. These show the static pressures for a material with 30.5% of the weight retained in the 1mm sieve or smaller. The static pressure recorded for a 3 metre column of this material was $73mmH_2O$ at a much lower superficial velocity of $0.01ms^{-1}$.

The screened waste trial produced very high static pressures for relatively low superficial velocities. For example 119 mmH_2O for a 2.4 metre column at a superficial velocity of $0.021ms^{-1}$this is compared to a 2.5 metre column of shredded waste in Figure 4.23. The reduced particle size had the effect of increasing the bulk density to over twice that of the freshly shredded composts. The reduced particle size dramatically increased the bulk density and greatly reduced the free air space. The increase in static pressure requirements for increased quantities of fine material is in agreement with the work carried out by Ergun (1952) and McGurkin *et al.* (1999) as well as with the work on grains performed by Giner and Denisiena (1996).

It is important to consider the cost implications of design. If the wrong power of fan is sourced at the construction stage replacement with a more powerful fan can be costly, alternatively over specification may cause unnecessary expense at an early stage. It may also be likely that the equipment will not be operating at its most efficient duty point. Running costs may also be an important issue. A column of compost 3 metres high with a bulk density of $400kgm^{-3}$ would require a superficial velocity of $0.01ms^{-1}$, Figure 4.24 shows that this air would need to be supplied at a static pressure of

approximately 10 mmH_2O. For a compost of density 800 kgm^{-3} a greater quantity of air would be required. Figure 3.15 states that 6×10^{-3} $m^3s^{-1}m^{-3}$ of air would be required for the denser compost to allow a composting rate of 30 $gCO_2kgVS^{-1}day^{-1}$- this gives a superficial velocity of 0.02 ms^{-1}. Figure 4.24 shows that a static pressure of approximately 100 mmH_2O would be required to supply this air. As fan power is a function of both flow rate and static pressure it can be determined that the denser compost would require approximately 40 times the energy to aerate than the less dense compost. This increase in power may cause problems with sites that have chosen to use the 12mm treatment profile to ensure sanitisation of the compost.

The figures recorded for static pressure were similar to those found by other researchers. For example Sadaka *et al.* (2002) recorded a pressure drop of approximately 45 mmH_2O at a depth of 1.5 metres and superficial velocity of 0.143 ms^{-1}. Figure 4.7 shows at a depth of 1.5 m and superficial velocity of 0.149 ms^{-1} a static pressure of 36 mmH_2O was recorded. The material used by Sadaka *et al.* (2002) had a slightly higher bulk density of 387kgm^{-3} rather that 349 kgm^{-3} for the material shown in Figure 4.7 which may explain the higher static pressures.

The graph shown in Figures 4.24 shows the variation in static pressures for a 3 metre column of compost with the compost's bulk density. The data points were calculated using the trend lines from figures 4.2 to 4.22. There is a quadratic relationship between the static pressures and the bulk density. In Figure 4.25 further data from models presented by Mu and Leonard (1999) and Giner and Denisienia (1996) have been added. The majority of the added data were in a range not covered by the tests performed at the CERT composting facility in Carmarthen. The data further reinforce the quadratic relationship and only slightly modify the trend lines. The Ergun equation includes terms for the particle size and the proportion of free air space. As these parameters change the bulk density of the material will be affected. The bulk density of a material is relatively easy to determine and as was seen in Chapter 3 will affect the actual quantity of aeration required by the composting process. Because of the ease of determination it is an ideal parameter for compost practitioners and facility designers to use for calculating aeration requirements.

4.9 Conclusions

Decreased particle size and increased bulk density increase the required static pressures.

The bulk density of compost appears to have a large affect on the airflow resistance and cost of aeration.

An allowance should be made at the design stage of composting equipment for the compaction of the compost.

An understanding of the physical properties of the feedstock at an early stage will allow fairly accurate design of composting equipment, this may reduce refitting or initial costs.

There are certain cases where a laminar model for static pressure against superficial velocity appears to give the best fit, however generally turbulent flow models were more accurate.

5 Windrow Composting Trials

5.1 The CERT Composting Facility

The Carmarthenshire Environmental Resources Trust (CERT) composting facility was originally constructed as a research facility for the composting of green waste in windrows. The site layout is shown in Figure 5.1. It consists of a large concrete pad with a covered area (C) approximately 50 metres long by 30 metres wide. The site was equipped with a Seko 600/200 tractor driven shredder, a Menart SP4000 tractor powered windrow turner, a Menart screen and two tractors-one with a front end loader. Photographs of these are shown in Figure 5.2. The building was capable of housing 4 windrows which were approximately 1.7 metres high, 4 metres wide and 50 metres long.

Using the equipment shown in Figure 5.2 the building was capable of holding 4 windrows. In order to meet the quality assurance aspect of BSI PAS 100 (2002) each of the 4 locations for a windrow within a building was given a number. Each consecutive windrow was given a letter, for example the first windrow in position 1 was called W1A and the second was W1B. This allowed various batches to be recognised and traced from material delivered to product sold. The same designation is used for the green waste windrows described in Section 5.3.

5.2 The Composting Rate

Often with much of composting the only parameter being measured is the temperature but this however is highly dependant upon not only the quantities of heat being produced but also the heat being lost by the compost as was discussed in Chapter 3. It therefore may be the case that temperature is not a good indicator of the composting activity and it is important to find an appropriate measure of the activity. This would also allow comparison between different techniques and methods allowing optimum conditions to be found.

C.E.R.T COMPOSTING FACILITY

NANTYCAWS

CARMARTHEN

A	WASTE RECEPTION AND INSPECTION AREA
B	SHREDDING AND SCREENING AREA
C	COMPOST BUILDING
D	LEACHATE TANK CAPACITY 35000 LITERS
E	STORAGE OF NON COMPOSTABLE WASTE
F	FIRE FIGHTING EQUIPMENT
S	SPILLAGE CONTROL EQUIPMENT
W	WATER SUPPLY
O	SITE OFFICE
P	LEACHATE RE-CYCLING PUMP
G	ATTENUATION TANK
H	INTERCEPTOR TANK
J	MATURATION AREA
K	COVERED WINDROWS (SUMMER ONLY)
L	WOOD STORAGE

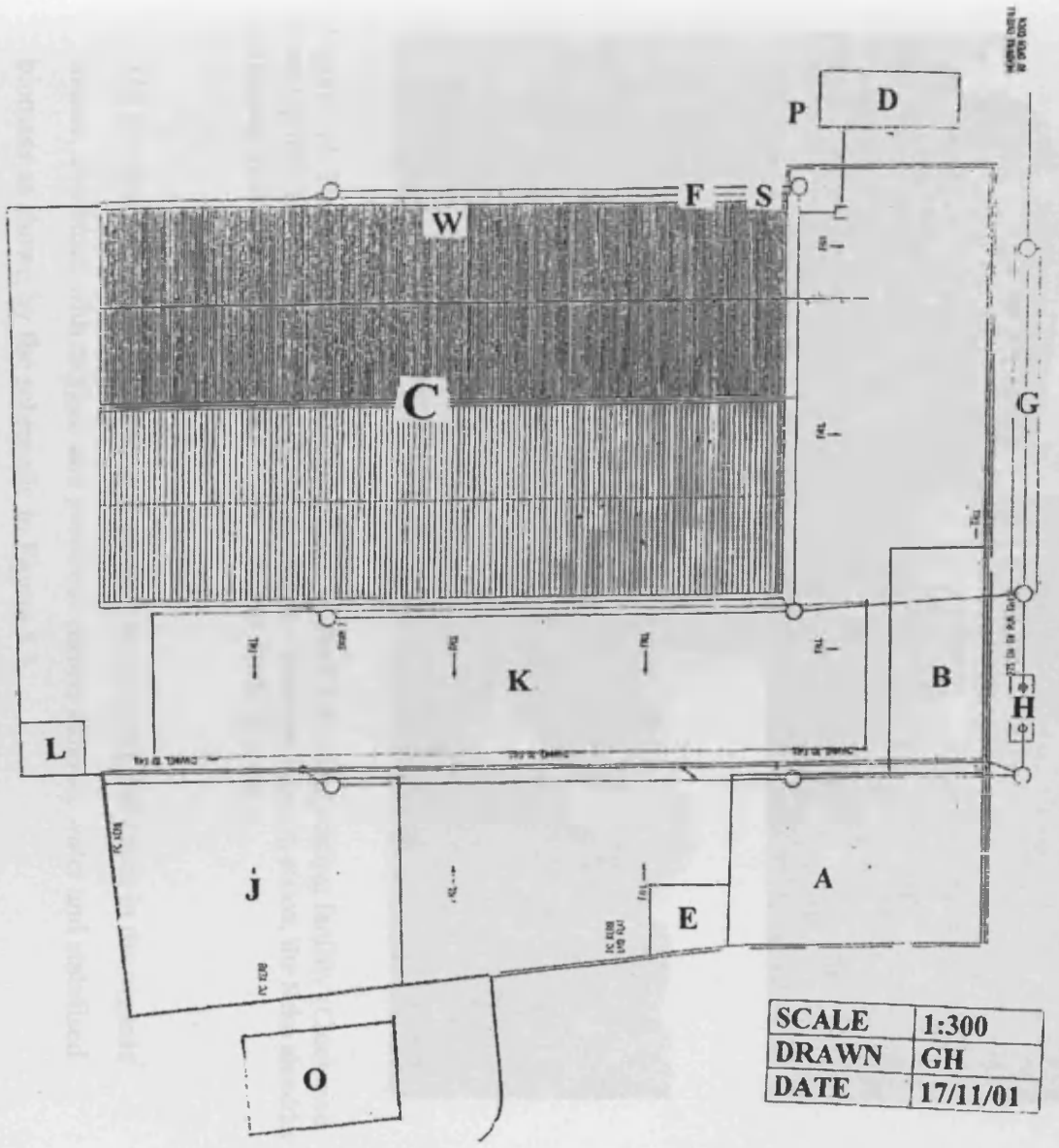

Figure 5.1. Layout of CERT composting facility

Figure 5.2. The composting equipment used on the CERT composting facility (Clockwise from top left: The Menart trommel screen, the Menart windrow turner in action, the Seko shredder unloading freshly shredded material and the shredder from the side)

The production of compost from a feedstock is a process that takes in the organic matter, combines with oxygen and produces carbon dioxide, water and stabilised biomass as shown by the schematic in Figure 5.3.

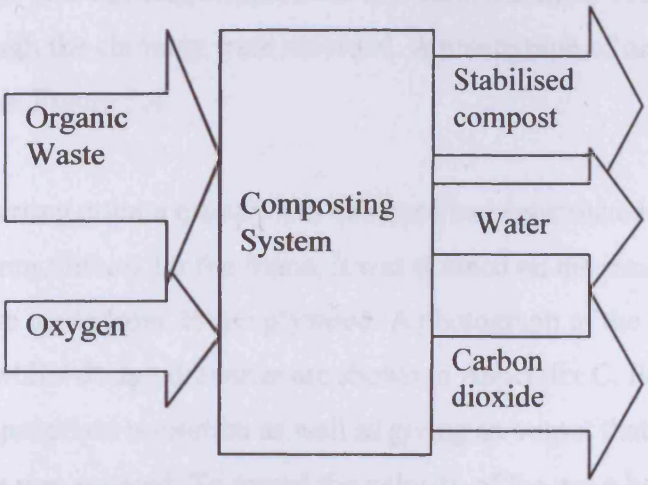

Figure 5.3. Schematic of the composting process, showing main inputs and outputs

By measuring one of these parameters the rate at which the material is composting can be quantified. The simplest of all of these to measure is either the rate at which oxygen is utilised or the rate at which carbon dioxide is produced. It is not a new concept to use these two parameters as an indicator of composting activity as they are often used in small scale stability tests such as those discussed in Chapter 2. However, to the knowledge of the author they have not been used in-situ to monitor the reaction rate of the composting material.

By monitoring the quantity of carbon dioxide in the exhaust air leaving the composting system and combining this with the air temperature and the volumetric flow rate the rate of production of carbon dioxide can be found. It is then useful to base this on the mass of volatile solids present within the composting mass as this is the fraction that is being stabilised, the result is a rate measured in grams of carbon dioxide evolved per kilogram of initial volatile solids per day or g CO_2 $kgVS^{-1}$ day^{-1}.

5.2.1 The Canopy System

The canopy system was developed in order to monitor the composting rate. Initial trials were carried out simply by using a tarpaulin stretched over several planks of wood which were supported by the windrow. A length of 110mm soil pipe was used as a chimney. The velocity, temperature and carbon dioxide concentration of the gas exiting through the chimney were recorded. A photograph of one of the initial trials can be seen in Figure 5.4.

From this starting point a canopy was designed and constructed from wood, using 50mm x 50mm timbers for the frame, it was skinned on the inside with chipboard and the ends were made from 25mm plywood. A photograph of the canopy is shown in Figure 5.5. whilst design drawings are shown in Appendix C. Equipment capable of giving an appropriate resolution as well as giving an output that could be connected to a data logger was sourced. To record the velocity of the gas a hot film anemometer (E+E Electronik series EE65 or EE66) was mounted in the centre of the chimney. A thermistor (RS 813-828) was mounted in the chimney to record the temperature of the

gas. Both the anemometer and thermistor were connected to a data logger (Delta T, DL2e) as was a type k thermocouple probe which was inserted into the core of the compost windrow to monitor the core temperature. The carbon dioxide concentration was measured using a separate meter with inbuilt logging capacity (Gas Data PCO_2). The data were then downloaded to a laptop computer for off line analysis using an RS232 serial connection and Delta T's Ls2win software.

Figure 5.4. A photograph of the tarpaulin with equipment for monitoring gas velocity, temperature and carbon dioxide concentration in the foreground

Figure 5.5. A photograph of the completed canopy system

5.2.2 Analysis of Data

The data recorded by the carbon dioxide meter and the logger were downloaded and fed into an Excel spreadsheet. The rate of carbon dioxide release is calculated by

$$\dot{M}_{CO2} = \frac{P \times \overline{U} \times A \times \Delta E_{CO2}}{R_{CO2} \times T_g \times 100 \times 1000} \tag{5.1}$$

where P is the atmospheric pressure 101325 Pa,

$\overline{U}$ is the mean velocity of gas through the chimney in m/s,

A is the cross sectional area of the chimney $8.22 \times 10^{-3} m^2$,

ΔE_{CO2} is the change in concentration of carbon dioxide in %v/v (between inlet and outlet),

R_{CO2} is the specific gas constant for carbon dioxide 188.96 Nm/kg K,

T_g is the temperature of the gas being released in Kelvin,

100 is used to convert the percentage of carbon dioxide to a concentration and 1000 converts from kilograms to grams

Equation 5.1 can be simply derived. First the volumetric flow rate through the chimney is calculated using the cross sectional area and the mean velocity. Turbulent flow is assumed through the chimney meaning that the mean velocity is equal to 0.82 multiplied by the maximum (centreline) velocity (Massy, 1989). The volumetric flow rate of carbon dioxide is then found by multiplying by the carbon dioxide concentration. The volumetric flow rate of carbon dioxide is converted into a mass flow rate by use of the perfect gas equation which gives temperature correction.

The mass of volatile solids present within the compost is determined in accordance with British Standards BS EN 13040:2000 and BS EN 13039:2000 (BSI, 2000b; 2000c). Generally the initial volatile solids content of the green waste was found to be in the range of 50-70% (d.b.). The spreadsheet was capable of reducing the volatile solids content remaining in the material as carbon dioxide left the windrow. The spreadsheet can also be used to determine the enthalpy and specific volume of the inlet and outlet air allowing heat lost via the air flow through the windrow to be calculated.

It is important to take into account the measurement errors encountered to give an indication of the accuracy of the results. The respiration rate is calculated by combining the gas velocity, temperature and carbon dioxide content with the mass of volatiles solids underneath the canopy. The usage of high resistance thermistors for the ambient and flue temperatures allows the minimisation of errors due to cable resistance. The thermistors used had a negative temperature coefficient meaning the resistance fell with increasing temperature, their resistance was 10 kΩ at 25°C with an accuracy of ±0.5°C. To measure the core temperature a type k thermocouple was used. A thermocouple gives a voltage output proportional to the difference in temperature between its hot and cold junctions and in order to ensure accuracy of this measurement a reliable cold junction is required. For these measurements the data logger's internal cold junction was used. The error of the hot film anemometer used to measure the gas velocity was $\pm 0.3 ms^{-1}$ or ±3% of the value; the anemometer was designed to allow for misalignment of up to 20 degrees. The thermistors, thermocouple and anemometer were all connected to the data logger for testing and calibration. The carbon dioxide meter was a separate unit capable of logging data, the accuracy of the meter was ±2% of full scale. Variations in static pressure occur throughout the day and these will have an effect on Equation 5.1. However these variations are unlikely to exceed 3%.

In order to analyse the large amount of data that were collected during the monitoring of the windrows some of the shorter sampling periods were averaged together to give a value with less noise than the raw data. It was of interest to test whether two variables were related; to do this the correlation between different variables was calculated and used for comparison. The correlation coefficient is the covariance of two series divided by the product of the standard deviations of the two data sets. It indicates the strength of a linear relationship between the two variables in question and is calculated by,

$$\rho_{xy} = \frac{\frac{1}{n}\sum_{j=1}^{n}(x_j - \mu_j)(y_j - \mu_j)}{\sigma_x \sigma_y}$$

(5.2 (after Bendat and Piersol, 1971))

where μ_x is the mean value of data set x,

μ_y is the mean value of data set y,

ρ_{xy} is the correlation coefficient between data set x and data set y,

σ_x is the standard deviation of data set x,

σ_y is the standard deviation of data set y and

x_j and y_j are data within the data sets.

A negative value indicates that as one variable rises the other will fall, whilst a positive value means that the two series move together. The absolute value of a correlation coefficient cannot exceed 1.

5.3 Green Waste Windrows

5.3.1 Introduction

In order to get a standard for comparison with other waste types and treatment processes several windrows constructed of green waste as described in Section 5.1 were monitored using the canopy system as described in Section 5.2.1. The green waste used came from civic amenity sites in the Carmarthenshire area.

5.3.2 Results

Although a large number of windrows were monitored the most coherent data are for two windrows in particular, windrow W1I and windrow W2F. The results for each of these windrows are presented in individual sections below. Much of the other data that were recorded consist of either only carbon dioxide measurements or were subject to equipment failure. Although the monitoring of any system is likely to interfere with the behaviour of the system, the daily monitoring required on site showed core temperatures beneath the canopy to be similar to the rest of the windrow. The canopy was also moved along the windrow showed similar behaviour at several points of the windrow.

5.3.2.1 Windrow W1I

Windrow W1I was constructed using the green waste that was delivered to the composting site between the 3rd and 10th of October 2002 and was monitored from the

18th of October, when the windrow was approximately 1 week old, until the 29th of November. It was turned on the 23rd of October, the 30th of October, 12th of November, the 20th of November and the 27th of November, creating 6 periods between turning events. As the windrow was already one week old when the monitoring period had started the core had already heated up and was above 60°C for most of the time it was monitored. The data for the monitoring phase were recorded at five minute intervals and as such contained a large quantity of noise and in order to filter out some of this noise, 25 minute averages have been taken and are presented in the following figures.

Figure 5.6 shows the data recorded during Period 1 for windrow W1I, between the 18th and 23rd of October 2002. During this period the airspeed through the flue varied between 0.89 and 1.83 ms^{-1} whilst the CO_2 content of the exhaust gas varied between 0.54 and 1.38 percent causing the composting rate to vary between 7.9 and 37.8 g CO_2 kg VS^{-1} day^{-1}. This is a large range and greater than the range for either the airspeed or CO_2 content alone. During this period the core temperature experiences a generally upwards trend until approximately midday on the 22nd of October when there is a small sharp increase followed by a larger fall. This rise and fall in the core temperature coincides with an increase in the CO_2 concentration observed in the chimney and some erratic behaviour in the readings from the hot wire anemometer (which has just suffered a breakdown). The composting rate, which had been approximately $20gCO_2kgVS^{-1}day^{-1}$ throughout much of this period, fell to approximately $12gCO_2kgVS^{-1}day^{-1}$ after this brief rise and fall in the core temperature. The airflow may have been increased due to increased core temperatures, strong prevailing winds or weather pressure fronts. The increased airflow could have lead to increased oxygen availability within the windrow. But the high temperatures experienced may have had a detrimental effect upon the microbial population within the compost. As would be expected both airflow and CO_2 concentration have strong correlations with the respiration rate, these returned correlation coefficients of 0.65 between airflow and respiration rate and 0.87 between CO_2 concentration and respiration rate.

The ambient and flue temperatures are also strongly correlated with each other, this is to be expected as the difference between ambient and flue temperatures gives an

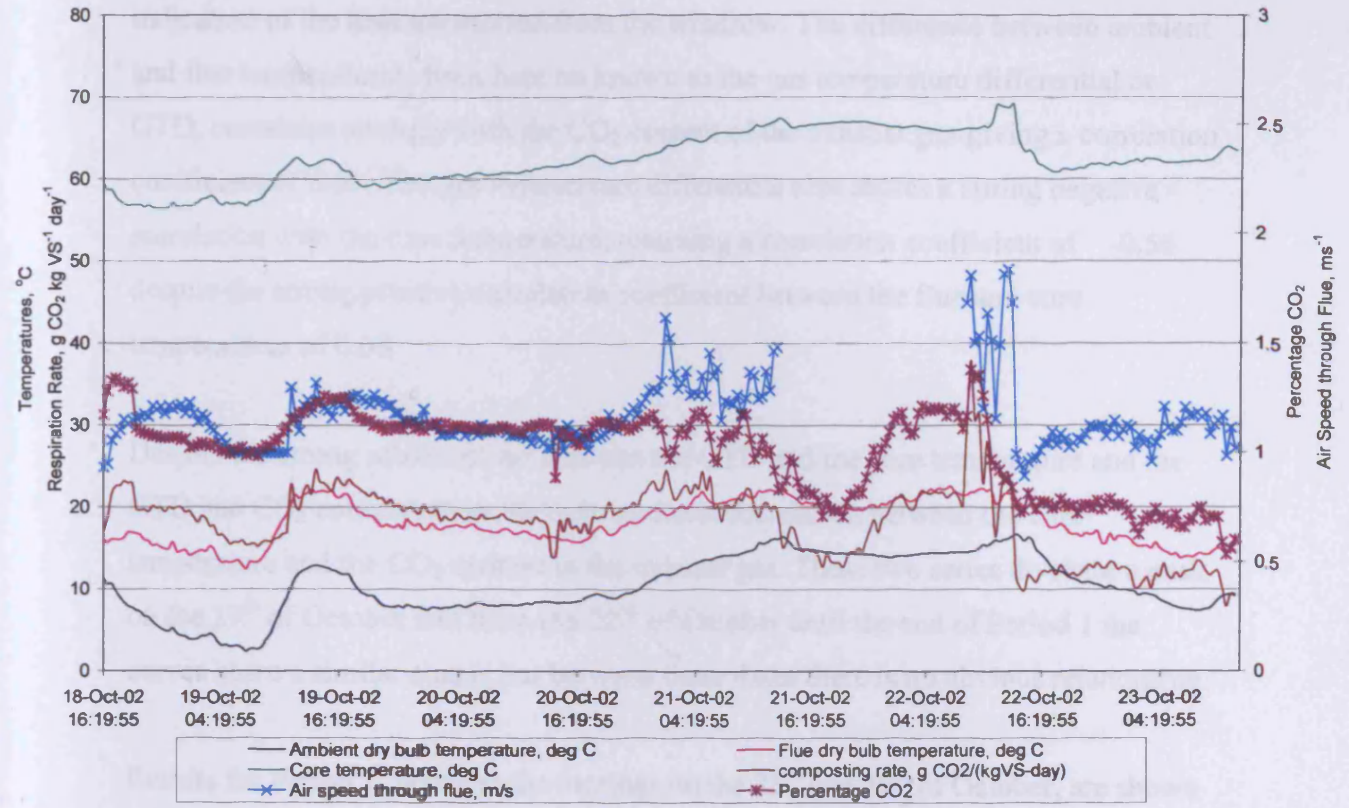

Figure 5.6. Data recorded from windrow W1I during Period 1

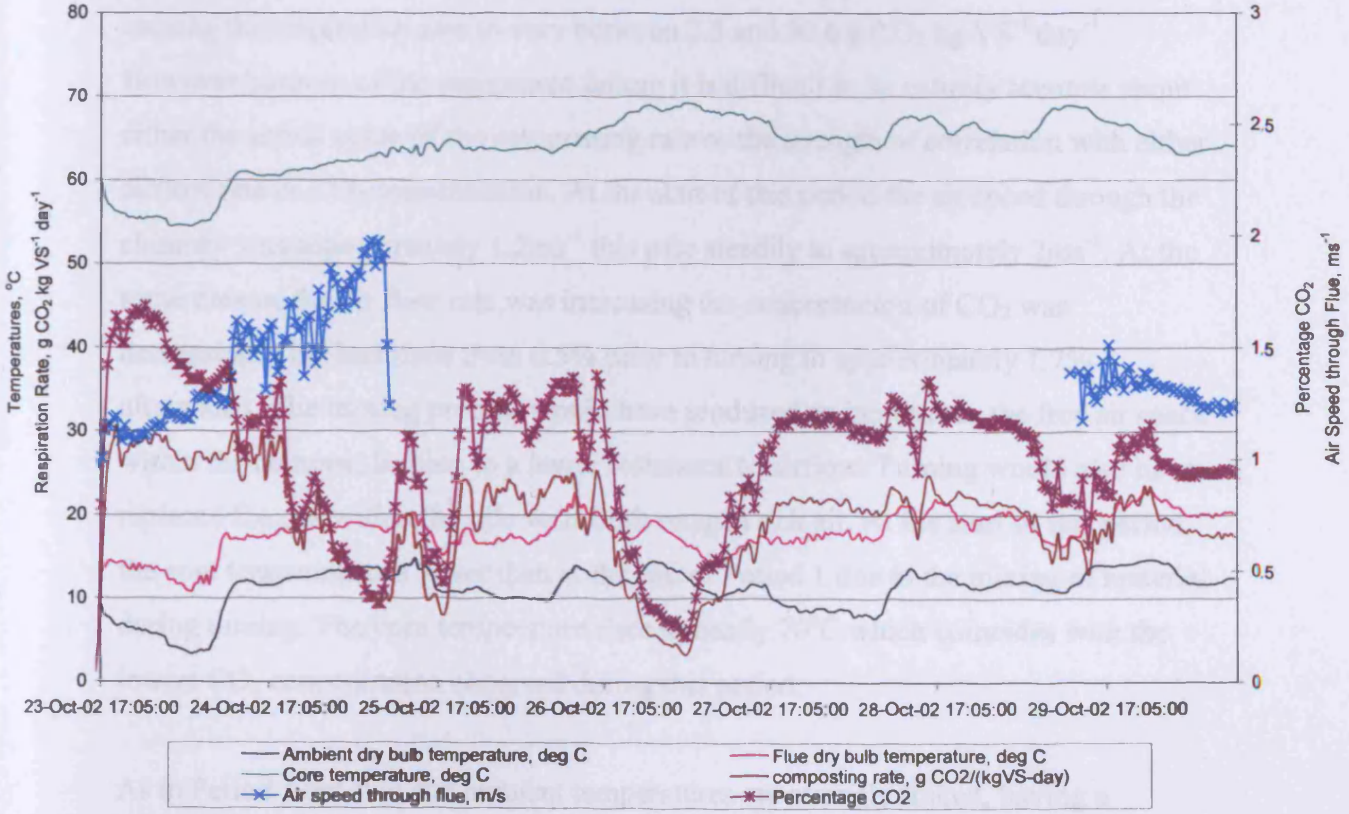

Figure 5.7. Data recorded from windrow W1I during Period 2

indication of the heat transferred from the windrow. The difference between ambient and flue temperatures, from here on known as the gas temperature differential or GTD, correlates strongly with the CO_2 content of the exhaust gas-giving a correlation coefficient of 0.61. The gas temperature differential also shares a strong negative correlation with the core temperature, returning a correlation coefficient of -0.56 despite the strong positive correlation coefficient between the flue and core temperatures of 0.68.

Despite the strong relationships between the GTD and the core temperature and the GTD and CO_2 concentration, there is no direct correlation between the core temperature and the CO_2 content in the exhaust gas. These two series do share a peak on the 19th of October and from the 22nd of October until the end of Period 1 the curves share a similar shape, but between these dates there is no obvious relationship.

Results for Period 2, between the turnings on the 23rd and 29th of October, are shown in Figure 5.7. During this period there was a breakdown of the hot film anemometer, the data that were recorded show the air speed varying between 0.96 and 1.98 ms^{-1}. The CO_2 concentration of the exhaust gas varied between 0.04 and 1.69 percent, causing the respiration rate to vary between 3.3 and 30.6 g CO_2 kg VS^{-1} day^{-1}. However because of the equipment failure it is difficult to be entirely accurate about either the actual value of the composting rate or the strength of correlation with either airflow rate or CO_2 concentration. At the start of this period the air speed through the chimney was approximately 1.2ms^{-1} this rose steadily to approximately 2ms^{-1}. At the same time as the air flow rate was increasing the concentration of CO_2 was decreasing. This had risen from 0.5% prior to turning to approximately 1.7% afterwards. The turning process would have produced an increase in the free air space within the compost leading to a lower resistance to airflow. Turning would also have replaced the gas within the pile with fresh oxygen rich air. At the start of this period the core temperature is lower than at the end of Period 1 due to the mixing of material during turning. The core temperature rises to nearly 70°C which coincides with the lowest CO_2 concentration observed during this period.

As in Period 1 the flue and ambient temperatures are strongly linked, having a correlation coefficient of 0.80. The relationship between the GTD and the CO_2

content of the exhaust gas is also strong during Period 2, giving a correlation coefficient of 0.74. As in Period 1 the flue and core temperatures share a strong correlation, however unlike Period 1 the GTD and the core temperature show no correlation. There is a very weak correlation between the CO_2 content of the exhaust gas and the core temperature , however on the 23rd, 26th and 29th of October increases in the core temperature were accompanied by decreases in the concentration of CO_2 and hence respiration rate. When the temperature falls on the 27th and 29th the CO_2 concentration increases again.

Data for Period 3 of windrow W1I is shown in Figure 5.8. These data were recorded between the 30th of October and 11th of November. As with the previous turning event the core temperature fell, but rose again and was in the range 65°C to 70°C for most of this period. The CO_2 concentration also rose after turning and fell as the core temperature increased. Unlike the previous two periods there is a very strong negative correlation between the core temperature and the CO_2 concentration of the exhaust gas giving a correlation coefficient of -0.79. Over this period the core temperature increased from approximately 55°C to 70°C, before settling at approximately 65°C. This corresponds with the general falling trend in the CO_2 concentration which starts at a high of 1.89% and falls to a value of approximately 1%. Small peaks in the core temperature series correspond with several troughs in the data for CO_2 concentration. There is also a strong negative correlation between the GTD and the core temperature with a coefficient of -0.61, the GDT and CO_2 content of the exhaust gas are strongly correlated with a coefficient of 0.71

The hot wire anemometer was again functional for this period and the airflow varied between 0.84 and 1.89 ms^{-1}, but remains relatively constant when compared to the carbon dioxide content which shows values in the range of 0.17 to 1.89 percent. As a result of this the composting rate ranges from 2.9 to 35.1 g $CO_2 kgVS^{-1} day^{-1}$ with the rate being highest towards the start of this period and at its lowest at the end with several peaks and troughs in between. The composting rate is highly correlated to the CO_2 content of the exhaust gas, with a coefficient of 0.95, whilst the composting rate and airflow only give a correlation coefficient of 0.35.

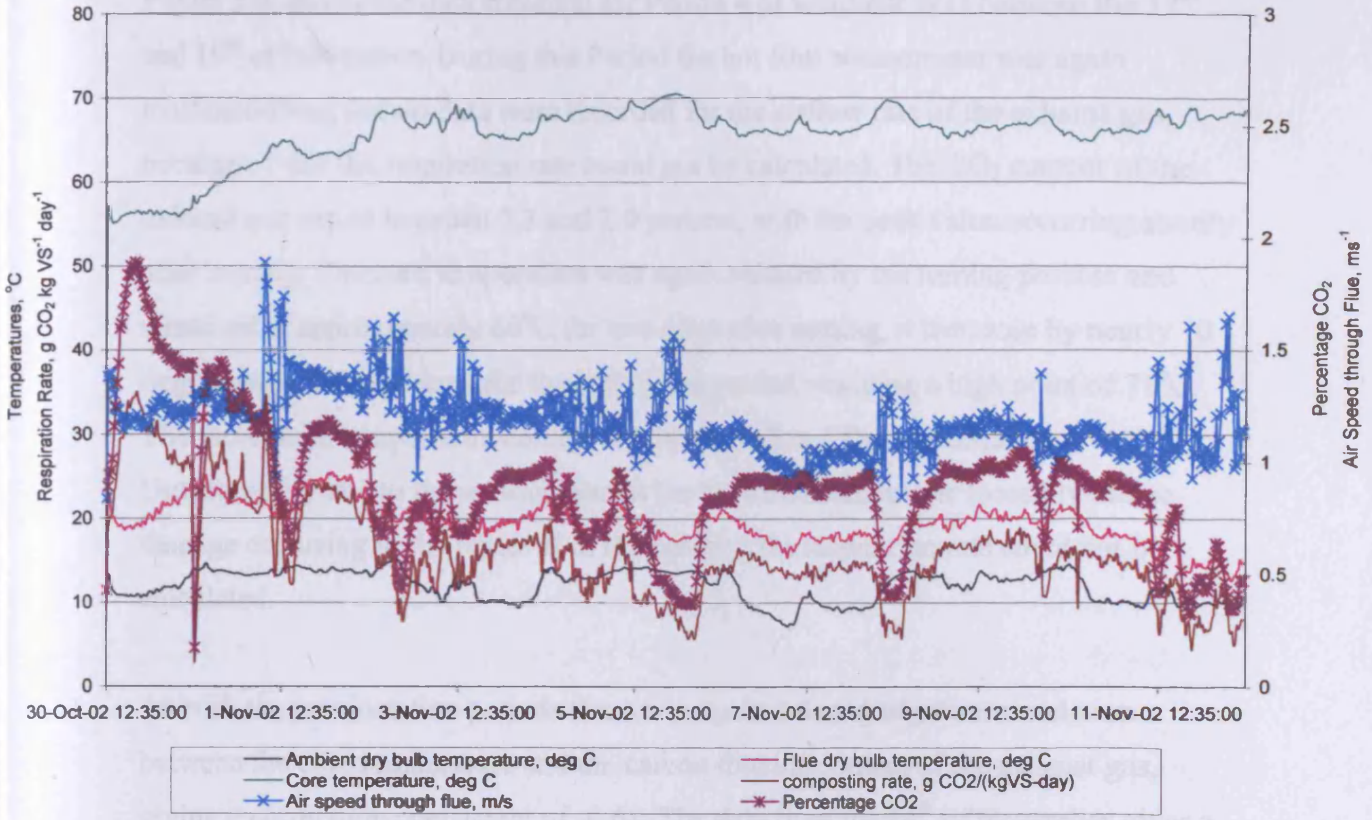

Figure 5.8. Data recorded from windrow W1I during Period 3

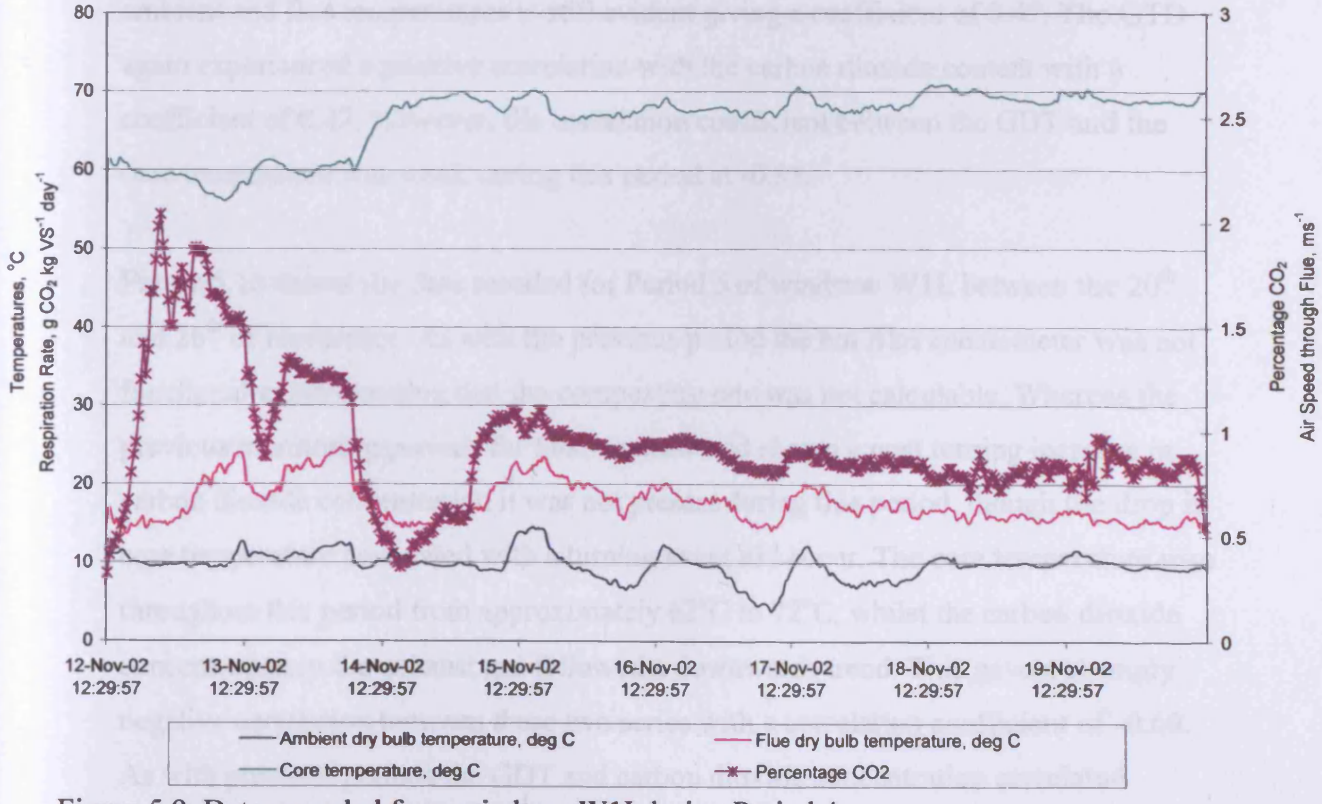

Figure 5.9. Data recorded from windrow W1I during Period 4

Figure 5.9. shows the data recorded for Period 4 of windrow W1I between the 12th and 19th of November. During this Period the hot film anemometer was again malfunctioning and no data were recorded for the airflow rate of the exhaust gas, because of this the respiration rate could not be calculated. The CO_2 content of the exhaust gas varied between 0.3 and 2.0 percent, with the peak value occurring shortly after turning. The core temperature was again reduced by the turning process and remained at approximately 60°C for two days after turning, it then rose by nearly 10 degrees where it remained for the rest of this period, reaching a high point of 71°C. The increase in temperature coincides with the fall in CO_2 concentration. Unfortunately due to the malfunction in the hotwire anemometer (possibly due to damage occurring in the removal of the canopy) the respiration rate could not be calculated.

As with the previous two periods there was again a strong negative correlation between the core temperature and the carbon dioxide content of the exhaust gas, giving a correlation coefficient of -0.61. The data from the 14th of November gives a strong demonstration of this as the core temperature rises above 60°C there is a large decrease in carbon dioxide concentration. The positive correlation between the ambient and flue temperatures is still evident giving a coefficient of 0.47. The GTD again experienced a positive correlation with the carbon dioxide content with a coefficient of 0.47. However, the correlation coefficient between the GDT and the core temperature was weak during this period at -0.33.

Figure 5.10 shows the data recoded for Period 5 of windrow W1I, between the 20th and 26th of November. As with the previous period the hot film anemometer was not functional-again meaning that the composting rate was not calculable. Whereas the previous monitoring periods for this windrow had shown a post turning increase in carbon dioxide concentration it was not present during this period, though the drop in core temperature associated with a turning event did occur. The core temperature rose throughout this period from approximately 62°C to 72°C, whilst the carbon dioxide concentration in the exhaust gas followed a downwards trend. This gave a strongly negative correlation between these two series with a correlation coefficient of -0.69. As with previous periods the GDT and carbon dioxide concentration correlated strongly giving a coefficient of 0.71. This period showed no correlation between the

flue and ambient temperatures and a very weak negative correlation between the GTD and the core temperature.

The final period for which data were recorded for windrow W1I is shown in Figure 5.11. Period 6 is much shorter than the other monitoring periods recording only data from the 27th to the 29th of November 2002. As opposed to previous periods the core temperature and carbon dioxide concentration both increase, despite the core temperature reaching 70°C. This gives a correlation coefficient of 0.65 between the core temperature and the carbon dioxide concentration, although the shortened timescale of this period and the proximity to turning may have affected this. Periods 2 to 4 all showed similar behaviour during the days immediately post turning with a peak in carbon dioxide concentration occurring whilst the core temperature increases. The gap between the flue and ambient temperatures, the GTD, increases during this period giving a correlation coefficient of 0.91 between the GTD and the carbon dioxide concentration. The relationship between the core temperature and GTD for this period displays a positive correlation having a coefficient of 0.43.

The data shown in Figures 5.6 to 5.11 generally shows that the core temperature and carbon dioxide concentrations move in opposite directions to each other. During a turning event there appears to be a decrease in the core temperature. This may be caused by heat dispersal during the turning event or by mixing of the cooler material from the edges of the windrow with the hotter core material. The concentration of carbon dioxide observed in the chimney generally increases post turning, often maintaining an elevated level for up to 2 days. The turning event will release excess moisture from the void space within the compost and replace the gases present with fresh air. The respiration rate of the compost often follows the carbon dioxide concentration very strongly, whilst the GDT also appears to be a strongly correlated with composting activity.

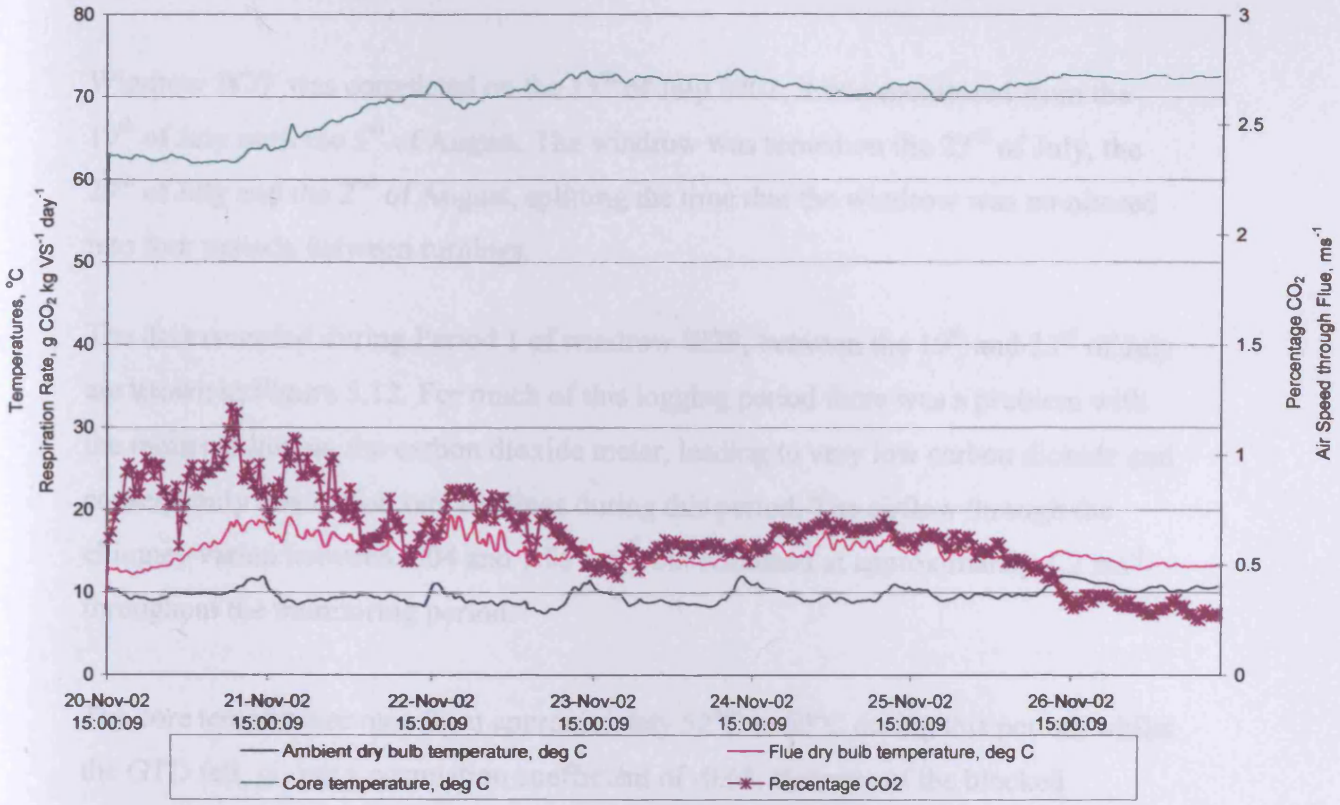

Figure 5.10. Data recorded from windrow W1I during Period 5

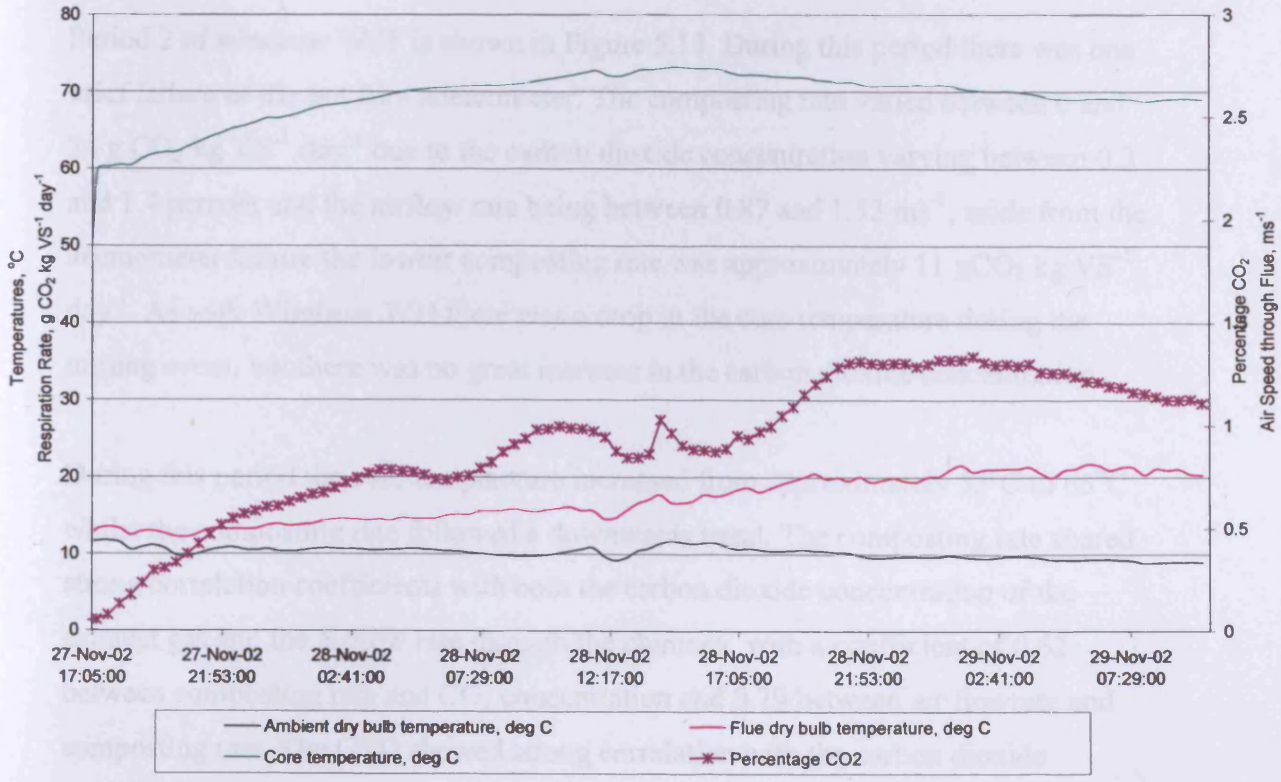

Figure 5.11. Data recorded from windrow W1I during Period 6

5.3.2.2 Windrow W2F

Windrow W2F was completed on the 15th of July 2002; it was monitored from the 19th of July until the 5th of August. The windrow was turned on the 23rd of July, the 29th of July and the 2nd of August, splitting the time that the windrow was monitored into four periods between turnings.

The data recorded during Period 1 of windrow W2F, between the 19th and 23rd of July are shown in Figure 5.12. For much of this logging period there was a problem with the moisture trap on the carbon dioxide meter, leading to very low carbon dioxide and consequently respiration rate readings during this period. The airflow through the chimney varied between 1.04 and 1.55 ms^{-1}, but remained at approximately 1.2 ms^{-1} throughout the monitoring period.

The core temperature rose from approximately 52°C to 60°C during this period, whilst the GTD fell, giving a correlation coefficient of -0.68. Because of the blocked moisture trap which lead to low carbon dioxide readings it is not possible to gain an insight into the respiration rate.

Period 2 of windrow W2F is shown in Figure 5.13. During this period there was one brief failure of the hot film anemometer. The composting rate varied between 0 and 24 g CO_2 kg VS^{-1} day^{-1} due to the carbon dioxide concentration varying between 0.3 and 1.4 percent and the airflow rate being between 0.87 and 1.53 ms^{-1}, aside from the anemometer failure the lowest composting rate was approximately 11 gCO_2 kg VS^{-1} day^{-1}. As with Windrow W1I there was a drop in the core temperature during the turning event, but there was no great increase in the carbon dioxide concentration.

During this period the core temperature increased from approximately 55°C to 65°C whilst the composting rate followed a downwards trend. The composting rate shared strong correlation coefficients with both the carbon dioxide concentration of the exhaust gas and the airflow rate through the chimney, with a coefficient of 0.62 between composting rate and CO_2 concentration and 0.79 between air flowrate and composting rate. The GTD showed strong correlation with the carbon dioxide concentration with a coefficient of 0.66, however the carbon dioxide concentration

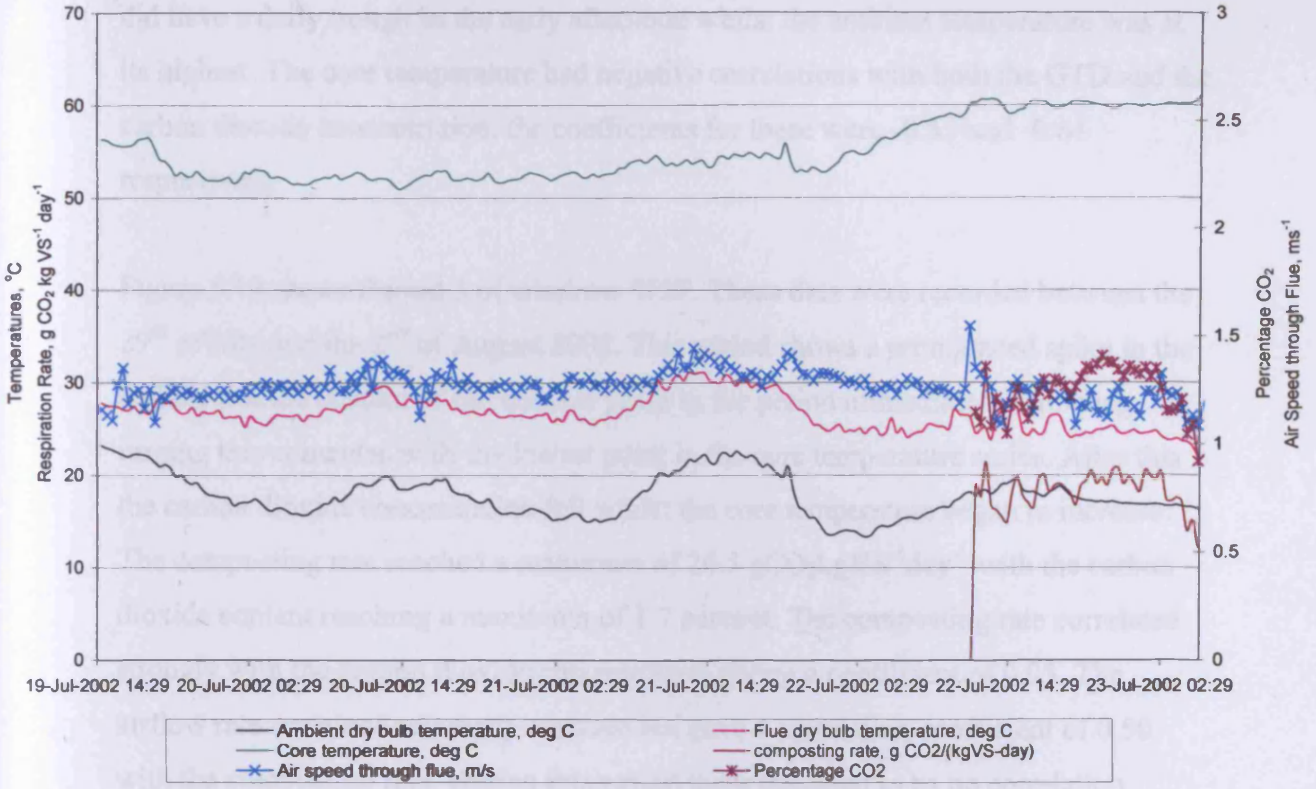

Figure 5.12. Data recorded from windrow W2F during Period 1

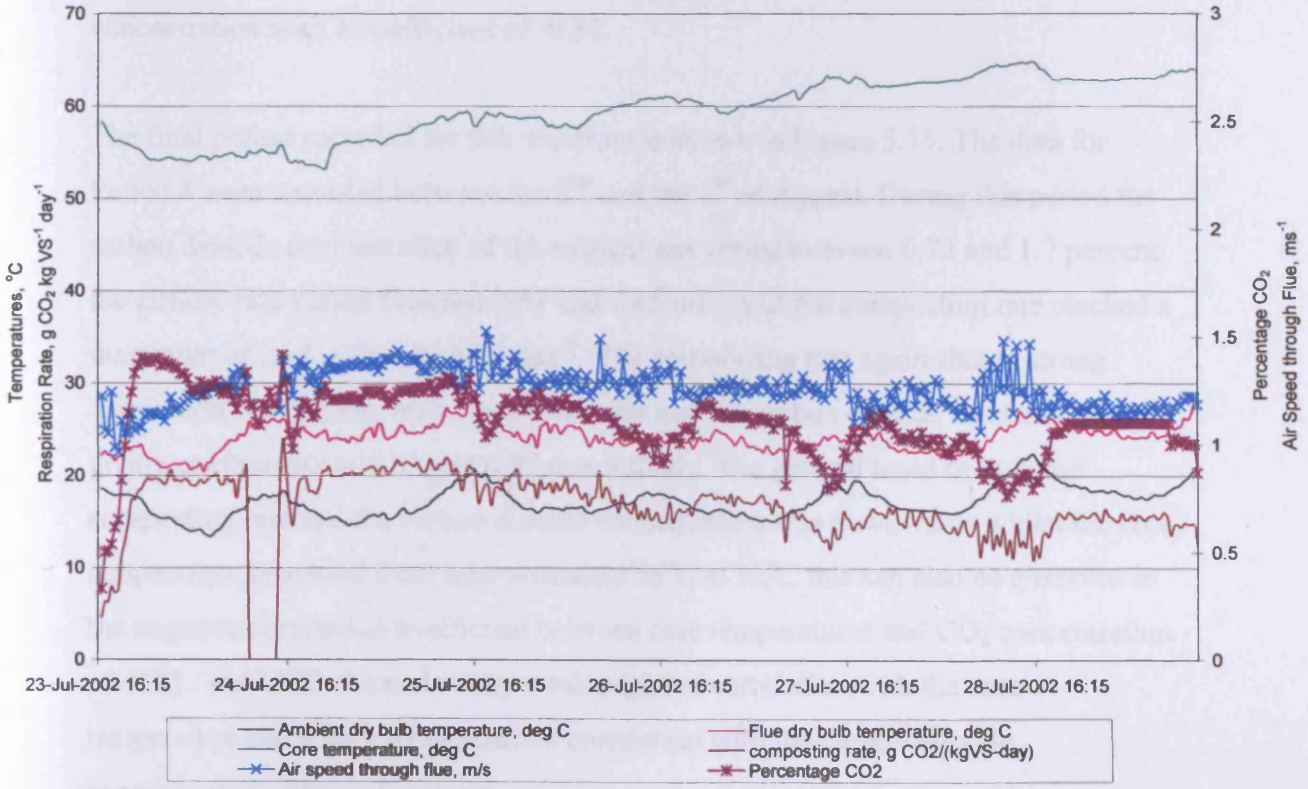

Figure 5.13. Data recorded from windrow W2F during Period 2

did have a daily trough in the early afternoon whilst the ambient temperature was at its highest. The core temperature had negative correlations with both the GTD and the carbon dioxide concentration, the coefficients for these were -0.53 and -0.61 respectively.

Figure 5.14 shows Period 3 of windrow W2F. These data were recorded between the 29th of July and the 2nd of August 2002. This period shows a pronounced spike in the carbon dioxide content of the exhaust gases in the period immediately following turning this coincides with the lowest point in the core temperature series. After this the carbon dioxide concentration fell whilst the core temperature began to increase. The composting rate reached a maximum of 26.3 $gCO_2kgVS^{-1}day^{-1}$ with the carbon dioxide content reaching a maximum of 1.7 percent. The composting rate correlated strongly with the carbon dioxide concentration giving a coefficient of 0.95. The airflow rate remained relatively constant but gave a correlation coefficient of 0.50 with the composting rate. During this period there appeared to be no correlation between the GDT and the core temperature or carbon dioxide concentration in the exhaust gas, but the core did have a negative correlation with the carbon dioxide concentration with a coefficient of -0.53.

The final period recorded for this windrow is shown in Figure 5.15. The data for Period 4 were recorded between the 2nd and the 5th of August. During this period the carbon dioxide concentration of the exhaust gas varied between 0.72 and 1.7 percent, the airflow rate varied between 0.93 and 1.45 ms^{-1}, and the composting rate reached a maximum of 26.1 g CO_2 kg VS^{-1} day^{-1}. The composting rate again shared strong correlation coefficients with the airflow rate and the carbon dioxide concentration giving coefficients of 0.61 and 0.97 respectively. The general trend of both the composting rate and the carbon dioxide concentration was downwards whilst the core temperature increased from approximately 55°C to 72°C this can also be observed in the negative correlation coefficient between core temperatures and CO_2 concentration of -0.81. The GTD showed a very weak negative correlation with the core temperature and a very weak positive correlation with the carbon dioxide concentration of the exhaust gas.

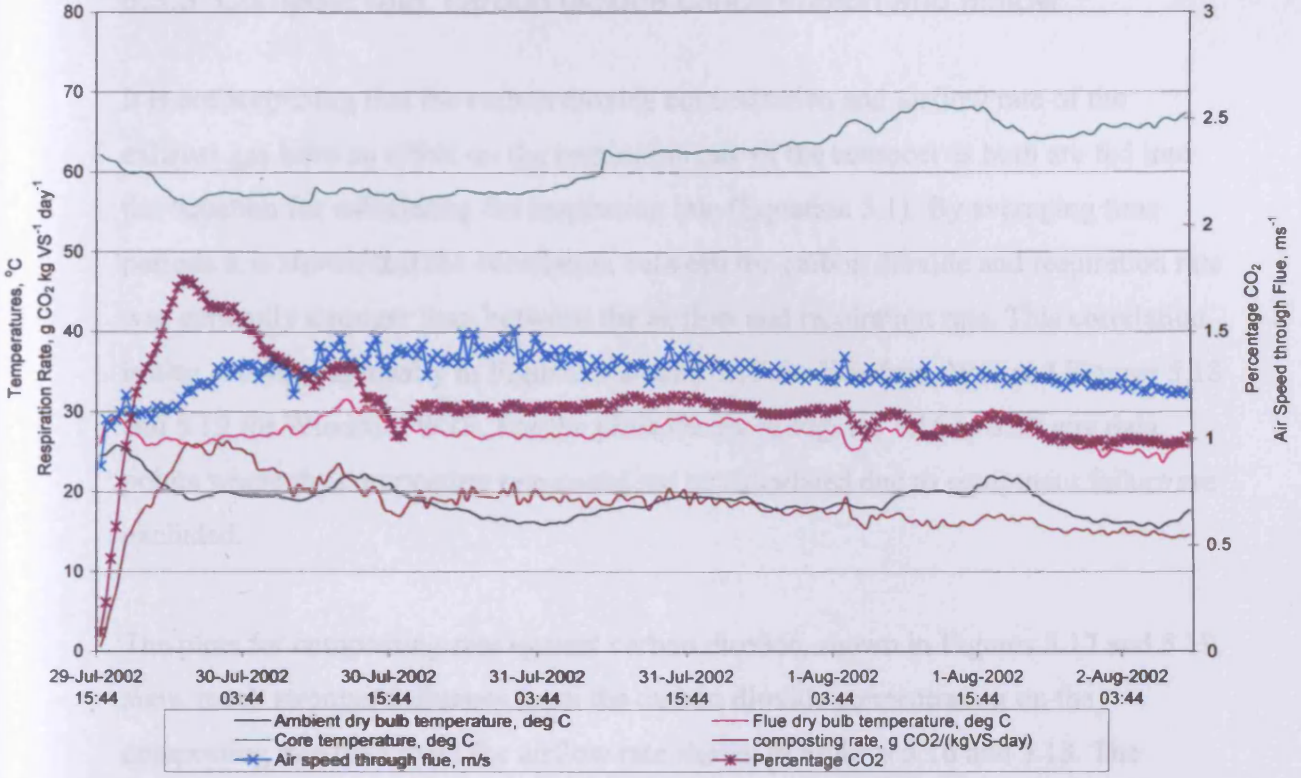

Figure 5.14. Data recorded from windrow W2F during Period 3

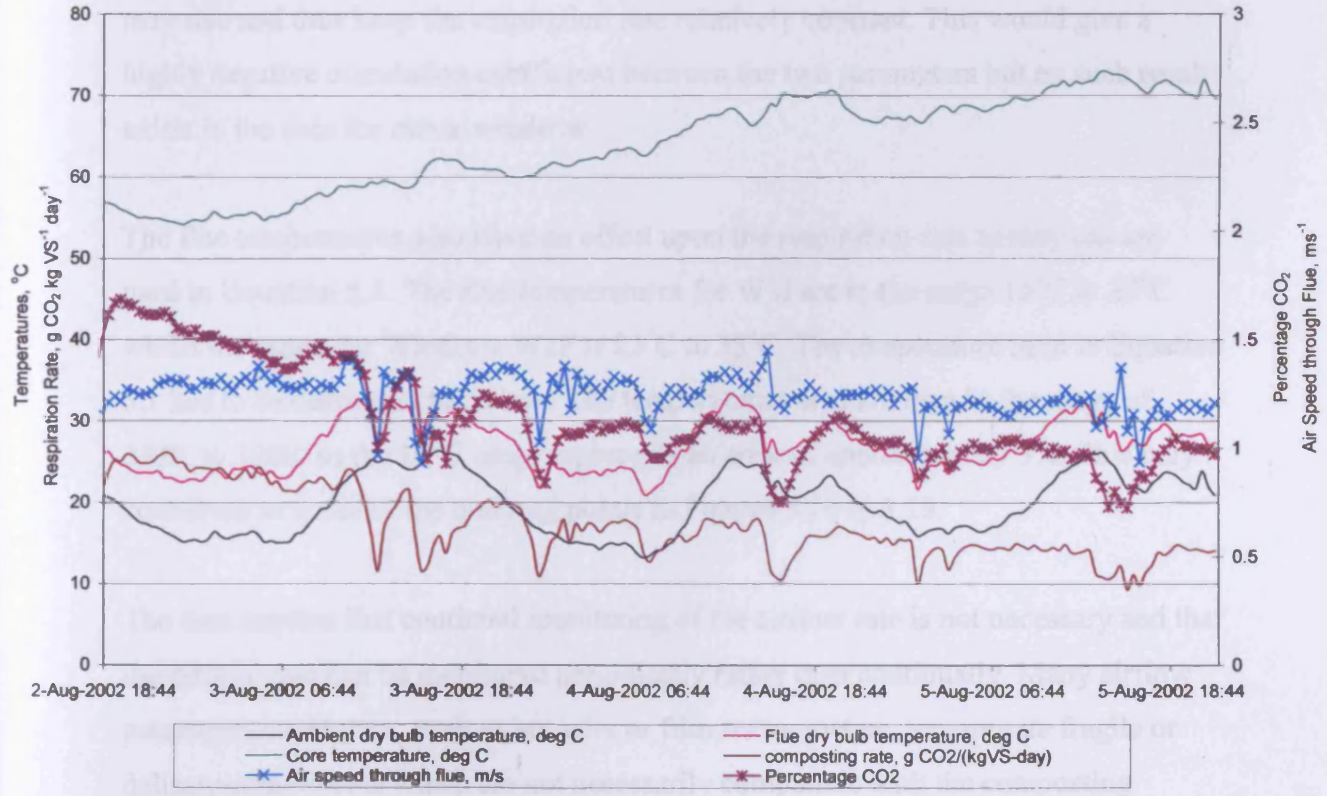

Figure 5.15. Data recorded from windrow W2F during Period 4

5.3.3 Compost rate, carbon dioxide concentration and airflow

It is not surprising that the carbon dioxide concentration and airflow rate of the exhaust gas have an effect on the respiration rate of the compost as both are fed into the equation for calculating the respiration rate (Equation 5.1). By averaging time periods it is shown that the correlation between the carbon dioxide and respiration rate was generally stronger than between the airflow and respiration rate. This correlation is also shown graphically in Figures 5.16 and 5.17 for Windrow W1I and Figures 5.18 and 5.19 for Windrow W2F. For the plots shown in Figures 5.16 to 5.19 any data points where the composting rate could not be calculated due to equipment failure are excluded.

The plots for composting rate against carbon dioxide, shown in Figures 5.17 and 5.19, show much stronger influence from the carbon dioxide concentration on the composting rate than from the airflow rate shown in Figures 5.16 and 5.18. The carbon dioxide concentration varied more than the airflow rate which in many cases remains relatively constant. It was thought that as the respiration rate depends on both the airflow and the carbon dioxide concentration that if one were to drop the other may rise and thus keep the respiration rate relatively constant. This would give a highly negative correlation coefficient between the two parameters but no such result exists in the data for either windrow.

The flue temperatures also have an effect upon the respiration rate as they too are used in Equation 5.1. The flue temperatures for W1I are in the range 15°C to 25°C whilst the range for Windrow W2F is 25°C to 35°C. The temperature used in Equation 5.1 has to be converted to Kelvin. The temperatures used are then in the range of 288K to 308K so the 10°C range represents an error of approximately 3%. This may contribute to some of the outlying points in Figures 5.16 to 5.19.

The data implies that continual monitoring of the airflow rate is not necessary and that the airflow rate can be monitored periodically rather than continually. Many airflow measurement devices, such as hot wire or film anemometers, incorporate fragile or delicate components which are not necessarily compatible with the composting

process and the associated environments of elevated temperature, high humidity and airborne particles.

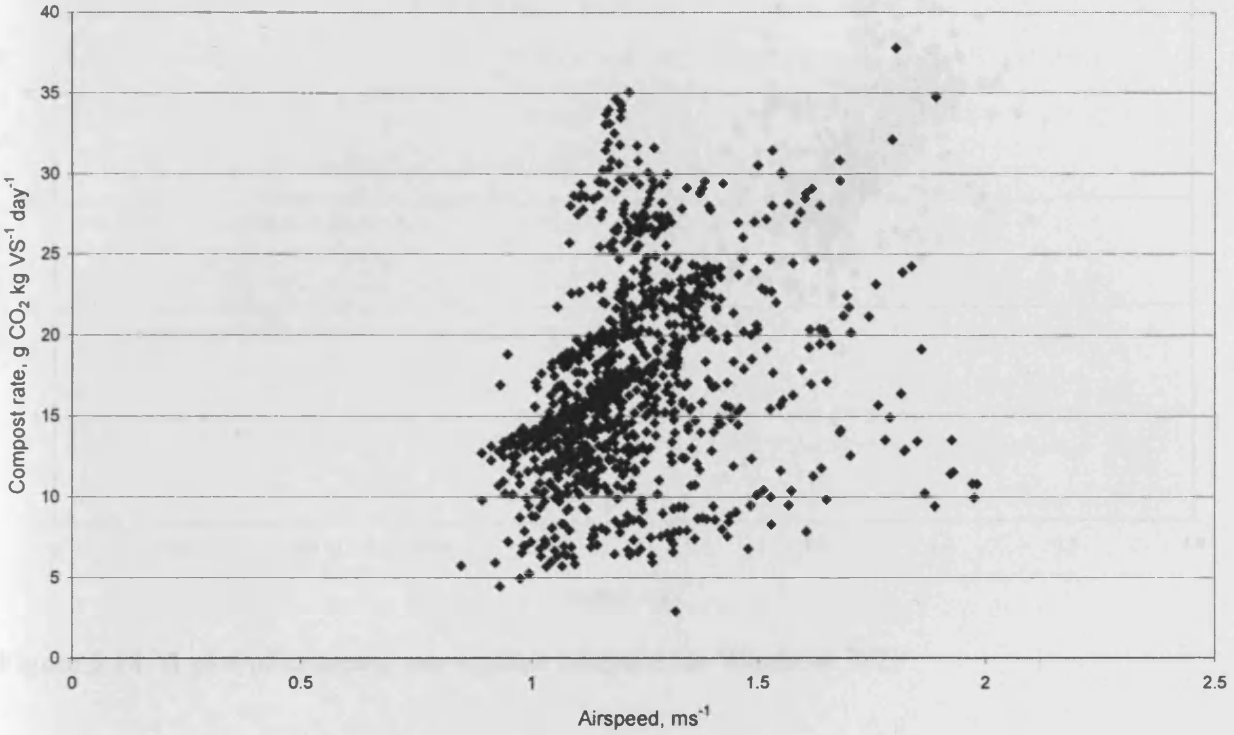

Figure 5.16. A plot of compost rate against airspeed for Windrow W1I

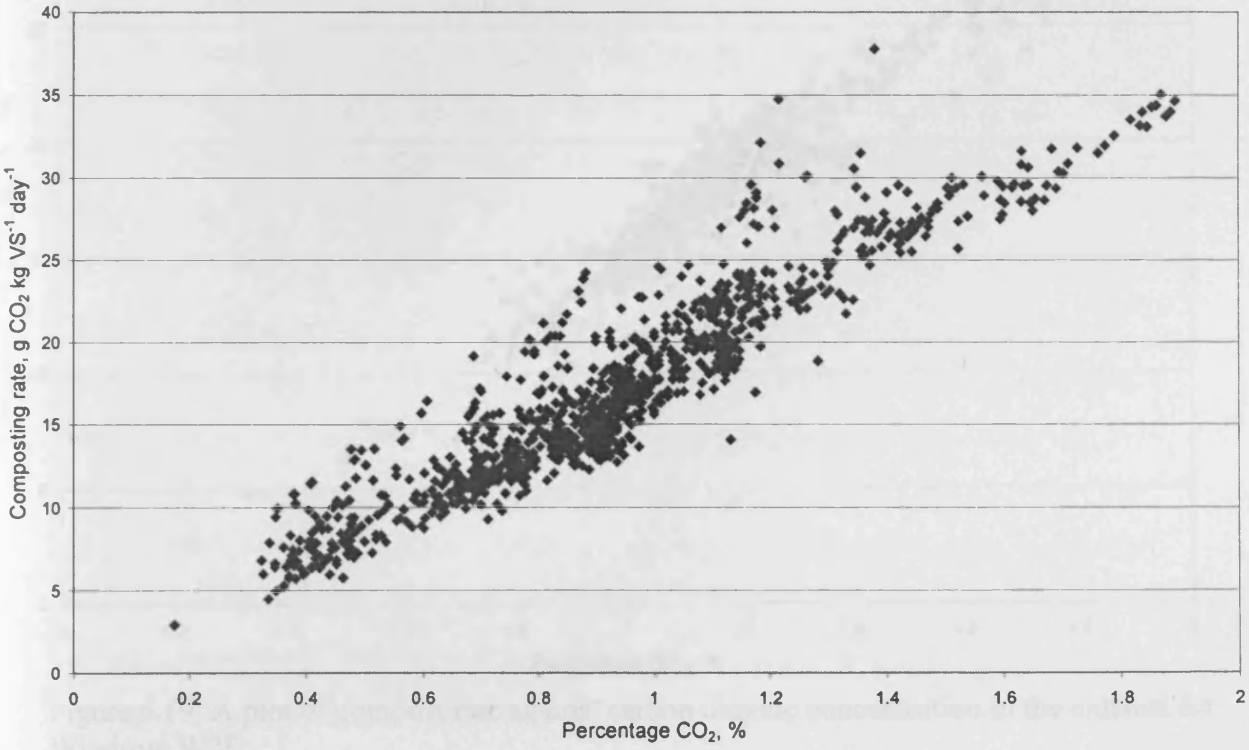

Figure 5.17. A plot of compost rate against carbon dioxide concentration in the exhaust for Windrow W1I

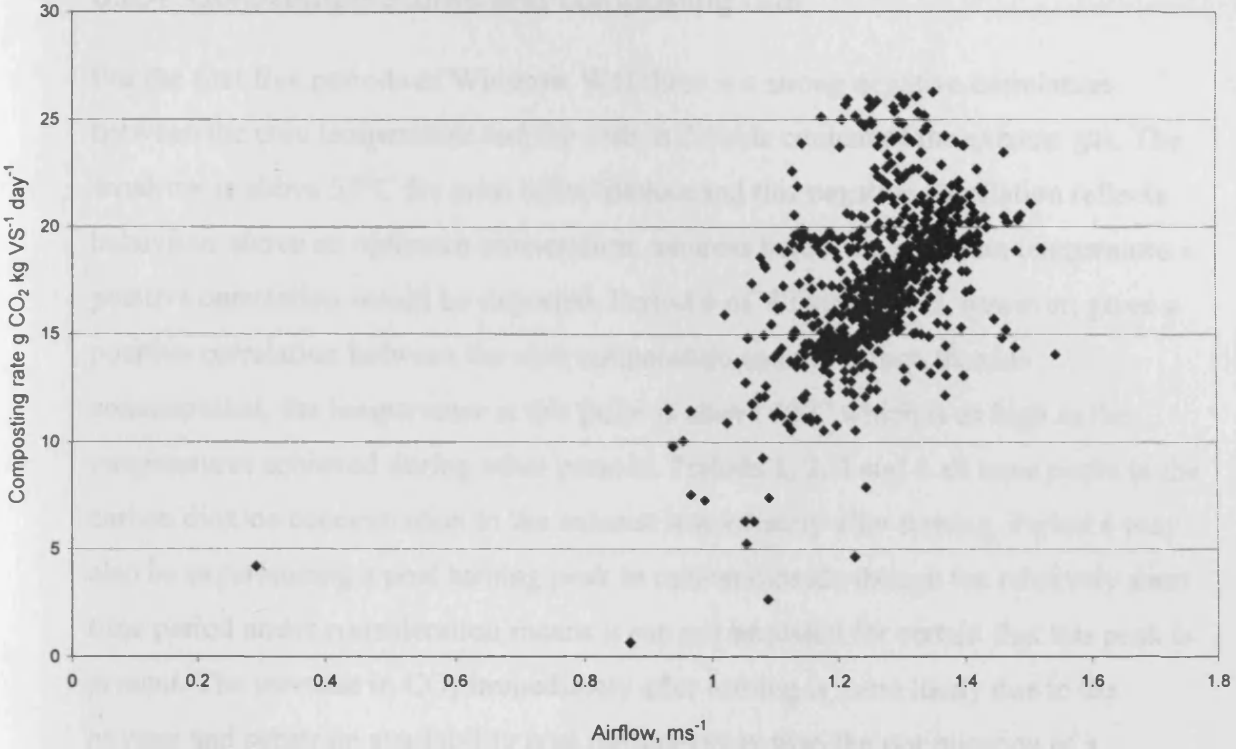

Figure 5.18. A plot of compost rate against airspeed for Windrow W2F

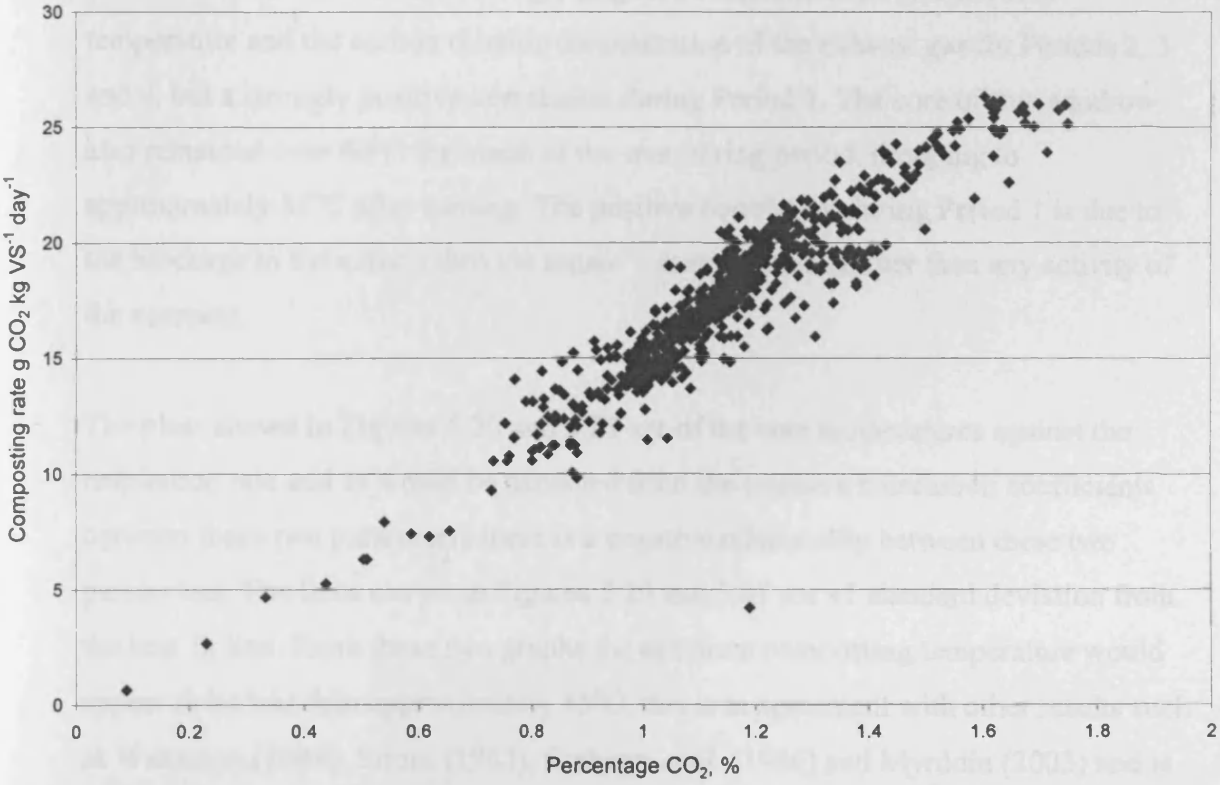

Figure 5.19. A plot of compost rate against carbon dioxide concentration in the exhaust for Windrow W2F

5.3.4 Core temperatures and composting rate

For the first five periods of Windrow W1I there is a strong negative correlation between the core temperature and the carbon dioxide content of the exhaust gas. The windrow is above 55°C for most of its lifetime and this negative correlation reflects behaviour above an optimum temperature, whereas below the optimum temperature a positive correlation would be expected. Period 6 of Windrow W1I, however, gives a positive correlation between the core temperature and the carbon dioxide concentration, the temperature at this point is above 60°C which is as high as the temperatures achieved during other periods. Periods 1, 2, 3 and 4 all have peaks in the carbon dioxide concentration in the exhaust immediately after turning. Period 6 may also be experiencing a post turning peak in carbon dioxide though the relatively short time period under consideration means it can not be stated for certain that this peak is present. The increase in CO_2 immediately after turning is more likely due to the oxygen and substrate availability post turning rather than the optimisation of a parameter such as temperature.

Windrow W2F also shows a strongly negative correlation between the core temperature and the carbon dioxide concentration of the exhaust gas for Periods 2, 3 and 4, but a strongly positive correlation during Period 1. The core of this windrow also remained over 60°C for much of the monitoring period, dropping to approximately 55°C after turning. The positive correlation during Period 1 is due to the blockage in the carbon dioxide sensor's sampling tube rather than any activity of the compost.

The plots shown in Figures 5.20 and 5.21 are of the core temperatures against the respiration rate and as would be expected from the negative correlation coefficients between these two parameters there is a negative relationship between these two parameters. The lines shown in Figures 5.20 and 5.21 are ±1 standard deviation from the best fit line. From these two graphs the optimum composting temperature would appear to be less than approximately 55°C, this is in agreement with other results such as Waksman (1949), Strom (1985), Cathcart *et al.* (1986) and Myrddin (2003) and is in very strong agreement with Wiley (1956;1957) who found optimum carbon dioxide production to occur at 56°C.

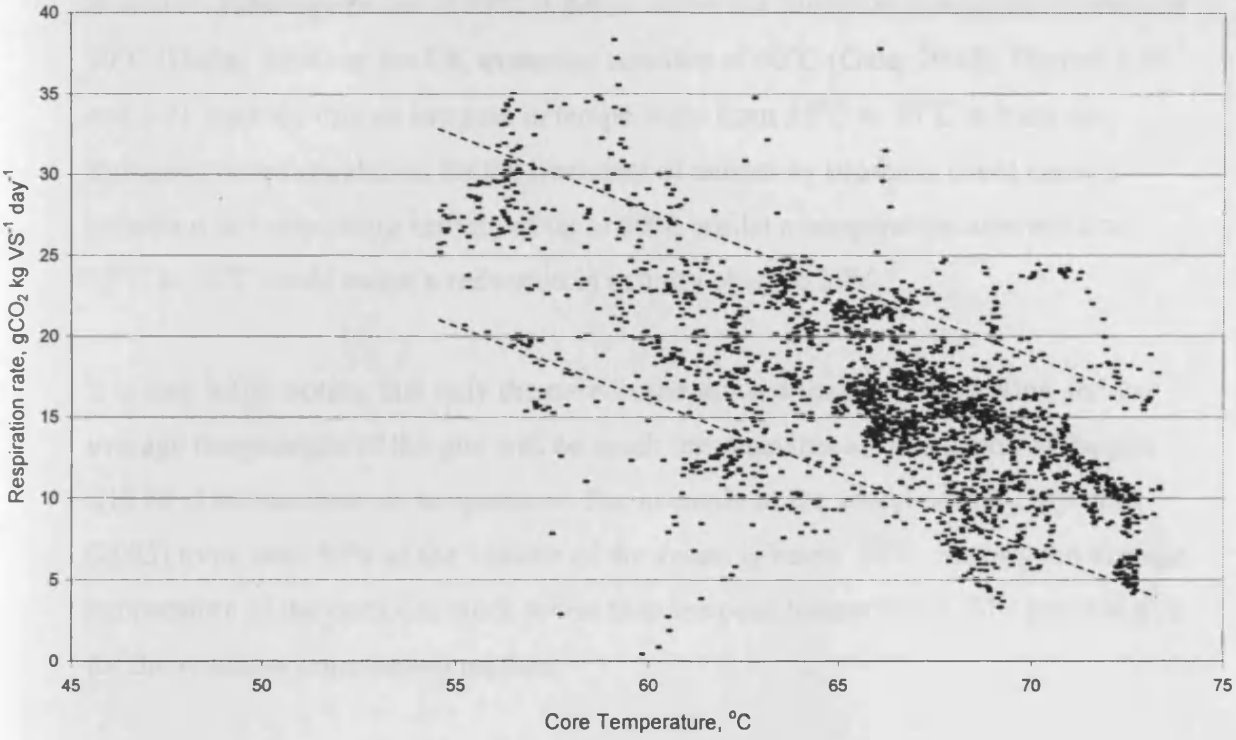

Figure 5.20. Graph of windrow core temperatures against respiration rate for windrow W1I

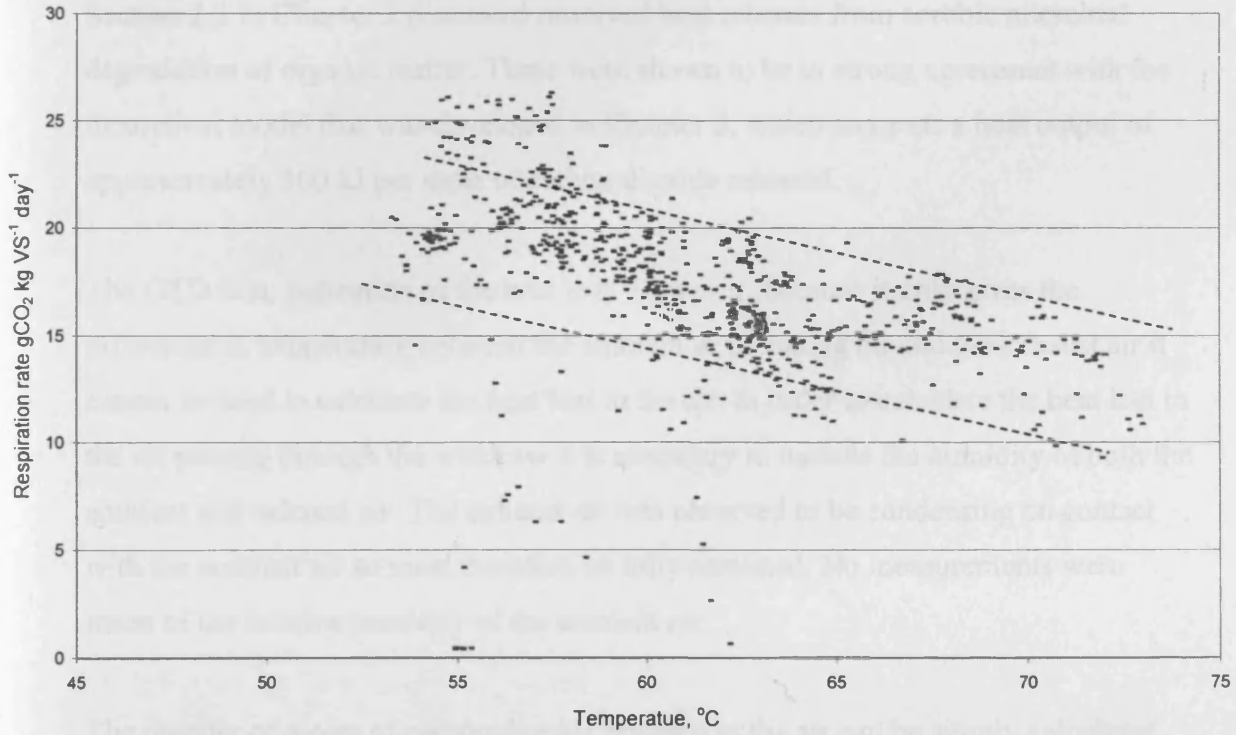

Figure 5.21. Graph of windrow core temperatures against respiration rate for windrow W2F

However, the temperature of 55°C is below either the European treatment standard of 70°C (Defra, 2004) or the UK treatment standard of 60°C (Gale, 2002). Figures 5.20 and 5.21 indicate that an increase in temperature from 55°C to 70°C to meet the European union regulation for the treatment of animal by products could cause a reduction in composting activity of up to 50%, whilst a temperature increase from 55°C to 60°C could cause a reduction in activity of up to 20%.

It is also worth noting that only the core temperature is under consideration and the average temperature of the pile will be much less than this as the outside of the pile will be at the ambient air temperature. For example in the vessel used by Myrddin (2003) more than 50% of the volume of the vessel is below 55°C, making the average temperature of the compost much lower than the peak temperatures. The same is true for the windrow composting method.

5.3.5 Heat release

Section 2.2 in Chapter 2 discussed observed heat releases from aerobic microbial degradation of organic matter. These were shown to be in strong agreement with the theoretical model that was developed in Chapter 3, which suggests a heat output of approximately 500 kJ per mole of carbon dioxide released.

The GTD is an indication of the heat lost. However, because it only gives the difference in temperature between the ambient or incoming air and the exhaust air it cannot be used to calculate the heat lost to the air. In order to calculate the heat lost to the air passing through the windrow it is necessary to include the humidity of both the ambient and exhaust air. The exhaust air was observed to be condensing on contact with the ambient air so must therefore be fully saturated. No measurements were taken of the relative humidity of the ambient air.

The number of moles of carbon dioxide released to the air can be simply calculated using the air flow rate and the carbon dioxide concentration, both of which were recorded by the data loggers. If a value of 70% relative humidity is applied to the

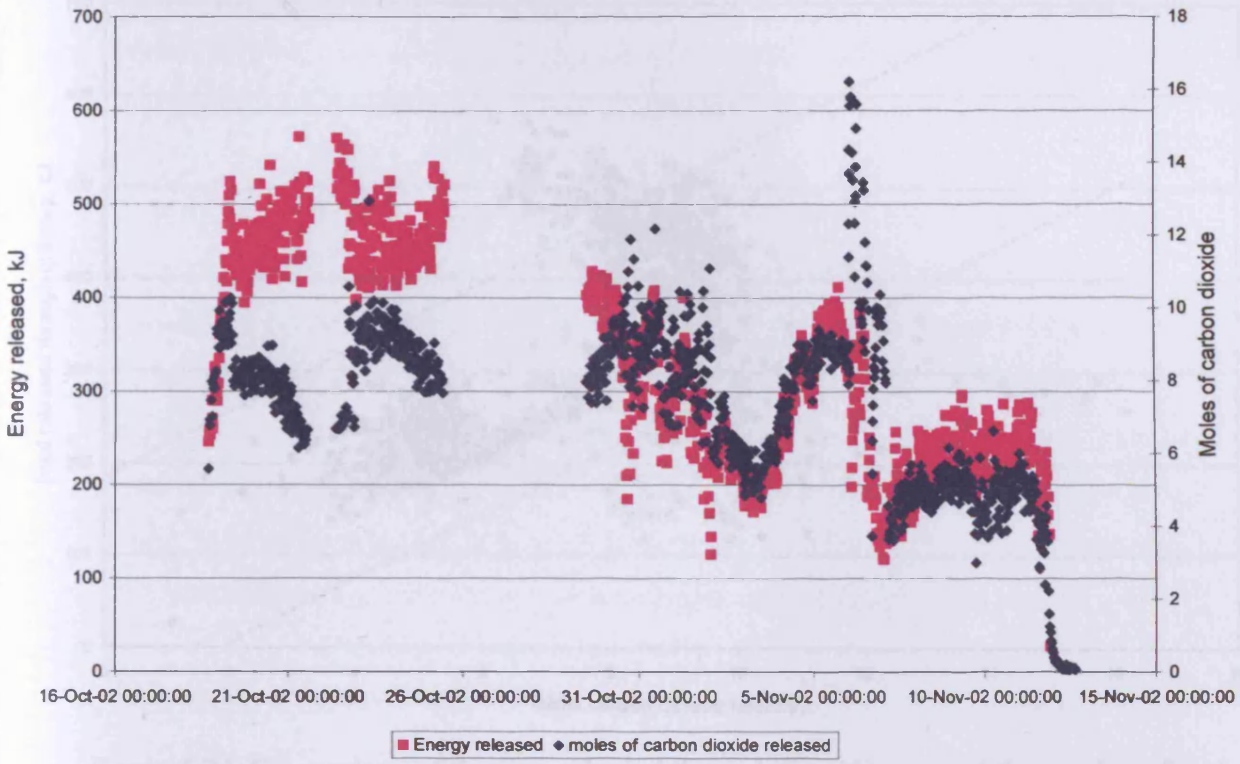

Figure 5.22. Energy and CO_2 emissions from windrow W1I (during each 25 minute time period)

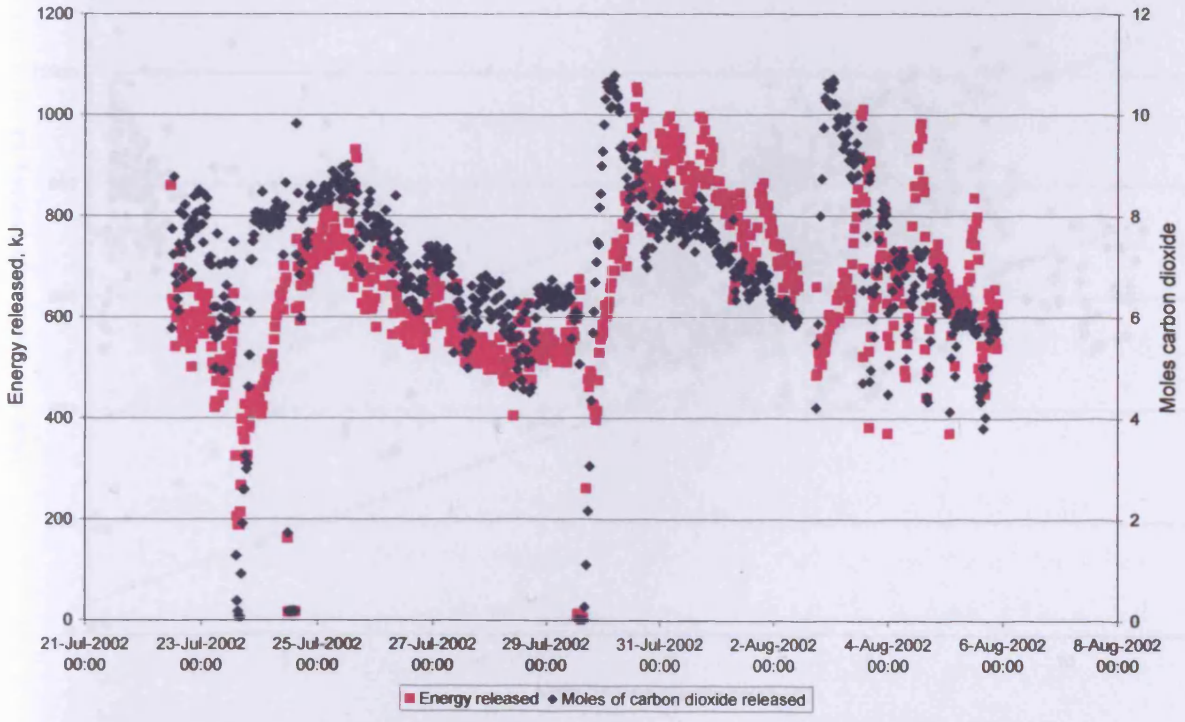

Figure 5.23. Energy and CO_2 emissions from windrow W2F (during each 25 minute time period)

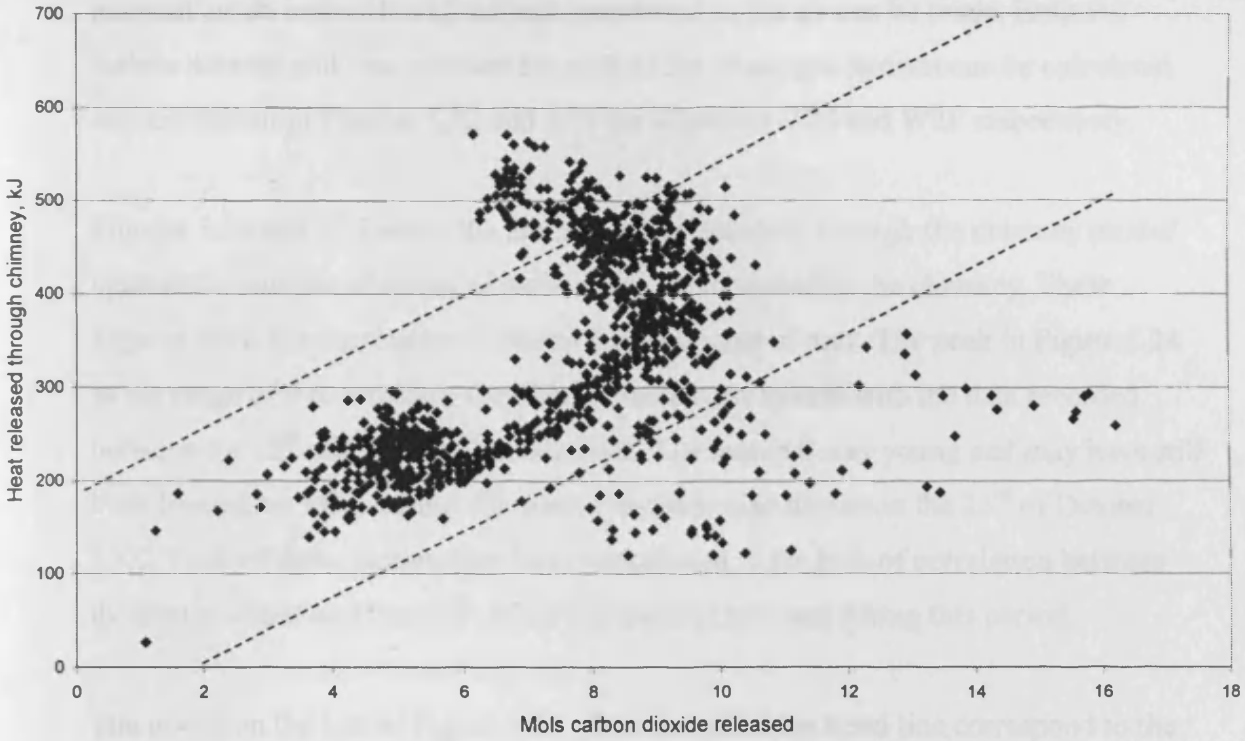

Figure 5.24. Comparison of the heat released through the chimney and the number of mols of carbon dioxide released for Windrow W1I (during each 25 minute time period)

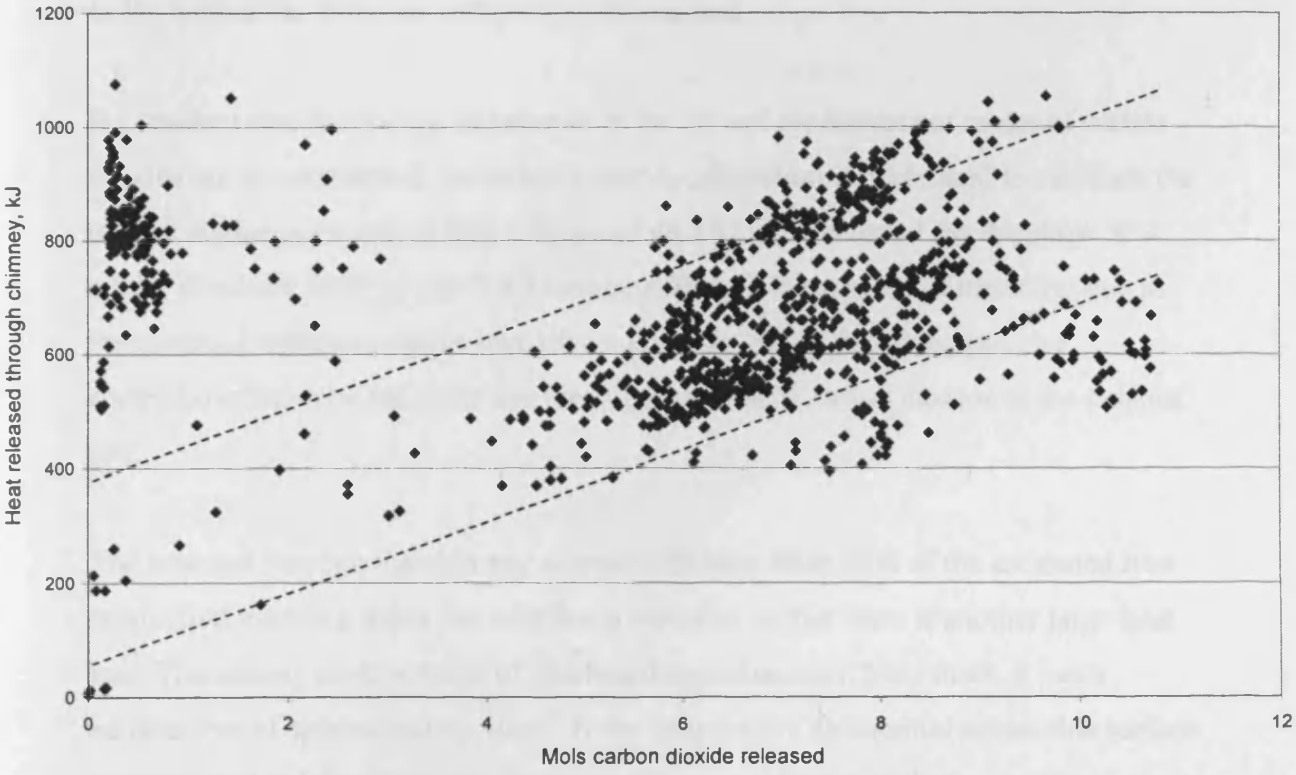

Figure 5.25. Comparison of the heat released through the chimney and the number of mols of carbon dioxide released for Windrow W2F (during each 25 minute time period)

ambient air an estimation of the heat transferred to the air can be made. Both the carbon dioxide and heat releases for each of the 25 minute periods can be calculated and are shown in Figures 5.22 and 5.23 for Windows W1I and W2F respectively.

Figures 5.24 and 5.25 show the amount of heat released through the chimney plotted against the number of moles of carbon dioxide measured in the chimney. These Figures show the correlation between these two sets of data. The peak in Figure 5.24 in the range of 6 to 8 moles of carbon dioxide corresponds with the data recorded between the 18th and 25th of October 2002. The material was young and may have still been heating up fully during this period and was also turned on the 23rd of October 2002. Both of these factors may have contributed to the lack of correlation between the heat released and the mols of carbon dioxide released during this period.

The points on the left of Figure 5.25 which lie off of the trend line correspond to the dates between the 22nd and 25th of July 2002. The material was turned on the 23rd of July which may have caused this anomaly. Other turning events on the 29th of July and 2nd of August also produce spikes on Figure 5.23 where the heat released appears to lag behind the moles of carbon dioxide released.

It is evident that the energy transferred to the air and the number of moles of carbon dioxide are closely linked, but when a simple calculation is performed to calculate the energy release per mole of CO_2 a figure of 43.3 kJ/mole is found for Windrow W1I whilst Windrow W2F gives 93.4 kJ/mole. Although this method is imperfect due to the assumed ambient relative humidity it is reinforced by the strong positive correlations between the GTD and the concentration of carbon dioxide in the exhaust gas.

The heat lost through the chimney accounts for only 10 to 20% of the estimated heat production meaning either the estimate is incorrect or that there is another large heat loss. The canopy itself is made of chipboard approximately 3mm thick, it has a surface area of approximately 10 m^2. If the temperature differential across this surface is considered to be the same as the gas temperature differential then a simple conductive heat loss through the canopy skin can be calculated. A conductivity of 0.1 W/m K (WPIF, 2004) was used for the chipboard skin of the canopy. When the heat

lost through conduction through the canopy was combined with heat lost to the air passing through the windrow figures of 559.7 kJ/mole and 624 kJ/mole were found for Windrows W1I and W2F respectively. These figures are within 25% of the calculated value of 500 kJ/mole of carbon dioxide predicted by Chapter.

There are differences between the theoretical value of energy released per mole of carbon dioxide released and the recorded value, but they are very close and there are several contributing factors, such as:

- Not all of the CO_2 produced by the composting process will be transferred into the air passing through the windrow. Some will remain within the interstitial void of the windrow only to be released at a turning event. This leads to an under estimation of the number of moles of carbon dioxide evolved and an over estimation of the heat release per mole of carbon dioxide.

- The assumed value for the relative humidity of the ambient air will vary not only with the seasons but with the time of day. This may lead to an incorrect estimation of the energy transferred to the air passing through the windrow. However, as the amount of heat transferred to the air is around 20% of the total produced the effect of the estimation is somewhat limited.

- Changes in overall internal average temperature of the windrows have not been taken into account. The average temperature of the windrow is an indicator of the quantity of heat stored within the windrow; as the temperature increases more heat is stored within the compost and less released. This gives an underestimate of the heat release per mole of carbon dioxide. Only the core temperature of each windrow was measured and without details of the temperature distribution through the windrow the average temperature cannot be calculated.

5.3.6 Conclusions

It is not necessary to record airflow rate continuously as it varies less than other parameters such as CO_2 concentration.

The optimum core composting temperature appears to be below 55°C, with the average windrow temperature being below this.

There is still a level of composting activity at high core temperatures, though this is likely to be due to activity in the cooler sections of the windrow.

The heat output of the composting process as calculated in Chapter 3 is validated by these results.

Results for temperature against composting rate and for estimated heat releases, agree with many other sources. This shows that the canopy is a reliable method of monitoring windrow composting activity.

5.4 Green Waste Augmented with Chicken Litter

Windrow W2I was built on the 25th of November 2002 from a mixture of chicken litter and green waste. As chicken litter has a lower carbon to nitrogen ratio than green waste this should have brought the windrow into the optimum range for composting. To achieve this 67,085 kg of green waste was mixed with 34,300 kg of chicken litter as it had previously been calculated that this should reduce the carbon to nitrogen ratio of the green waste from approximately 70:1 to 20:1. The windrow was turned on the 3rd of December, 6th of December, 10th of December and 13th of December.

5.4.1 Preparation of mixture

Calculations were performed using values of the carbon to nitrogen ratio of different organic materials. This allowed the quantity of chicken litter required to reduce the carbon to nitrogen ratio to be calculated prior to its delivery to the CERT composting facility. The estimate made using the data from Rynk (1992) is shown in Table 5-1. The estimate was based on a windrow of approximately 100 tonnes and a final C:N ratio of approximately 20:1. Samples of the mixture were taken and the carbon to nitrogen ratio of the mixture was analysed. The nitrogen content was analysed using the modified Kjeldahl method as specified in BS EN 13654-1:2001(BSI, 2001) and found to be 1.65% of the dry weight. The carbon content was analysed using a Shimadzu SSM 5000A total organic carbon analyser and was found to be 35.12% of the dry weight, giving a carbon to nitrogen ratio of 21.3:1.

The mixture was formed into a windrow approximately 4 metres wide, 2 metres high and 35 metres long. The average mass per metre length of windrow was 2,897 kg, the volume of one metre of windrow was calculated as 4.2 m^3, the total density of the mixture was 688 kg m^{-3} a value higher than for a windrow made solely of green waste.

Table 5-1. Estimation of the carbon to nitrogen ratio of the mixture

	Chicken litter	Green waste
Total weight	34,300 kg	67,085 kg
Dry weight	27,440 kg	22,542.5 kg
Volatile solids	16,460 kg	23,479.8 kg
Organic Carbon	8,890 kg	12,679 kg
Nitrogen	889 kg	181.1 kg
Calculated total carbon to nitrogen ratio 20.2:1		

5.4.2 Results

The results from the 29th of November 2002 to the 16th of December 2002, covering the first three weeks of the windrow's composting activity, were processed and split into five periods, which are defined as the period of time between turning events. The logger recorded the data every five minutes. In order to remove some of the noise the data has been grouped into sets of five giving averages for 25-minute periods. The data for each period are shown in Figures 5.26, 5.27, 5.28, 5.29 and 5.30. The core temperature of this windrow was generally below 60°C and dropped after turning events.

During Period 1, shown in Figure 5.26, the windrow is still heating up. As the windrow core heats up from 40°C to 55°C the concentration of carbon dioxide in the exhaust gas and the core temperature mirror each other i.e. as the core temperature rises the concentration of carbon dioxide falls. The carbon dioxide concentration is at its highest value of 1.9% whilst the core temperature is approximately 40°C. The two peaks in the core temperature on the 30th of November and the 1st of December coincide with troughs in the carbon dioxide concentration. Once the core temperature has reached 55°C the carbon dioxide concentration begins to rise again. As would be expected from this behaviour these two data series give a strongly negative correlation coefficient of -0.85.

The carbon dioxide concentration also appears to correlate strongly with both the flue temperature and the GTD with a correlation coefficient of 0.97 between carbon dioxide concentration and flue temperature, whilst the carbon dioxide concentration and GTD correlate with a coefficient of 0.95. This effectively means that as the core temperature increases both the GDT and the flue temperature fall.

During Period 2, shown in Figure 5.27, the carbon dioxide content does not appear to follow the flue temperature as closely as it did during Period 1. Correlating the carbon dioxide content with the flue temperature gives a coefficient of 0.47, correlating it with the gas temperature differential gives a very weak coefficient of 0.21. Comparison of the carbon dioxide content and the core temperature gives a correlation of 0.22, the only period to give a positive correlation between these two

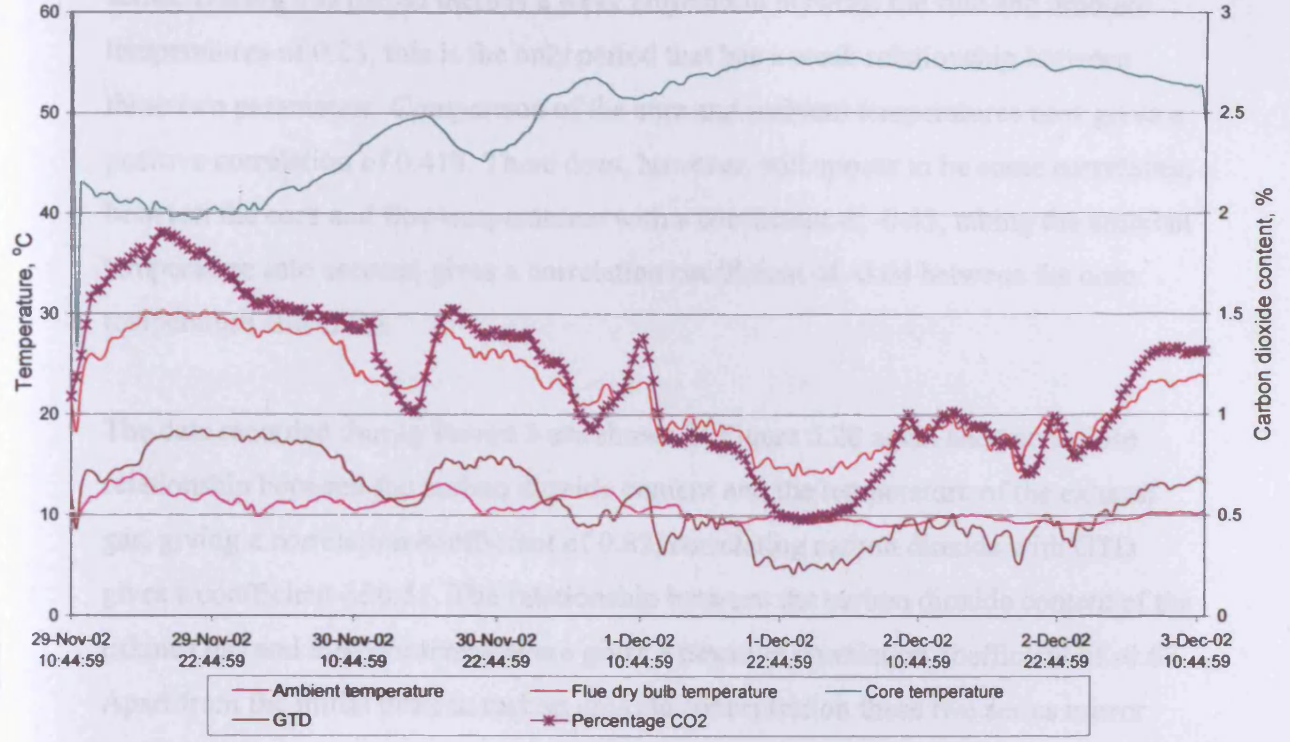

Figure 5.26. Data recorded during Period 1 of the windrow augmented with chicken manure

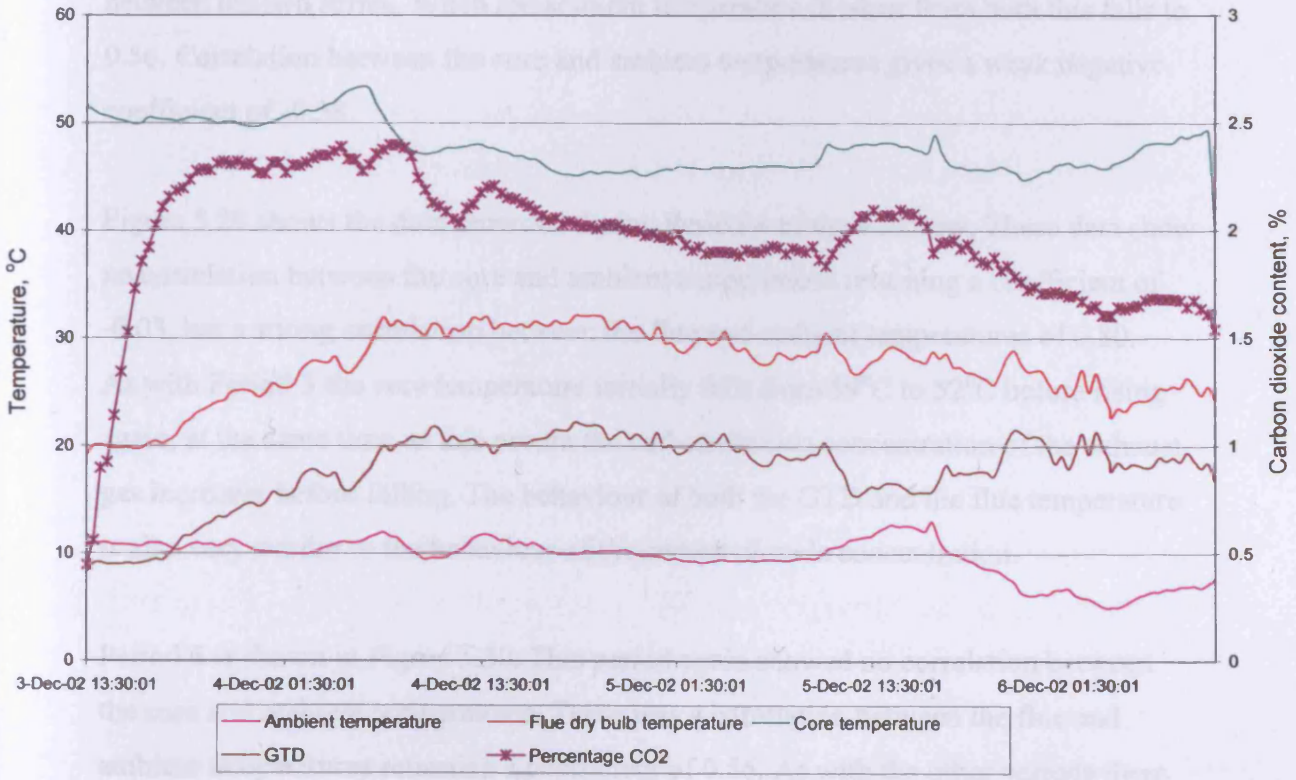

Figure 5.27. Data recorded during Period 2 of the windrow augmented with chicken manure

series. During this period there is a weak correlation between the flue and ambient temperatures of 0.23, this is the only period that has a weak relationship between these two parameters. Comparison of the core and ambient temperatures now gives a positive correlation of 0.418. There does, however, still appear to be some correlation between the core and flue temperatures with a coefficient of -0.43, taking the ambient temperature into account gives a correlation coefficient of -0.64 between the core temperature and GTD.

The data recorded during Period 3 are shown in Figure 5.28 again showed a close relationship between the carbon dioxide content and the temperature of the exhaust gas, giving a correlation coefficient of 0.82, correlating carbon dioxide with GTD gives a coefficient of 0.51. The relationship between the carbon dioxide content of the exhaust gas and the core temperature gives a negative correlation coefficient of -0.67. Apart from the initial peak in carbon dioxide concentration these two series mirror each other with the highest carbon dioxide concentration of 1.4% occurring at the lowest core temperature of 49°C. The relationship between the core and flue temperatures in Period 3 is again strong with a correlation coefficient of -0.86, between the two series. When the ambient temperature is taken from both this falls to 0.56. Correlation between the core and ambient temperatures gives a weak negative coefficient of -0.38.

Figure 5.29 shows the data recorded during Period 4 of the windrow. These data show no correlation between the core and ambient temperatures returning a coefficient of -0.03, but a strong correlation between the flue and ambient temperatures of 0.80. As with Period 3 the core temperature initially falls from 59°C to 52°C before rising again, at the same time as this occurs the carbon dioxide concentration of the exhaust gas increases before falling. The behaviour of both the GTD and the flue temperature is also very similar to the behaviour of the carbon dioxide concentration.

Period 5 is shown in Figure 5.30. This period again showed no correlation between the core and ambient temperatures. There was a correlation between the flue and ambient temperatures returning a coefficient of 0.56. As with the other periods there was a negative correlation between the core-ambient and GTD with a coefficient of -0.66. Unlike the other periods there was a negligible correlation between the carbon

dioxide content and the GTD with a coefficient of 0.08, but like the other periods there was a good negative correlation between the carbon dioxide content in the exhaust gas and the core temperatures with a coefficient of -0.53.

Unfortunately there were some breakdowns with the logging equipment during the lifetime of the windrow, Periods 1 to 5 cover days 3 to 20 of the windrow's lifetime. Further data were also recorded between the 9th and 13th of January which corresponds with the windrow being between 45 and 49 days old, the 30th and 31st of January corresponding with the windrow being 65 and 66 days old, the 3rd and the 11th of February corresponding with the windrow being between 69 and 77 days old and finally the 13th of February and 5th of March which corresponds to an age of between 78 and 98 days. The hot film anemometer used to record the gas velocity proved to be most problematic with very little data being recorded for this parameter.

The data recorded during the period between the 9th and 13th of January are shown in Figure 5.31. During this period there is a strong correlation between flue and ambient temperatures as with the earlier periods. Comparing the flue temperature with the carbon dioxide content of the exhaust gas gives a positive correlation coefficient of 0.44, if the CO_2 content is compared with the gas temperature differential this increases to 0.55. The strong negative correlation between the core temperature and the GTD is also present during this period with a coefficient of -0.72. This again gives a strong negative correlation between the carbon dioxide content and the core temperatures with a coefficient of -0.71 between the two series.

As previously mentioned the velocity of the gas leaving the windrow was not recorded, however data from later on during the composting period does show the gas velocity. Figure 5.32 shows data recorded between the 30th and 31st of January 2003 for the core temperature, carbon dioxide concentration and velocity of the exit gas. At this point the windrow was 65 days old and the core temperature had risen above 60°C and the carbon dioxide concentration had fallen below 1%. Over this short period the core temperature dropped very slightly from 65.7°C to 64°C, whilst the concentration of carbon dioxide in the exhaust gas increased from 0.15% to 0.66%. The velocity of the gas through the chimney remained relatively constant at approximately 0.8 ms^{-1}.

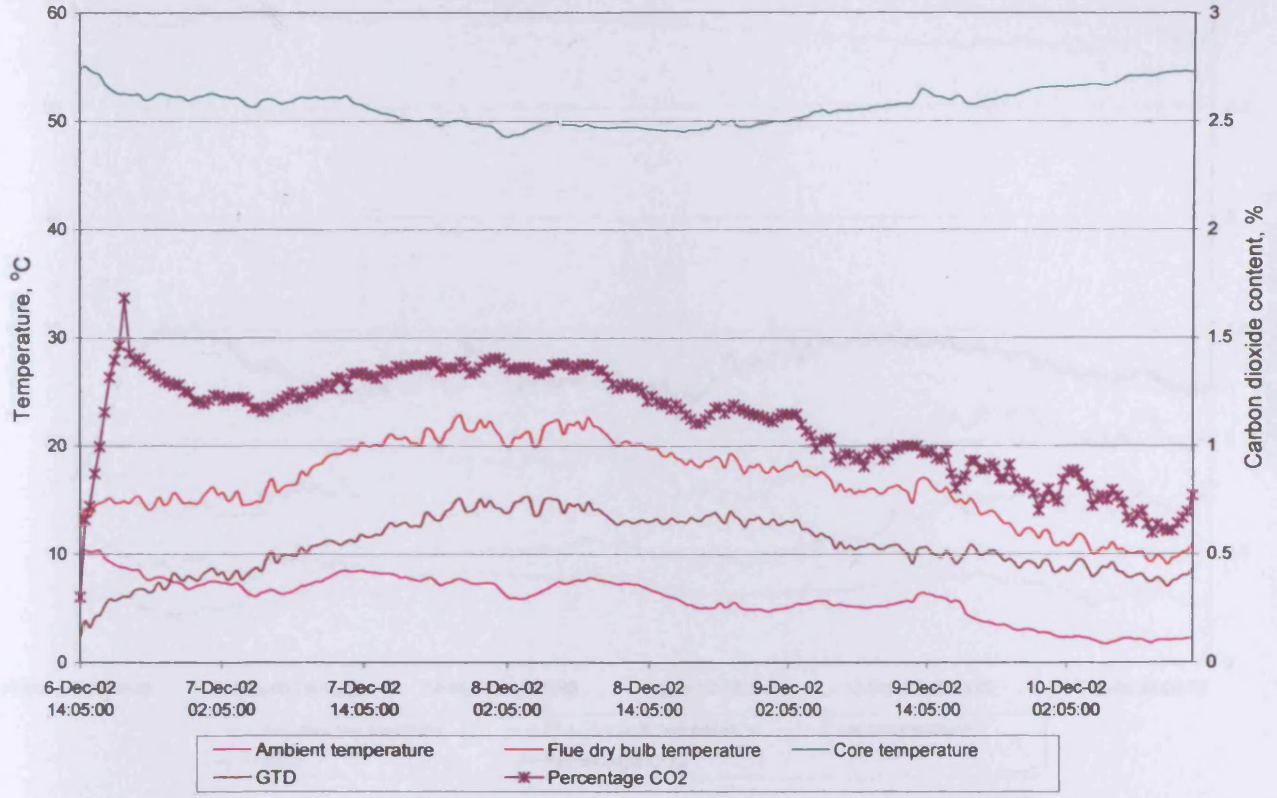

Figure 5.28. Data recorded during Period 3 of the windrow augmented with chicken manure

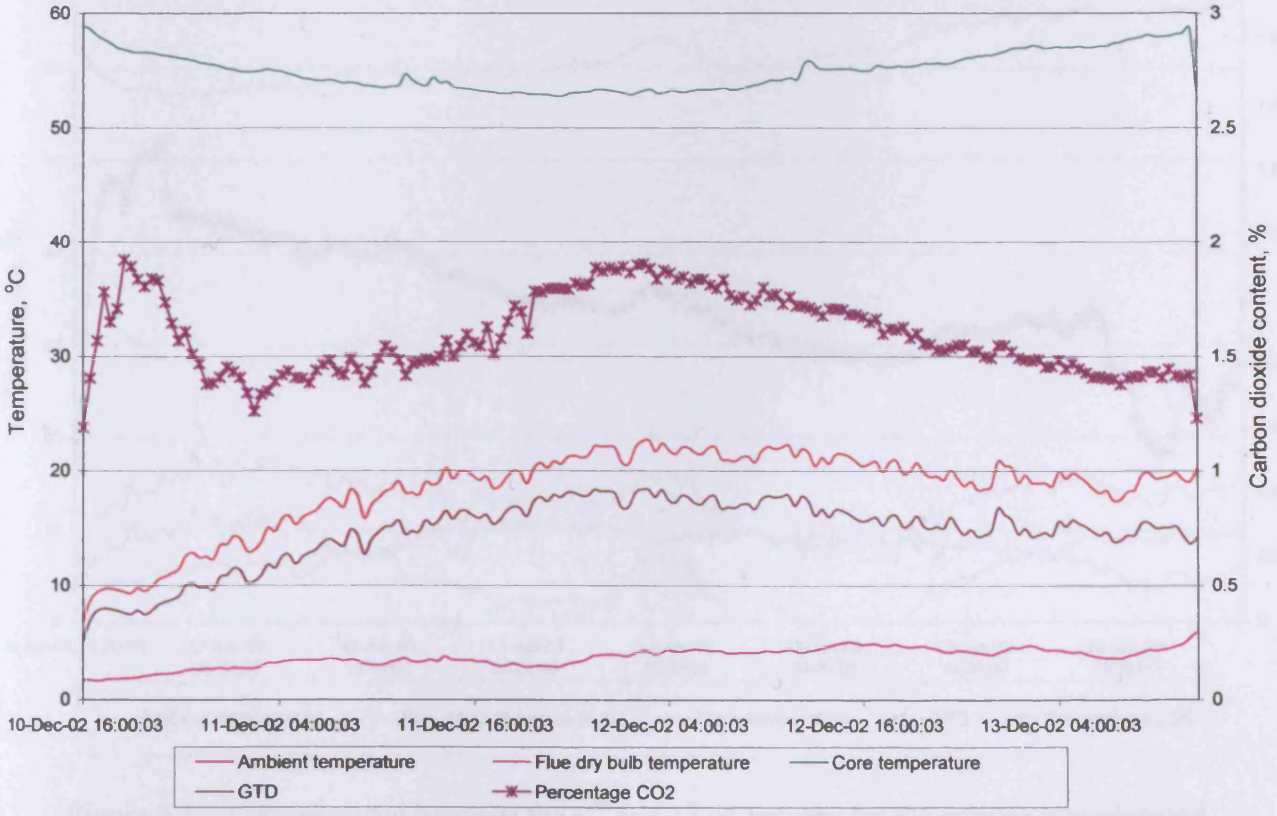

Figure 5.29. Data recorded during Period 4 of the windrow augmented with chicken manure

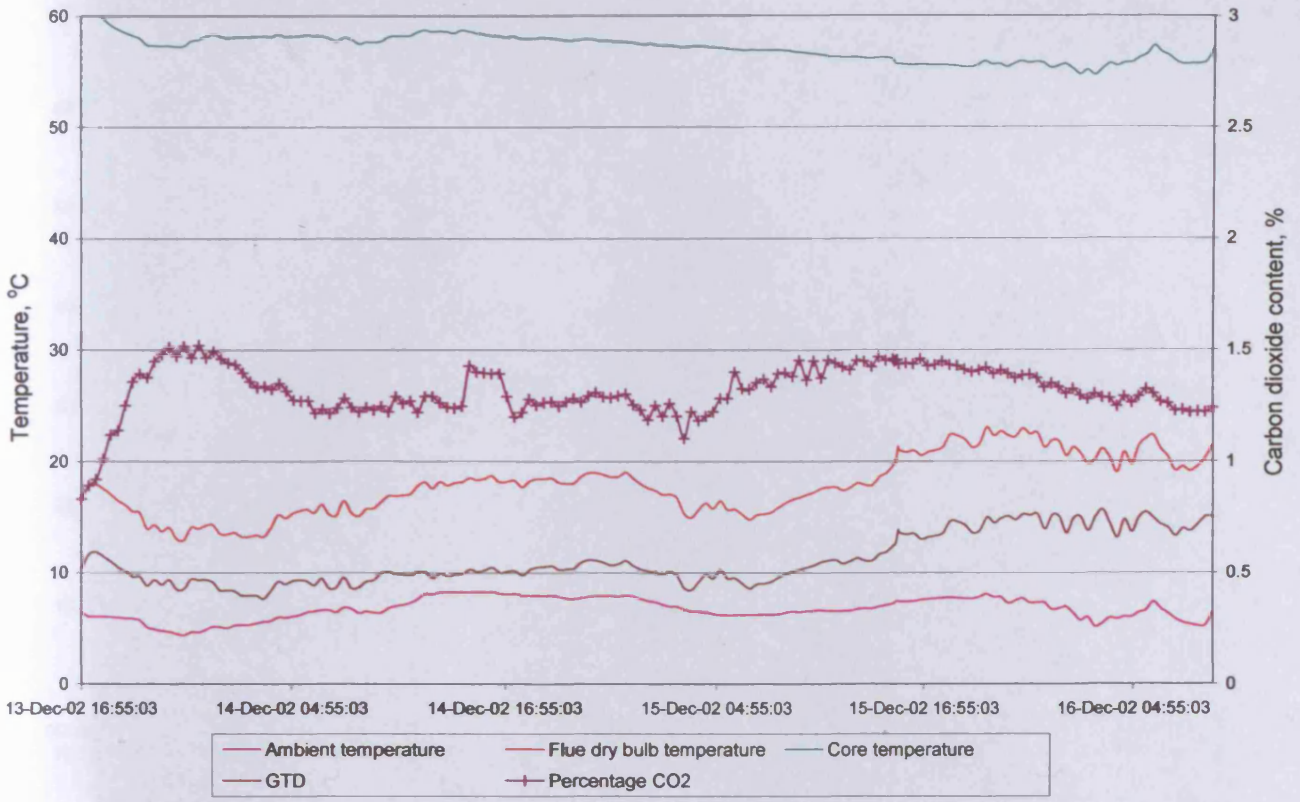

Figure 5.30. Data recorded during Period 5 of the windrow augmented with chicken manure

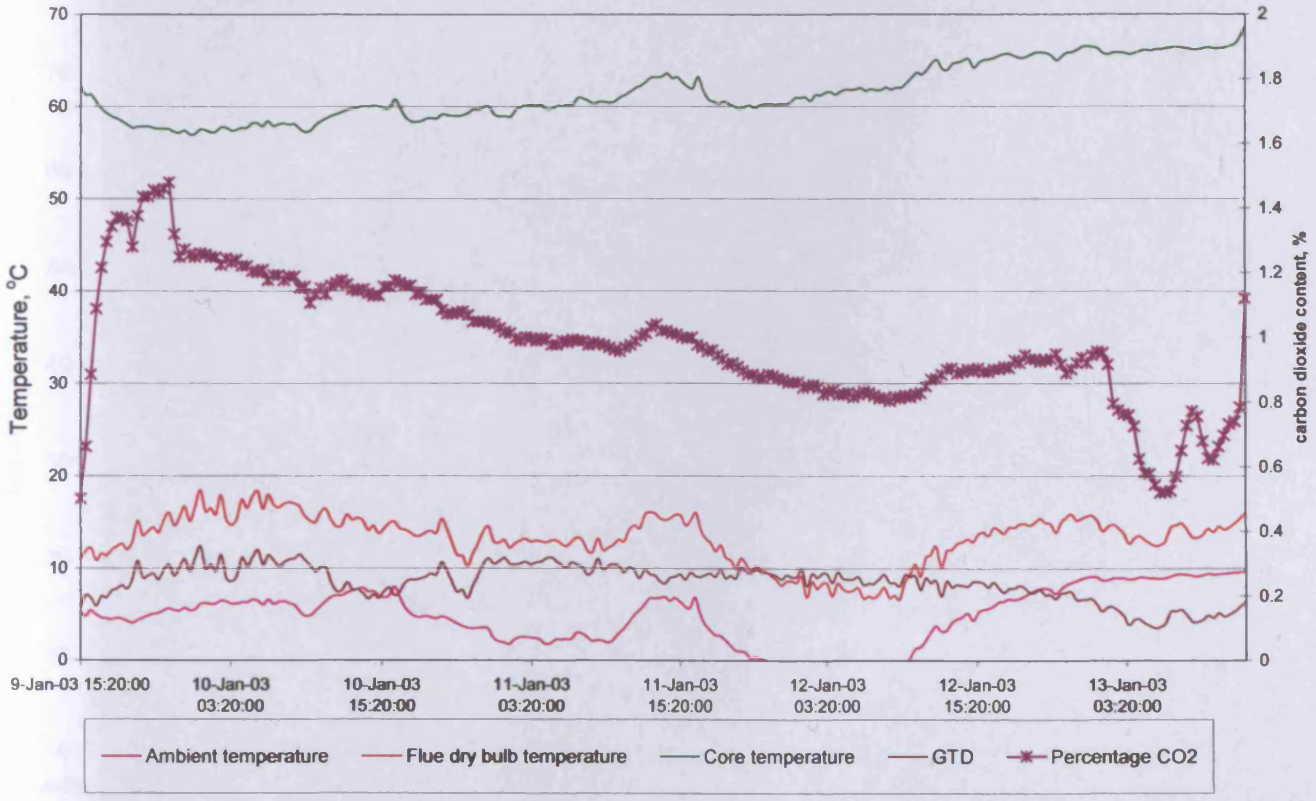

Figure 5.31. Data recorded between the 9th and 13 of January for the windrow augmented with chicken manure

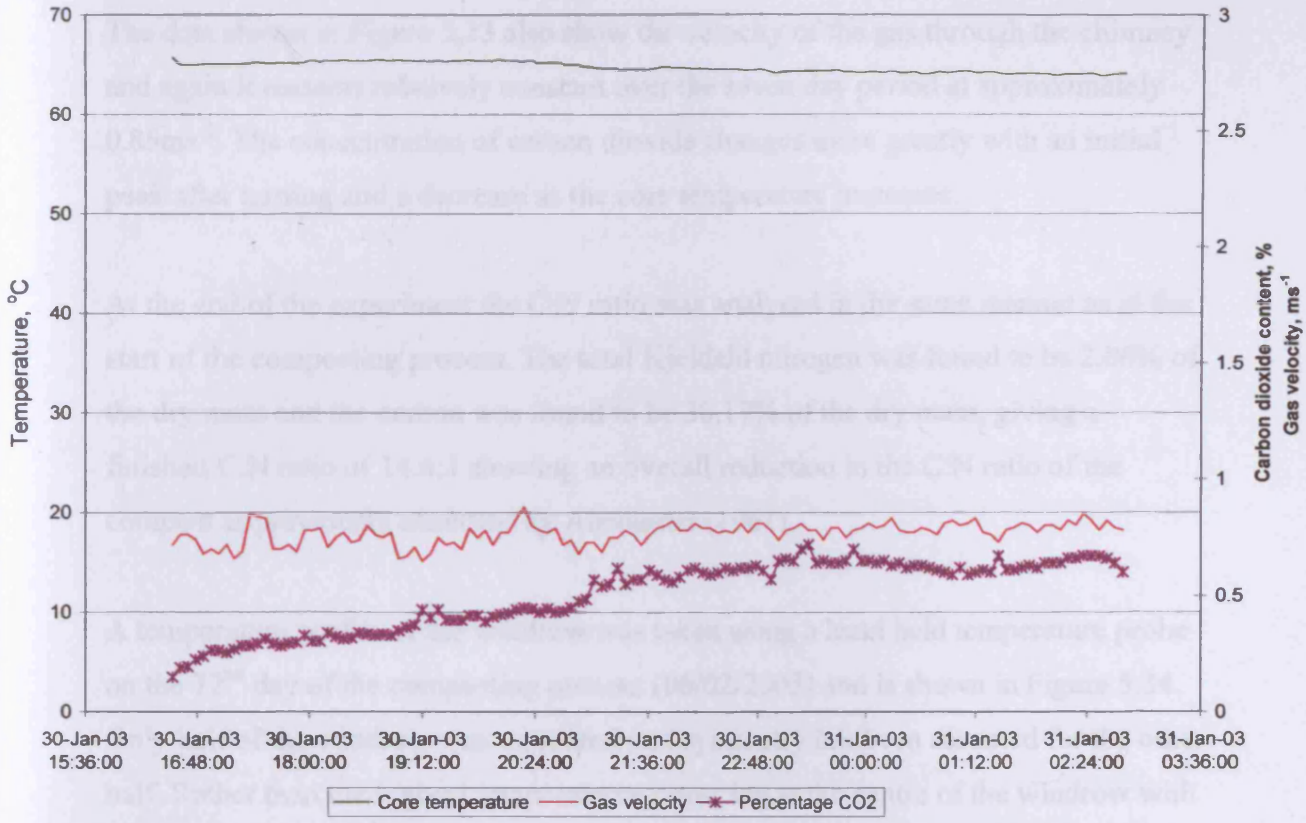

Figure 5.32. Data recorded between the 30th and 31st of January for the green waste and chicken litter windrow

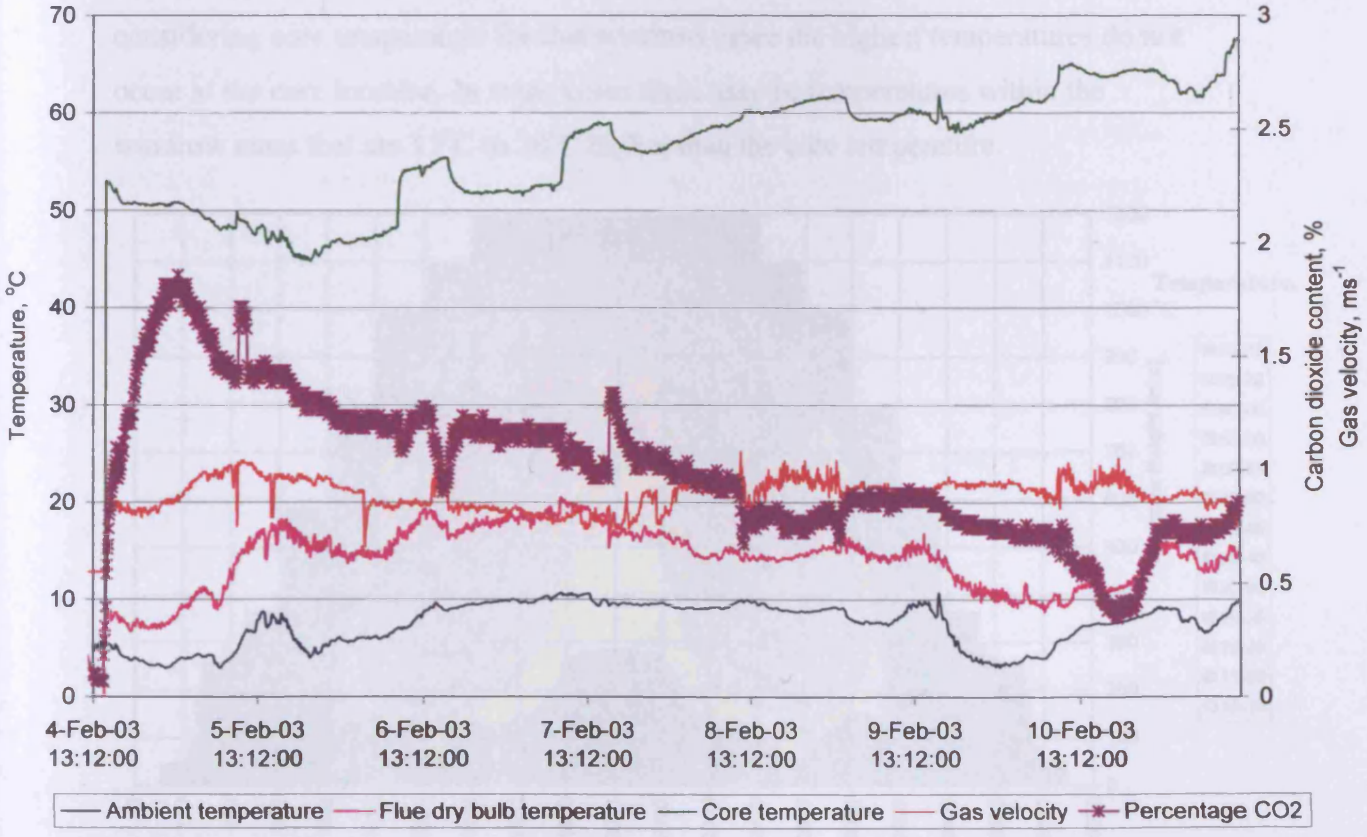

Figure 5.33. Data recorded between the 4th and 11th of February for the green waste and chicken litter windrow

The data shown in Figure 5.33 also show the velocity of the gas through the chimney and again it remains relatively constant over the seven day period at approximately 0.85ms^{-1}. The concentration of carbon dioxide changes more greatly with an initial peak after turning and a decrease as the core temperature increases.

At the end of the experiment the C:N ratio was analysed in the same manner as at the start of the composting process. The total Kjeldahl nitrogen was found to be 2.06% of the dry mass and the carbon was found to be 30.17% of the dry mass, giving a finished C:N ratio of 14.6:1 showing an overall reduction in the C:N ratio of the compost as previously observed by Alexander (1961).

A temperature profile of the windrow was taken using a hand held temperature probe on the 72nd day of the composting process (06/02/2003) and is shown in Figure 5.34. Only half of the windrow was measured and symmetry has been assumed for the other half. Rather than the highest temperatures occurring at the centre of the windrow with contour rings of decreasing temperature concentrically around the core, as shown by Polprasert (1989) and Hewings *et al.* (2002); the hottest area was in a zone ("saddle" or "n" shaped) above and nearer the surface. Care must, therefore, be exercised in considering core temperature for this windrow since the highest temperatures do not occur at the core location. In some cases there may be temperatures within the windrow mass that are 15°C to 20°C higher than the core temperature.

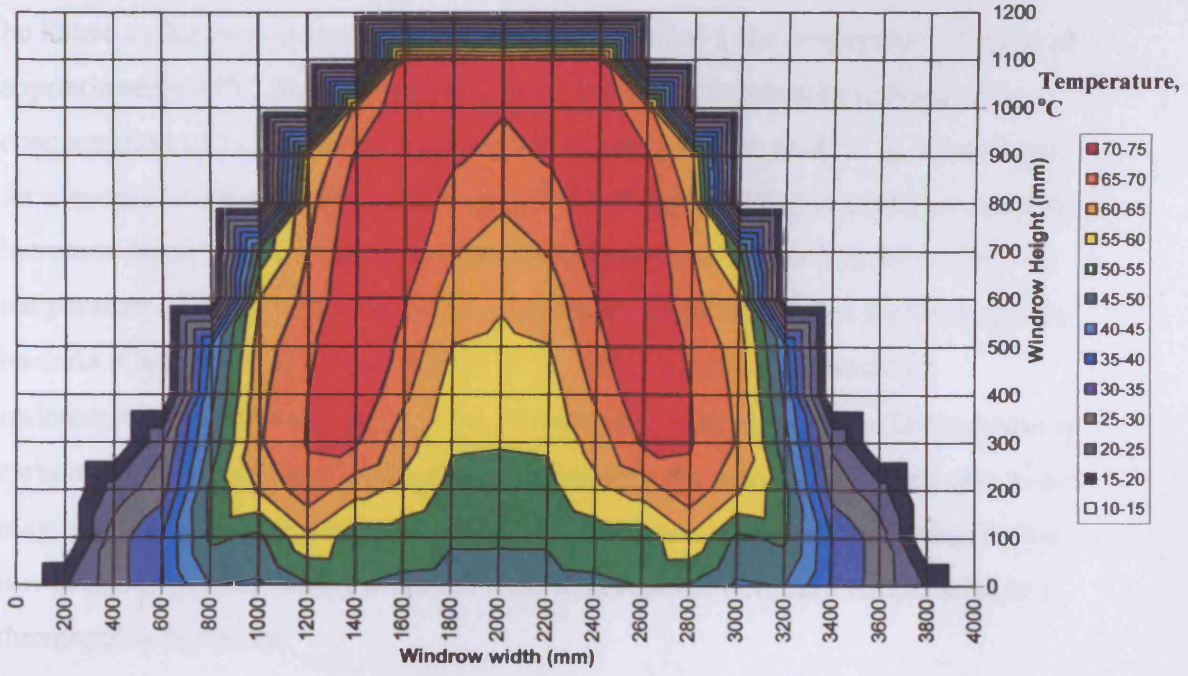

Figure 5.34. Temperature profile of windrow amended with chicken litter, taken on day 72

5.4.3 Discussion

The inclusion of chicken litter increased the density of the composting mixture, the litter was also very fine causing a decrease in the average particle size. As discussed in Chapter 4 the static pressure required to drive air through a static bed is dependant on both of these variables, it is therefore likely that the temperature gradient was not great enough to supply adequate aeration to the composting material and air was unable to penetrate the core of the windrow. This is further supported by the temperature profile shown in Figure 5.34, where the core of the windrow is cooler than the saddle shaped area above. This implies that air was unable to penetrate into the centre of the windrow, so that less composting activity took place at the core leading to the reduced temperature.

A strong correlation between the flue and ambient temperatures would be expected as the flue temperature is a function of the ambient temperature and the heat picked up as the air passes through the windrow, it is therefore somewhat odd that there is a weak correlation between these two series during Period 2.

The carbon dioxide content and core temperature series are evidently related and these two variables for the first five periods are plotted against each other in Figure 5.35. There is always a sharp increase in the concentration of carbon dioxide within the exhaust gas immediately after a turning event. However, after this, the behaviour can be linked to the core temperature series. During Period 1 the temperature remains at approximately 40°C for the first day shown, but as the temperature increases the concentration of carbon dioxide decreases. The temperature of 40°C is the optimum for mesophilic bacteria (Jeris and Regan, 1973; Kutzner 2000) so as the temperature increases the activity of the mesophiles decreases. On the 1st of December the core temperature reached 55°C one of the quoted optimum temperatures for thermophilic bacteria (Cathcart *et al.*, 1986; Wiley, 1956; 1957), shortly afterwards the concentration of carbon dioxide in the exhaust gas began to increase. The increase in carbon dioxide concentration implies an increase in the activity within the pile which may be due to the compost having reached an optimum temperature. During Period 1 it is possible that the windrow moved from a mesophilic optimum temperature to a thermophilic optimum.

The pattern of increasing and decreasing concentrations of carbon dioxide as the core temperature moves away from an optimum is reflected through much of the rest of the data. In Figure 5.28, Period 3, the core temperature gradually decreases from approximately 55°C to 49°C, over a period of 2 days before increasing back to 55°C over the next two days. Apart from the initial post-turning increase in carbon dioxide the concentration of CO_2 in the exhaust gas increases until the core temperature is at 49°C, before falling as the temperature begins to increase. For this period the optimum would appear to be 49°C rather than 55°C but this could purely be due to the positioning of the probe recording the core temperature. The same pattern is repeated in Figure 5.29, Period 4 and to a lesser extent in Figure 5.30 for Period 5 with 55 °C appearing to be the optimum composting temperature. Figure 5.31, Period 5, shows the windrow at a late stage and the temperature within the windrow is continuously increasing and the concentration of carbon dioxide within the exhaust gas continually decreases.

Due to the failure of the hot wire anemometer it is not possible to give an accurate representation of the composting rate. However, the concentrations of carbon dioxide observed in the chimney were similar to those for green waste. Figures 5.32 and 5.33 give an indication of the velocity through the chimney being approximately 0.85ms^{-1} as opposed to approximately 1 ms^{-1} for the green waste windrows discussed in Section 5.3. During this trial there was approximately double the mass of volatile solids beneath the canopy than during the green waste only trials. The exhaust gas temperatures were similar to those observed during the green waste trials. Combining these factors gives the composing rate as being approximately 45% of that of the green waste only windrows. So where a carbon dioxide concentration in the exhaust of 1% would give a rate of approximately 20 g CO_2 $kgVS^{-1}day^{-1}$ for the green waste only, the same concentration of CO_2 for the augmented windrow indicates a rate of approximately 9 $CO_2kgVS^{-1}day^{-1}$.

The strongly negative correlation coefficients between the core temperature and the concentration of carbon dioxide in the exhaust reflect the existence of an optimum temperature for composting. This relationship is also seen in Figure 5.35. Period 2 however, shown in Figure 5.27 does not show this behaviour and in fact has a weak positive correlation between the carbon dioxide concentration and the core

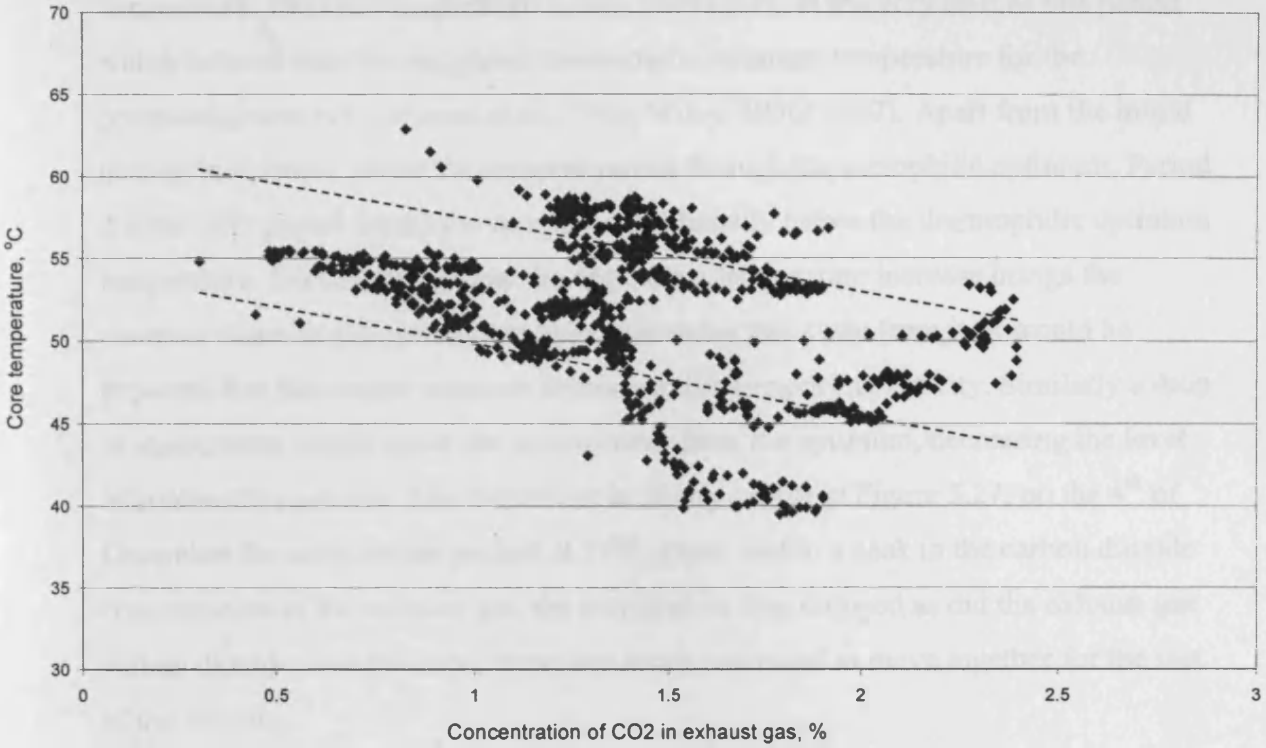

Figure 5.35. Core temperature against CO_2 concentration in the exhaust gas for the first 5 periods of the windrow augmented with chicken litter against core temperature

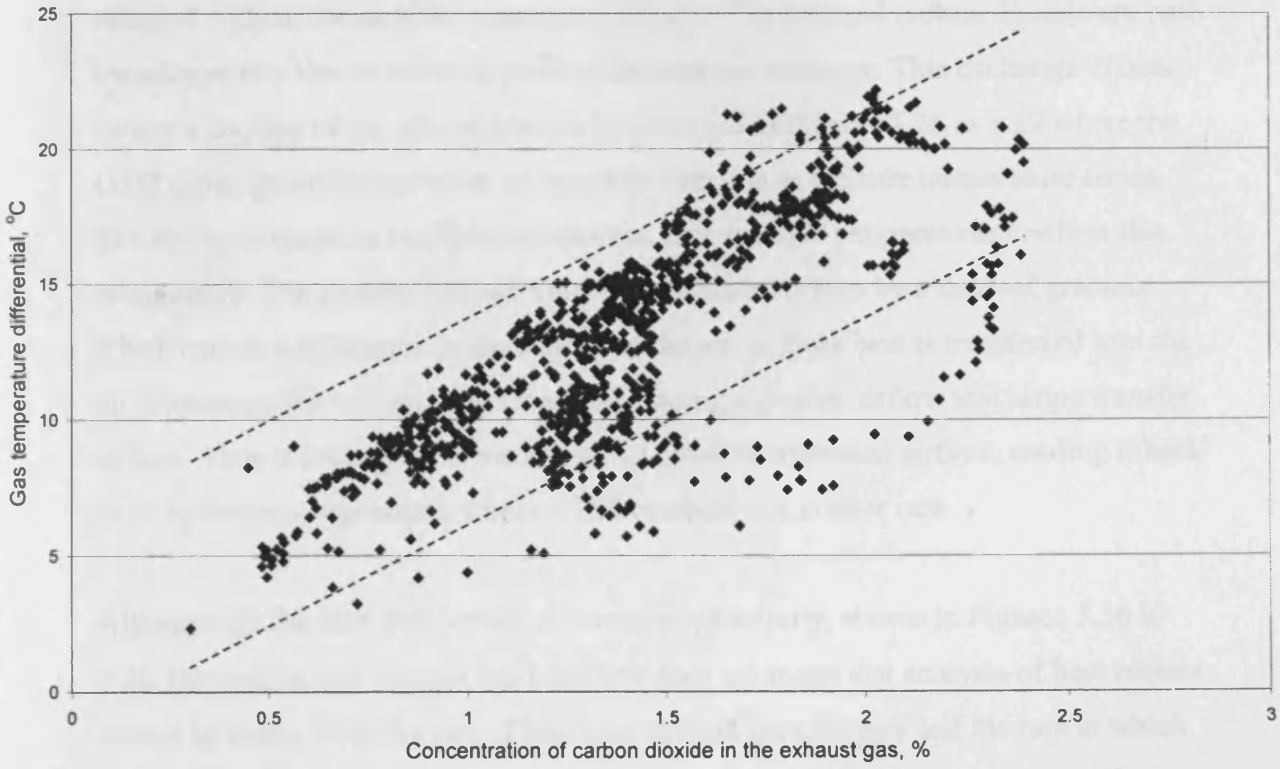

Figure 5.36. GTD against CO2 concentration in the exhaust gas for the first 5 periods of the windrow augmented with chicken litter against core temperature

temperature. The core temperature is only above 50°C at the very start of this period which is lower than the suggested thermophilic optimum temperature for the composting process (Cathcart *et al.*, 1986; Wiley, 1956; 1957). Apart from the initial heat up in Period 1 where the compost passes through the mesophilic optimum, Period 2 is the only period where the compost is continually below the thermophilic optimum temperature. Because it is below the optimum a temperature increase brings the compost closer to the optimum temperature rather that away from it. It would be expected that this would cause an increase in the composting activity. Similarly a drop in temperature would move the system away from the optimum, decreasing the level of composting activity. This behaviour is clearly visible in Figure 5.27; on the 4th of December the temperature peaked at 53°C which lead to a peak in the carbon dioxide concentration of the exhaust gas, the temperature then dropped as did the exhaust gas carbon dioxide concentration, these two series continued to move together for the rest of the period.

The positive correlation between the carbon dioxide concentration and the GTD can be seen in Figure 5.36. This is simply due to the increased quantities of heat that are released with an increase in composting activity. The heat and carbon dioxide are both transferred into the air which is passing through the windrow. This exchange of heat causes a cooling of the pile-which can be observed in Figures 5.26 to 5.29 where the GTD series generally moves in an opposite direction to the core temperature series. The strong correlation coefficients between core and flue temperatures confirm this relationship. The airflow through the windrow is also driven by a thermal gradient which causes a difference in the density of the air, as more heat is transferred into the air it becomes warmer and more buoyant causing a greater airflow and larger transfer of heat. Thus if a windrow is too hot it will cause an increased airflow, cooling it back to an optimum temperature, where it will compost at a greater rate.

Although for the first five periods of composting activity, shown in Figures 5.26 to 5.30, the airflow rate was not recorded this does not mean that analysis of heat release cannot be made. Both the rate of heat loss through the chimney and the rate at which moles of carbon dioxide leave through the chimney are dependant on the velocity through the chimney. However, calculating the heat released per mole of carbon dioxide released means that the flow rate of gas through the chimney is not important

as it will cancel itself out. The same assumptions about the air humidity were made as in Section 5.3.5; that the exhaust air is fully saturated whilst the inlet air has a relative humidity of 70%. The heat release through the chimney per mole of carbon dioxide for the first 5 periods is shown in Figure 5.37. The average value is 84 kJ/mole, lower than estimated in Chapter 3 but in the range of values for Windrows W1I and W2F found in Section 5.3.5 of 43.3 kJ/mole and 93.4 kJ/mole. As was shown in Section 5.35 it is possible to account for the remainder of the heat as being lost through the canopy.

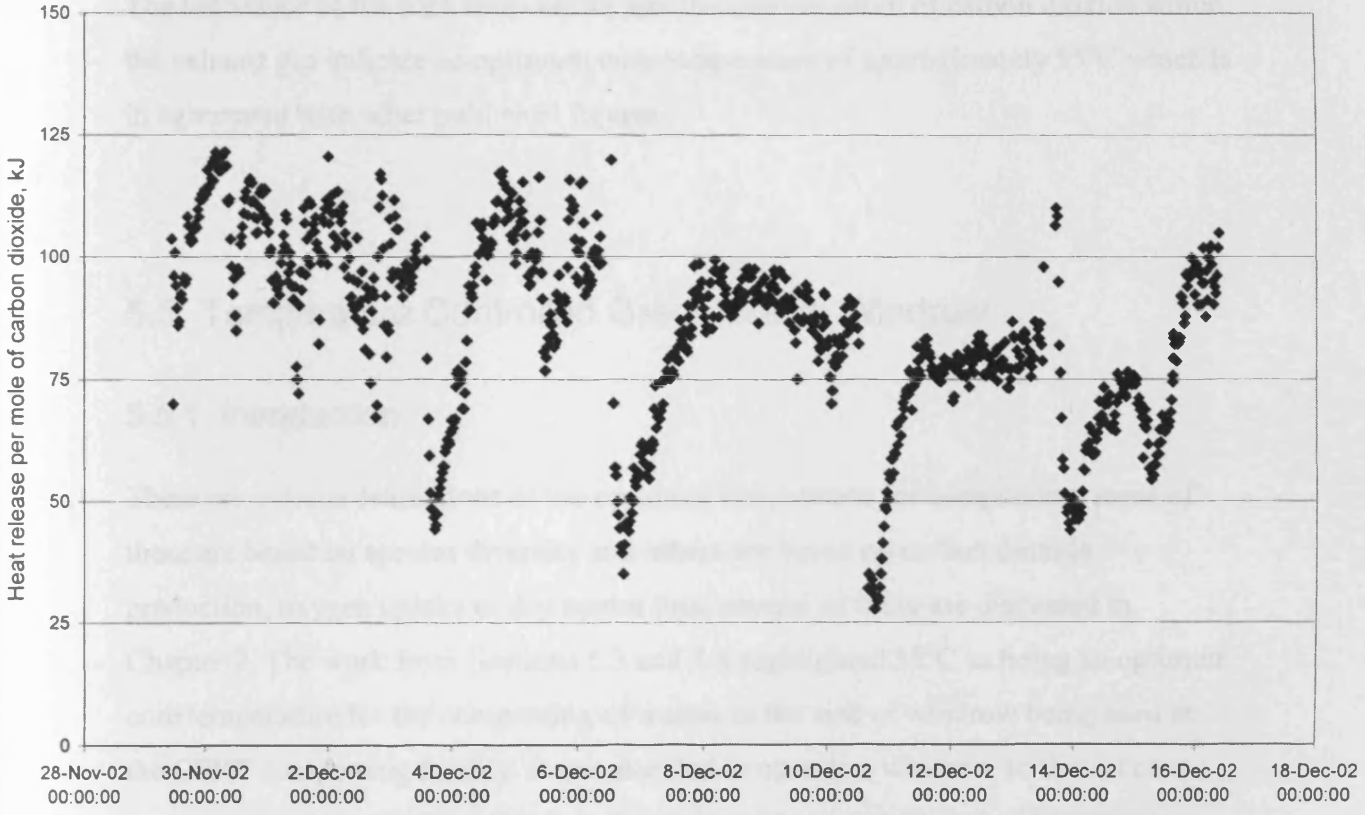

Figure 5.37. Heat release per mole of carbon dioxide for the first 5 Periods of the augmented windrow (during each 25 minute time period)

5.4.4 Conclusions

The mixture did achieve a level of stabilisation during the composting process as noted in the reduction in C:N ratio.

The levels of heat released to the air passing through the windrow are similar to those for green waste.

The rate of airflow through a windrow does not vary greatly over its lifespan. Meaning that changes in activity are accompanied by increased temperatures and CO_2 concentrations in the exhaust gas.

The size of the windrow and reliance on natural ventilation combined with the increased density and reduced particle size resulted in reduced airflow through the compost which inhibited the composting process.

The behaviour of the core temperature and the concentration of carbon dioxide within the exhaust gas indicate an optimum core temperature of approximately 55°C which is in agreement with other published figures.

5.5 Temperature Controlled Green Waste Windrow

5.5.1 Introduction

There are various estimations of the optimum temperature for composting, some of these are based on species diversity and others are based on carbon dioxide production, oxygen uptake or dry matter loss; several of these are discussed in Chapter 2. The work from Sections 5.3 and 5.4 highlighted 55°C as being an optimum core temperature for the composting of wastes in the size of windrow being used at the CERT composting facility. It was decided to operate a windrow so that its core temperature was at 60°C, as this was the optimum temperature quoted by various researchers (Strom, 1985;Rothbaum, 1961; Wiley 1956;1957). The aeration supplied to the windrow may also lead to more uniform temperature distribution within the windrow (Sesay *et al.*, 1998). To supply a large enough quantity of air to remove the excess heat a forced ventilation system was used and this was controlled by an internal relay in the data logging equipment that monitored the core temperature of the windrow. However the results from Chapter 3 suggest that the supply of enough air to cool the windrow will also remove moisture from the windrow which may affect composting activity.

5.5.2 Method

Some initial investigations were required in order to assess the quantity of air needed in order to remove the excess heat. A 15 metre long 4 metre wide and 2 metre high windrow was constructed on top of a 20 metre long section of 100 mm diameter perforated pipe. The windrow is shown in Figure 5.38. The pipe was bent into a "U" shape so that the arms were 1 metre apart under the centre of the windrow. The canopy was placed in the middle of the aerated section of the windrow in order to negate the end effects.

Figure 5.38. The short windrow built to determine air requirements for temperature control during the scoping studies

A blower was borrowed from a local agricultural equipment suppliers (J. Davies & Sons, Pencader) which was attached to the perforated pipe. Several tests were performed on the 1st of April 2003. A U-tube manometer capable of reading up to 300 mmH_2O was used to measure pressure and this along with the blower is shown in Figure 5.39. The static pressure that the fan could deliver at no flow was measured at 118 mmH_2O. The static pressure recorded at the outlet of the blower was 48 mmH_2O, much less than the figure of 203 mmH_2O assumed by Keener *et al.* (1997) for a column 2.4 metres high. The velocity head at the centre of the pipe was found to be 53 mmH_2O, this is equivalent to a maximum velocity through the pipe of 32.6 ms^{-1} and assuming turbulent flow through the pipe a volumetric flow rate of 0.21 m^3s^{-1} can be determined. This is approximately $2.8\times10^{-3}m^3\ s^{-1}m^{-3}$ (cubic metres of air per cubic metre of compost per second).

Theoretical aeration requirements were calculated in Chapter 3. Plots of aeration requirements for oxygen supply, heat removal and moisture removal as a function of composting rate and bulk density are shown in Figures 3.14, 3.15 and 3.16. The shredded green waste composted at the CERT composting facility has a bulk density of approximately 370 kgm^{-3}. The composting rate for the green waste shown in Section 5.3 was generally between 20 and 30 $gCO_2kgVS^{-1}day^{-1}$. Figure 3.15 shows that the aeration requirement for heat removal would be between $2\times10^{-3}m^3\ s^{-1}m^{-3}$ and $3\times10^{-3}m^3s^{-1}m^{-3}$. The quantity of air supplied to the trial windrow, shown in Figure 5.38, of $2.8\times10^{-3}m^3\ s^{-1}\ m^{-3}$lies within this range.

The blower was turned on and the effect on temperature of the core, carbon dioxide concentration of the exhaust gas and flue temperature was monitored over a period of several hours. These results are shown in Table 5-2.

Table 5-2. Data recorded during the temperature control scoping test

Time / Variable	12.35	14.00	15.45
Core Temperature	76.4°C	68.7°C	64.7°C
Flue Temperature	16.0°C	22.5°C	18.0°C
CO_2 Concentration	2.38%	0.47%	1.18%

The aeration successfully cooled the windrow during the first 85 minutes of continual blowing. The initial peak in the carbon dioxide concentration of 2.38 percent reflects the CO_2 being blown out from the interstitial voids within the windrow. As was expected the windrow cooled rapidly as a greater quantity of heat was transferred into the air passing through it. Over the next 105 minutes the rate of cooling reduced but the concentration of carbon dioxide in the exhaust gas built up, possibly reflecting a larger amount of composting activity within the windrow.

For the monitoring period a blower capable of delivering 1500 m^3hour^{-1} or 0.42 m^3s^{-1} at a pressure of 1000 Pascals (100 mmH_2O) was sourced to supply the windrow. A photograph of the experimental set up is shown in Figure 5.40. One of the data logger's internal relay channels was used to control the fan. The logger sampled and recorded values for core temperature, flue temperature, ambient temperature and gas velocity every 5 minutes. If the core temperature was over the preset value of 60°C

Figure 5.39. Equipment used to determine static pressure and flow rate to cool a windrow during the trial period

Figure 5.40. Canopy and cover on the green waste windrow during the monitoring period (the air supply fan is in the foreground)

the relay channel supplied a 12V D.C. voltage to the coil of another relay which turned the fan on. The comparison was made every five minutes when the logger recorded temperatures. If the temperature was below 60°C then the fan would be turned off for the next five minutes.

As can be seen in Figure 5.40 the parts of the windrow that were not covered by the canopy were covered with a breathable membrane, this was done for regulatory reasons to comply with the waste management licence of the CERT composting facility.

5.5.3 Aeration Calculations

Theoretical estimation of the required airflow to the windrow can be made using the figures presented in Chapter 3. These can be used to give an estimate of the airflow rate that should be expected through the chimney of the canopy. For a windrow composting at a rate of 15 gCO_2 kg $VS^{-1}day^{-1}$ and a density of 370kg m^{-3} approximately $2\times10^{-3}m^3s^{-1}$ of air per cubic metre of compost would be required to remove excess heat. Beneath the canopy there are approximately 12 cubic metres of compost. This gives a total aeration requirement of $2.4\times10^{-2}m^3s^{-1}$. At the chimney this airflow would be observed as an average velocity of 1.44 ms^{-1}, or as this is turbulent flow, a peak velocity of 1.76 ms^{-1}.

5.5.4 Results

The construction of the windrow was finished on the 1st of June 2003, and it was monitored from the 4th of June 2003. During the monitoring period there were a variety of breakdowns including the datalogger, the hot wire anemometer and the switching mechanism for the fan. Data are available for the windrow up to the 22nd of June and have been split into 3 periods. In order to allow greater clarity in the results

instead of the period being defined as the time between turnings it is in this case, unfortunately, defined as the period between equipment breakdowns.

The data collected by the data logging equipment between the 4th and 10th of June 2003 are shown in Figure 5.41, as with the data presented in earlier sections of this chapter the data have been slightly smoothed by averaging 25 minute periods from the raw data that were recorded every five minutes. The CO_2 concentration in the exhaust gas reaches quite high concentrations of up to 4%. It also appears to follow a diurnal pattern causing the composting rate to move with it. The airflow appears to move inversely to the carbon dioxide concentration and there is a strong negative correlation of -0.61 between these two series. As with the green waste windrow there is a strong correlation between the rate and the carbon dioxide concentration of 0.62, whilst the correlation between the rate and the airflow is a very weak 0.16. During this period the logger was housed in a box above the windrow so the cold junction temperature is shown. This is still within the loggers operating range.

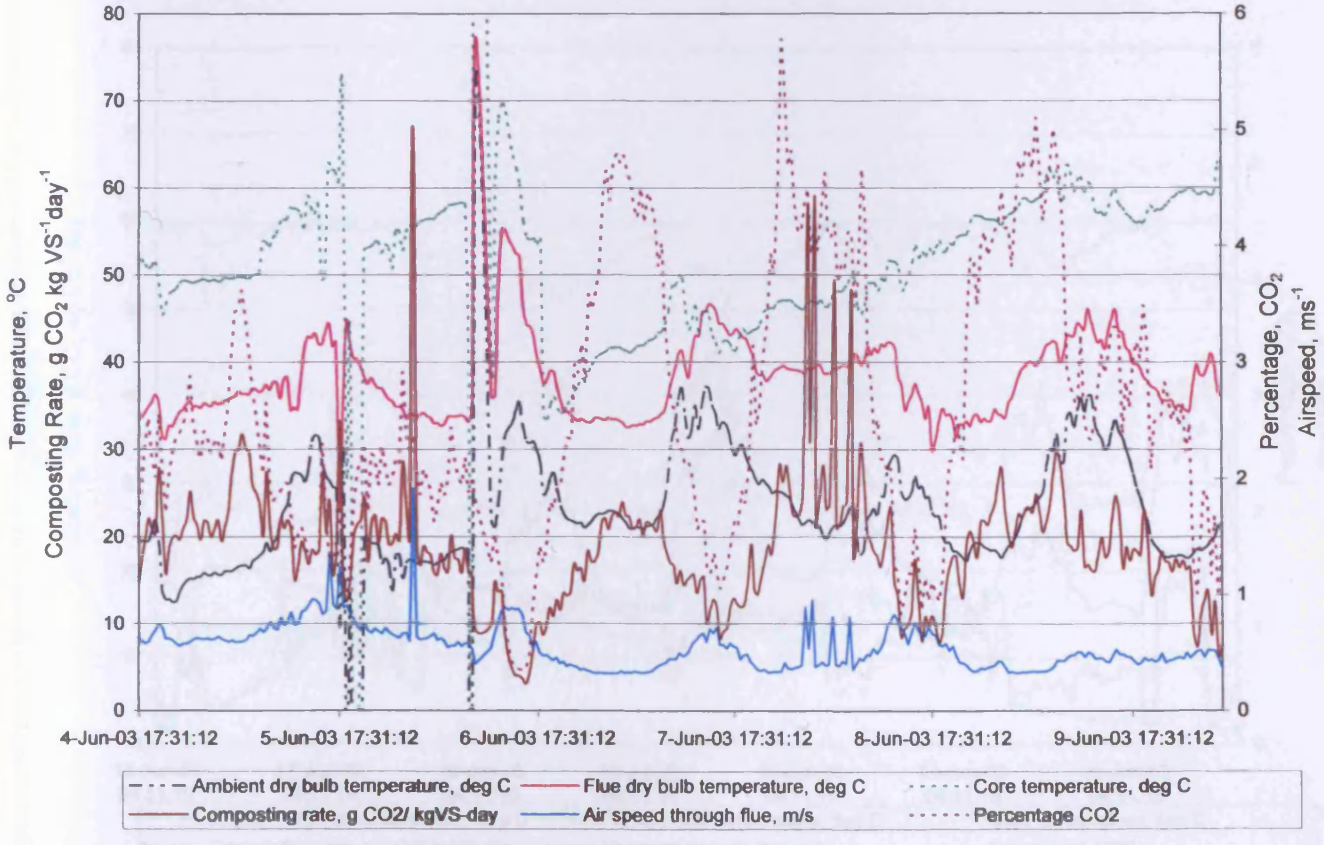

Figure 5.41. Data from the temperature controlled windrow during Period 1

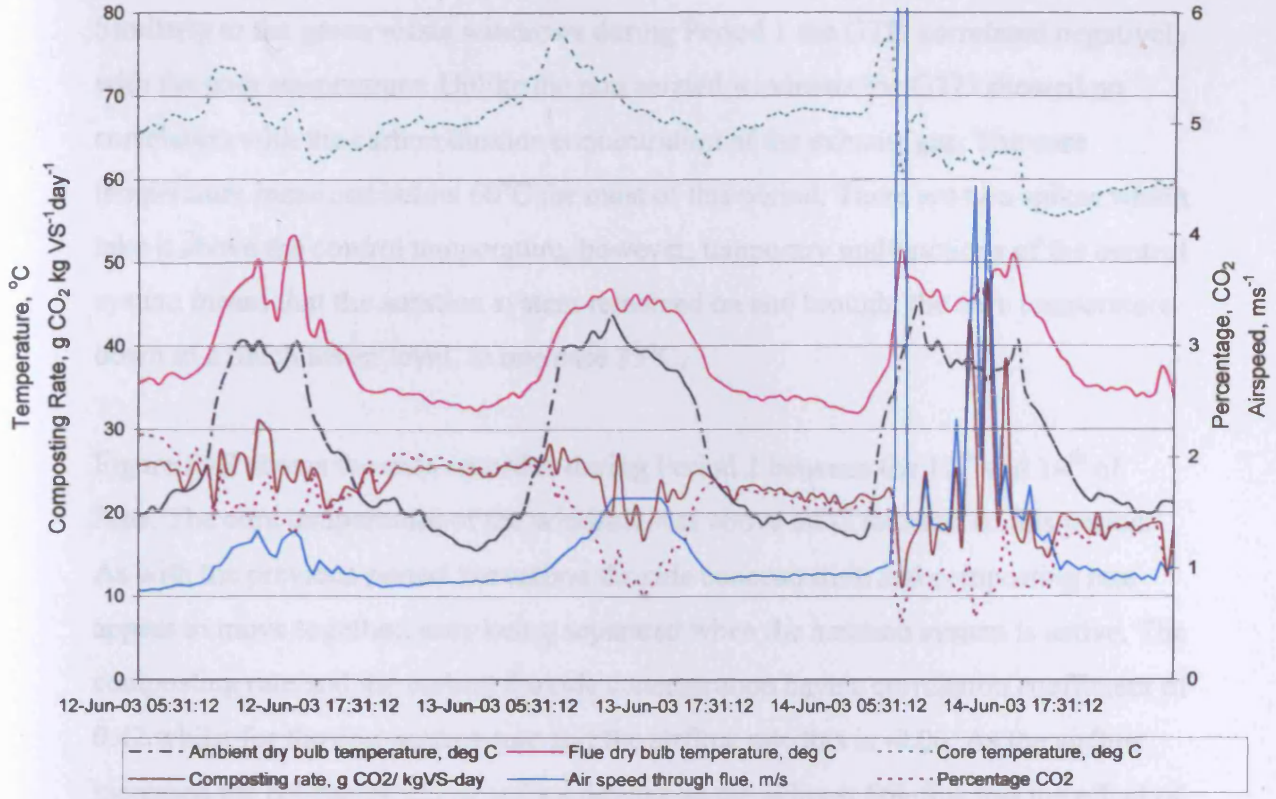

Figure 5.42. Data from the temperature controlled windrow during Period 2

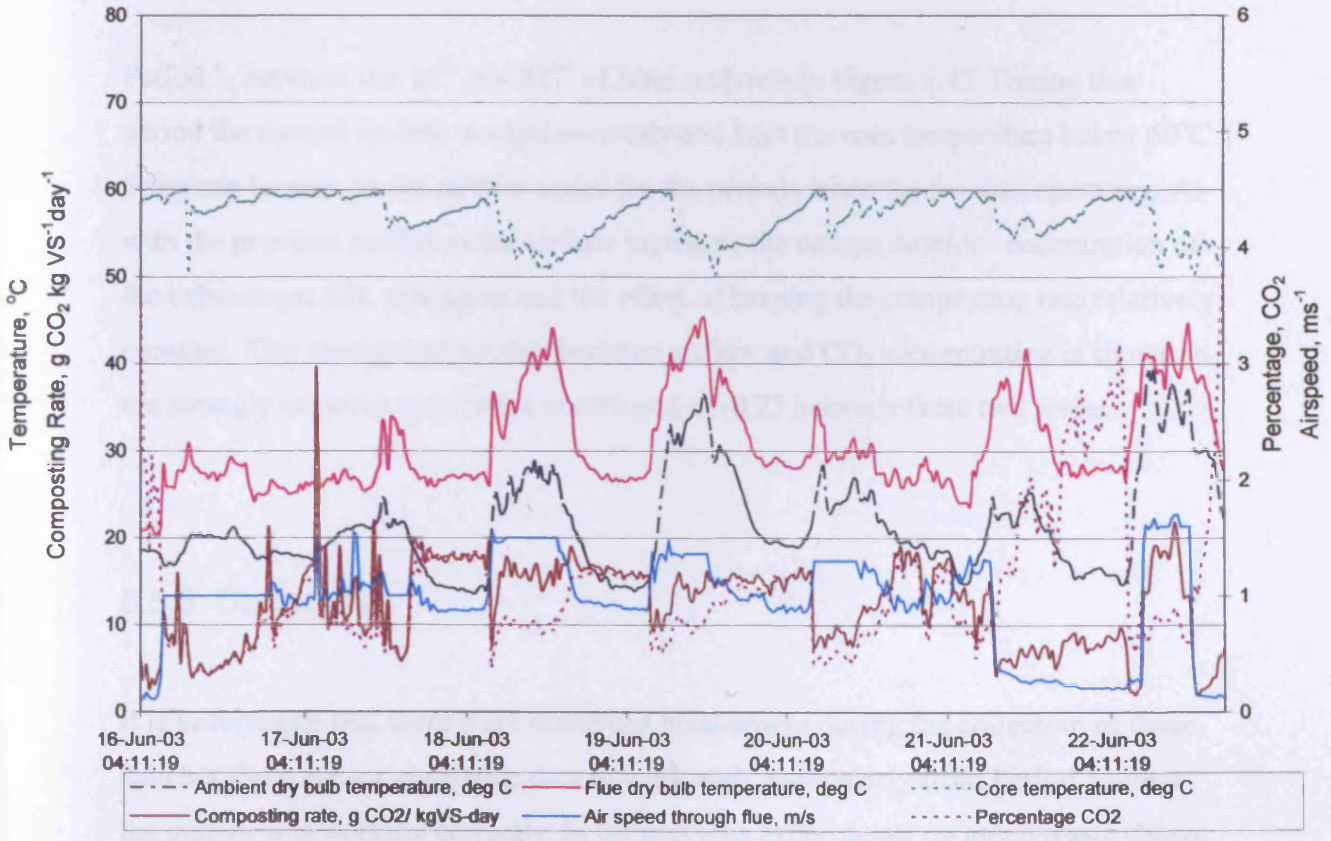

Figure 5.43. Data from the temperature controlled windrow during Period 3

Similarly to the green waste windrows during Period 1 the GTD correlated negatively with the core temperature. Unlike the non aerated windrows the GTD showed no correlation with the carbon dioxide concentration of the exhaust gas. The core temperature remained below 60°C for most of this period. There are two spikes which take it above the control temperature, however, temporary malfunctions of the control system meant that the aeration system remained on and brought the core temperature down to a much lower level, in one case 35°C.

Figure 5.42 shows the data recorded during Period 2 between the 12th and 14th of June. The core temperature of the windrow was above 60°C for most of this period. As with the previous period the carbon dioxide concentration and composting rate appear to move together, only being separated when the aeration system is active. The composting rate and the carbon dioxide concentration have a correlation coefficient of 0.42 whilst for the composting rate and the airflow rate this is -0.06. As the airflow increased the concentration of carbon dioxide in the exhaust fell, this had the effect of keeping the composting rate relatively constant. Unlike the non aerated windrows there was no correlation between the GTD and the carbon dioxide concentration.

Period 3, between the 16th and 22nd of June is shown in Figure 5.43. During this period the control system worked correctly and kept the core temperature below 60°C. Steps can be seen in the airflow series for the periods when the fan was operating. As with the previous period as the airflow increased the carbon dioxide concentration of the exhaust gas fell, this again had the effect of keeping the composting rate relatively constant. This strong relationship between airflow and CO_2 concentration is shown in the strongly negative correlation coefficient of -0.73 between these two series.

5.5.5 Discussion

It is unfortunate that there were numerous breakdowns during the collection of these data but there are some suitable data to work with, particularly from Period 3 where the system was working correctly. In the previous experiments on green waste shown in Section 5.3, the composting rate was shown to be more dependant on the carbon

dioxide concentration of the exhaust gas than its flow rate; Figures 5.41 and 5.42 show that this is true for the first two periods of this experiment. However, the data recorded during Period 3, shown in Figure 5.43, show that the composting rate is highly dependant upon the airflow rate. This was the only period where the control system worked correctly.

The carbon dioxide concentration and airflow rate also moved inversely to each other for all three periods whereas in the green waste composting trials these two series appeared to be unrelated. This movement causes the respiration rate to remain relatively constant (particularly during periods 2 and 3). The increase in one parameter offsets the decrease in the other.

Figure 5.44 shows a plot of composting rate against core temperature for the temperature controlled windrow. Unlike the non controlled windrows shown in Figures 5.20 and 5.21 there is no definite trend linking the two parameters. There is a strong vertical cluster around the temperature of 60°C, this is the temperature at which the fan came on to aerate the windrow. During fan start up and run down periods a variety of carbon dioxide concentrations would have been observed leading to a variety of composting rates.

Between aeration periods it is likely that the interstitial carbon dioxide concentration will build up. Because the fan is controlled by the data logger once it is turned on the readings are not taken by the logger for another 5 minutes. It is likely that some of the interstitial carbon dioxide is blown out during the five minute interval between the fan being turned on and the next sample that the logger takes. It may then be the case that there is then no stored reservoir of carbon dioxide and all the CO_2 that is produced is blown out and monitored. Figure 5.43 shows this well, once the aeration increases there is a sharp decrease in the respiration rate as all the interstitial CO_2 is blown out. The respiration rate then recovers.

The composting rates, shown in Figure 5.44, above 60°C are as high as those below 60°C, this may be a reflection of a more evenly distributed temperature within the composting pile or may be a result of mis-measurement of carbon dioxide levels due to aeration. For the green waste windrows a graph of estimated energy release and

moles of carbon dioxide released, as shown in Figure 5.22 and 5.23, gave a good correlation between the two series. For the temperature controlled windrow the overall average for energy release was 1005 kJ per mole of carbon dioxide released, nearly twice the level predicted in Chapter 3-this alone suggests that not all of the carbon dioxide release was recorded.

Figure 5.45 shows the estimated energy lost to air and the moles of carbon dioxide measured for the temperature controlled windrow. During the time covered by Period 1 where the temperature controller did not work there were peaks in both series. However Periods 2 and 3 have no peaks in the data for moles of carbon dioxide released but several in the estimated energy release. This further implies that much CO_2 was lost and not measured during the period that the fan started up. The previously observed positive correlation between the gas temperature coefficient and the carbon dioxide concentration was not present during this experiment and this further suggests the incomplete measurement of carbon dioxide production.

The lack of relationship between the GTD and the core temperature, which for the non aerated windrows proved to be strongly negative, is due to the aeration system. Whilst the control system was malfunctioning (during Period 1) there is a strong negative correlation between these two parameters. During Periods 2 and particularly 3 the relationship was less prevalent, because the control system was either partially or fully operational during these periods. This suggests that the forced aeration changed this characteristic of the windrow composting process.

The airflow rates recorded were quite obviously higher than for the non aerated green waste windrows whilst the fan was operational. When the fan was not operating the flow rate was similar to the non aerated windrows-which would be expected. The airflow rate whilst the fan was operating was slightly lower than the requirement predicted in Section 5.5.3, reaching a high of $1.7ms^{-1}$ during Period 3 rather than the predicted $1.76ms^{-1}$. The difference in values may be due to the assumptions taken in calculating the quantity of air required, but it is nonetheless in the correct range and validates the calculations performed in the theoretical analysis presented in Chapter 3.

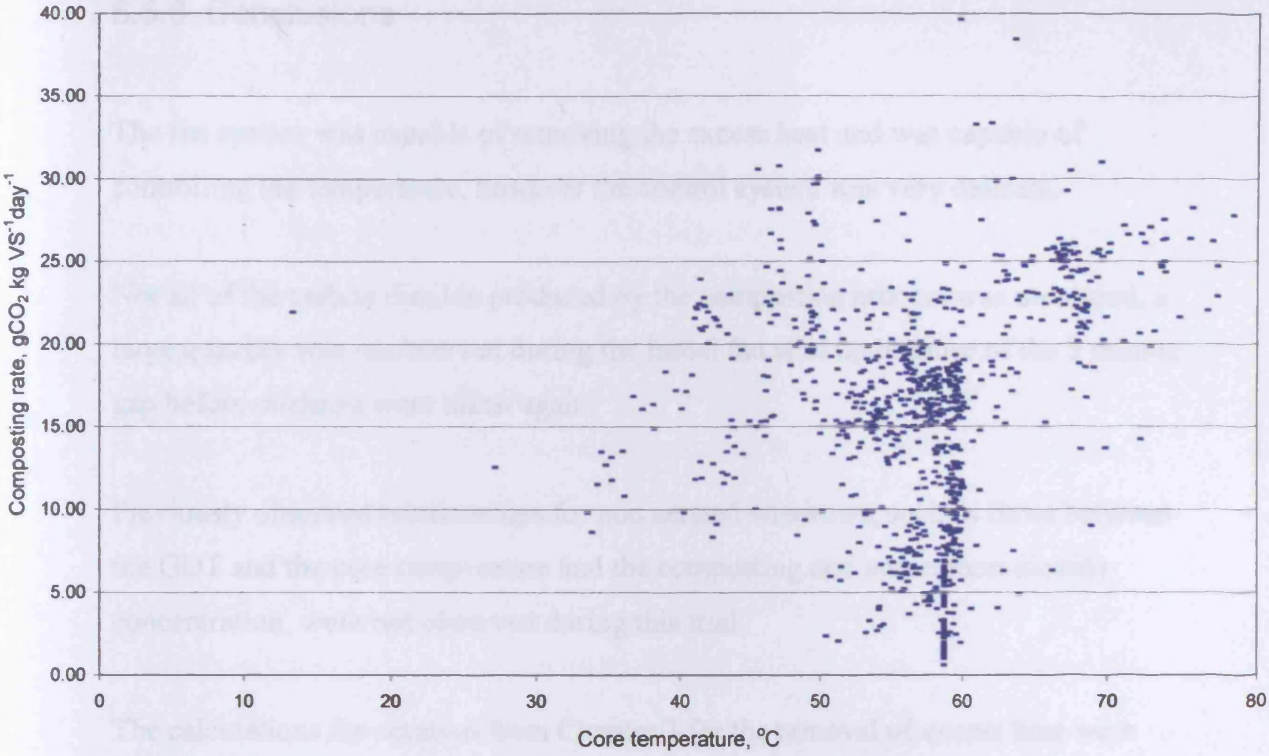

Figure 5.44. Plot of composting rate against core temperature for the temperature controlled windrow

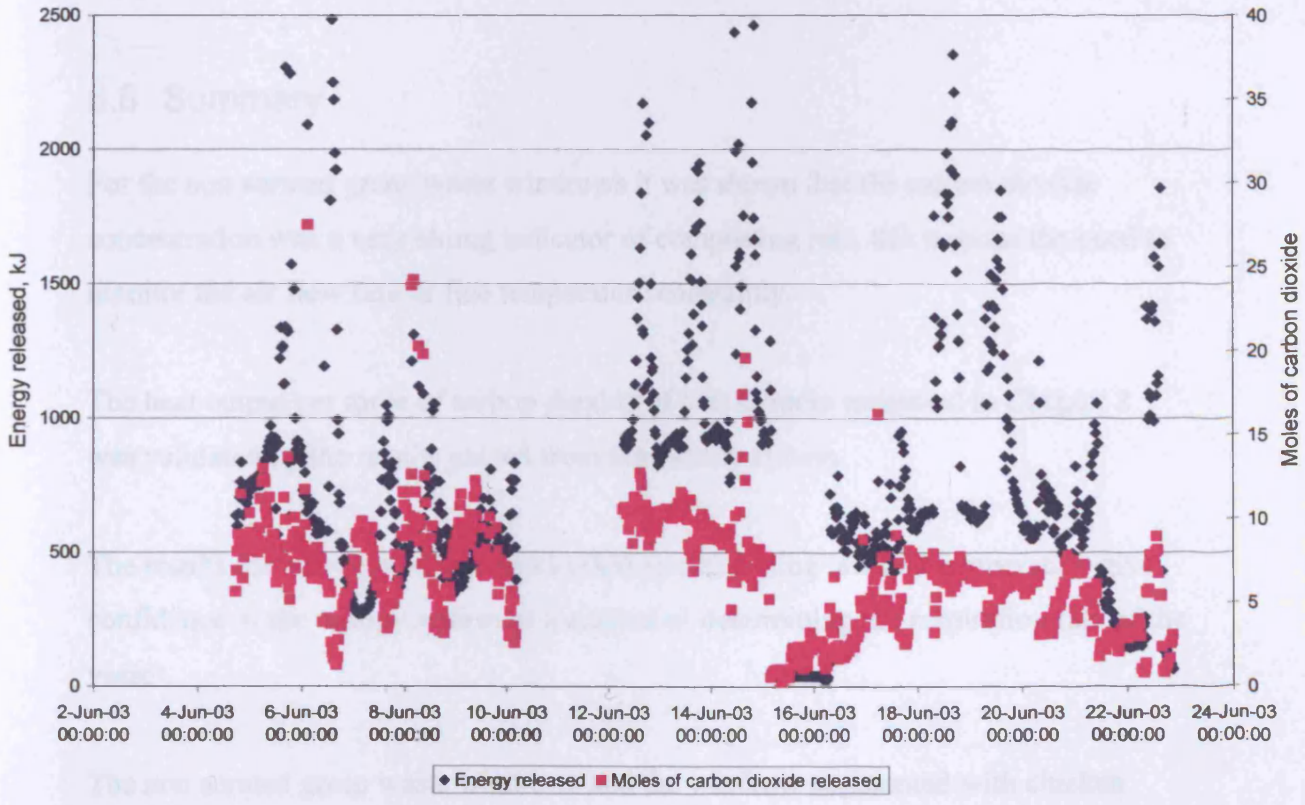

Figure 5.45. Energy and CO_2 emissions for the temperature controlled windrow (during each 25 minute time period)

5.5.6 Conclusions

The fan system was capable of removing the excess heat and was capable of controlling the temperature, however the control system was very delicate.

Not all of the carbon dioxide produced by the composting process was measured, a large quantity was unobserved during the initial fan start up because of the 5 minute gap before readings were taken again.

Previously observed relationships for non aerated windrows, such as those between the GDT and the core temperature and the composting rate and carbon dioxide concentration, were not observed during this trial.

The calculations for aeration from Chapter 3 for the removal of excess heat were shown to be in the correct range with a predicted velocity of 1.76 ms^{-1} being supplied whilst the fan was operational.

5.6 Summary

For the non aerated green waste windrows it was shown that the carbon dioxide concentration was a very strong indicator of composting rate, this negates the need to monitor the air flow rate or flue temperature constantly.

The heat output per mole of carbon dioxide of 500 kJ/mole estimated in Chapter 3 was validated by the results gained from the canopy system.

The results for non aerated windrows relating composting rate and temperature give confidence in the canopy system as a method of determining the respiration rate of the vessel.

The non aerated green waste windrows and the windrow augmented with chicken litter showed the optimum core temperature to be approximately 55°C.

The highest recorded respiration rate for a green waste windrow was approximately 35 $gCO_2\ kgVS^{-1}day^{-1}$.

The airflow rate through compost varied for all the experiments, the fan obviously provided the highest flow rates and the chicken litter augmented windrow gave the lowest-due to the increased density and reduced free air space.

Although correction of C:N ratio may be an important facet of composting it is important not to gain it at the expense of something else of importance-such as airflow.

Monitoring equipment can be extremely sensitive to the harsh environments found within composting plants, the greatest number of failures being due to the hot film anemometer.

6 Containerised Composting System

6.1 The Composting Vessel

There are a variety of in-vessel composting technologies available and an outline of these is available in the Composting Association's publication "A guide to In-Vessel Composting" (Edwards *et al.*, 1998). Containerised composting systems offer a modular system of composting allowing a well planned site to expand the volume of compost being processed. Systems of this type available on the market include Alpheco, Stinnes Enerco and NaturTech. These systems, amongst others, were compared by Myrddin (2003) for a variety of categories, such as: residence time, temperature distribution and throughput. The throughput per unit area of this type of composting system was shown to vary between 16.97 and 46.15 $kgm^{-2}week^{-1}$.

The vessel used in the current research was supplied by Wormtech Ltd. and is based on the roll-on-off skips allowing simple transportation of the vessels using standard equipment. Drawings for the vessel are shown in Appendix B and photographs of the vessel are shown in Figure 6.1. The vessel is essentially a container of height 2.37 metres, width 2.25 metres and 5.8 metres long and a mass of 3.5 tonnes when empty.

Figure 6.1. Photographs of the Wormtech vessel

The vessel has a false floor which has a number of slits cut into it (see photograph on the right of Figure 6.1) air enters the plenum beneath the floor though three vents, one of which can be easily seen on the front of the vessel in Figure 6.1 (brown circle to the right of the ladder). Initially the vessel was configured to draw air out of the top of the vessel. The maximum depth of the compost in this vessel when filled is approximately 1.6 metres.

6.2 Positive Aeration

6.2.1 Introduction

In the configuration shown in Figure 6.1 the fan drew air from the top of the vessel and vented it to atmosphere. The fan was operated by a simple time clock, initially it was set to come on for 30 minute intervals spaced evenly throughout the day: 4 a.m., 12 p.m. and 8 p.m. Initially the vessel was sited at the Rhondda Cynon Taff Materials Reclamation Facility in Llantrisant, South Wales. The material used to fill it was shredded green waste from the doorstep collection service.

6.2.2 Method

Two runs using green waste were performed in the positive aeration mode. Gemini Tiny Tag miniature data loggers were used to record the temperatures. The data loggers consisted of a 100mm long probe containing a negative temperature coefficient thermistor with an accuracy of ±0.2°C. The probe was connected via a 2 metre cable to a small box which provided power through batteries and was capable of storing 16, 000 readings. The recorded data could then be downloaded to a computer for off-line analysis. Two of these probes were mounted within 1 metre long steel sheaths to allow them to be inserted into the core of the vessel whilst a further 6 probes were inserted to measure the temperature near the wall. The layout of these probes for the first run is shown in Figure 6.2 and the distances are relative to the ground and the front of the vessel. The layout for the second run is shown in Figure

6.3, with one of the long probes being inserted from the end. For the second run 25mm of expanded polystyrene was used to insulate the corner of the vessel.

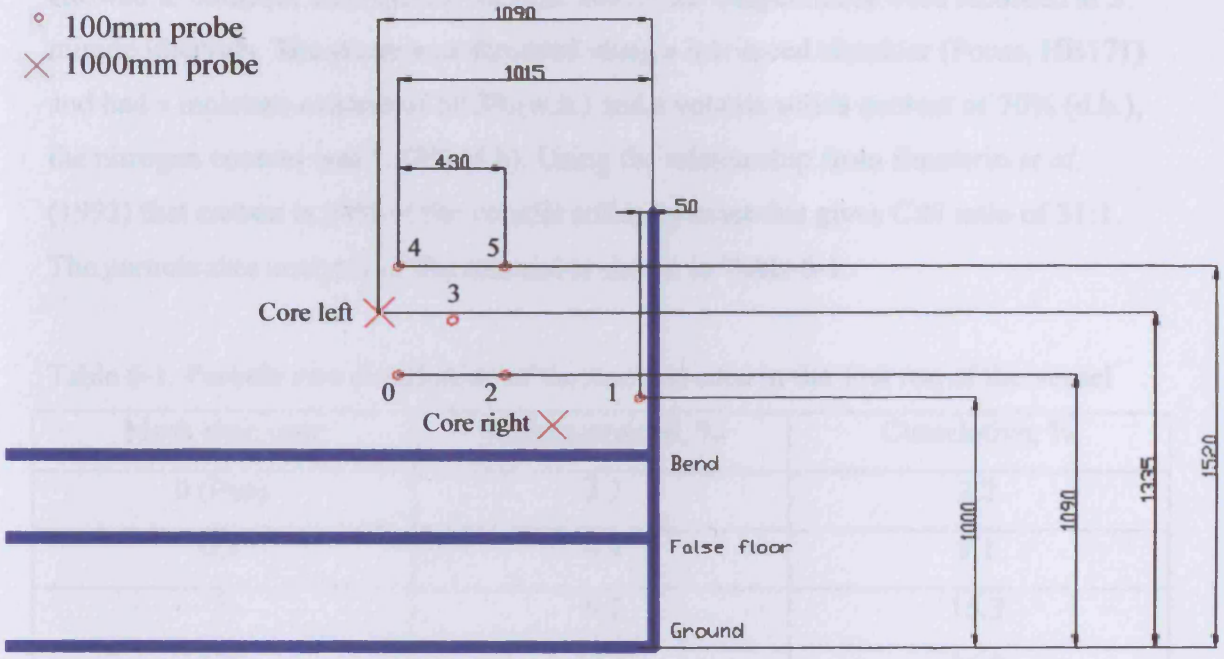

Figure 6.2. Location of probes during the first run of the vessel

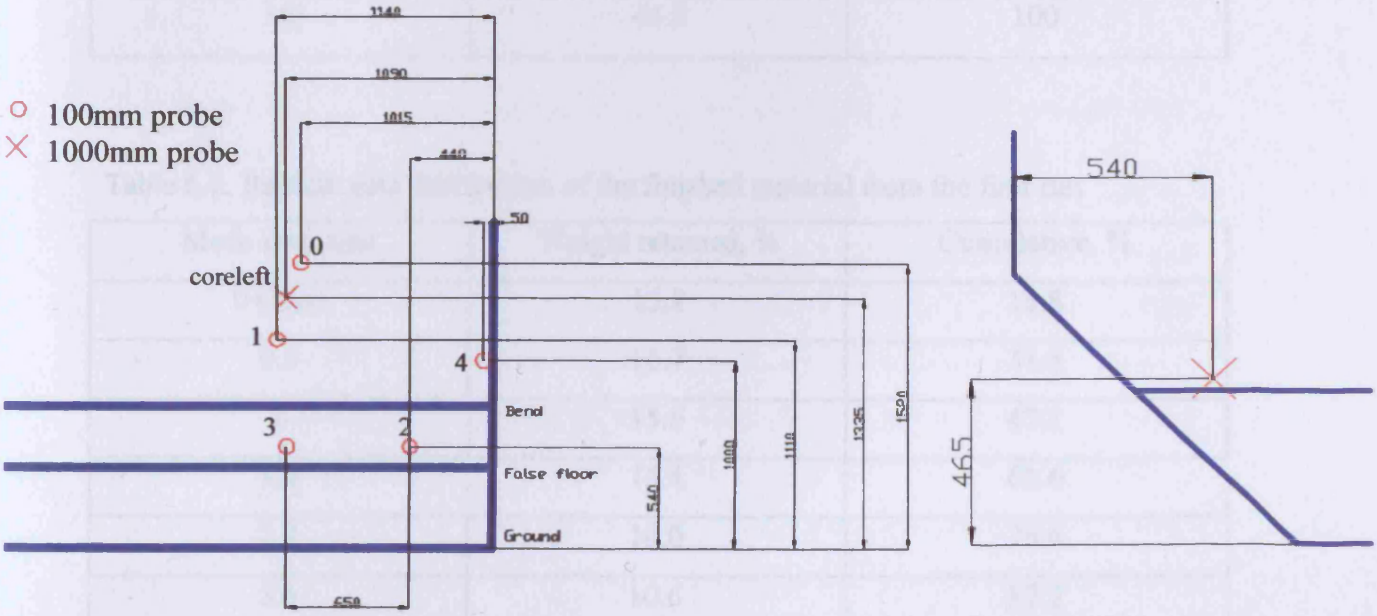

Figure 6.3. Position of probes for the second run

6.2.3 Results

The material for the first run was loaded into the vessel on the 9th of June 2003 and allowed to compost until the 19th of June 2003. The temperatures were recorded at 5 minute intervals. The waste was shredded using a low speed shredder (Forus, HB171) and had a moisture content of 50.3%(w.b.) and a volatile solids content of 70% (d.b.), the nitrogen content was 1.22% (d.b). Using the relationship from Emeterio *et al.* (1992) that carbon is 54% of the volatile solids by mass this gives C:N ratio of 31:1. The particle size analysis of the material is shown in Table 6-1.

Table 6-1. Particle size distribution of the material used in the first run of the vessel

Mesh size, mm	Weight retained, %	Cumulative, %
0 (Pan)	2.2	2.2
0.5	6.9	9.1
1	6.2	15.3
1.4	11.6	26.9
2.8	14.2	41.1
5.6	6.5	47.6
8	7.6	55.2
16	44.8	100

Table 6-2. Particle size distribution of the finished material from the first run

Mesh size, mm	Weight retained, %	Cumulative, %
0 (Pan)	15.8	15.8
0.5	15.7	31.5
1	15.6	47.1
1.4	15.4	62.6
2.8	14.0	76.6
5.6	10.6	87.2
8	8.2	95.5
16	4.5	100.0

The finished material had a slightly increased moisture content of 56.3% (w.b.). The particle size distribution for the finished material is shown in Table 6-2 and a comparison between the distributions of the feed and composted material is shown graphically in Figure 6.4. Figure 6.4 shows a reduction in larger material and an increase in small particle sizes during the composting period. Much of the initial large material consisted of leaves and grass but this was less evident in the finished material.

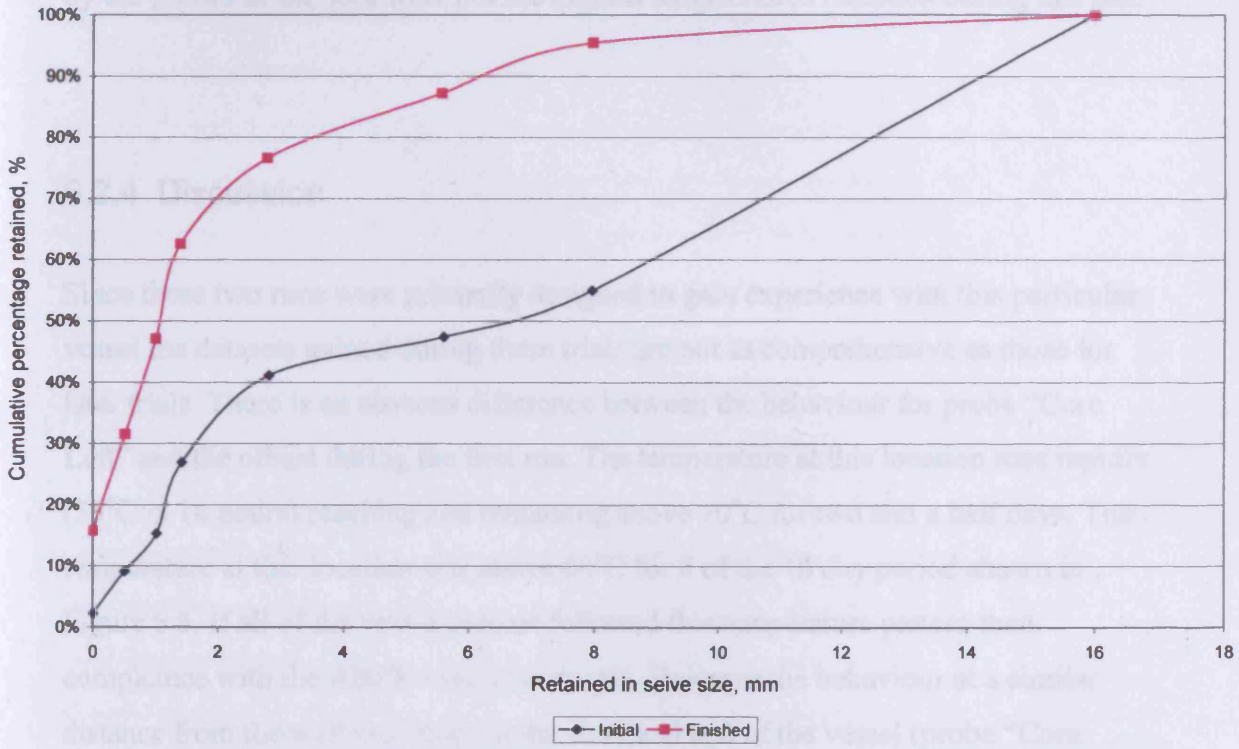

Figure 6.4. Comparison of initial and final particle size distributions for the first trial

The temperatures recorded during the first run of the vessel are shown in Figure 6.5, the numbers in the legend refer to the positions of the temperature probes as given in Figure 6.2, whilst the vertical lines represent the aeration periods. The core left series remained above 60°C for much of the trial, whilst many of the probes at the side of the vessel were over 40°C. Although many of the probes cooled during the aeration period and increased in temperature between aeration, probe 5 did not. Instead the temperature of probe 5 increased during the aeration periods and decreased between them. The temperatures recorded at position 1 also bore no relationship to the aeration periods, these were the lowest temperatures recorded and it comes as no surprise that this probe was in the corner of the vessel.

The second run was started on the 3rd of July 2003, the material again came from the doorstep collection of green waste but had a slightly higher moisture content of 58% (w.b.). The temperatures recorded for the second run are shown in Figure 6.6, during this run probe 5 was monitoring the ambient temperatures. The temperatures achieved were lower than those from the first run despite the addition of insulation. All the probes that were within the compost show behaviour of cooling during the aeration period and heating between the aeration periods. The temperatures recorded by the probes in the core were not the highest temperatures recorded during this run.

6.2.4 Discussion

Since these two runs were primarily designed to gain experience with this particular vessel the datasets gained during these trials are not as comprehensive as those for later trials. There is an obvious difference between the behaviour for probe "Core Left" and the others during the first run. The temperature at this location rose rapidly (55°C in 16 hours) reaching and remaining above 70°C for two and a half days. The temperature at that location was above 60°C for 8 of the 10 day period shown in Figure 6.5. If all of the vessel content followed this temperature pattern then compliance with the ABPR would be simple. However the behaviour at a similar distance from the wall but closer to the floor and end of the vessel (probe "Core Right") is not so encouraging. Here the temperature rise is also rapid (40°C within 8 hours) but reaches a maximum of 65°C and then steadily declines, remaining above 60°C for only 12 hours. The reason for this behaviour is probably due to the increased heat loss through the adjacent walls rather than a poor composting rate, since it would be expected that the composting rate would be lower near probe "Core Left" (high temperature at that point and probably lower air supply as indicated by the reduced response to aeration pulses).

Five of the shorter probes (0, 2, 3, 4 and 5) were grouped closely together, it would therefore be expected that the behaviour of these points would be similar to each other. Probes 0, 2, 3 and 4 all behave in a similar fashion to each other generally showing temperatures in the range of 40°C to 50°C. The temperature at these locations

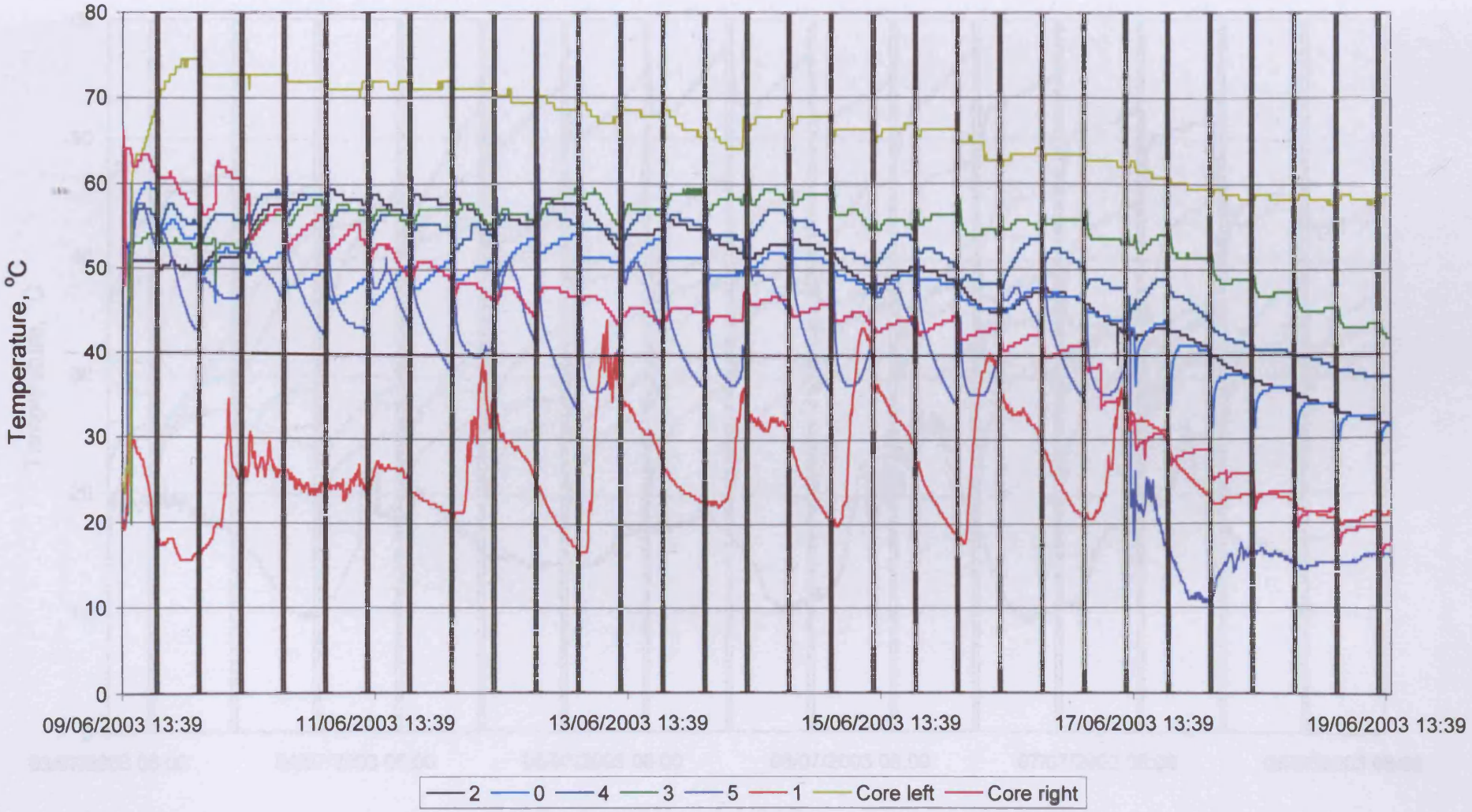

Figure 6.5. Temperatures recorded during the first run of the in-vessel composter

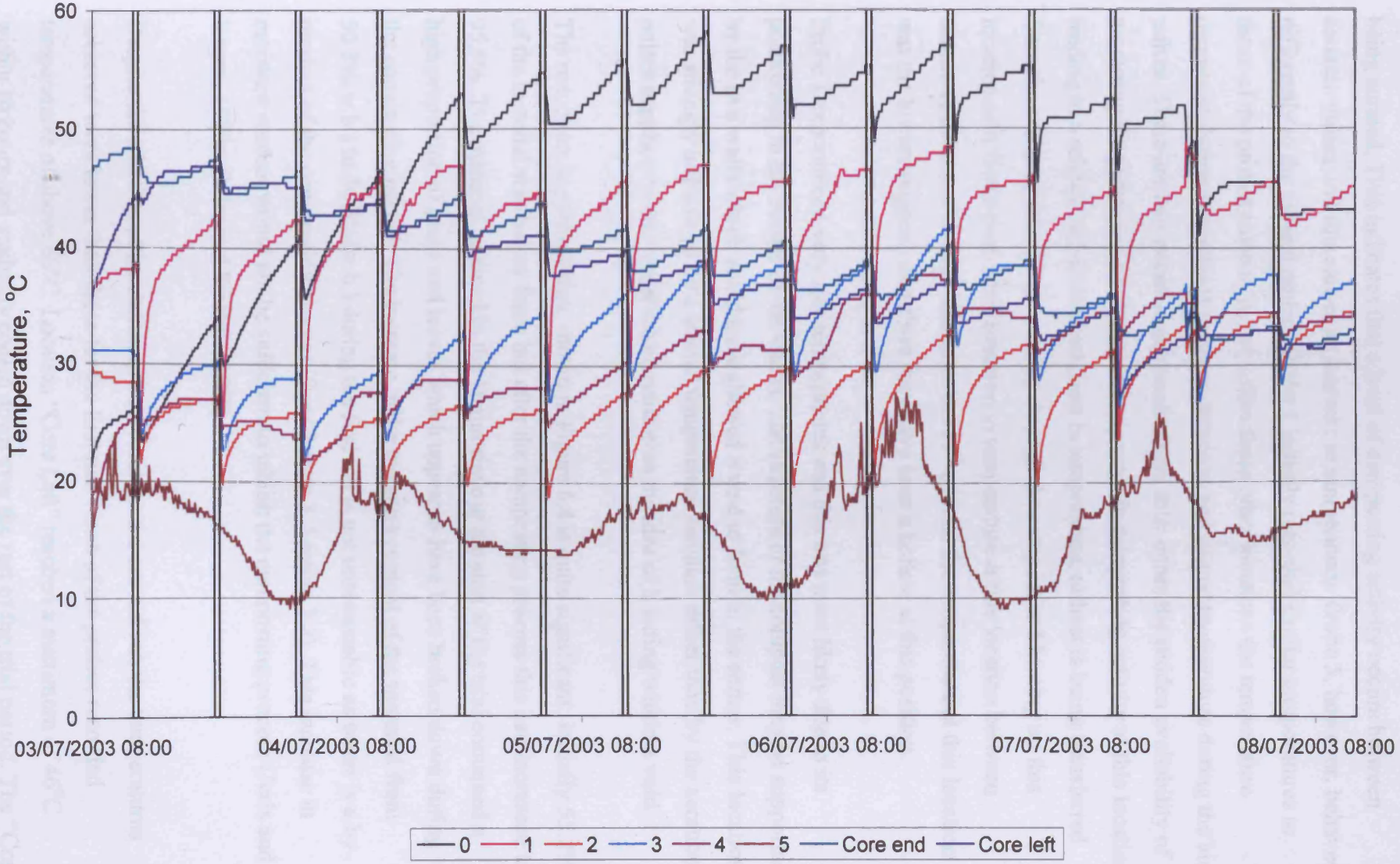

Figure 6.6. Temperatures recorded during the second run of the in-vessel composter

increases between aeration periods with a fall in temperature while the material is being aerated. This indicates that a level of composting activity occurs between aeration pulses and this causes an increase in temperature. Probe 5, however, behaved differently to the other 4 probes. Probe 5 initially recorded similar temperatures to those of the probes close to it, but unlike those other locations the temperature decreased during the periods between aerations and gained temperature during the air pulses. There are two possible explanations for this: either the sudden availability of air during the aeration period causes an upsurge in composting activity at this location leading to a release of heat and increase in temperature, or heat is being transferred from the compost into the air passing through the compost and heating up this location as it flows past. The reduction in temperature at this location between aeration pulses and the fact that after the 17th of June the temperature at this location was the lowest suggests that there may have been a hollow at this position.

Probe 1 experienced very low temperatures and this was most likely due to its positioning in the corner of the vessel. The structure of the compost may be supported by the two walls which could have allowed a void to form in the corner. This location was strongly influenced by a diurnal temperature variation rather than by the aeration pulses supplied to the vessel which reinforces the idea of it sitting within a void.

The reduction in particle size, shown in Figure 6.4 is quite significant; initially 55.2% of the material was below 8mm but after the composting process this had increased to 95.5%. The material retained in the 16mm sieve at the start of the trial contained a high proportion of grass and leaves which appear to have been broken down during the composting period. The increase in the moisture content of the material from 50.3%(w.b.) to 56.3%(w.b.) during the first run is not unreasonable as water is a by-product of the composting process (See Chapter 3, Section 3.2). This increase in moisture content would not be sufficient to inhibit the composting process (Jeris and Regan, 1973a; Suler and Finstein, 1977).

Despite the addition of insulation to the vessel for the second run the temperatures achieved were lower than those for the first run. None of the probes recorded temperatures of above 60°C. Location "Core Left" reached a maximum of 46°C within 16 hours and gradually cooled down over the rest of the trial period. The "Core

End" probe recorded similar, though slightly higher temperatures to the "Core Left" location despite being close to the false floor of the vessel.

The highest temperatures recorded during this trial were at location 0. This was also the highest probe, indicating that heat was rising through the vessel. Locations 2 and 3 located near to the false floor experience lower temperatures, generally between 20°C and 30°C. Probe 1 experienced higher temperatures than probe 4 even though they were at a similar height, however probe 4 was only 50 mm away from the end wall so the difference in temperature is likely to be due to the increased heat losses.

The probes all increased in temperature in the intervals between aeration. For several of the probes the rate of temperature increase diminishes during the period. This may be due to a limiting factor such as oxygen availability or high temperature. Unlike run 1 the "Core Left" location was affected by the aeration periods and lost heat during them. However the reductions in temperature of the two core series were smaller than those experienced by the surface locations-suggesting that although the aeration was reaching the core most of it is being provided to the edges.

During the second run none of the material within the vessel achieved the appropriate temperatures to meet the Animal By-Products Regulations (2003). For the first run, applying a straight line temperature profile between the core probes and the edge probes, approximately one quarter of the material in the vessel reached temperatures high enough to meet the Animal By-Products Regulations. A statistical analysis (Hewings *et al.*, 2004) shows that this would require the vessel to be emptied, cleaned and reloaded 21 times to reach the 99.8% level as stipulated by the Defra risk assessment (Gale, 2002).

6.2.5 Conclusions

The temperatures within the vessel were too low, meaning that although composting did occur the vessel in this configuration did not meet the Animal By-Products Regulations (2003).

The insulation applied to the vessel for the second run did not increase temperatures.

6.3 Factory waste trial

6.3.1 Introduction

The main benefit of an in-vessel composting system is its ability to compost catering waste to the standards specified under the Animal By-Products Regulations. Green waste can be composted easily in windrow systems, but without the composting of catering waste it is not possible to meet the targets set out in Wise About Waste (WAG, 2002).

The initial tests of the containerised system were performed using green waste only. It was necessary to find a suitable waste stream to use as a substitute for waste covered by the Animal By-Products Regulations to combine with the green waste to allow investigation of how the vessel would behave. Ideally this would have been kitchen waste from doorstep collection, but without a doorstep collection service for kitchen waste in place the quantity required would have been difficult to obtain. Instead a source was located from a factory which only processes vegetables meaning that it was outside the remit of the Animal By-Products Regulations (2003). The waste was delivered to site and used in both the containerised system as well as a turned bay system that was being developed (Hewings *et al.*, 2004).

Whereas the previous trials had taken place at the Rhondda Cynon Taff Materials Reclamation Facility in Llantrisant, South Wales, prior to this trial the vessel was moved to the University's Composting Research Station at the CERT facility near Carmarthen, West Wales.

6.3.2 Method

In order to prepare the feed for the composting trial the shredded green waste was mixed with the vegetable waste in a ratio of 3:1 by volume. Approximately 12 tonnes of material were used in total to fill the vessel with around one third of that weight being vegetable waste. Due to the unknown composition of the material it was decided to manually monitor the interstitial CO_2 concentration during the composting process and adjust the aeration appropriately. The CO_2 concentration was recorded using a Gas Data PCO_2 carbon dioxide meter with inbuilt data logging facility. A brass pipe of diameter 6mm and length 1 metre was inserted into the core of the compost to allow sampling of the interstitial gas. The sampled gas was passed through a moisture trap made from a 250ml Dreschel vessel filled with silica gel crystals to remove water which would inhibit the performance of the CO_2 meter.

A Seko shredder was used to shred the green waste, as shown in Chapter 4 approximately 50% of the shredded material has a particle size of less than 8mm. The density of the shredded green waste was shown by Hewings *et al.* (2002) to be approximately 360 kg m^{-3} and to remain below 400 kg m^{-3} for the first 20 days of windrow composting. The addition of the vegetable waste increased the density of the feed to 460 kg m^{-3}.

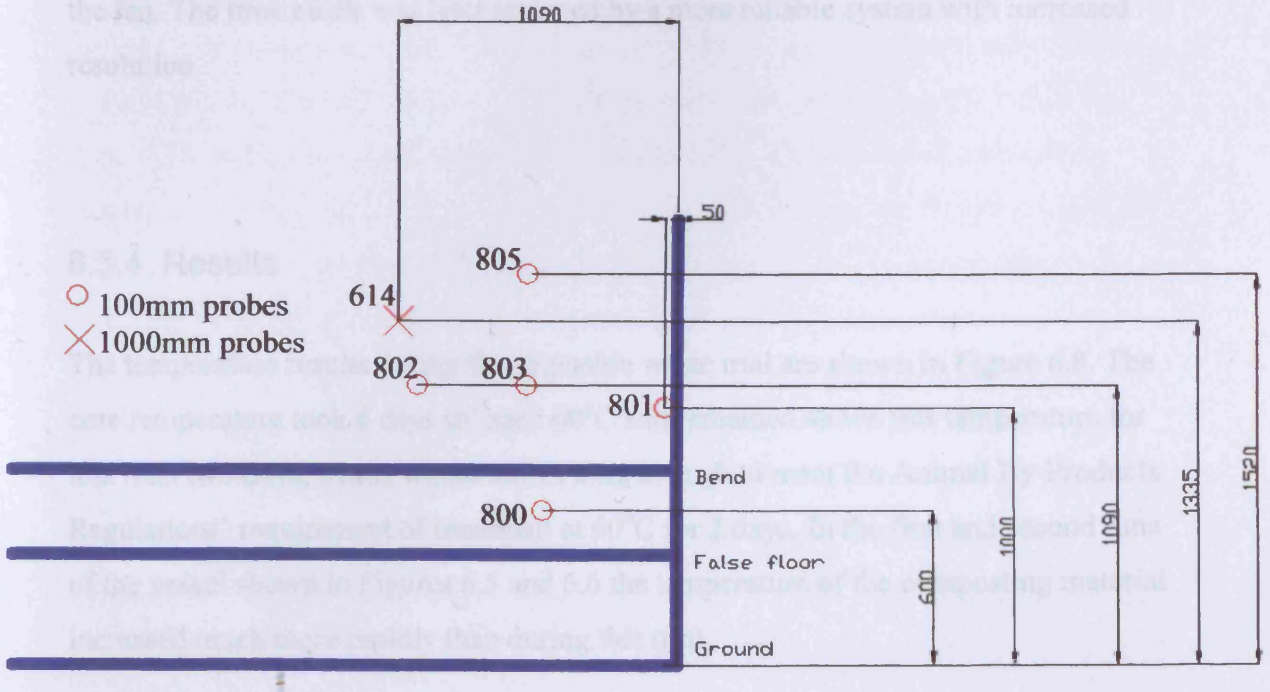

Figure 6.7. Location of probes during the vegetable waste trial

Several probes were used to monitor the temperature of the vessel, laid out as shown in Figure 6.7. As with the previous trials these were Gemini Tiny Tag data loggers, as described in Section 6.2.2. Two of these probes had failed either due to the corrosive nature of the compost or the settling action of the material during the composting period causing physical damage.

6.3.3 Aeration

For this trial the vessel was in the negative aeration mode. This means that the air was being blown by the fan into the void space at the top of the vessel, flowing downwards through the compost and leaving through the three vents beneath the false floor. The original control strategy for aeration of the vessel during this trial was based on human monitoring and to keep the interstitial CO_2 concentration of the compost below 10% so that composting activity would not be impeded. If the interstitial CO_2 was found to be above 10% then the duration or frequency of the aeration periods would be adjusted and the same would happen if the interstitial CO_2 content were too low. However during this trial it was discovered that the time clock on the control circuit of the fan was malfunctioning leading to inaccurate control of the fan. The time clock was later replaced by a more reliable system with increased resolution.

6.3.4 Results

The temperature results during the vegetable waste trial are shown in Figure 6.8. The core temperature took 6 days to reach 60°C and remained above this temperature for less than two days, which would not be long enough to meet the Animal By-Products Regulations' requirement of treatment at 60°C for 2 days. In the first and second runs of the vessel shown in Figures 6.5 and 6.6 the temperature of the composting material increased much more rapidly than during this trial.

In order to meet the Animal By-Products Regulations it is necessary for the entirety of the vessel to experience a temperature greater than 60°C for 2 days or more provided that the particle size is less than 400mm. As can be seen from Figure 6.8 none of the probes located close to the side wall (800, 801, 802, 803 and 805) recorded temperatures in excess of 60°C. Four of these probes (801, 802, 803 and 805) took approximately two and a half days to reach their peak temperatures, whilst probe 800 took 7 days to reach a peak temperature of 59°C.

Due to the manual intervention in the control of this trial there are a lot of data relating to the control of the system in the log book kept at site and this is detailed as follows. The vessel was filled on the 18th of November and the temperatures remained static until approximately 1300 hours on the 19th. At this time the interstitial CO_2 concentration in the core of the vessel was observed to be 42% CO_2. Because of this high concentration the fan was switched on manually until 1415 hours, this is likely to have caused a large release of heat from the vessel, but it also coincided with the first increase in temperature within the vessel.

The temperatures recorded by the probes began to fall at 2244 on the 19th of November. On the 20th of November it was observed that the CO_2 concentrations had been very high all night and was recorded to be at 31% at 0815. Again the fan was manually set to operate until 0900 when the interstitial CO_2 concentration had fallen to 4.6%. By 1005 it had reached 15% so the blower was again manually turned on until 1115, when the concentration had fallen to 3.7%. The blower was turned on constantly at 1300 and left on overnight, the CO_2 concentration on the morning of the 21st was 1.5%. The manual operation of the fan during the 20th of November coincides with the second increase in temperatures shown in Figure 6.8.

Apart from one brief period the fan was left constantly running until the morning of the 24th of November. During the constant aeration period between the 21st and 24th of November the core temperature probe and probe 800 both record increasing temperatures. Probes 801 and 805, however, experienced falls in temperature during this period while probes 802 and 803 experienced a fall in temperature followed by an increase.

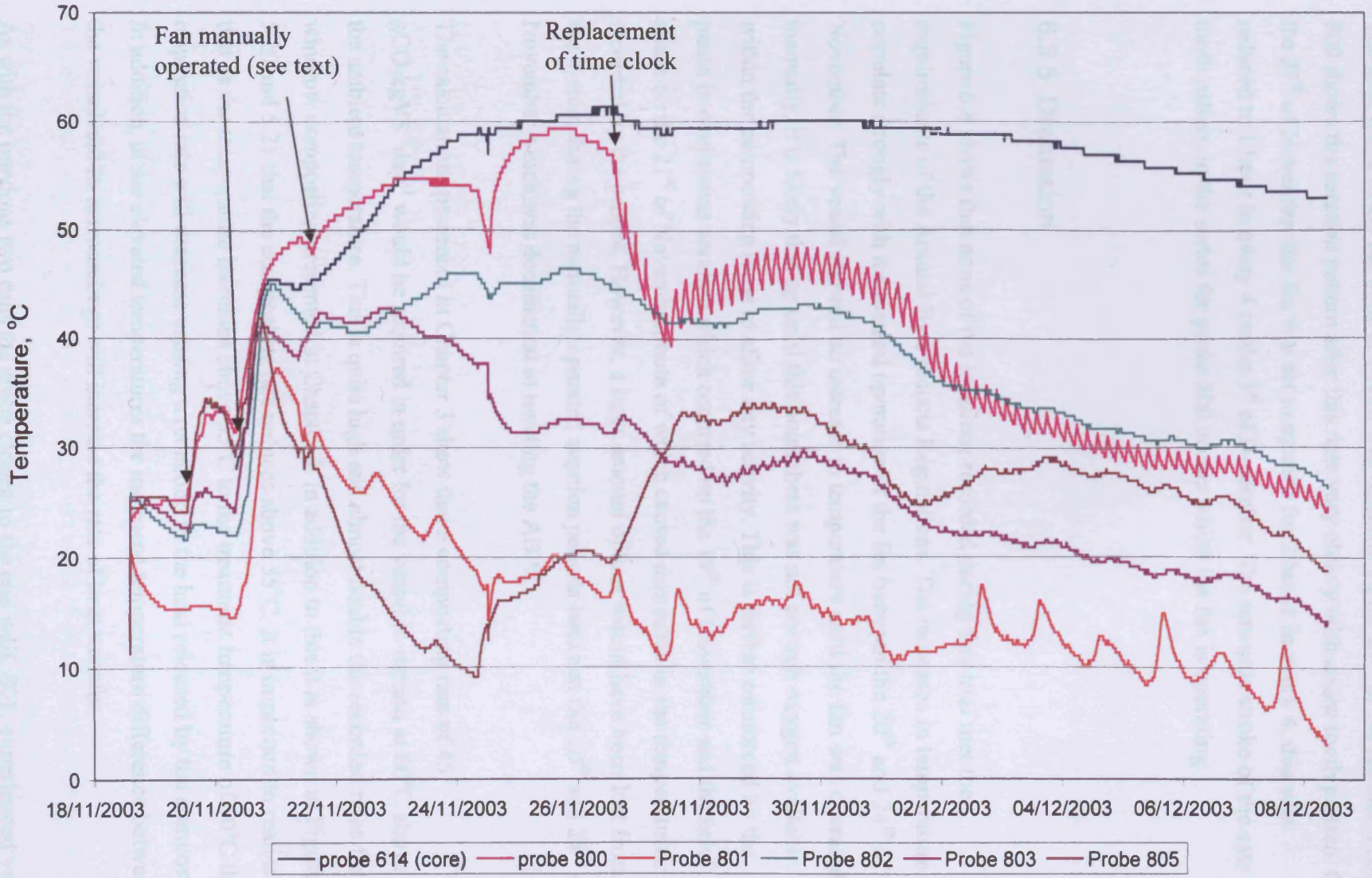

Figure 6.8. Temperature results for the vegetable waste trial

The time clock in the fan control circuit was replaced on the 26th of November. Probe 800 shows the aeration pattern after this date very clearly with a saw tooth pattern. On the 27th of November the fan was set to operate for 2 hours in every 4, this was reduced to 1 hour in every 4 on the 1st of December. The upwards stroke of the saw tooth pattern in the series for probe 800 occurs whilst the fan is operating.

6.3.5 Discussion

Figure 6.8 shows that none of the locations recorded during this trial met the requirements of the Animal By-Products Regulations. The increases in temperature correlate strongly with the manual operation of the fan between the 20th and 24th of November. The vessel showed no increase in temperature until the fan was operated manually, it is likely that up until this point there was not enough oxygen available within the composting mass to allow any activity. This is further reinforced by the pause in continuous aeration which occurred on the 19th of November and the brief pause on the 21st of November, both of which caused decreases in the temperatures recorded by the probes. However, a large amount of heat would have been lost from the system during the manually operated aeration periods between the 20th and 24th of November which was detrimental to meeting the ABPR.

The calculations presented in Chapter 3 show that a composting rate of 45 $gCO_2kgVS^{-1}day^{-1}$ would be required in order for the vessel to remain at 60°C above the ambient temperature. This is quite high and almost double the recorded rates for windrow composting presented in Chapter 5. In addition to this it is shown in Figures 5.20 and 5.21 that the composting rate reduces above 55°C. It is important to realise that as the temperature increases above 55°C to the treatment temperature of 60°C the respiration rate will decrease causing a reduction in the heat released by the compost. In addition, at the elevated temperatures the increased temperature difference between the vessel and its surroundings will increase the rate of heat transfer.

As with the previous two runs the probe closest to the end wall, 801, experienced very low temperatures. As with the previous runs this is likely to be related to its position

close to two walls meaning that it experiences greater heat transfer to the atmosphere. Although this location reached 37°C as a result of the constant aeration on the 21st of November it was below 20°C for the majority of the trial. In order to ensure treatment of material at this location either more heat needs to be released or introduced here or the rate of heat loss needs to be reduced.

Probe 800 experienced the highest temperatures of all of the probes on the side wall. After the replacement of the time clock this location increases in temperature during the aeration periods. Figure 6.7 shows that this is the closest probe to the vessel's false floor. As the vessel was configured for negative aeration it is likely that heat is being moved downward by the air flow into this location. This location is also hotter than the core during the constant aeration further implying that heat is being transferred downwards through the vessel. The low temperatures experienced by probe 805, the highest probe location, further reinforce this.

The density of the material may have affected air flow. During runs 1 and 2 many of the probes experienced changes in temperature which were related to the aeration pulses. However during this vegetable waste trial this only occurred at the location of probe 800. The implication of this is that the air flow through the composting material was reduced compared to the green waste only trials. The particle size analysis of the material used in Run 1 shows that 55% of that material was less than 8 mm. As shown in Chapter 4 approximately 60% of the green waste shredded by the Seko shredder will pass through an 8 mm sieve and all of the vegetable waste was less than 8mm. This means that there was a much higher proportion of fine material in this trial than in the previous tests. Although this creates a larger surface area on which composting can occur it also increases the resistance to airflow of the material. The increased density of the mixture, 460 kg m^{-3}, rather than 360 kg m^{-3} for green waste reflects the reduction in particle size. The increase in density will also lead to a reduction in available pore space further inhibiting airflow.

The malfunction of the time clock required an increased level of manual operation of the system during the start of the trial. The increases in core temperature were strongly related to the periods during which the fan was operational. This implies that

the composting process within the vessel when the fan was not operating there was insufficient oxygen within the vessel to allow composting to occur.

6.3.6 Conclusions

The vessel did not reach the required treatment temperatures, due to either insufficient respiration or excessive heat loss.

As the respiration rate was not recorded during this trial the system can not be compared to the windrow composting trials in Chapter 5.

Appropriate aeration is critical to allow the system to meet the Animal By-Products Regulations (2003).

The increased density and higher proportion of fine material appeared to impede airflow within the vessel.

6.4 Citrus Waste Trial

6.4.1 Introduction

It was decided to use factory processing waste as a replacement to the kitchen waste in the mix to feed the vessel as treatment of such wastes may have a commercial future. A difficult waste, namely citrus waste, was sourced from a factory in South Wales and incorporated into the feedstock. For this trial various improvements were made to the operation of the vessel including the recirculation of air as described in Section 6.4.3. Unlike the previous trials data on respiration rates were recorded and a larger dataset is available.

6.4.2 Preparation of the feedstock

The factory waste consisted mainly of orange pulp and peel and is shown in Figure 6.9. To prepare the feedstock for the trial 4,460 kg of the factory waste were combined with 8, 240 kg of green waste. The green waste was first shredded using a Jenz hammer mill shredder, then mixed with the factory waste in batches using a Seko shredder. Photographs of the waste being prepared are shown in Figure 6.10. The photograph on the left of Figure 6.10 shows the mixture after it has been unloaded from the Seko shredder, orange flecks can be made out within the mixture. The waste mixture was then loaded into the vessel using a telehandler and levelled off by hand.

Figure 6.9. A photograph of the citrus waste as delivered

The final depth of compost within the vessel was approximately 1.25 metres. The weights of each of the wastes were analysed by towing trailers of wastes over the weighbridge on the Nantycaws landfill site owned by CWM Environmental. The final density of the mixture was 780 kg m^{-3}, much higher than green waste by itself. Samples were taken in accordance with BS EN 12579:2000 of the individual feedstocks and the mixture that was used to fill the vessel. These were analysed at the School of Engineering's laboratories in Cardiff and the results of the analysis are given in Table 6-3.

Figure 6.10. Photographs of the mixture of green and citrus waste and the mixture being loaded into the vessel

Table 6-3. Analysis of samples taken on day of filling the vessel

	Factory Waste	Green Waste	Mix Used in Vessel
pH (BS EN 13037:2000)	3.96	7.04	5.33
Electrical Conductivity, mS/cm (BS EN 13038:2000)	0.30	0.50	0.73
Moisture content (w.b.) (BS EN 13040:2000)	79.9%	46.7%	63.6%
Volatile solids content (d.b.) (BS EN 13039:2000)	95.5%	49.5%	61.6%

6.4.3 Method

The vessel was configured to recirculate the air through positive aeration. This mode of aeration was chosen due to previous operational problems with too much condensation remaining in the plenum. A knock-out pot was also added to the aeration circuit to allow removal of some of the excess moisture. The knock-out pot was manufactured from a barrel approximately 400mm in diameter and 600mm high. The air was blown in tangentially allowing the excess moisture to condense on the side of the pot. Air left through a pipe at the top of the vessel. A tap located at the

bottom of the knock-out pot allowed the moisture condensed from the air to be drained and quantified. Ten k type thermocouples were attached to the inside wall of the vessel to monitor the wall temperature. The thermocouples were connected to the datalogger (Delta T, DL2e). In addition to the wall thermocouples the inlet and exhaust air temperatures and the inlet relative humidity of the air were recorded and this information was also stored on the datalogger. A Gemini Tiny Tag data logging probe, as used in previous trials was inserted into the core to monitor the internal temperatures of the vessel. A 1 metre long 6mm diameter gas pipe was inserted horizontally into the compost, this was connected to a CO_2 meter which recorded the interstitial concentration of CO_2 within the composting mass.

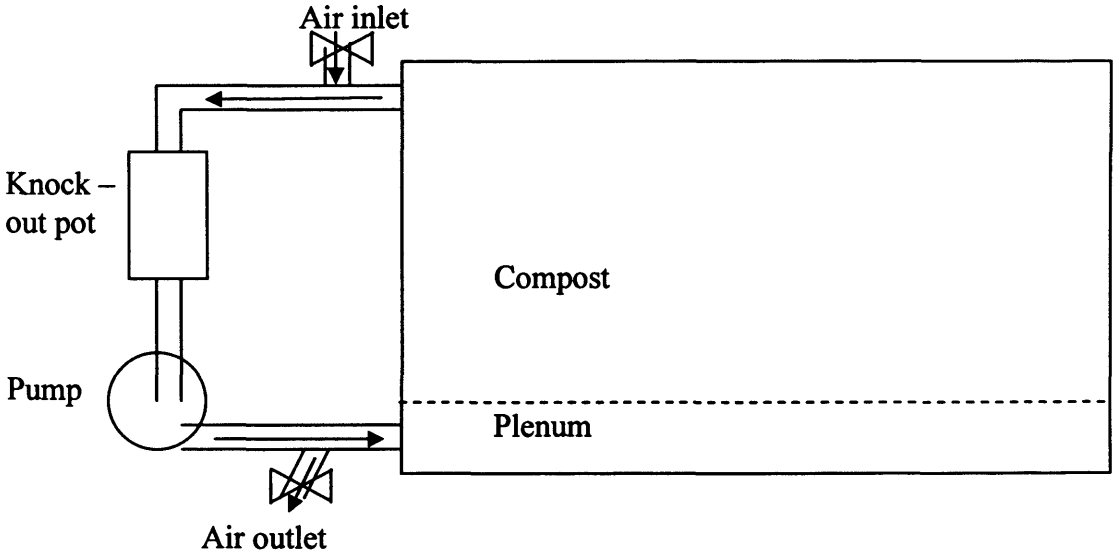

Figure 6.11. Schematic of the vessel's air recirculation system

During the trial the method of supplying air was changed, initially the air was supplied into the plenum beneath the false floor and sucked out of the top as shown schematically in Figure 6.11. Approximately 5% of the air was replaced through the inlet valve whilst the fan was operating with the remaining 95% being recirculated. Part way through the trial a new air delivery system was employed. Three 1½"BSP pipes were driven into the composting pile at a height of half a metre above the false floor. The last 200mm of each pipe had a number of holes and the ends were capped. The central pipe was half way along the vessel with the other two being 1.5 metres either side of it, a photograph of this new air distribution system is shown in Figure 6.12.

During the composting period several samples were taken for analysis of moisture, volatile solids, pH and electrical conductivity. Unlike the previous trials the respiration rate of the compost was analysed on days 11, 13 and 19 of the composting process. This was done by monitoring the CO_2 concentration, temperature and airflow rate of the exhaust gas. The final weight of the material in the vessel was measured by loading the vessel on to the back of a lorry and driving over the weigh bridge on the landfill site. At the end of the composting period the weight of material in the vessel was 8,280 kg. This represents a mass loss of 35 percent.

Figure 6.12. The new aeration system that was designed to supply air to the core of the vessel

6.4.4 Life story

The life story of this trial is quite complicated and is shown in Figure 6.13. The line represents the proportion of the time that the fan was operational, this is shown on the right hand axis. For the majority of the life of the vessel the fan operated for 15 minutes in every hour, on day 7 the aeration frequency was reduced to 15 minutes in every two hours, this was changed back on day 13 of the composting period. The

brown columns shown in Figure 6.13 represent the amount of moisture drained from the knock out pot or the plenum; these correspond to the left hand axis.

The red vertical lines represent the days when the respiration rate was recorded at the outlet of the vessel, whilst the blue lines show when the aeration system was changed as described in Section 6.4.3. The line on day 26 shows the new system being installed whilst the line on day 43 is when the system was changed back to the original aeration system.

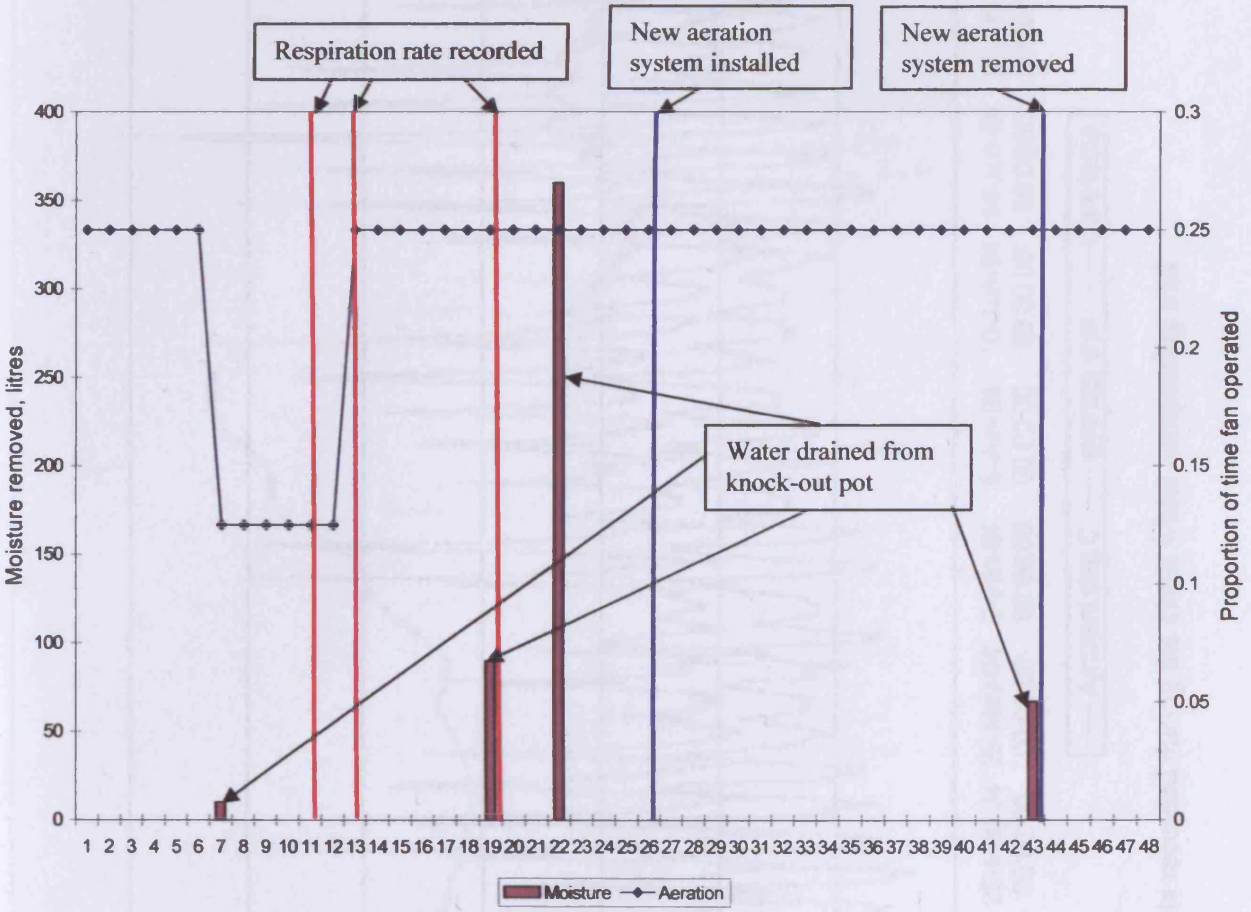

Figure 6.13. The life story of the vessel during the citrus waste trial

6.4.5 Results

The results for the core and wall temperatures are shown in Figure 6.14. Although 10 wall temperature readings were taken these have been averaged and this is shown as the average wall series. The ambient temperature is also shown on Figure 6.15 for

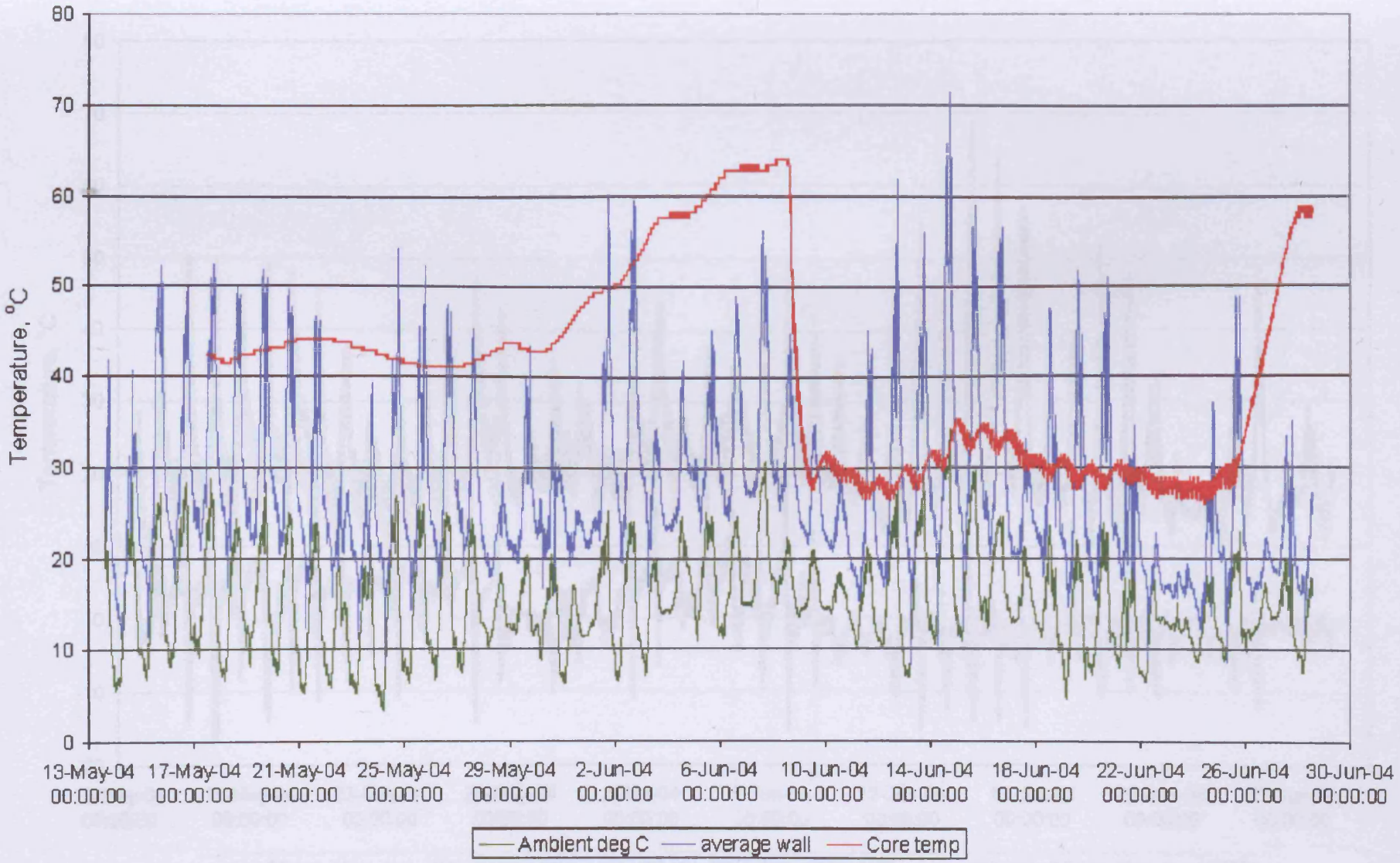

Figure 6.14. Temperature data recorded during the citrus waste composting trial

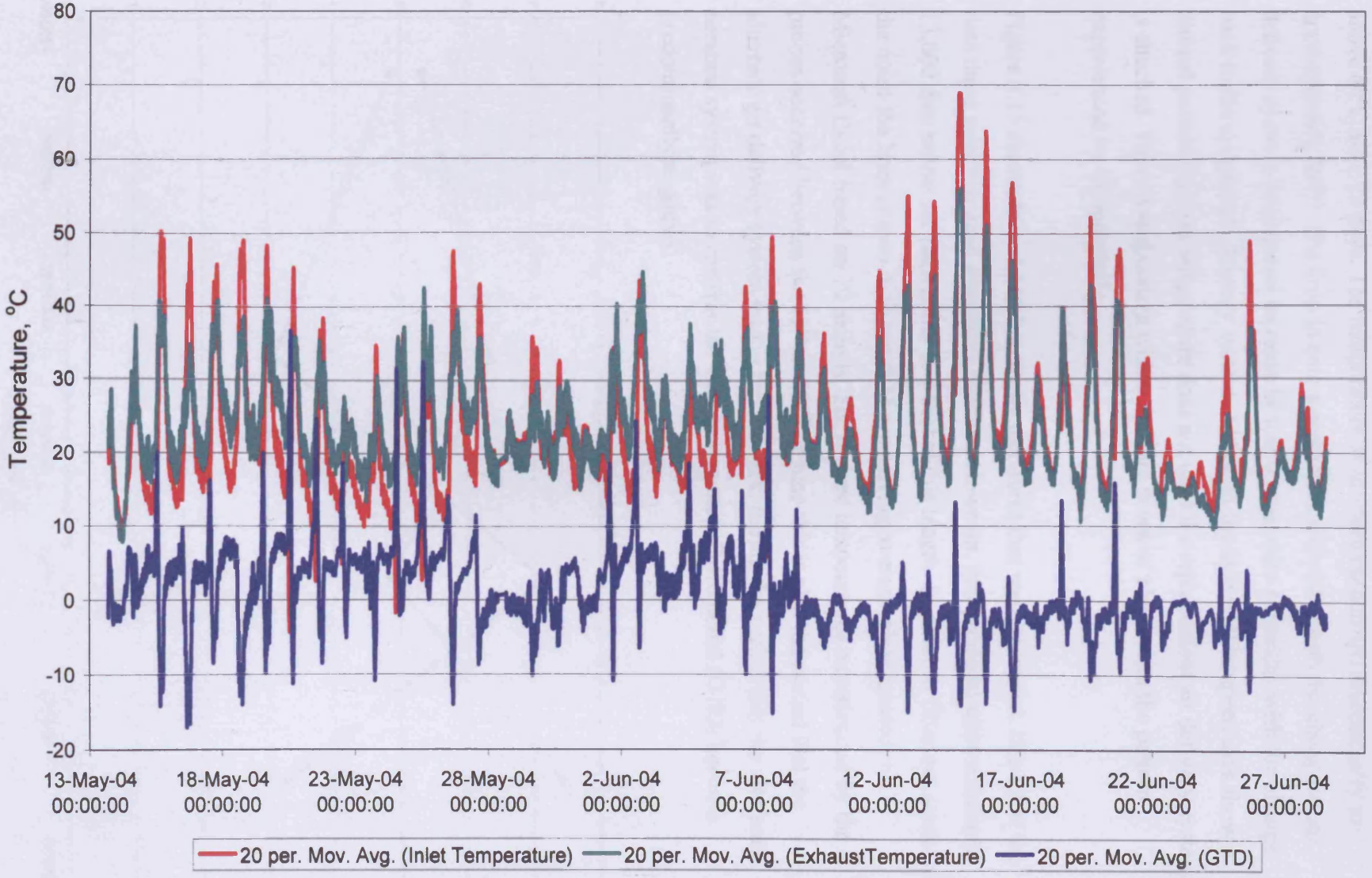

Figure 6.15. Inlet and outlet temperatures and GTD for the composting vessel

comparison. Despite an initially slow start the core temperature does eventually reach above 60°C after 23 days. The temperature of the core then drops dramatically to approximately 30°C. The drop in core temperature coincides with the change in air delivery system. The second increase in core temperature coincides with the change back to the original air delivery system. Although the side wall temperatures show a diurnal pattern the core temperature does not until the replacement air delivery system is attached. This diurnal pattern within the core is out of phase with the pattern experienced by the sidewalls

Figure 6.15 shows the inlet and outlet temperatures that were recorded, like all of the data these were recorded every five minutes. However, this produces approximately 13,000 data points for each series in a trial of this length. In order to filter out some of the noise the lines shown in Figure 6.15 are moving average plots created in Microsoft Excel based on 20 periods. The highest temperatures experienced by the probes occurred between the 11th and 21st of June-this is also the period that the alternate air delivery system was in use. It is also during the period that the alternate aeration system was in use that the Gas Temperature Differential (GTD) became predominantly negative.

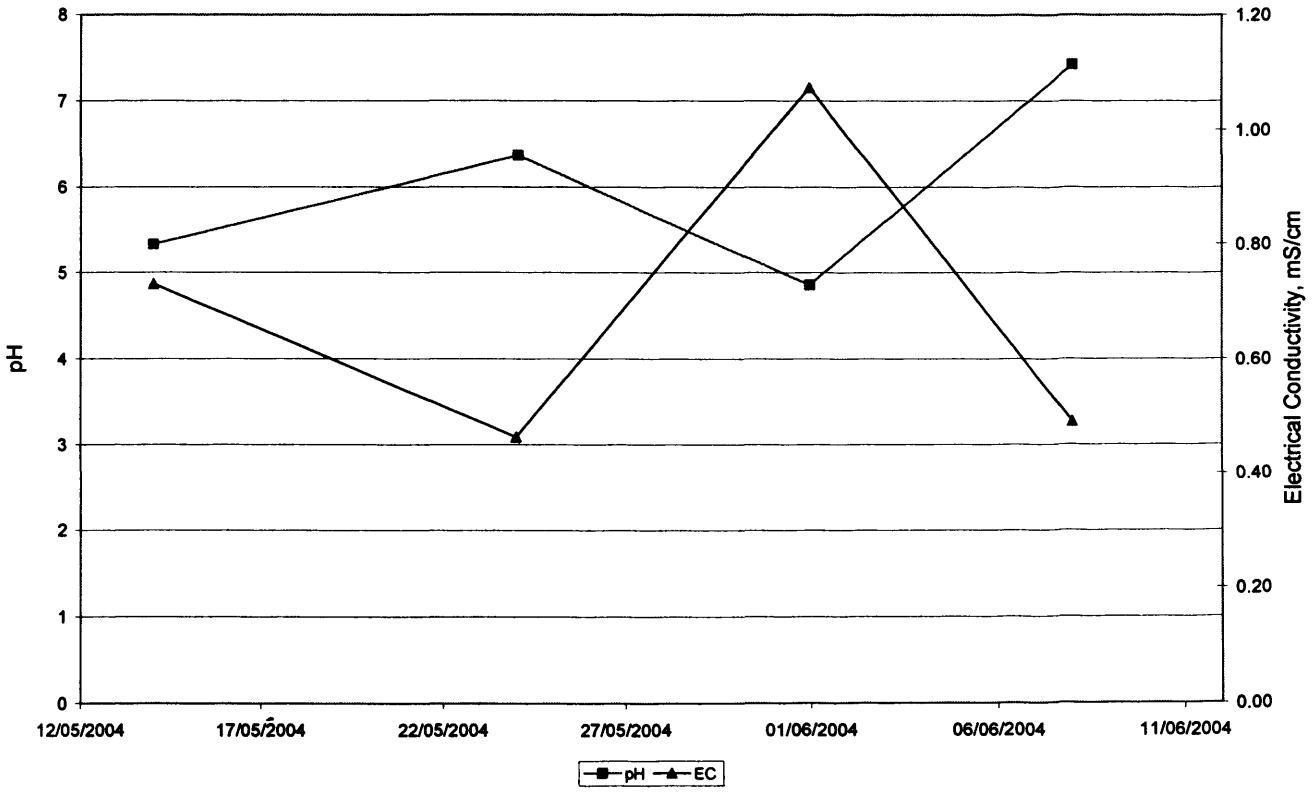

Figure 6.16. pH and electrical conductivity of the composting material during the citrus waste trial

Figure 6.16 shows the electrical conductivity and pH of samples taken from the vessel during the composting trial, these are averages of 3 sub samples. Electrical conductivity and pH were measured in accordance with BS EN 13037:2000 and BS EN 13038:2000 (BSI, 2000e; 2000f) using a Hanna Instruments metre. The pH of the compost increases after the 1st of June to approximately 7.5 on the 8th of June. Due to the acidic nature of the citrus waste the initial pH of the material was quite low. The electrical conductivity varies between 0.46 and 1.07 mS/cm.

6.4.6 Respiration rate

There are essentially three methods for the measurement of respiration rate within the containerised composter, these are:

- Direct measurement of CO_2 lost at the outlet port,
- Measurement of interstitial CO_2 recovery between aeration periods
- Analysis of the mass balance to work out volatile solids reduction during composting.

The first method, direct measurement at the outlet port was performed 3 times during the trial, on days 11, 13 and 19. The sampling tube of a CO_2 meter was inserted into the outlet port of the vessel. The meter was set to record the CO_2 concentration automatically at one minute intervals. The velocity of the gas leaving the vessel was recorded manually using a Testo 425 hot wire anemometer. The CO_2 records are shown in Figures 6.17, 6.18 and 6.19. Occasionally, as with the third peak in Figure 6.17 and peak E in Figure 6.18 there may have been a failure with the meter-for example a blockage within the moisture trap or pipe.

The data for airflow rate, CO_2 concentration and air temperature can be combined to give a respiration rate. These respiration rates along with the volumetric flow rate of air leaving the vessel and the proportion of time that the fan was operating are shown in Table 6-4. As can be seen from Table 6-4 the greatest respiration rate occurred on day 13 of the composting process, with a high of 47.2 $gCO_2\ kgVS^{-1}day^{-1}$. This maximum value of respiration rate coincides with the increase in aeration frequency and the dramatic rise in core temperature shown in Figure 6.14. However, two days

prior this, the recorded rate was approximately one third of the maximum, whilst the aeration frequency was half. Once the core temperature had reached 50°C the rate had fallen to levels nearer a quarter of the maximum.

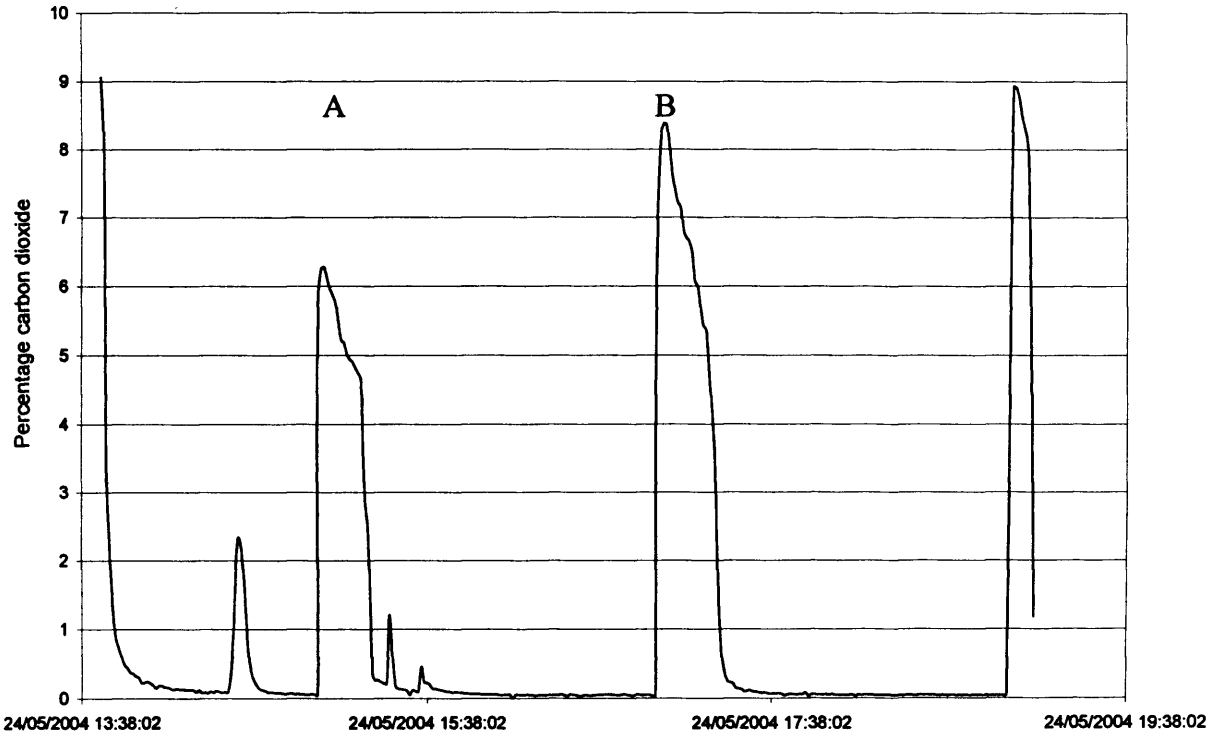

Figure 6.17. Carbon dioxide data for the vessel from day 11 (24th of May 2004)

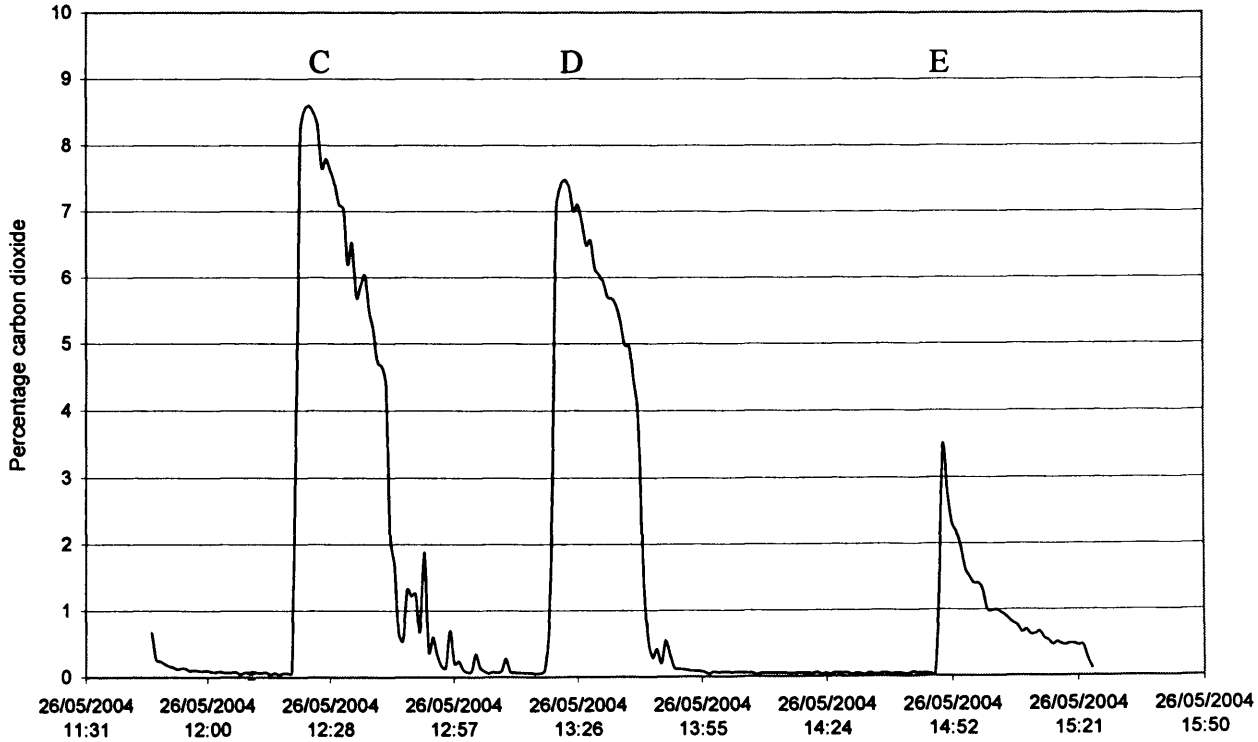

Figure 6.18. Carbon dioxide data for the vessel from day 13 (26th of May 2004)

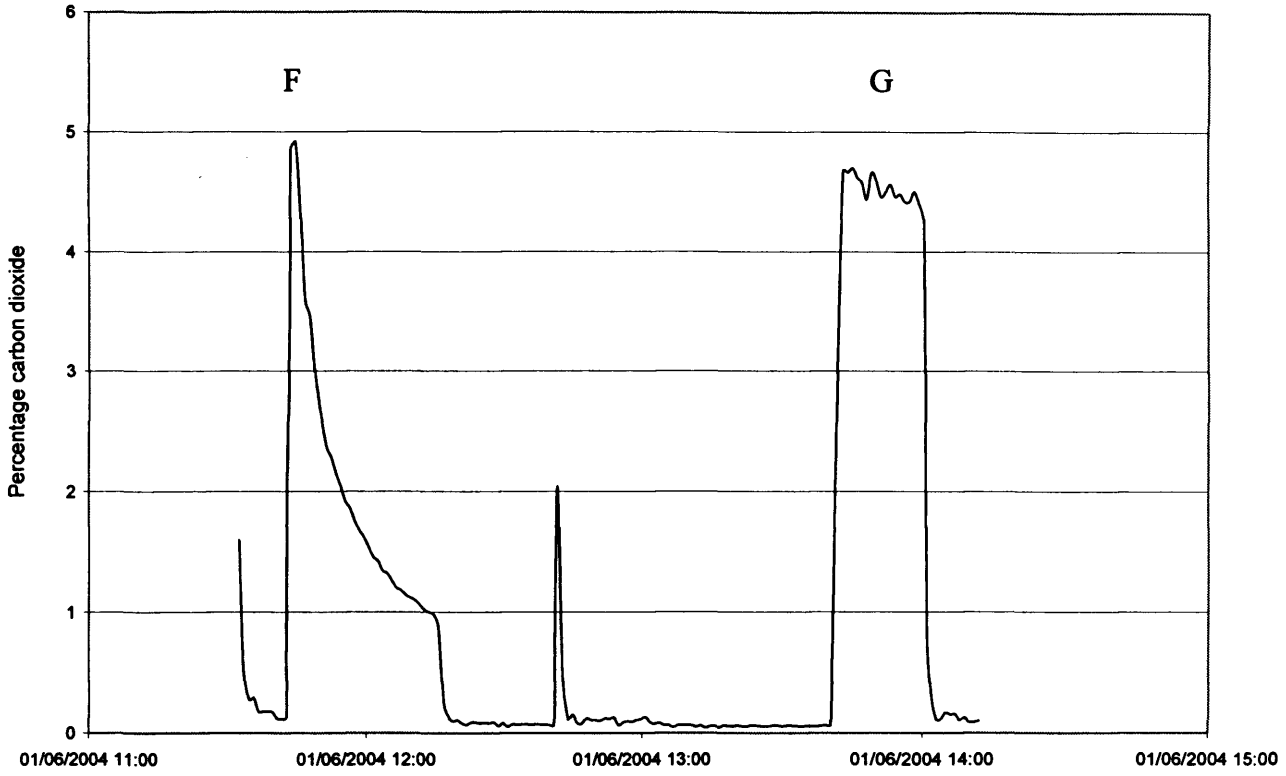

Figure 6.19. Carbon dioxide data for the vessel from day 19 (1st of June 2004)

Table 6-4. Respiration rates recorded at outlet of vessel

Peak	Day	Volumetric flow rate, m^3s^{-1}	Proportion aeration operating	Respiration rate, $gCO_2\ kgVS^{-1}\ day^{-1}$
A	11	0.053	0.125	14.3
B	11	0.053	0.125	18.6
C	13	0.052	0.25	47.2
D	13	0.052	0.25	41.3
E	13	0.052	0.25	3.2
F	19	0.050	0.25	8.3
G	19	0.050	0.25	13

The next method that can be used to assess respiration rate is the measurement of the interstitial CO_2 concentration. The interstitial CO_2 content was monitored for this trial in order to develop a strategy to keep it below 10%. Within the composting mass there is a volume of free air space. Equations 4.10 and 4.11 from Chapter 4 allow this volume to be calculated as a function of compost bulk density, moisture content and volatile solids content. The recovery rate of interstitial CO_2 concentration can be

combined with the volume of free air space and the mass of volatile solids to allow estimation of the respiration rate.

Figures 6.20, 6.21 and 6.22 show interstitial CO_2 data for three key periods during the compost trial. Figure 6.20 shows interstitial CO_2 data between the 17th and 23rd of May. During the time shown in this figure the aeration period decreased from 15 minutes in every hour to 15 minutes in every 2 hours. The decrease in frequency of aeration can be clearly seen in the data. Figure 6.21 shows interstitial CO_2 recorded between the 23rd and 29th of May. During this period the aeration was increased from 15 minutes in every two hours to 15 minutes in every hour. The increase in aeration can be clearly seen in the data. The period shown in Figure 6.21 coincides with the maximum recorded respiration rate shown in Table 6-4 and with the increase in core temperature shown in Figure 6.14. Finally, Figure 6.22 shows the data for interstitial CO_2 when the method of air delivery was changed as described in Section 6.4.3. The result of this was a dramatic fall in core temperatures. In this case the frequency of aeration pulses remained the same but the recovery rate of interstitial CO_2 was greatly reduced.

The estimation of composting rate from these figures is rather difficult and assumes no loss of CO_2 from the vessel when the fan is not operating. Approximately 12 tonnes of waste were used to fill the vessel, the initial density of that material was 780 kgm^{-3} and the moisture and volatile solids contents are shown in Table 6-3. Applying Equations 4.10 and 4.11 gives a proportion of free air space within the compost of 0.35. The total volume filled by the compost was 16.3 m^3, therefore the total free air space within the compost was 5.7 m^3. In addition to this there is a volume of air above the composting material in the headspace and a volume below beneath the false floor. It is likely that some of the CO_2 from the composting process will leak into these volumes. However, it is unlikely that the gas in the headspace and the plenum will reach the same CO_2 concentration as the gas in the interstitial void.

Figure 6.20 shows the decrease in aeration frequency that occurred on day 11. The aeration was initially for 15 minutes in every hour but was changed to 15 minutes in every two hours. Before this change in the aeration frequency the interstitial CO_2 concentration increased by approximately 3% in the 45 minute period between

aerations. After the reduction in aeration frequency the CO_2 concentration increased by approximately 5% in the 105 minute period between aerations. After a further day's composting this reduced to around a 3.5% increase in interstitial CO_2 in a 105 minute period.

Figure 6.21 shows the interstitial CO_2 data from when the aeration frequency was increased from 15 minutes in every two hours to 15 minutes in every hour. Prior to the change the concentration of CO_2 was increasing by 5% in the 105 minute interval between aerations. After the change in aeration frequency this had reduced to a 3% increase, but in the shorter period of 45 minutes.

Figure 6.22 shows what happened when the replacement air delivery system was installed. The recovery of interstitial CO_2 concentration was initially 8% in 45 minutes. This initially reduced to 6% in 45 minutes but after one day the recovery of interstitial CO_2 had diminished until it was approximately 2% in 45minutes. This is approximately a quarter of the rate prior to the change.

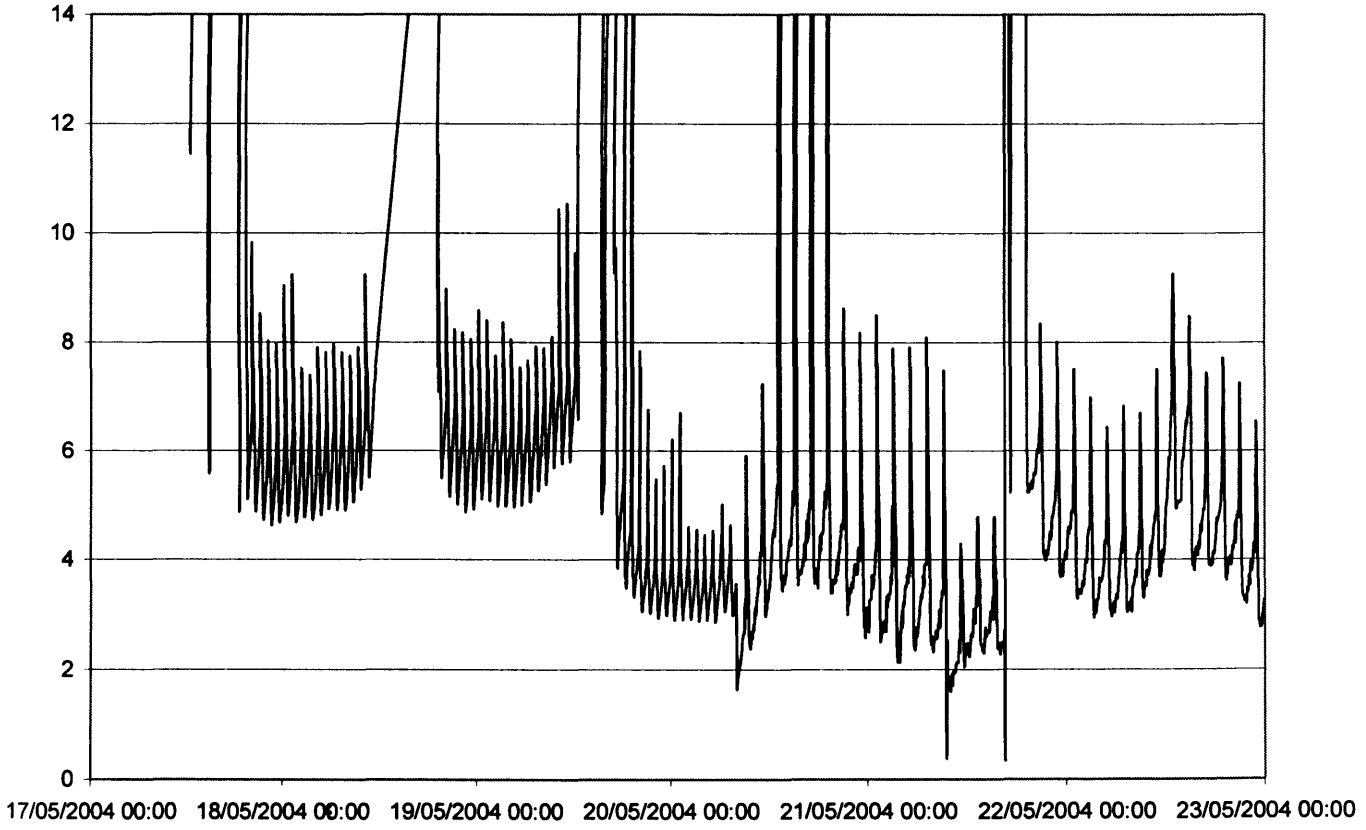

Figure 6.20. Interstitial carbon dioxide recorded between the 17th and 23rd of May for the citrus waste composting trial

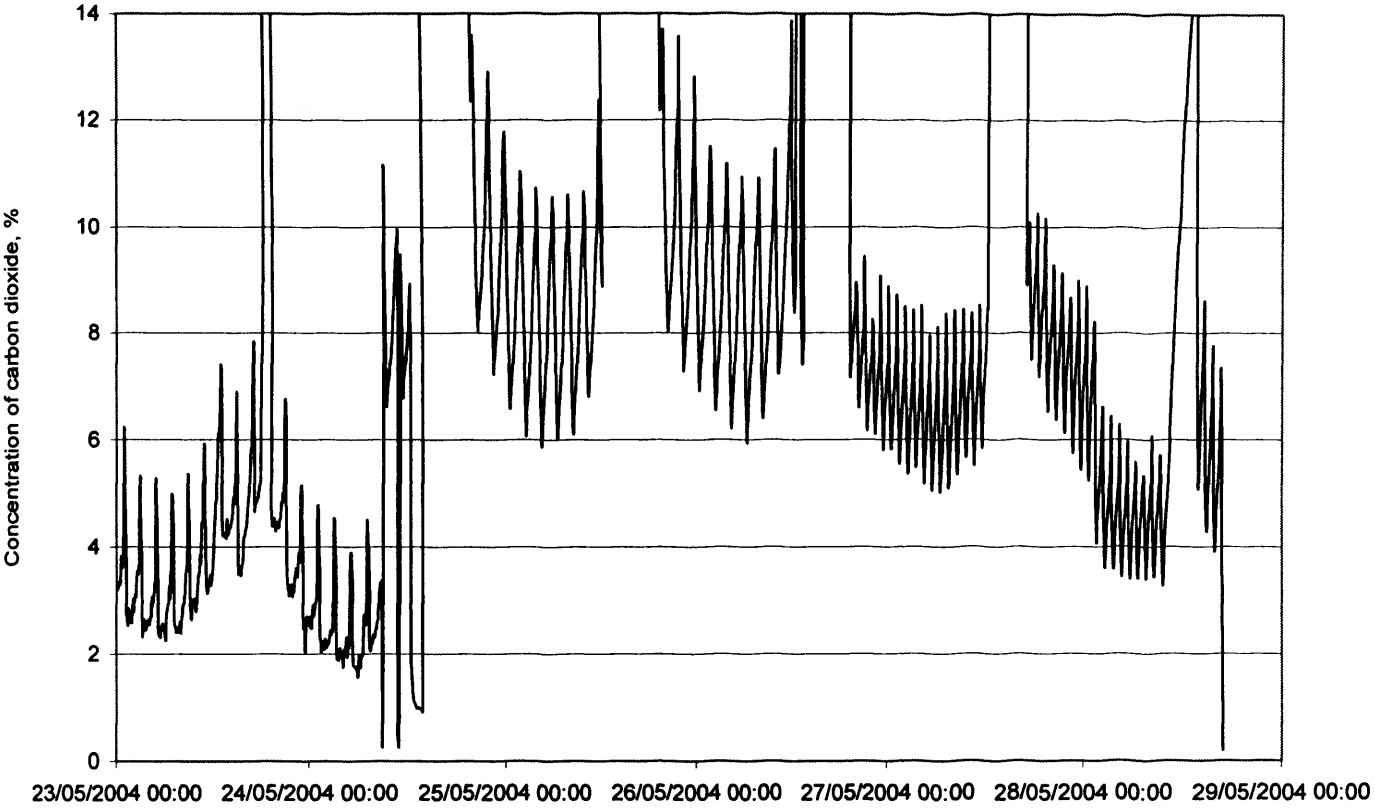

Figure 6.21. Interstitial carbon dioxide recorded between the 23rd and 29th of May for the citrus waste composting trial

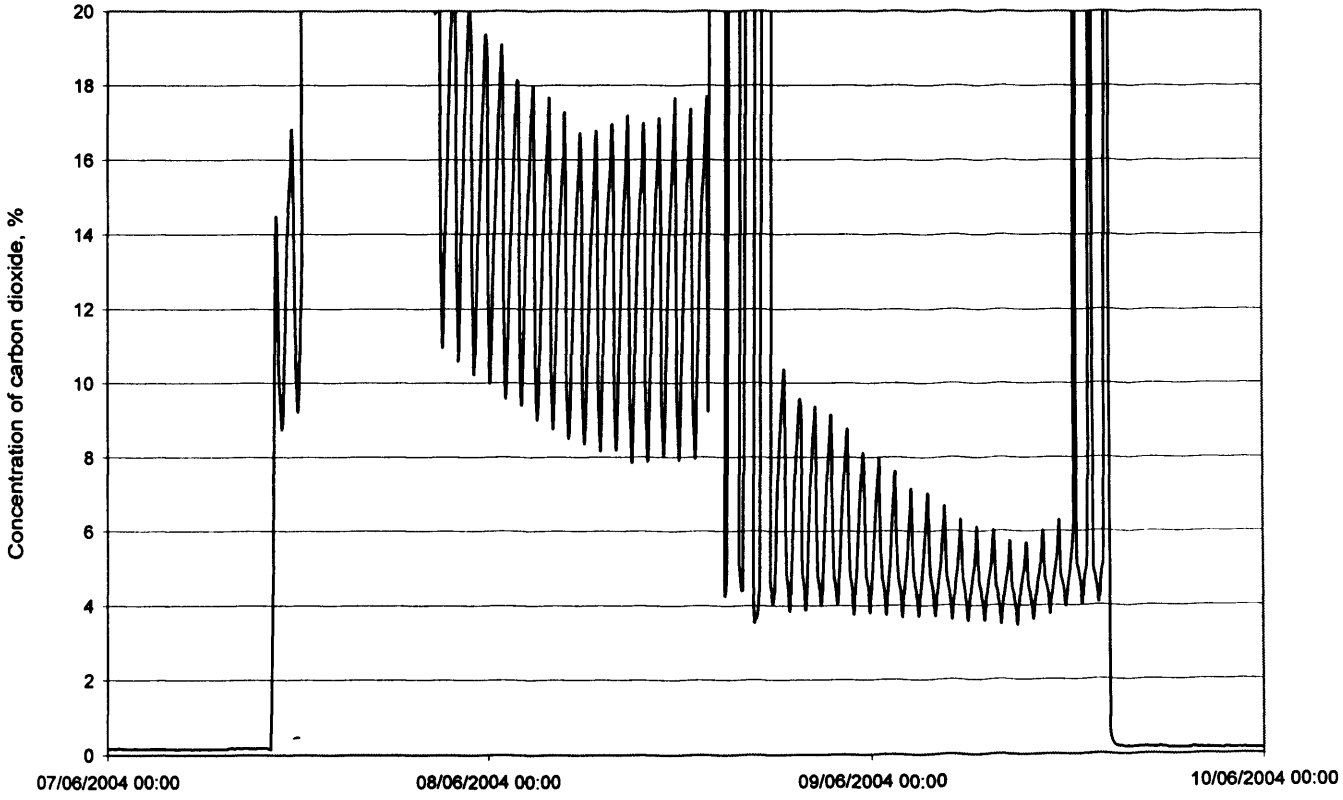

Figure 6.22. Interstitial carbon dioxide recorded between the 7th and 10th of June for the citrus waste composting trial

Table 6-5 shows an estimation of the respiration rate based on interstitial CO_2 recovery combined with the void space. Two rates are shown in the last two columns of the table. The final column assumes that the headspace above the compost reached the same concentration of CO_2 as the interstitial volume, whilst the other rate given assumes that all of the CO_2 remained within the interstitial void and none was released into the void space. The true rate will lie somewhere between these two extremes.

The rates shown in Table 6-5 are far lower than those shown for respiration rate as recorded at the outlet of the vessel shown in Table 6-4. For example the maximum rate shown in Table 6-4 of 47.3 $gCO_2kgVS^{-1}day^{-1}$ occurred on the 26th of May. One day later the rate calculated from interstitial CO_2 recovery was 6.1 $gCO_2kgVS^{-1}day^{-1}$. Though the maximum rate recorded by this method occurred on the 8th of June prior to the installation of the alternate aeration system. At that point the core temperature was 64°C and the respiration rate was 15.5 gCO_2kgVS^{-1}.

Table 6-5. Respiration rate estimated from interstitial carbon dioxide increase

Date	Recovery percentage, %	Time to recover, minutes	Rate excluding headspace $gCO_2kgVS^{-1}day^{-1}$	Rate including headspace $gCO_2kgVS^{-1}day^{-1}$
20/05/04	3	45	1.9	6.1
21/05/04	5	105	1.3	4.4
26/05/04	5	105	1.3	4.4
27/05/04	3	45	1.9	6.1
08/06/04	8	45	4.7	15.5
09/06/04	2	45	1.3	4.3

The final method of calculating the respiration rate concerned the materials balance within the vessel. The initial moisture content of the material loaded into the vessel was 63.6%(w.b.) with a volatile solids content of 61.6%(d.b.). The total mass was 12,700 kg with a density of 780 kgm^{-3}. Forty three days later when the final samples were taken there was 8,280kg of material in the vessel with a moisture content of 51%(w.b.) and a final volatile solids content of 55%(d.b.). The total mass, mass of

water present and mass of volatile solids present at the start and end of the process are shown in Table 6-6.

Table 6-6. Total mass, mass of moisture and mass of volatile solids (in kilograms)

Constituent	On Filling	After 43 days
Total mass	12,700	8,280
Mass of water	8,077	4,223
Mass of volatile solids	2,848	2,231
Mass of ash	1,775	1,826

It is not unreasonable that the quantity of ash present would remain constant. The difference between weight of ash on filling and after 43 days given in Table 6-6 is less than 3% of the weight of ash on filling. Much of the weight loss comes from a reduction in moisture-3,854 kilograms were lost between the start and end of the composting trial. During the trial 527kg of leachate was drained off from the knock-out pot. The calculations from Chapter 3 suggest that an approximately even number of moles of CO_2 and water are produced by the composting process, so quantification of the average respiration rate should also allow calculation of water produced during the composting process.

Overall 617kg of volatile solids were lost. It has been suggested that volatile solids consist of approximately 55% carbon (Emeterio and Garcia, 1992; Haug, 1993), this can be reinforced by the figures shown in Table 3-2 in Chapter 3. Therefore it can be calculated that a total mass of 339,350 grams of carbon or 1.2 kg of CO_2 were released during the 43 day composting period. This can then be divided by the initial mass of volatile solids, 2,848 kg, and the number of days to give an average composting rate of 10.2 $gCO_2\ kgVS^{-1}day^{-1}$. This is generally higher than the values given in Table 6.5, which shows calculated rates based on interstitial CO_2 increase. This average rate is comparable with those shown in Table 6-4 where low rates were recorded at the start and towards the end of the trial, with the higher rates being associated with the rapid heating of the vessel. A similar mixture of citrus waste and green waste was tested in a turned bay composting system (Hewings *et al.*, 2004a)

and a respiration rate based on interstitial CO_2 recovery of approximately 17 gCO_2 $kgVS^{-1}day^{-1}$ was recorded.

As previously mentioned water is released by the composting process, the calculations in Chapter 3 predict that approximately 1 mole of water is produced for every mole of CO_2 released. The previous calculations show that 28,279.2 moles of CO_2 were released. Application of the 1:1 molar ratio between CO_2 and H_2O gives 509 kg of water produced by the process. This means a total of 4,363 kg of water were removed from the vessel during this composting trial.

6.4.7 Discussion

It is evident from Figure 6.14 that the wall temperature of the vessel did not reach an appropriate temperature to ensure sanitisation of the composting material. The core temperature eventually reached 64°C but took 23 days to reach 60°C. The wall temperatures were strongly influenced by the diurnal variation in air temperature. After the addition of the new aeration system the temperature differential between the wall and ambient temperatures increased. This implies that the heat previously stored within the core of the vessel was being moved outwards by the new air delivery configuration. The core also experienced a diurnal fluctuation which lagged behind the diurnal trends recorded for the average wall temperature and ambient temperature.

In previous trials using the vessel it was not possible to calculate whether the quantity of air being supplied was appropriate. For example the moisture content for the first run increased from 50.3%(w.b.) to 56.3%(w.b.) during the trial. However because volatile solids are used by the composting process the actual weight of water in the vessel could have decreased, increased or remained the same. For the citrus waste trial the initial and final weights of the feedstock were measured and are shown in Table 6-6. Chapter 3 showed estimates of air requirements for composting material as a function of bulk density and composting rate (Figures 3.14, 3.15 and 3.16). The bulk density of this mixture was 780 kgm^{-3} and the required rate was 45 $gCO_2kgVS^{-1}day^{-1}$.

The calculations from Chapter 3 suggest that an airflow rate of $6\times10^{-3}m^3s^{-1}$ would be required to supply oxygen (assuming that all the oxygen is used), $0.15m^3s^{-1}$ would be required to remove excess heat and $0.11m^3s^{-1}$ would be required to remove excess moisture. The figures for airflow presented in Table 6-4 suggest that on day 11 there was an airflow rate of $6.63\times10^{-3}m^3s^{-1}$. When the frequency of aeration was increased the air flow rate rose to $1.3\times10^{-2}m^3s^{-1}$, approximately double the estimate from Chapter 3. The estimate from Chapter 3 assumes that all oxygen in the air is used, as the control strategy was to keep the interstitial CO_2 concentration below 10% this rate needs to be doubled. Once the airflow rate was at $1.3\times10^{-2}m^3s^{-1}$ the CO_2 concentration could be kept to 10% so as not to inhibit activity and the respiration rate could increase to the target value allowing the vessel to heat up.

The compost activity as indicated by measurement at the outlet port showed the greatest rate occurring on day 13 whilst the compost was approximately 42°C and the aeration had been increased. This precedes the rapid warm up of the vessel and perhaps implies a mesophilic optimum temperature. By day 19, the 1st of June, the core temperature had risen to approximately 58°C but activity had dropped to around a quarter of the previously recorded level. The airflow rate was still at the calculated level for oxygen supply so implies that there is some other limiting factor within the vessel. This may be due to a reduction in mesophilic bacteria as the temperature moved towards a thermophilic optimum but without a thermophilic population developing to take over the composting process.

Prior to the replacement air delivery system's installation the GTD was generally positive meaning that the exhaust air was warmer than the inlet air. After the installation the GTD moved closer to 0°C and drops below 0°C quite frequently. In Chapter 5 it was observed that the GTD was an indicator of compost activity, the reduction in GTD which coincides with the installation of the new air delivery system implies a drop in composting activity.

Figure 6.22 shows large recoveries in interstitial CO_2 recovery-approximately 8% in 45 minutes equivalent to a rate of 15.5 $gCO_2kgVS^{-1}day^{-1}$ prior to the aeration system being replaced, at this point the core temperature was approximately 63°C. After the replacement air delivery system was installed the core temperature dropped to

approximately 30°C and the compost rate to 4.3 $gCO_2\,kgVS^{-1}day^{-1}$, as with the windrow composting this suggests a relationship between the temperature and the composting rate.

The average composting rate as determined by a mass balance was 10.2 gCO_2kgVS^{-1} day^{-1}. This is lower than the rates recorded for the windrow composting in Chapter 5. Whilst the replacement aeration system was being used the composting rate appeared to be very low and it is likely to be this period of low activity that produced such a low rate of composting for the overall trial.

The pH rises once the material entered the thermophilic stage. It is usual for the pH of a compost to initially drop with the formation of CO_2 and organic acids and then increase once the thermophilic stage begins (Haug, 1993). Lei *et al.* (2000) observed that while the adjustment of the pH affected microbial structure it did not affect oxygen consumption. This implies that the initially low pH was not necessarily a problem for the composting process, the material also moved into the optimum range of 7-8 (Nagasaki *et al.*, 1992).

6.4.8 Conclusions

The replacement aeration system appeared to move heat from the centre of the vessel to the extremities which also impeded composting activity at the core due to the reduced temperatures.

The replacement air delivery system did not supply adequate air to support higher respiration rates and did not redistribute the heat within the vessel appropriately.

An average respiration rate of 10.2 $gCO_2kgVS^{-1}day^{-1}$ was recorded, approximately a quarter of the rate suggested in Chapter 3.

Interstitial CO_2 concentrations of greater than 10% inhibited the composting process.

A total mass reduction of 35% was recorded. This was made up of approximately 1,244 kg of CO_2 and 4,363 kg of water, meaning that much of the mass reduction comes from reducing the moisture content of the material.

The vessel system did not meet the requirements of the Animal By-Products Regulations during this trial. In order to meet these requirements better air distribution management may be required as well as minimisation of heat losses.

6.5 Insulation

6.5.1 Introduction

As calculated in Chapter 3 the vessel requires a rate of approximately 45 $gCO_2\ kgVS^{-1}\ day^{-1}$ in order to maintain a temperature of 60°C above ambient and allow it to meet the Animal By-Products Regulations (2003). As can be seen from Chapter 4 this rate is approximately double that of windrow composting. A rate of this magnitude was reached during the heat-up of the vessel during the citrus waste trial, but could not be sustained. By reducing the temperature differential between the ambient air and the outer vessel wall a lower composting rate would be required to keep the vessel at the required treatment temperature. The development of a turned bay system by Hewings *et al.* (2004) used 50mm thick insulation. This demonstrated that high internal wall temperatures could be maintained. It was deduced that the thickness and type of insulation was important. During the second run of the vessel described in Section 6.2 the vessel had been insulated with 25mm of expanded polystyrene and low temperatures had been recorded.

6.5.2 Method

The vessel was lined on the inside using 50mm high density foam insulation. The floor of the vessel was left clear of insulation except for the 300mm next to the walls.

It was hoped that this would channel more of the air to the core of the vessel. The air was supplied in the positive airflow direction and was recirculated. The k type thermocouples which had been previously mounted on the internal wall of the vessel during the citrus waste trial were moved to the internal side of the insulation, thus keeping them in contact with the compost. The thermocouples were applied to the wall at heights of 0.5m, 1m and 1.5 metres above the false floor in three different locations along the vessel, in the corner, 1 metre from the corner and 2 metres from the corner. As with the previous trials a Gemini Tiny Tag temperature probe was inserted into the core of the compost to record internal temperatures at 5 minute intervals.

The vessel was filled with green waste collected at local civic amenity sites. This was shredded using a Jenz hammer mill shredder. The aeration was controlled to keep the interstitial CO_2 concentration in the range of 5 to 10% so as not to inhibit the composting activity. Initially the fan was on for 15 minutes in every hour as this had been shown to cause the increase in temperature and high respiration rate during the citrus waste trial. The frequency was later reduced to 15 minutes in every two hours after the core of the material had begun to cool.

6.5.3 Results

The core temperature was recorded at 5 minute intervals and is shown in Figure 6.23. The probe was inserted whilst the core was at approximately 33°C and recorded the rise in temperature to 75°C over the next 24 hours. The core temperature then declined over the next 5 days to approximately 70°C before rising back up again. The re-growth of temperature within the core coincides with the reduction in frequency of aeration from 15 minutes in every hour to 15 minutes in every 2 hours. The maximum recorded temperature was 81.7°C.

Unfortunately the junction box through which the thermocouples were routed before being fed into the logger was flooded with leachate at the start of the trial. This caused irreparable damage to the connections within the box meaning that the wall

temperatures could not be automatically logged. Temperatures were however taken manually by plugging the thermocouples into the handheld meter used for daily recording of temperature on site. The manually recorded temperatures are shown in Table 6-7. The temperatures recorded are almost all below the limit of 60°C required by the Animal By-Products Regulations.

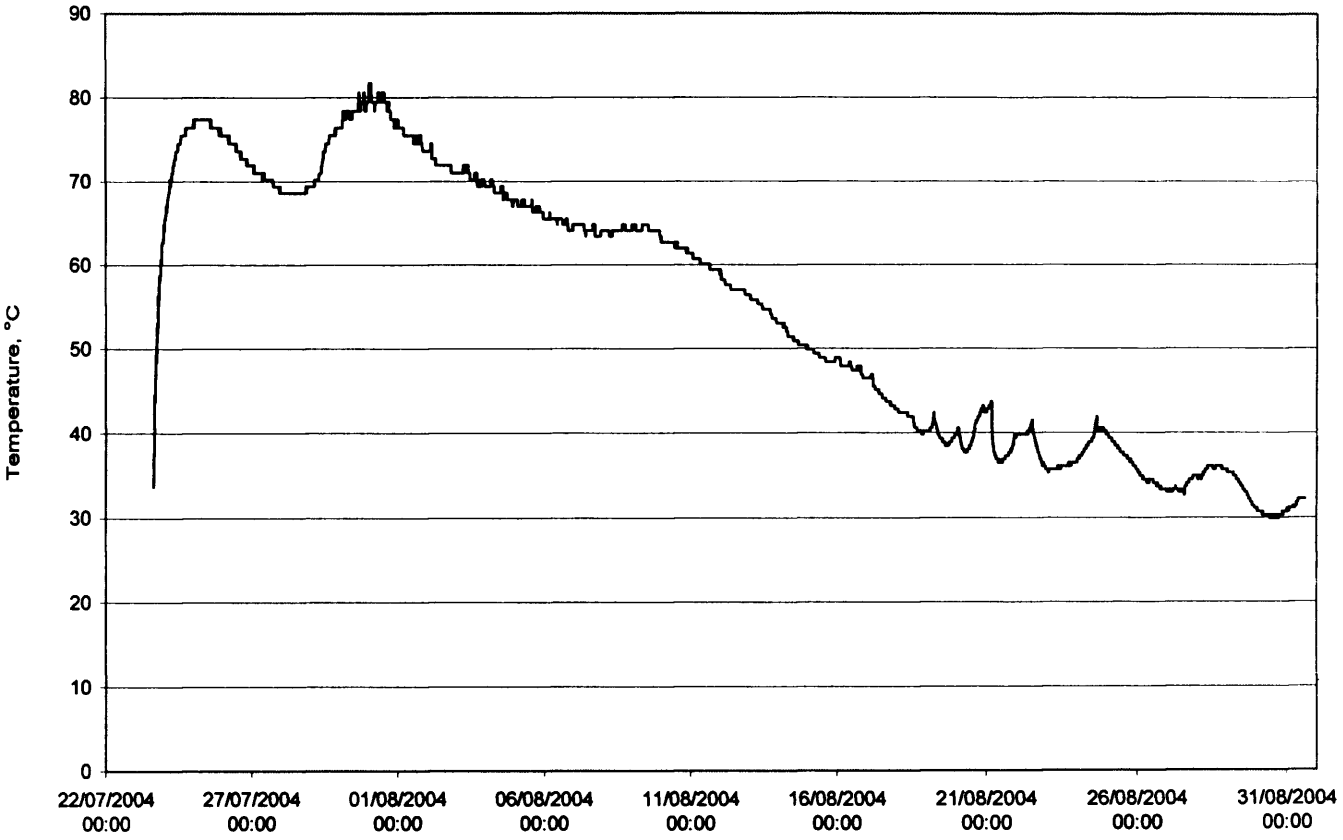

Figure 6.23. Core temperatures recorded during the insulated trial

6.5.4 Discussion

The core temperatures recorded were the highest observed whilst using the vessel and if this temperature pattern had been experienced by the entire vessel it would have meant that the system would be capable of meeting the European treatment standard for animal by-products as well as the UK treatment standards for catering waste. The high temperatures recorded during this trial suggest that the expanded polystyrene insulation applied in Section 6.2 was inadequate. The board used in this trial has a thermal conductivity of 0.04 $Wm^{-1}K^{-1}$ and although expanded polystyrene has a lower

thermal conductivity of 0.03 $Wm^{-1}K^{-1}$ the depth of insulation during this trial was 50mm as opposed to the 25mm of polystyrene used. A brief analysis of these properties shows that the 25mm of expanded polystyrene would lose 50% more heat than the 50mm of board used in this trial for the same area and temperature difference.

The data shown in Chapter 4 for windrow composting suggest a reduction in composting activity for temperatures above 55°C. The rapid increase in temperature at the start of this trial is an indicator of high composting activity, but the high temperatures reached would imply a reduction in the rate of composting occurring within the core. However with the reduction in heat losses due to the insulation it would require a reduced rate of heat release to keep the core at the elevated temperatures.

Unfortunately the volumetric air flow was not recorded during this trial. The initial aeration frequency of 15 minutes in every hour allowed a rapid rise in the core temperature of the vessel. The core temperature then decreased because it was losing too much heat. When the frequency was reduced to 15 minutes in every 2 hours the core temperature again increased. This implies that the initial quantity of air supplied was enough to provide oxygen to the bacteria but not remove the excess heat, Chapter 3 shows that for a given composting rate the quantity of air for heat removal is two orders of magnitude greater than for oxygen supply. However, once the high temperatures had been reached the previously high levels of activity were inhibited by temperature. The same amount of air was now enough to remove more heat than was being created, this lead to a fall in temperature. The aeration frequency was reduced to a level where less heat was being removed than was released by the composting process and the core temperature rose again.

Although these were the highest recorded core temperatures for the vessel the temperatures recorded at the wall shown in Table 6-6 show that the extremities of the compost still do not reach an appropriate temperature to ensure sanitisation. Sanitisation could be achieved through either turning or mixing of the material, which would require a great deal of mechanical handling at increased expense or through

direct addition of heat which is allowed under the 6th draft of the guidance for treatment by composting to meet the Animal By-Products Regulations (Defra, 2004).

Table 6-7. Manually recorded temperatures (in °C) from the vessel sidewall

	DAY	3	5	6
LOCATION		TEMPERATURE		
CORNER	UPPER	34	23	40
	MIDDLE	39	27	46
	LOWER	46	40	32
SIDE 1 1m from corner	UPPER	36	34	50
	MIDDLE	42	39	69
	LOWER	57	43	46
SIDE 2 2m from corner	UPPER	37	33	NA
	MIDDLE	48	NA	59
	LOWER	37	33	46

6.5.5 Conclusions

The insulation increased the core temperature of the vessel by reducing the rate at which heat was lost.

The core temperatures during this trial were the highest recorded in the vessel so far.

The vessel still did not meet the Animal By-Products Regulations.

The heat released by the initial high composting rate needs to be more evenly distributed around the vessel to allow compliance with the Animal By-Products Regulations.

The vessel requires an energy input of either mechanical handling or heating to meet the Animal By-Products Regulations.

6.6 Summary

The calculations in Chapter 3 showed that the vessel needed to achieve a composting rate of approximately $45gCO_2kgVS^{-1}day^{-1}$ to provide enough heat to maintain the vessel at a temperature which would meet the Animal By-Products Regulations. This is a rate approximately 50% greater than the highest rate recorded during the windrow composting trials. However the results from the citrus waste trial showed that this rate could be achieved in the vessel. The citrus waste results also showed that the estimates for air requirements from Chapter 3 were reasonable.

The trials performed using the vessel have shown that the use of insulation, method of air delivery and frequency of aeration all have a critical impact on the composting process. The recent inclusion of heat addition in the Defra guidance note (Defra, 2004) suggests that compost practitioners may also be finding difficulty in meeting the Animal By-Products Regulations.

There are several available brands of this type of composting vessel, based on roll-on-off skips, whilst they are useful for materials handling and transportation and are modular many were designed before the advent of the Animal By-Products Regulations. This means that they were not designed to meet the criteria laid out to ensure sanitisation.

7 Conclusions and Recommendations

Depending on the growth rate of waste, by 2020 Wales will need to compost between 585,000 and 1,569,000 tonnes. This is a huge amount and much of it will need to be treated to the Animal By-Products Regulations to ensure that it does not cause any health problems. Despite the growth of interest in composting as a method for waste treatment and materials recovery it can be difficult to find useful data to aid the design of composting facilities. The importance of a relatively simple parameter, the bulk density, of compost is highlighted in this work. As well as allowing the throughput of composting systems to be determined the bulk density also affects both the rate at which air is supplied and the static pressure at which it must be supplied.

The models for energy release demonstrate that although the biomass yield coefficient can vary, the quantity of heat that is released per mole of carbon dioxide evolved remains almost constant at approximately 500kJ. This value is similar to those observed experimentally and from the windrow composting trials performed at the CERT composting facility. The calculations also indicate a value other than unity for the CO_2:O_2 ratio during the composting process with approximately 450kJ released for each mole of oxygen utilised. The quantification of heat release allows respiration rates to be expressed as a power output and energy balances on composting systems to be performed.

By using a canopy system to cover a portion of a windrow it has been possible in the present study to measure in-situ respiration rates. A relationship between the core temperature and the respiration rate similar to those observed in small scale laboratory-based experiments was observed. The optimum core temperature for windrow composting was approximately 55°C although the average temperature of the windrow will be lower than this. The highest composting rate recorded for windrow composting was 38 $gCO_2kgVS^{-1}day^{-1}$.

When they reach the optimum temperature windrows appear to self limit. At the optimum temperature for composting a large amount of heat is produced, some of this heat will be used to increase the temperature of the compost. As the compost's

temperature increases the respiration rate, and hence quantity of heat released, will decrease. Due to the increased temperature there will be an increased thermal drive of the air passing through the windrow. Both of these effects will act to cool the windrow back to its optimum temperature and highest respiration rate.

In the static non-aerated windrows the carbon dioxide content of the exhaust gas was a very strong indicator of composting activity. The Gas Temperature Differential (GDT) generally showed a strong positive correlation with the concentration of carbon dioxide for the green waste windrows and this was also observed for the windrow augmented with chicken litter. This would allow monitoring of compost without use of carbon dioxide measuring equipment-generally the most expensive of the sensors used.

The GTD is a very basic measure of the heat transferred into the air passing through the compost. It is also comparatively cheap to measure, requiring only 2 thermocouples whilst the respiration rate requires measurement of carbon dioxide concentration, temperature and airflow rate.

The chicken litter windrow highlighted the importance of the physical properties of compost. The small particle size of the chicken litter decreased the pore space in the compost causing an increase in the bulk density. The diminished pore space and greater surface area of this material inhibited the airflow through the windrow inhibiting composting activity at the core of the windrow, despite the enhanced C:N ratio of approximately 20:1 compared to a normal green waste of about 70:1.

At the start of this project the addition of heat to composting vessels in order to allow them to meet the Animal By-Products Regulations was not allowed. Because of this it was important to understand the operation of the containerised in-vessel composting system and to attempt to optimise its performance. The vessel that was discussed in Chapter 6 had numerous design features that would require some improvement, not least in the loading of the vessel which required a large level of manual handing.

The latest guidance note to the Animal By-Products Regulations issued by Defra allows the addition of heat to composting systems provided that the appropriate time

and temperature profiles are met. Composting plants that are adding heat to compost still need to prove that biological degradation is taking place. To heat up the compost for treatment would require a large energy input so it would be preferable that as much of the heat required for composting comes from the composting process.

After several trials the vessel was shown to be able to meet the respiration rate of $45gCO_2kgVS^{-1}day^{-1}$ which should allow it to maintain a temperature of 60°C, this occurred during the citrus waste trial during its rapid heat up phase. One of the key problems to overcome in this type of composting system is the distribution of temperature and it would seem that air management is the key to this.

Further work on the composting process should look at optimising air management to a composting vessel to ensure that there is an even temperature profile. If the entirety of the vessel can meet the treatment profiles then there is no need for mechanical handling to turn the material. If this can be done through heat released from bacterial degradation then there will be no energy costs associated with heating the material. If up to 1.596 million tonnes of material are to be composted it is important to ensure that there is a market for approximately 800,000 tonnes of compost that will be produced. It may also be possible to use some of the data developed in this thesis to model the composting process using computational fluid dynamics software. This would allow more rapid modelling and testing of composting systems and their potential to meet the Animal By-Products Regulations.

8 References

1999 No.646 The Animal By-Products Order 1999.

2001 No. 1704 The Animal By-Products (Amendment)(Wales) Order 2001.

2003 No.1482 The Animal By-Products Regulations 2003.

Adani, F. Ubbiali, C. Tambone, F. Scaglia, B. Centemero, M. Genevini, P. L. 2002. Static and dynamic respirometric indexes-Italian research and studies. Biological Treatment of Biodegradable Waste-Technical Aspects. European Commission EUR 20517 EN.

AESA (Alberta Environmentally Sustainable Agriculture Council). 2001. Greenhouse Gas Emissions from Composting of Agricultural Wastes. Number 6, February 2001.

Agnew, J. M. Leonard, J. J. Feddes, J. Feng, Y. 2003. A modified Pycnometer for Compost Air Volume and Density Determination. Cadadian Biosystems Engineering 45, pp 6.27-6.35.

Agnew, J. M. Leonard, J, J. 2003. Literature Review: The Physical Properties of Compost. Compost Science & Utilization 11 (3), pp. 238-264.

Alexander, M. 1961. Introduction to Soil Microbiology. Wiley, New York.

Ali, M. Williams, K. P. Griffiths, A. J. 2004. The Application of Rotary In-Vessel Composting Process to the Treatment of Biodegradable Waste. Cardiff University report number 3069.

Anonymous. 2002. In vessel composting. The Composting Association News Spring 2002 vol 6 (2), pp. 14-16.

ASAE, 2000. ASAE D272.3 mar96 Resistance to Airflow of Grains, Seeds, Other Agricultural Products and Perforated Metal Sheets.

Baker, S.M., T.L. Richard, Z. Zhang and S. Monteiro da Rocha. 1998. Determining the free air space inside compost mixtures using a gas pycnometer. ASAE Paper No. 98-4094. St. Joseph, MI: ASAE.

Bari, Q. H. Koenig, A. 2001. Effect of Air Recirculation and Reuse on Composting of Organic Solid Waste. Resources, Conservation and Recycling 33, pp. 93-111.

Barrington, S. Choinière, D. Trigui, M. Knight, W. 2002. Compost Airflow Resistance. Biosystems Engineering 81 (4), pp. 433-441.

Beck-Friis, B. Smars, S. Jonsson, H. Eklind, Y. and Kirchmann, H. 2003, Composting of Source Separated Household Organics At Different Oxygen Levels: Gaining an Understanding of the Emission Dynamics. Compost Science & Utilization 11 (1). pp 41-50.

Bendat, J. S. Piersol, A. G. 1971. Random data: Analysis and measurement procedures. Wiley-Interscience. New York.

Bidlingmaie, W. Scheelhaase, T. Becker, G. 2002. Characterisation of the stabilitity of solid waste by AT_4 and other methods. Biological Treatment of Biodegradable Waste-Technical Aspects. European Commission EUR 20517 EN.

Brewer, L. J. Sullivan, D. M. 2003. Maturity and Stability Evaluation of Composted Yard Trimmings. Compost Science and Utilization 11 (2), pp. 96-112.

Bryson, B. 2003. A short History of Nearly Everything. Transworld Publishers, London.

BSI. 2000a. BS EN 12579:2000. Soil Improvers and growing media-Sampling.

BSI. 2000b. BS EN13040:2000. Soil Improvers and growing media-Sample preparation for chemical and physical tests, determination of dry matter content, moisture content and laboratory compacted bulk density.

BSI. 2000c. BS EN 13039:2000. Soil Improvers and growing media-Determination of organic matter content and ash.

BSI, 2000d. BS EN 13041:2000. Soil Improvers and growing media-Determination of physical properties-Dry bulk density, air volume, water volume, shrinkage value and total pore space.

BSI, 2000e. BS EN 13037:2000. Soil Improvers and growing media-Determination of pH.

BSI, 2000f. BS EN 13038:2000. Soil Improvers and growing media-Determination of electrical conductivity.

BSI. 2001. BS EN 13654-1:2001. Soil improvers and growing media-Determination of Nitrogen-Part 1: Modified Kjeldahl method.

BSI, 2002, BSI PAS 100 Specification for composted materials.

Cathcart, T. P. Wheaton, F. W. Brinsfield, R.B. 1986. Optimizing Variables Affecting Composting of Blue Crab Scrap. Agricultural Wastes 15. pp. 269-287.

Composting Assocciation, The. 1999. Standardised Protocol for the Sampling and Enumeration of Airborne Micro-organisms at Composting Facilities. ISBN 0 9532546 2 3.

Composting Association, The. 2000. Standards for Compost-Working Document, ISN 0-9532546-3-1.

Composting Association, The. 2004. Information Sheet 5- Feedstock characteristics. http://www.compost.org.uk/images_client/resource/05%20Feedstock%20characteristics.pdf accessed 18th May 2004.

Cooney, C. L. Wang, D. I. C. Mateles, R. I. 1969. Measurement of Heat Evolution and Correlation with Oxygen Consumption during Microbial Growth. Biotechnology and Bioengineering vol XI, pp. 269-281

Coulson, J. M. Richardson, J. F. Backhust, J. R. Harker, J. H. 1978. Chemical Engineering vol 2 3rd edition. Pergamon Press, Oxford.

Cronje, A. L. Turner, C. Williams, A. G. Barker, A. J. Guy, S. 2004. The Respiration rate of Composting Pig Manure. Compost Science and Utilization 12 (2), pp 119-129.

Dairo, O. U. Ajibola, O. O. 1994. Resistance to Airflow of Bulk Sesame Seed. Journal of Agricultural Engineering Research 58, pp.99-105.

Das, K. Keener H. M. 1997. Moisture Effect on Compaction and Permeability in Composts. Journal of Environmental Engineering 123 (3), pp. 275-281.

Defra. 2002. Digest of Environmental Statistics.
http://www.defra.gov.uk/environment/statistics/index.htm

Defra. 2003. The Environment in your pocket 2003.
http://www.defra.gov.uk/environment/statistics/eiyp/pdf/eiyp2003.pdf

Defra. 2003a. Draft Guidance on the treatment in Approved Composting or Biogas Plants of Animal By-Products and Catering Waste. Draft 6: 7th July 2003.
http://www.defra.gov.uk/animalh/by-prods/publicat/compost_guidance.pdf

Defra. 2004. Draft Guidance on the treatment in Approved Composting or Biogas Plants of Animal By-Products and Catering Waste. Draft 7: 7th June 2004.
http://www.compost.org.uk/images_client/resource/compost%20guidance%20v7%20apr04.doc accessed 28/05/04.

Droffener, M. L. Brinton Jr, W. F. Evans, E. 1995. Evidence for the Prominence of Well Characterized Mesophilic Bacteria in Thermophilic (50-70°C) Composting Environments. Biomass and Bioenergy. 8 (3). pp. 191-195.

Eden Project, 2004, Soil Matters-Making the Earth.
http://www.edenproject.com/3440_3477.htm

Edwards, M. A. Cox, A. Gale, C. Walker, M. Wood, K. 1998. A Guide to In-Vessel Composting plus A Directory of Systems. The Composting Association.

Eklind, Y. Kirchmann, H. 2000. Composting and storage of organic household waste with different litter amendments. II: nitrogen turnover and losses. Bioresource Technology 74. pp. 125-133.

Emery, A. D. Gibbs, A. J. Griffiths, A. J. Myrddin, S. Williams, K. P. 2000. Analysis of Waste Entering a Typical Small Landfill Site in the South Wales Valleys-Phase 2. Cardiff University School of Engineering Report No. 2683.

Emeterio, I. J. Garcia, P. 1992. Relationships between organic carbon and total organic matter in municipal solid wastes and city refuse composts. Bioresource Technology 41 (3). pp. 265-272.

Ergun, S. 1952. Fluid Flow Through Packed Columns. Chemical Engineering Progress 48. pp. 89-94.

European Commission. 1999. Council Directive 1999/31/EC of the 26th April 1999 on the landfill of waste.

European Commission. 2001.Working Document-Biological Treatment of Biological Waste 2nd draft.

European Commission. 2004. Draft Discussion Document for the ad-hoc meeting on Biowastes and Sludges 15-16 January 2004, Brussels.

Feachem, R. G. Bradley, D. J. Garelick, H. Mara, D. D. 1983. Sanitation and Disease: Health Aspects of Excreta and Wastewater Management. Wiley, Chichester.

Fischer, J. L. Beffa, T. Lyon, P. F. Aragno, M. 1998. Aspergillus fumigatus in windrow composting:effect of turning frequency. Waste Management & Research 16 (4), pp 320-329.

Fowler, W. H. 1968. Fowler's Mechanical Engineer's Pocket Book. Scientific Publishing Company, Manchester.

Gale, P. 2002. Risk Assessment: Use of Composting and Biogas Treatment to Dispose of Catering Waste Containing Meat. http://www.defra.gov.uk/animalh/by-prods/publicat/report5.pdf accessed 15/8/2002.

Golueke, C. G. 1972. Composting-A study of the Process and its Principals. Rodale Press Inc. Emmaus.

Giner, S. A. Denisienia, E. 1996, Pressure Drop Through Wheat as Affected by Air Velocity, Moisture content and Fines. Journal of Agricultural Engineering Research 63, pp.73-86.

Grüneklee, C. E. 1998. Comparing Open Versus In-Vessel Composting. Proceedings of Asian-North American Conference on Solid Waste Management, Los Angeles. pp 68-79.

Gunasekaran, S. Jackson, C. Y. 1987. Resistance of Airflow of Grain Sorghum. ASAE Paper No. 87-6041.

Gustaffson, K. Gustaffson, L. 1983. Heat changes, respiratory activities, ATP pools and metabolic potentials in natural sediment samples treated with quaternary amines, Oikos 41 (1), pp 64-72.

Hamoda, M. F. Abu Qdais, H. A. Hewham, J. 1998. Evaluation of municipal solid waste composting kinetics. Resources, Conservation and Recycling 23, pp. 209-223.

Hannon, J. B. Mason, I. G. 2003. Composting of Green Waste Shredded by a Crush/Cut Roller versus a Low Speed Counter-Rotating Shear Shredder. Compost Science & Utilization 11 (1), pp 61-71.

Harper, E. Miller, F.C. Macauley, B. J. 1992. Physical management and interpretation of an environmentally controlled composting ecosystem. Australian Journal of Experimental Agriculture 32, pp 657-667.

Haug, R. T. 1980. Compost Engineering, Principals and Practices. Ann Arbor Sciences Publishers Inc, Mich.

Haug, R. T. 1993. The Practical Handbook of Compost Engineering. Lewis Publishers, Boca Raton.

Hellebrand, H. J. 1998. Emission of Nitrous Oxide and other Trace Gasses during Composting of Grass and Green Waste. Journal of Agricultural Engineering Research 69. pp 365-375.

Hewings G, Notton D J, Griffiths A J, Williams K P. 2002. Full Scale Composting Research Facility Progress report 1. Cardiff University Report number 2914.

Hewings G, Notton D J, Griffiths A J, Williams K P. 2004. Full Scale Composting Research Facility Progress report 4. Cardiff University Report number 3078.

Hewings G, Notton D J, Griffiths A J, Williams K P. 2004a. Full Scale Composting Research Facility Progress report 5. Cardiff University Report number 3094.

Hibbard, C. S. Ferro, A. R. 1996. Review of potential health effects associated with bioaerosols (Aspergillus fumigatus) at composting facilities and recommended design and prudent avoidance measures. Proceedings of the Air & Waste Management Association's Annual Meeting & Exhibition 1996.

Higgins, A. J. Chen, S. Singley, M. E. 1982. Airflow resistance in sewage sludge composting aeration systems. Transactions of the ASAE 24(4). Pp 1010-1014.

Hoitink, H. A. J. Keener, H. M. 1995. Composting organics in the Netherlands. Biocycle 36 (1).

Holman, J. P. 1976, Heat Transfer, McGraw-Hill, Kogakusha.

Jeong, Y. K. Kim, J. S. 2001. A new method for conservation of nitrogen in aerobic composting processes. Bioresource Technology 79. pp 129-133.

Jerris, J. S. Regan, R.W. 1973. Controlling Environmental Parameters for Optimum Composting-I: Experimental Procedures and Temperature. Composting Science, pp 10-15.

Jerris, J. S. Regan, R.W. 1973a. Controlling Environmental Parameters for Optimum Composting-II: Moisture, free air space and recycle. Composting Science 14.

Jha, A. 2003. Unboilable bug points to hotter origin of life. The Guardian Friday August 15th 2003. http://www.guardian.co.uk/uk_news/story/0,3604,1019156,00.html accessed 18/08/2003.

Keener, H. M. Marugg, C. Hanson, C. Hoitink, H. A. J. 1993. Optimizing the efficiency of the composting process. In Science and Engineering of Composting: Design, Environmental, Microbiological and Utilization Aspects, ed. Hoitink, H. A. J. and Keener, H. M. Renaissance Publications, Columbus, Ohio. Pp 59-94.

Keener, H. M. Hansen, R. C. Elwell, D. L. 1997. Airflow Through Compost: Design and Cost Implications. Applied Engineering in Agriculture 13 (3), pp. 377-384.

Kraft, E. 2002. Methods for Determining Physical, Particle Related Characteristics Relevant to Fluid Flow Phenomena in Biowaste. Bioprocessing of Solid Waste & Sludge 2 (1), pp.9-17

Kutzner, H. J. 2000. Microbiology of Composting. in Biotechnology volume 11c Environmental Processes III editors Klein, J. Winter, J.

Larney, F. J. Olsen, A. F. Carcamo, A. A. Chang, C. 2000. Physical changes during active and passive composting of beef feedlot manure in winter and summer. Bioresource Technology 75, pp 139-148.

Lasaridi, K. E. 1997. Compost Stability: A Comparative Evaluation of Respirometric Techniques. Ph.D. thesis, University of Leeds, Department of Civil Engineering, UK.

Lhadi, E. K. Tzi, H. Aylaj, M. Tambone, F. Adani, F. 2004. Cocomposting Separated MSW And Poultry Manure in Morocco. Compost Science & Utilization 12 (2), pp137-144.

Lei, F. VanderGheynst, J. S. 2000. The effect of microbial inoculation and pH on microbial community structure during composting. Process Biochemistry 35, pp 923-929

Li, L. I. Kock, C. M. Mckinney, D. E. 1991. Composting, Past, Present and Future. Proceedings of the ASCE conference on environmental engineering 1991, New York.

MAFF, 2001, Guidance note on the disposal of Animal By-Products and Catering Waste. www.defra.gov.uk/animalh/by-prods/publicat/dispguide.pdf accessed 3rd June 2004.

Mari, I. Ehaliotis, C. Kotsou, M. Balis, C. Georgakakis, D. 2003. Respiration profiles in monitoring the composting of by-products from the olive oil agro-industry. Bioresource Technology 87, pp 331-336.

Massey, B. S. 1989, Mechanics of Fluids, sixth edition. Chapman and Hall, London.

MacGregor, S. T. Miller, F. C. Psarianos, K. M. Finstein, M. S. 1981. Composting Process Control Based on Interaction Between Microbial Heat Output and Temperature. Applied and Environmental Microbiology 41 (6), pp 1321-1330.

McCartney, D. Raichura, A. 2003. Does Size Matter? The Effect of Woodchip Particle Size on the Composting Process. The Composting Council of Canada's 13th Annual National Composting Conference.

McGuckin, R. L. Eiteman, M. A. Das, K. 1999. Pressure Drop Through Raw Food Waste Compost Containing Synthetic Bulking Agents. Journal of Agricultural Engineering Research 72, pp. 375-384.

Mears, D. R. Singley, M. E. Ali, C. Rupp, F. 1975. Thermal and Physical Properties of Compost, in Energy, Agriculture and Waste Management, W. J. Jewell, Ed. Ann Arbor, Michigan.

Metcalf & Eddy, Tchobanoglous, G. Burton, F. Stensel, H. D. (Eds), 2002, Wastewater Engineering: Treatment-Disposal-Reuse. McGraw Hill.

Michel, F. C. Forney, L. J. Huang, A. J. F. Drew, S. Czuprenski, M. Lindebergy, J. D. Reddy, C. A. 1996. Effects of turning frequency, leaves to grass mix ratio and windrows vs. pile configuration on the composting of yard trimmings. Compost Science and Utilization 4(1), pp 26-43.

Mu, R. Leonard, J. 1999. Measurement of air flow through MSW-sewage sludge compost. Canadian Agricultural Engineering 41 (2), pp. 93-97.

Myrddin, S. 2003. In-Vessel Composting as a Solution to the Management of Biodegradable Municipal Waste. Ph.D. Thesis University of Wales, Cardiff.

Nakasaki, K. Shoda, M. Kubota, H. 1986. Effects of a bulking agent on the reaction rate of thermophilic sewage sludge composting. Journal of Fermentation Technology 64(6), pp 539-544.

Nagasaki, K. Yaguchi, H. Sasaki, Y. Kubota, H. 1992. Effects on pH on control on composting of garbage. Waste Management and Research 11, pp 117-125.

National Trust, 2002, Policy Statement-The use of Peat in Gardens. http://www.nationaltrust.org.uk/main/policy/documents/Peat.pdf

Nicolai, R. E. Janni, K. A. 2001. Determining Pressure Drop Through Compost-Wood Chip BiofilterMedia. ASAE paper No. 014080.

NSCA. 2002. Comparison of Emissions from Waste Management Options. ISBN 0 9034 7459 0. www.nsca.org.uk.

Patumsawad, S. Cliffe, K. R. 2002. Experimental study on fluidised bed combustion of high moisture municipal solid waste. Energy Conversion and Management 43, pp 2329-2340.

Polprasert, C. 1989, Organic Waste Recycling. John Wiley & sons Ltd, Chichester.

Richard, D. Zimmerman, R. 1995. Respiration Rate-Reheating Potential: A Comparison of Measures of Compost Stability. Compost Science & Utilization 3(2), pp 74-79.

Roberts, P. Jones, D. L. Edwards-Jones, G. 2004. Spatial Variability and Plant Nutrient Dynamics During the Composting of Three Green Waste Combinations, using Ecopod Technology. Presented at the WARMNET conference "Tackling waste, 20th-21st July 2004

Rothbaum, H. P. 1961. Heat output of thermophiles occurring in wool. Journal of Bacteriology 81, pp. 164-171.

Rothbaum, H. P. Stone, H. M. 1961. Heat output of Escherichia coli. Journal of Bacteriology 81, pp. 172-177.

RSPB. 2001. Peatering Out-Towards a sustainable UK growing media industry. http://www.rspb.org.uk/Images/peateringout_tcm5-31088.pdf

Rynk, R. 1992. On-Farm Composting handbook, NRAES 54, Ithaca, NY.

Sadaka, S. Magura, C. R. Mann, D. D. 2002. Verticle and Horizontal Airflow Characteristics of Wood/Compost Mixtures. Applies Engineering in Agriculture 18 (6), pp. 735-741.

Sadaka, S. El-Taweel, A. 2003. Effects of Aeration and C:N Raio on Household Waste Composting in Egypt. Composting Science & Utilization 11 (1), pp 41-50.

Saint-Joly, C. Peyre, A. Bochu, J. L. N'Dao, O. 1989. Pressure losses during ventilation of manure. Biological wastes 30, pp 123-132.

Schaub-Szabo, S. M. Leonard, J. J. 1999. Characterizing the Bulk Density of Compost. Compost Science & Utilization 7 (4), pp. 15-24.

Schmidt, D. 2000. Odor, hydrogen sulfide, and ammonia emissions from the composting of caged layer manure. Final report to the Broiler and Egg Association of Minnesota. University of Minnesota.

Sesay, A. A. Lasaridi, K. E. Stentiford, E. I. 1998. Aerated static pile composting of municipal solid waste (MSW): a comparison of positive pressure aeration with highbred positive and negative aeration. Waste Management Research 16 (3), pp 264-272.

Shedd, C. K. 1953. Resistance of Grain and Seeds to Airflow. Agricultural Engineering 34 (9), pp. 616-619.

Singh, A. Sharma, S. 2003. Effect of Microbial Inocula on Mixed Solid Waste Composting, Vermicomposting and Plant Response. Compost Science and Utilization 11 (3), pp. 190-199

Sparling, G. P. 1983. Estimation of microbial biomass and activity in soil using microcalorimetry. Journal of Soil Science 34, pp. 381-390

Strom, P. F. 1985. Effect of Temperature on Bacterial Species Diversity in Thermophilic Solid-Waste Composting. Applied and Environmental Microbiology 50 (4), pp. 899-905

Spoehr, H. A. Milner, H. W. 1949. The Chemical Composition of Chlorella; Effect of Environmental Conditions. Plant Physiology 24

Suler, D. J. Finstein, M. S. 1977. Effect of temperature, aeration and moisture on CO_2 formation in bench-scale continuously thermophillic composting of solid waste. Applied and Environmental Microbiology 33, pp. 345-350.

Sullivan, D. M. Miller, R. O. 2001. Compost Quality Attributes, Measurements and Variability. In Stofella, P. J. Kahn, B. A. (ed.) Compost Utilization in Horticultural Cropping Systems. CRC Press. Boca Raton, Florida. Pp. 95-120

Tancho, A. Merckx, R. Schoovaerts, R. Vlassak, K. 1995. Relationship between substrate-induced respiration and heat loss from soil samples treated with various contaminents. Thermochimica Acta 251, pp. 21-28.

Tiquia, S. M. Tam, N. F. Y. 2002. Characterization and composting of poultry litter in forced-aeration piles. Process Biochemistry 37, pp 869-880.

Van Ginkel, J. T. Van Haneghem, I. A. Raats, P. A. C. 2002. Physical Properties of Composting Material: Gas Permeability, Oxygen Diffusion Coefficient and Thermal Conductivity. Biosystems Engineering 81(1), pp. 113-125.

Velikonja Bolta,S. Mihelic, R. Lobnik, F. Lestan, D. 2003. Microbial Community Structure During Composting With and Without Mass Inocula. Compost Sciense and Utilization 11 (1). Pp. 6-15.

WAG, 2002, Wise about Waste: The National Waste Strategy for Wales.

Waksman, S. A. Cordon, T. C. Hulpoi, N. 1939. Influence of Temperature Upon the Microbiological Population and Decomposition Processes in Composts of Stable Manure. Soil Science 47, pp. 83-113.

Walker, J. Goldstein, N. Chen, B. 1986. Evaluating the In vessel composting option. Biocycle 27 (5).

Weppen, P. 2001. Process calorimetry on composting of municipal organic wastes. Biomass and Bioenergy 21, pp.289-299.

Wiley, J.S. 1956. II Progress report on high-rate composting studies. Processing of Industrial Waste Conference. (Purdue University Publication No. 96) 11, pp. 334-341.

Wiley, J.S. 1957. III Progress report on high-rate composting studies. Processing of Industrial Waste Conference. (Purdue University Publication No. 96) 12, pp. 596-603.

Witter, E. Lopez-Real, J. M. 1988. Nitrogen losses during the composting of sewage sludge and the effectiveness of clay soil, zeolite and compost in adsorbing the volatized ammonia. Biological Wastes 23. pp. 279-294.

WPIF (Wood Panel Industries Federation), 2004, Panel guide, http://www.wpif.org.uk/panelguide.asp, accessed 05/10/04

Zanoni, A. E. Mueller, D. L. 1982. Calorific Value of Wastewater Plant Sludges. Journal of the Environmental Engineering Division ASCE 108(1), pp. 187-195.

Appendix A:

Results of Stoichiometric Equations for Bacterial Breakdown

Table A-1. Required reactants and products for composting of one mole of glucose ($C_6H_{12}O_6$)

Yield co-efficient	Moles ammonia required	Moles O_2 required	Moles of bacterial cell	Moles CO_2 evolved	Moles H_2O evolved	CO_2:O_2 ratio	CO_2:H_2O ratio
0.502	0.8	2.0	0.8	2.0	4.4	1	0.45
0.430	0.7	2.5	0.7	2.5	4.6	1	0.54
0.376	0.6	3.0	0.6	3.0	4.8	1	0.63
0.314	0.5	3.5	0.5	3.5	5.0	1	0.70
0.251	0.4	4.0	0.4	4.0	5.2	1	0.77
0.188	0.3	4.5	0.3	4.5	5.4	1	0.83
0.125	0.2	5.0	0.2	5.0	5.6	1	0.89
0.063	0.1	5.5	0.1	5.5	5.8	1	0.95

Table A-2. Required reactants and products for composting of one mole of protein ($C_{16}H_{24}O_5N_4$)

Yield co-efficient	Moles ammonia required	Moles O_2 required	Moles of bacterial cell	Moles CO_2 evolved	Moles H_2O evolved	CO_2:O_2 ratio	CO_2:H_2O ratio
0.502	-2.4	8.7	1.6	8.2	2.9	0.94	2.85
0.430	-2.6	9.7	1.4	9.2	3.3	0.95	2.81
0.376	-2.8	10.6	1.2	10.1	3.7	0.95	2.77
0.314	-3.0	11.6	1.0	11.1	4.0	0.96	2.75
0.251	-3.2	12.6	0.8	12.1	4.4	0.96	2.73
0.188	-3.4	13.6	0.6	13.1	4.8	0.96	2.71
0.125	-3.6	14.5	0.4	14.0	5.2	0.97	2.69
0.063	-3.8	15.5	0.2	15.0	5.6	0.97	2.68

Table A-3. Required reactants and products for composting of one mole of fat ($C_{50}H_{90}O_6$)

Yield co-efficient	Moles ammonia required	Moles O_2 required	Moles of bacterial cell	Moles CO_2 evolved	Moles H_2O evolved	CO_2:O_2 ratio	CO_2:H_2O ratio
0.502	3.5	52.0	3.5	32.5	38.0	0.63	0.86
0.430	3.1	54.2	3.1	34.7	38.9	0.64	0.89
0.376	2.6	56.4	2.6	36.9	39.8	0.65	0.93
0.314	2.2	58.6	2.2	39.1	40.6	0.67	0.96
0.251	1.7	60.8	1.7	41.3	41.5	0.68	0.99
0.188	1.3	63.0	1.3	43.5	42.4	0.69	1.03
0.125	0.9	65.1	0.9	45.6	43.3	0.70	1.06
0.063	0.4	67.3	0.4	47.8	44.1	0.71	1.08

Table A-4. Required reactants and products for composting of one mole of primary sludge ($C_{22}H_{39}O_{10}N$)

Yield co-efficient	Moles ammonia required	Moles O_2 required	Moles of bacterial cell	Moles CO_2 evolved	Moles H_2O evolved	CO_2:O_2 ratio	CO_2:H_2O ratio
0.502	1.1	15.4	2.1	11.4	13.8	0.74	0.83
0.430	0.9	16.7	1.9	12.7	14.3	0.76	0.89
0.376	0.6	18.1	1.6	14.1	14.8	0.78	0.95
0.314	0.3	19.4	1.3	15.4	15.4	0.79	1.00
0.251	0.1 -	20.7	1.1	16.7	15.9	0.81	1.05
0.188	-0.2	22.0	0.8	18.0	16.4	0.82	1.10
0.125	-0.5	23.4	0.5	19.4	16.9	0.83	1.14
0.063	-0.7	24.7	0.3	20.7	17.5	0.84	1.18

Table A-5. Required reactants and products for composting of one mole of wood ($C_{295}H_{420}O_{186}N$)

Yield co-efficient	Moles ammonia required	Moles O_2 required	Moles of bacterial cell	Moles CO_2 evolved	Moles H_2O evolved	CO_2:O_2 ratio	CO_2:H_2O ratio
0.502	29.9	151.8	30.9	140.6	146.7	0.93	0.96
0.430	26.0	171.1	27.0	159.9	154.4	0.93	1.04
0.376	22.2	190.4	23.2	179.2	162.2	0.94	1.10
0.314	18.3	209.7	19.3	198.5	169.9	0.95	1.17
0.251	14.4	229.0	15.4	217.8	177.6	0.95	1.23
0.188	10.6	248.3	11.6	237.1	185.3	0.95	1.28
0.125	6.7	267.6	7.7	256.4	193.1	0.96	1.33
0.063	2.9	286.9	3.9	275.7	200.8	0.96	1.37

Table A-6. Required reactants and products for composting of one mole of grass ($C_{23}H_{38}O_{17}N$)

Yield co-efficient	Moles ammonia required	Moles O_2 required	Moles of bacterial cell	Moles CO_2 evolved	Moles H_2O evolved	CO_2:O_2 ratio	CO_2:H_2O ratio
0.502	1.7	9.9	2.7	9.7	12.2	0.97	0.79
0.430	1.3	11.6	2.3	11.3	12.8	0.98	0.88
0.376	1.0	13.3	2.0	13.0	13.5	0.98	0.96
0.314	0.7	14.9	1.7	14.7	14.2	0.98	1.04
0.251	0.3	16.6	1.3	16.3	14.8	0.98	1.10
0.188	0.0	18.3	1.0	18.0	15.5	0.99	1.16
0.125	-0.3	19.9	0.7	19.7	16.2	0.99	1.22
0.063	-0.7	21.6	0.3	21.3	16.8	0.99	1.27

Table A-7. Required reactants and products for composting of one mole of combined sludge ($C_{10}H_{19}O_3N$)

Yield co-efficient	Moles ammonia required	Moles O_2 required	Moles of bacterial cell	Moles CO_2 evolved	Moles H_2O evolved	CO_2:O_2 ratio	CO_2:H_2O ratio
0.502	-0.1	8.0	0.9	5.5	6.2	0.69	0.89
0.430	-0.2	8.6	0.8	6.1	6.4	0.71	0.95
0.376	-0.3	9.2	0.7	6.7	6.7	0.73	1.00
0.314	-0.4	9.7	0.6	7.2	6.9	0.74	1.05
0.251	-0.6	10.3	0.4	7.8	7.1	0.76	1.09
0.188	-0.7	10.8	0.3	8.3	7.3	0.77	1.14
0.125	-0.8	11.4	0.2	8.9	7.6	0.78	1.18
0.063	-0.9	11.9	0.1	9.4	7.8	0.79	1.21

Table A-8. Required reactants and products for composting of one mole of Refuse (TOF) ($C_{64}H_{104}O_{37}N$)

Yield co-efficient	Moles ammonia required	Moles O_2 required	Moles of bacterial cell	Moles CO_2 evolved	Moles H_2O evolved	CO_2:O_2 ratio	CO_2:H_2O ratio
0.502	5.6	37.9	6.6	31.2	37.4	0.82	0.83
0.430	4.7	42.0	5.7	35.3	39.0	0.84	0.90
0.376	3.9	46.1	4.9	39.4	40.6	0.85	0.97
0.314	3.1	50.2	4.1	43.5	42.3	0.87	1.03
0.251	2.3	54.3	3.3	47.6	43.9	0.88	1.08
0.188	1.5	58.4	2.5	51.7	45.6	0.88	1.13
0.125	0.6	62.5	1.6	55.8	47.2	0.89	1.18
0.063	-0.2	66.6	0.8	59.9	48.9	0.90	1.23

Table A-9. Required reactants and products for composting of one mole of Refuse (TOF) ($C_{99}H_{148}O_{59}N$)

Yield co-efficient	Moles ammonia required	Moles O_2 required	Moles of bacterial cell	Moles CO_2 evolved	Moles H_2O evolved	CO_2:O_2 ratio	CO_2:H_2O ratio
0.502	9.2	54.8	10.2	48.0	52.1	0.88	0.92
0.430	7.9	61.1	8.9	54.4	54.7	0.89	1.00
0.376	6.6	67.5	7.6	60.8	57.2	0.90	1.06
0.314	5.4	73.9	6.4	67.1	59.8	0.91	1.12
0.251	4.1	80.3	5.1	73.5	62.3	0.92	1.18
0.188	2.8	86.6	3.8	79.9	64.9	0.92	1.23
0.125	1.5	93.0	2.5	86.3	67.4	0.93	1.28
0.063	0.3	99.4	1.3	92.6	70.0	0.93	1.32

Table A-10. Required reactants and products for composting of one mole of Garbage ($C_{16}H_{27}O_8N$)

Yield co-efficient	Moles ammonia required	Moles O_2 required	Moles of bacterial cell	Moles CO_2 evolved	Moles H_2O evolved	CO_2:O_2 ratio	CO_2:H_2O ratio
0.502	0.6	10.0	1.6	8.0	8.8	0.80	0.91
0.430	0.4	11.0	1.4	9.0	9.2	0.82	0.98
0.376	0.2	12.0	1.2	10.0	9.6	0.83	1.04
0.314	0.0	13.0	1.0	11.0	10.0	0.85	1.10
0.251	-0.2	14.0	0.8	12.0	10.4	0.86	1.15
0.188	-0.4	15.0	0.6	13.0	10.8	0.87	1.20
0.125	-0.6	16.0	0.4	14.0	11.2	0.87	1.25
0.063	-0.8	17.0	0.2	15.0	11.6	0.88	1.29

Results of Stoichiometric Equations for Fungal Breakdown.

Table A-11. Required reactants and products for composting of one mole of glucose ($C_6H_{12}O_6$)

Yield co-efficient	Moles ammonia required	Moles O_2 required	Moles of fungal cell	Moles CO_2 evolved	Moles H_2O evolved	CO_2:O_2 ratio	CO_2:H_2O ratio
0.502	0.37	2.16	0.37	2.34	3.44	1.08	0.68
0.430	0.32	2.64	0.32	2.80	3.76	1.06	0.74
0.376	0.27	3.12	0.27	3.26	4.08	1.04	0.80
0.314	0.23	3.60	0.23	3.71	4.40	1.03	0.84
0.251	0.18	4.08	0.18	4.17	4.72	1.02	0.88
0.188	0.14	4.56	0.14	4.63	5.04	1.02	0.92
0.125	0.09	5.04	0.09	5.09	5.36	1.01	0.95
0.063	0.05	5.52	0.05	5.54	5.68	1.00	0.98

Table A-12. Required reactants and products for composting of one mole of protein ($C_{16}H_{24}O_5N_4$)

Yield co-efficient	Moles ammonia required	Moles O_2 required	Moles of fungal cell	Moles CO_2 evolved	Moles H_2O evolved	CO_2:O_2 ratio	CO_2:H_2O ratio
0.502	-3.28	8.98	0.72	8.84	0.99	0.98	8.93
0.430	-3.37	9.92	0.63	9.74	1.62	0.98	6.02
0.376	-3.46	10.86	0.54	10.63	2.24	0.98	4.74
0.314	-3.55	11.80	0.45	11.53	2.87	0.98	4.02
0.251	-3.64	12.74	0.36	12.42	3.49	0.97	3.55
0.188	-3.73	13.68	0.27	13.32	4.12	0.97	3.23
0.125	-3.82	14.62	0.18	14.21	4.75	0.97	2.99
0.063	-3.91	15.56	0.09	15.11	5.37	0.97	2.81

Table A-13. Required reactants and products for composting of one mole of fat ($C_{50}H_{90}O_6$)

Yield co-efficient	Moles ammonia required	Moles O_2 required	Moles of fungal cell	Moles CO_2 evolved	Moles H_2O evolved	CO_2:O_2 ratio	CO_2:H_2O ratio
0.502	1.60	52.72	1.60	34.02	33.81	0.65	1.01
0.430	1.40	54.82	1.40	36.02	35.21	0.66	1.02
0.376	1.20	56.91	1.20	38.01	36.61	0.67	1.04
0.314	1.00	59.01	1.00	40.01	38.01	0.68	1.05
0.251	0.80	61.11	0.80	42.01	39.41	0.69	1.07
0.188	0.60	63.21	0.60	44.01	40.80	0.70	1.08
0.125	0.40	65.30	0.40	46.00	42.20	0.70	1.09
0.063	0.20	67.40	0.20	48.00	43.60	0.71	1.10

Table A-14. Required reactants and products for composting of one mole of primary sludge ($C_{22}H_{39}O_{10}N$)

Yield co-efficient	Moles ammonia required	Moles O_2 required	Moles of fungal cell	Moles CO_2 evolved	Moles H_2O evolved	CO_2:O_2 ratio	CO_2:H_2O ratio
0.502	-0.03	15.82	0.97	12.30	11.21	0.78	1.10
0.430	-0.15	17.09	0.85	13.51	12.06	0.79	1.12
0.376	-0.27	18.36	0.73	14.73	12.91	0.80	1.14
0.314	-0.39	19.64	0.61	15.94	13.76	0.81	1.16
0.251	-0.52	20.91	0.48	17.15	14.61	0.82	1.17
0.188	-0.64	22.18	0.36	18.36	15.45	0.83	1.19
0.125	-0.76	23.45	0.24	19.58	16.30	0.83	1.20
0.063	-0.88	24.73	0.12	20.79	17.15	0.84	1.21

Table A-15. Required reactants and products for composting of one mole of wood ($C_{295}H_{420}O_{186}N$)

Yield co-efficient	Moles ammonia required	Moles O_2 required	Moles of fungal cell	Moles CO_2 evolved	Moles H_2O evolved	CO_2:O_2 ratio	CO_2:H_2O ratio
0.502	13.13	157.87	14.13	153.69	109.58	0.97	1.40
0.430	11.36	176.42	12.36	171.35	121.95	0.97	1.41
0.376	9.60	194.97	10.60	189.01	134.31	0.97	1.41
0.314	7.83	213.51	8.83	206.68	146.68	0.97	1.41
0.251	6.07	232.06	7.07	224.34	159.04	0.97	1.41
0.188	4.30	250.61	5.30	242.01	171.41	0.97	1.41
0.125	2.53	269.16	3.53	259.67	183.77	0.96	1.41
0.063	0.77	287.70	1.77	277.34	196.14	0.96	1.41

Table A-16. Required reactants and products for composting of one mole of grass ($C_{23}H_{38}O_{17}N$)

Yield co-efficient	Moles ammonia required	Moles O_2 required	Moles of fungal cell	Moles CO_2 evolved	Moles H_2O evolved	CO_2:O_2 ratio	CO_2:H_2O ratio
0.502	0.22	10.44	1.22	10.80	8.96	1.03	1.21
0.430	0.07	12.04	1.07	12.33	10.03	1.02	1.23
0.376	-0.09	13.64	0.91	13.85	11.10	1.02	1.25
0.314	-0.24	15.24	0.76	15.38	12.16	1.01	1.26
0.251	-0.39	16.85	0.61	16.90	13.23	1.00	1.28
0.188	-0.54	18.45	0.46	18.43	14.30	1.00	1.29
0.125	-0.70	20.05	0.30	19.95	15.37	1.00	1.30
0.063	-0.85	21.65	0.15	21.48	16.43	0.99	1.31

Table A-17. Required reactants and products for composting of one mole of combined sludge ($C_{10}H_{19}O_3N$)

Yield co-efficient	Moles ammonia required	Moles O_2 required	Moles of fungal cell	Moles CO_2 evolved	Moles H_2O evolved	CO_2:O_2 ratio	CO_2:H_2O ratio
0.502	-0.59	8.21	20.97	0.41	5.91	0.72	1.15
0.430	-0.64	8.75	23.97	0.36	6.42	0.73	1.17
0.376	-0.69	9.28	27.96	0.31	6.93	0.75	1.18
0.314	-0.74	9.82	33.56	0.26	7.45	0.76	1.20
0.251	-0.80	10.35	41.95	0.20	7.96	0.77	1.21
0.188	-0.85	10.89	55.93	0.15	8.47	0.78	1.22
0.125	-0.90	11.43	83.89	0.10	8.98	0.79	1.23
0.063	-0.95	11.96	167.78	0.05	9.49	0.79	1.24

Table A-18. Required reactants and products for composting of one mole of Refuse 1 (TOF) ($C_{64}H_{104}O_{37}N$)

Yield co-efficient	Moles ammonia required	Moles O_2 required	Moles of fungal cell	Moles CO_2 evolved	Moles H_2O evolved	CO_2:O_2 ratio	CO_2:H_2O ratio
0.502	2.01	39.20	18.25	3.01	33.95	0.87	1.15
0.430	1.63	43.14	20.86	2.63	37.70	0.87	1.17
0.376	1.25	47.08	24.34	2.25	41.46	0.88	1.19
0.314	0.88	51.03	29.21	1.88	45.22	0.89	1.21
0.251	0.50	54.97	36.51	1.50	48.97	0.89	1.22
0.188	0.13	58.92	48.68	1.13	52.73	0.89	1.24
0.125	-0.25	62.86	73.02	0.75	56.49	0.90	1.25
0.063	-0.62	66.81	146.03	0.38	60.24	0.90	1.26

Table A-19. Required reactants and products for composting of one mole of Refuse 2(TOF) ($C_{99}H_{148}O_{59}N$)

Yield co-efficient	Moles ammonia required	Moles O_2 required	Moles of fungal cell	Moles CO_2 evolved	Moles H_2O evolved	CO_2:O_2 ratio	CO_2:H_2O ratio
0.502	3.66	56.77	4.66	52.36	39.85	0.92	1.31
0.430	3.08	62.90	4.08	58.19	43.93	0.93	1.32
0.376	2.50	69.02	3.50	64.02	48.01	0.93	1.33
0.314	1.92	75.14	2.92	69.85	52.09	0.93	1.34
0.251	1.33	81.26	2.33	75.68	56.17	0.93	1.35
0.188	0.75	87.38	1.75	81.51	60.26	0.93	1.35
0.125	0.17	93.51	1.17	87.34	64.34	0.93	1.36
0.063	-0.42	99.63	0.58	93.17	68.42	0.94	1.36

Table A-20. Required reactants and products for composting of one mole of Garbage ($C_{16}H_{27}O_8N$)

Yield co-efficient	Moles ammonia required	Moles O_2 required	Moles of fungal cell	Moles CO_2 evolved	Moles H_2O evolved	CO_2:O_2 ratio	CO_2:H_2O ratio
0.502	-0.27	10.29	0.73	8.66	6.86	0.84	1.26
0.430	-0.36	11.26	0.64	9.58	7.50	0.85	1.28
0.376	-0.45	12.22	0.55	10.49	8.15	0.86	1.29
0.314	-0.54	13.18	0.46	11.41	8.79	0.87	1.30
0.251	-0.63	14.15	0.37	12.33	9.43	0.87	1.31
0.188	-0.72	15.11	0.28	13.25	10.07	0.88	1.32
0.125	-0.82	16.07	0.18	14.16	10.72	0.88	1.32
0.063	-0.91	17.04	0.09	15.08	11.36	0.89	1.33

Appendix B:
Design of Static Pressure Test Rig

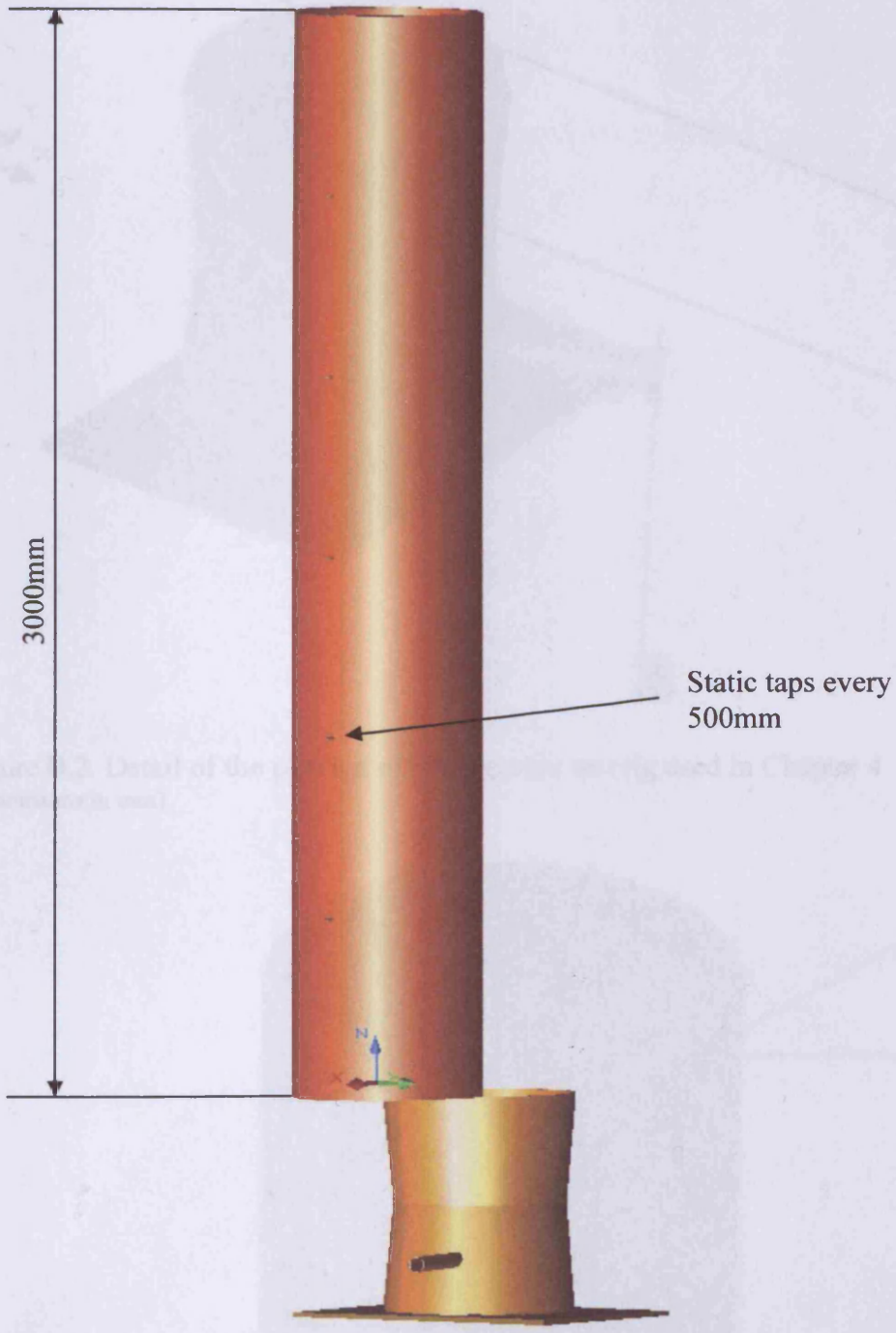

Figure B.1. Design of pressure test rig used for static pressure measurement in Chapter 4

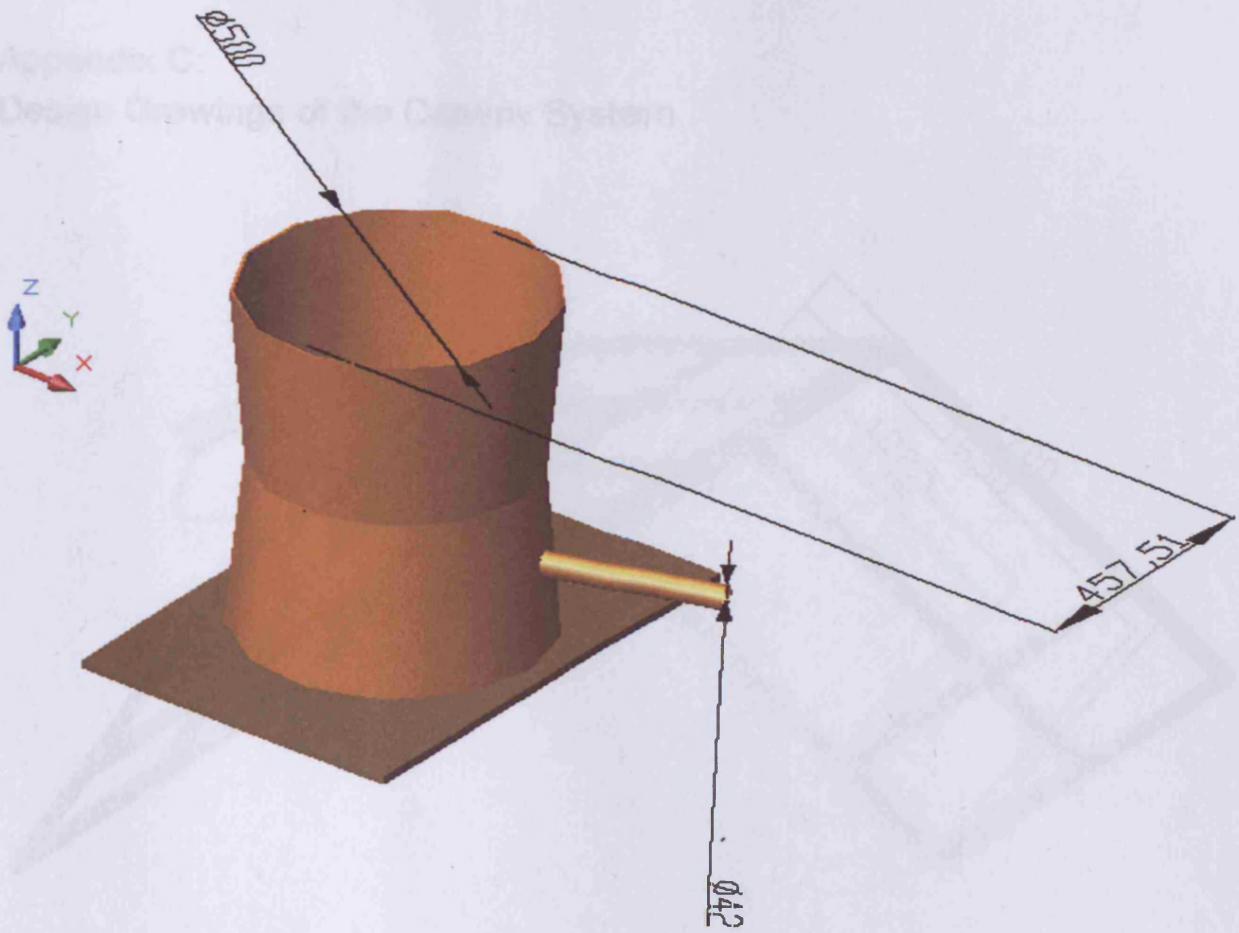

Figure B.2. Detail of the plenum of the pressure test rig used in Chapter 4 (dimensions in mm)

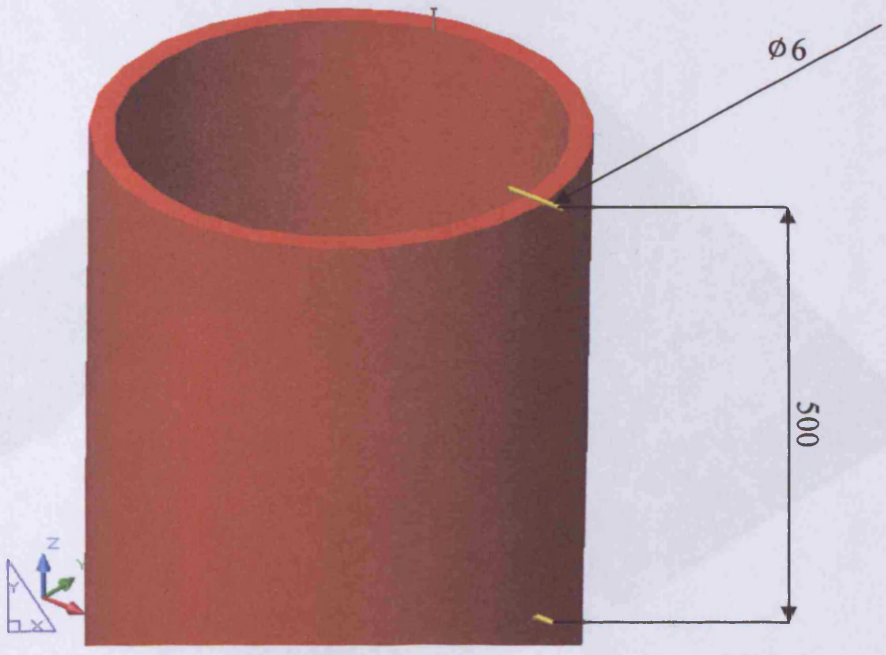

Figure B.3. Detail of the top of the column and static taps of the pressure test rig used in Chapter 4 (dimensions in mm)

Appendix C:
Design Drawings of the Canopy System

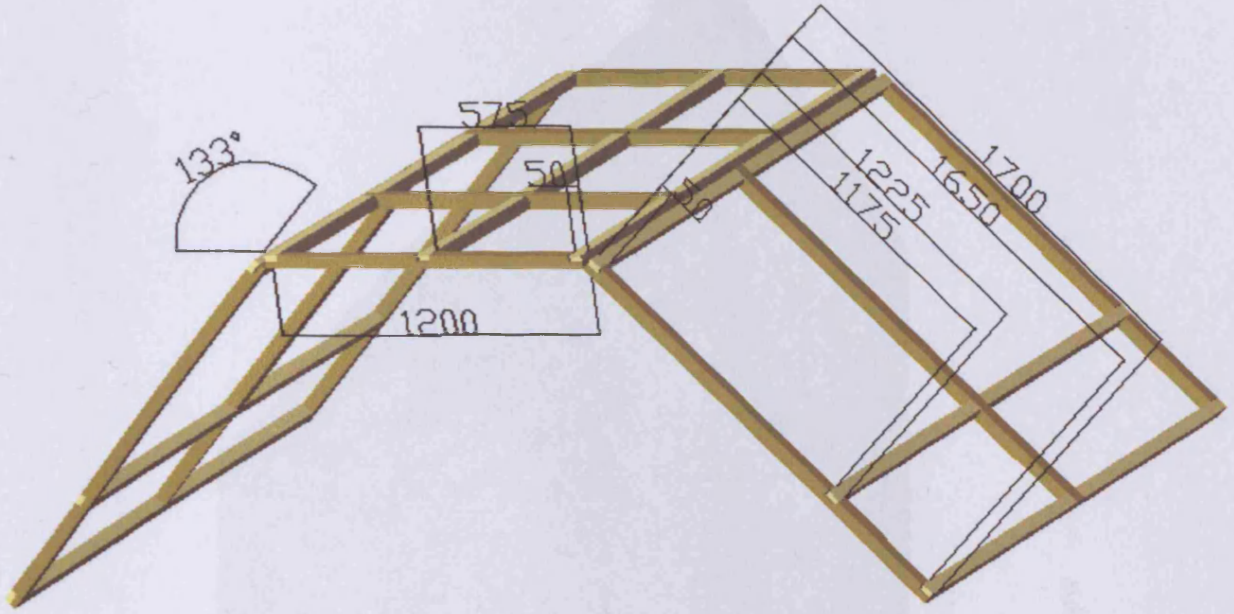

Figure C.1. The frame of the canopy, showing dimensions

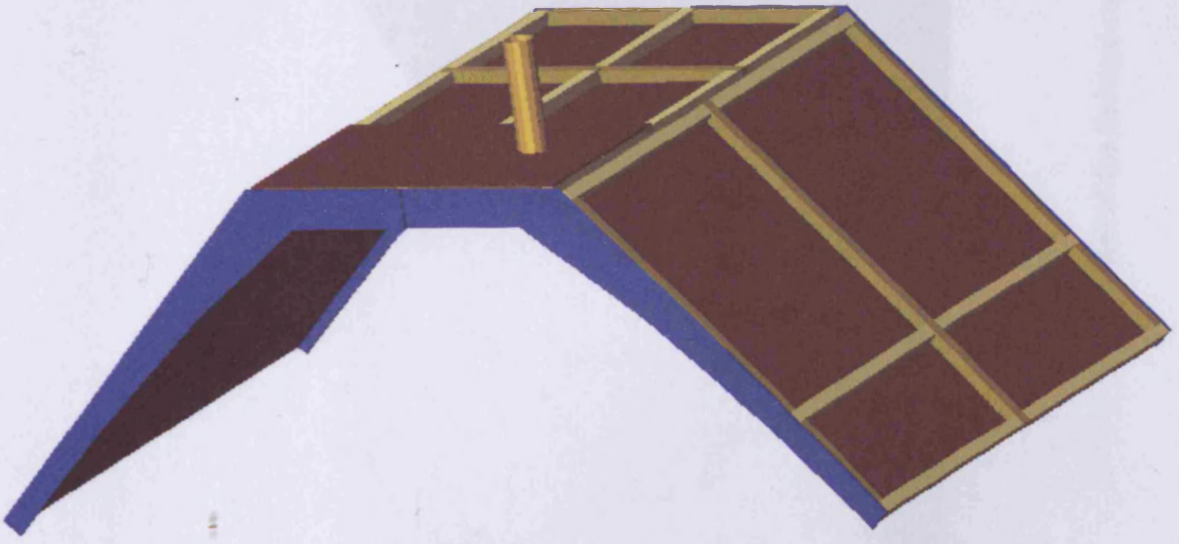

Figure C.2. The frame of the canopy skinned with fibreboard and 15mm plywood used as ends

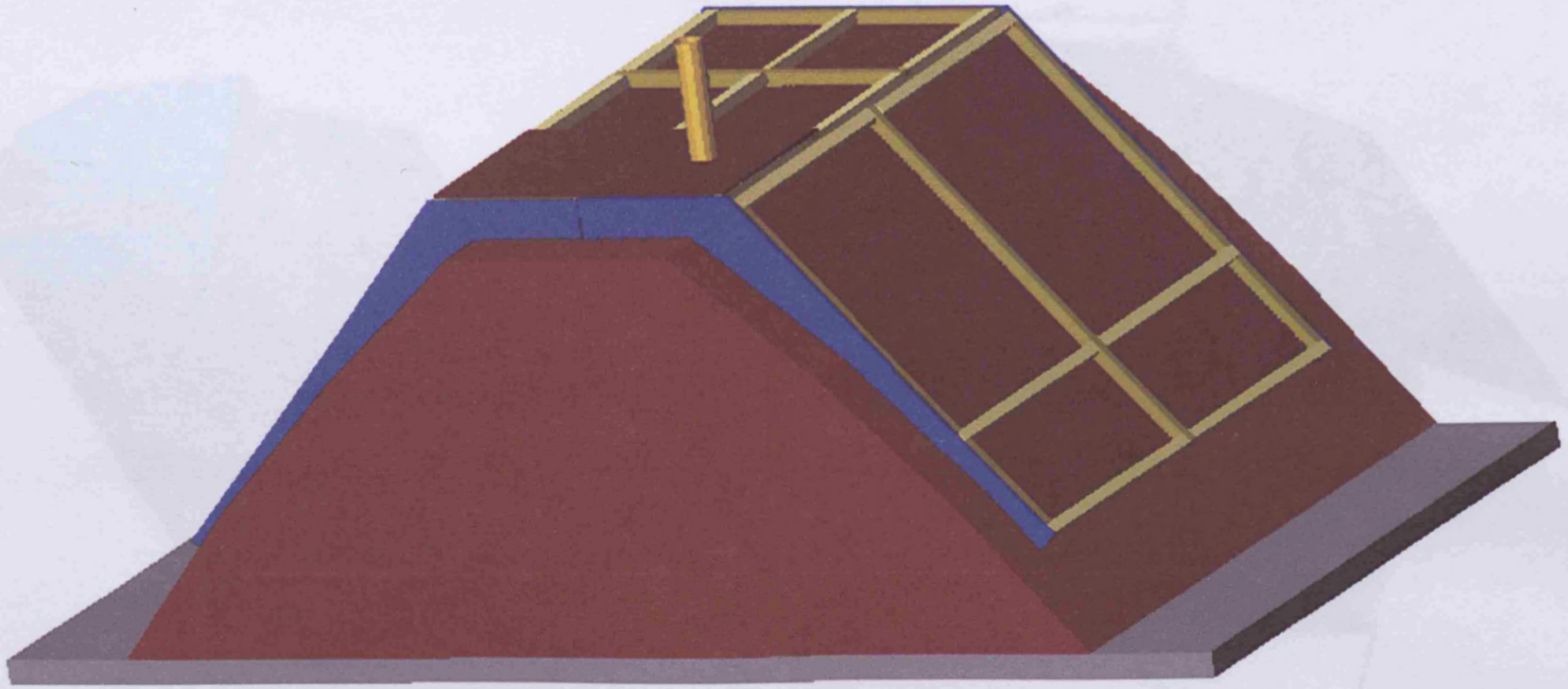

Figure C.3. Projection of the finished canopy on top of a windrow

Appendix D:
Wormtech Vessel Drawings

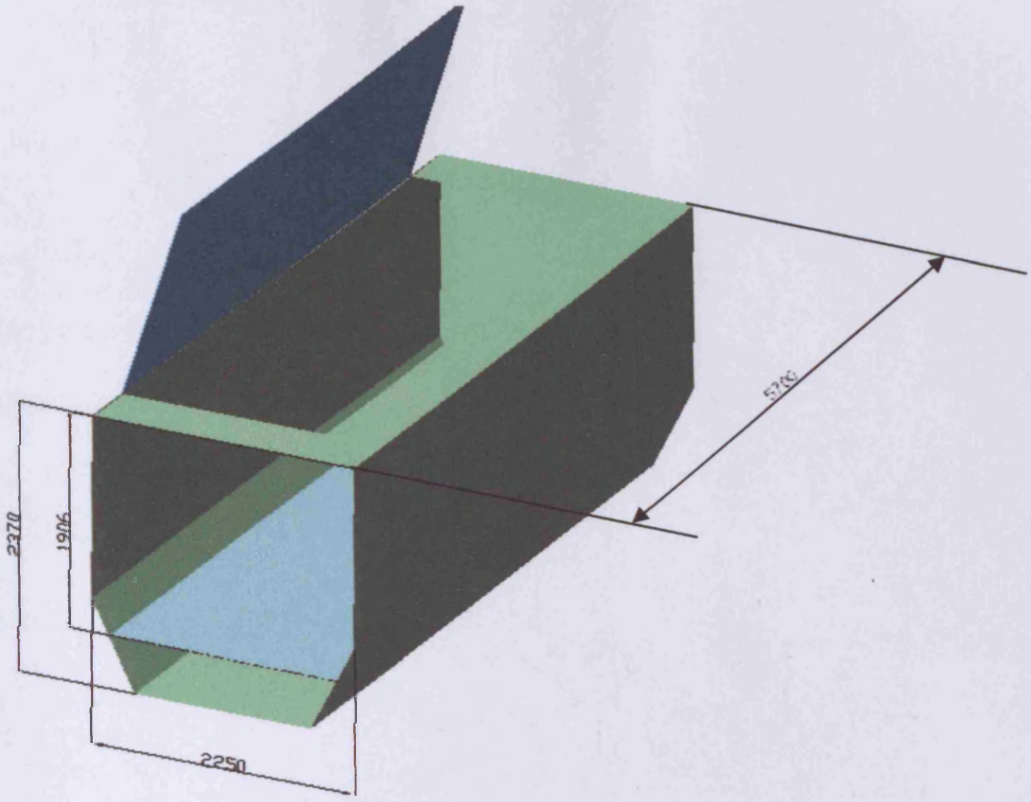

Figure D-1. The Wormtech vessel, with front panel removed showing the plenum beneath the false floor (dimensions in millimetres)

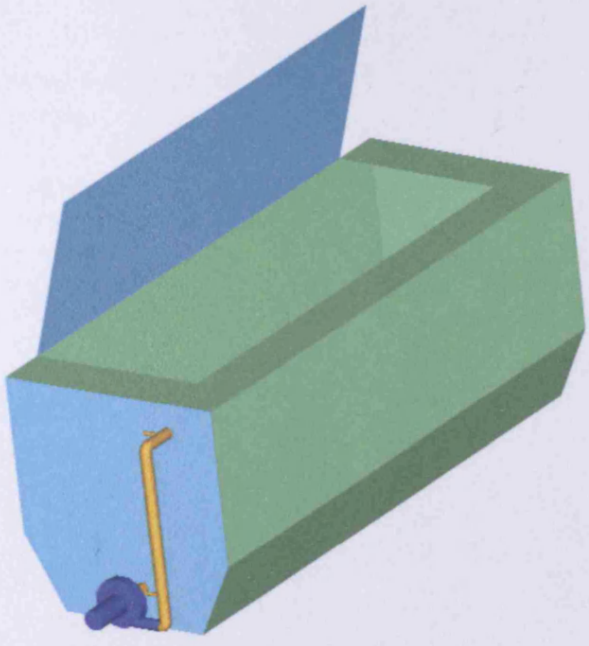

Figure D.2. Empty Wormtech vessel set up for recirculation of air

Appendix E: Risk Assessment for CERT Composting Facility

Risk assessment:

Site Name and address: CERT composting facility,
Nantycaws landfill site,
Llanddarrog road,
Nantycaws, Carmarthenshire, SA32 8BG

Performed by: David Notton
Date assessment carried out: 21/08/02
Review date: annually and with addition of new equipment

Contents:

Physical layout:

This is a new specially constructed compost facility standing on an engineered concrete base. There is a covered, labelled C in figure 1, where the composting process takes place. Other operations such as shredding and screening take place outside in the area marked B in figure 1. Other areas of the hard standing are set aside for specific tasks such as: Waste reception (A), Storage of wood, Maturation area (J) (L) and Storage of non-compostable waste (L).

The covered area is well lit with lights being shown by an X in figure 1. The drainage from the covered area is sealed and any liquid is stored in a leachate tank situated within a bund (D). In addition to the site there is also an office building (O) where there is a small kitchen and a basic laboratory.

Activities carried out:

Delivery of green waste to site by lorries up to 40 cubic yard capacity.
Sorting and litter picking of waste.
Shredding of green waste-including loading, unloading and manoeuvring of shredder
Building compost windrows.
Turning of compost windrows.
Screening of finished compost.
Sampling of Compost.
Maintaining machinery and equipment.

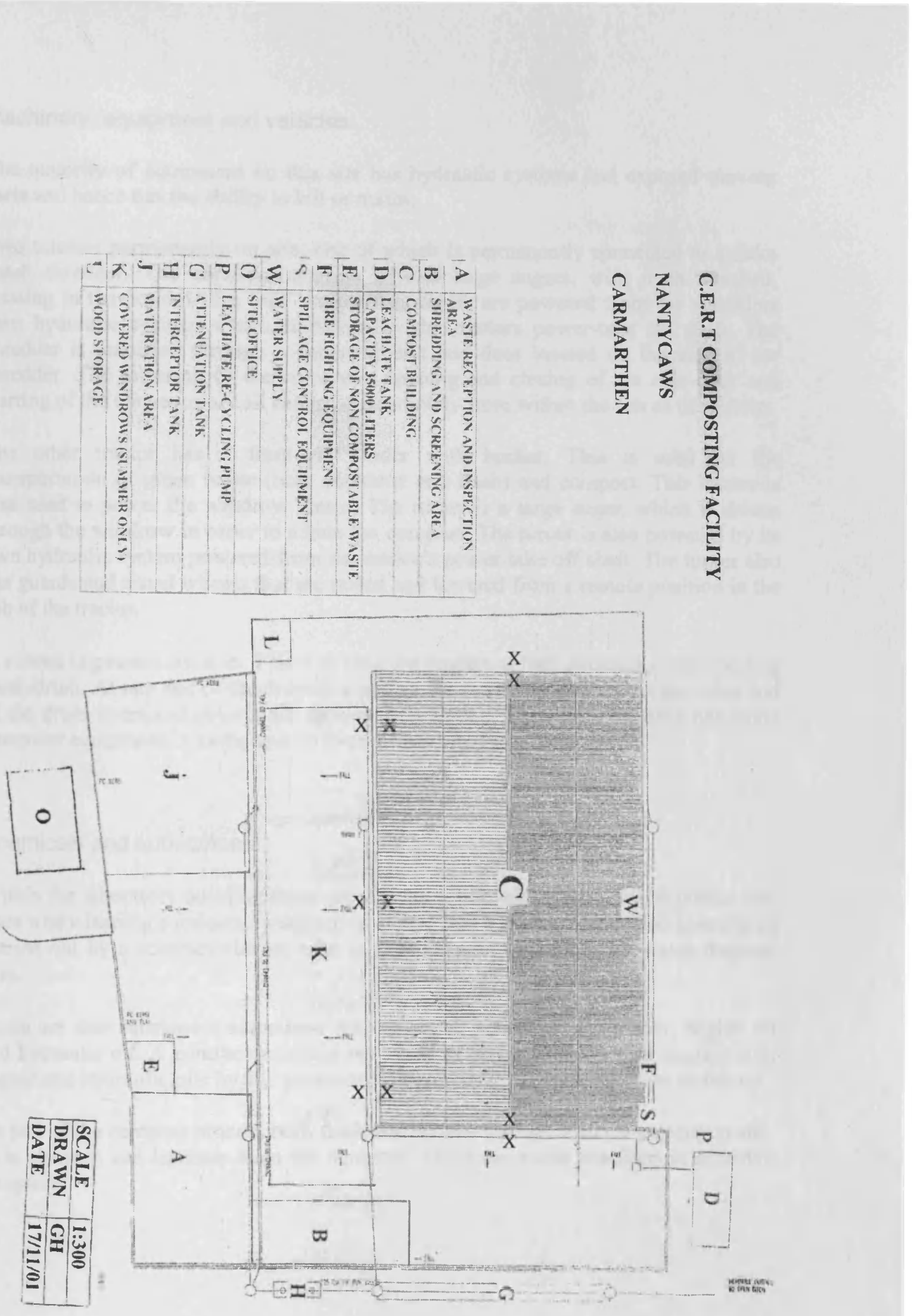

Figure 1. Layout of CERT composting site

Machinery, equipment and vehicles:

The majority of equipment on this site has hydraulic systems and exposed moving parts and hence has the ability to kill or maim.

Two tractors permanently on site, one of which is permanently connected to a Seko batch shredder. The shredder consists of two large augers, with teeth attached, rotating in the bottom of a feed trailer. The augers are powered from the shredders own hydraulic system, which is driven by the tractors power-take off shaft. The shredder is unloaded through a conveyor belt and door located on the side of the shredder. The lowering of the conveyor, opening and closing of the side door and starting of the conveyor are all carried out remotely from within the cab of the tractor.

The other tractor has a front-end loader with bucket. This is used for the transportation of green waste (both shredded and fresh) and compost. This tractor is also used to power the windrow turner. The turner is a large auger, which is driven through the windrow in order to aerate the compost. The turner is also powered by its own hydraulic system powered from the tractor's power-take off shaft. The turner also has guards and travel wheels that are raised and lowered from a remote position in the cab of the tractor.

A screen is present on site. This has its own engine, which drives a large rotating mesh drum. At one end of the drum is a hopper for finished compost. At the other end of the drum oversized objects are deposited in a heap. The office building has some computer equipment, a kettle and an oven.

Chemicals and substances:

Within the laboratory building there are various office substances such as printer ink, tipex and cleaning products (washing-up liquid and bleach). The office cleaning is carried out by a contract cleaner who is familiar with operations on waste disposal sites.

There are also substances associated with machinery such as: diesel fuel, engine oil and hydraulic oil. A contractor carries out much of the maintenance, so contact with engine and hydraulic oils by site personnel is minimised, except in the case of failure.

As part of the compost process both fresh and shredded green waste is present on site, as is compost and leachate from the compost. These can cause reactions in sensitive receptors.

Activity hazards:

Activity: Delivery of green waste to site

Description of activity: Fresh green waste is delivered on to site by lorries with up to a 40 cubic yard capacity. The waste is tipped off of the lorry in the area specified on the site plan.

Hazard	Description of existing workplace precautions	Severity	Likelihood	Risk
Risk of collision with site machinery	Before entering the site all vehicles should stop at the site entrance and make their presence known. Drivers will then be informed of any vehicle or personnel movements on site. Site tractors are fitted with an orange warning light to make them move visible. Speed limit of 10 miles per hour on site.	3	1	3
Risk of impact with site personnel	Before entering the site all vehicles should stop at the site entrance and make their presence known. Drivers will then be informed of any vehicle or personnel movements on site. Whilst on site, personnel are required to wear high visibility (day glow) vests or coats at all times	5	1	5
Accidental tipping of waste on to personnel or machinery	Drivers are responsible for the tipping of the waste. It is up to them to ensure that the waste is tipped in a safe manner in accordance with their training. If for any reason site personnel need to enter the tipping area they should make themselves known to the driver and await acknowledgement of their presence.	5	1	5

Activity hazards:

Activity: Inspection and shredding of green waste

Description of activity: The front-end loader is used to spread out a portion of the waste from the stockpile of green waste. This is then inspected for items that are unsuitable for composting, such as: metals, plastics and large logs. The inspected waste is then loaded into the running shredder again using the front-end loader. The waste is left resident in the shredder for an interval until the correct consistency has been achieved. The shredder is then unloaded. This is achieved through use of the shredder's integral conveyor belt that is located on its side. Whilst the shredded material is being unloaded the whole tractor/shredder assembly if moved forward to avoid the pile of shredded waste becoming too tall.

Hazard	Description of existing workplace precautions	Severity	Likelihood	Risk
Risk of impact between front end loader and site personnel	No personnel should be in the area of the shredder or loader whilst in operation. Site personnel are required to wear high visibility clothing at all times. Tractor has orange warning light to increase visibility. Anybody going on to site whilst a tractor is in use should make their presence known to the driver and await acknowledgement.	5	1	5
Risk of impact between shredder and personnel. Whilst the shredder is being moved/ remotely operated.	No personnel should be in the area of the shredder whilst it is in use. If anybody is required to go on to site whilst the shredder is in use should make their presence known to the driver and await acknowledgement. Site personnel are required to wear high visibility clothing at all times.	5	1	5
Risk of collision between shredder and delivery lorries.	All deliveries are required to stop at the site entrance and await permission to proceed. Good driving practises to be used- assume nothing Speed limit of 10mile per hour on site.	3	1	3

Damage to equipment making it unsafe and likely to cause an accident	All machinery is to be serviced at the recommended intervals. Equipment to be given a cursory daily check for any obvious dangerous defects. Waste entering shredder is to be inspected thoroughly to ensure that unsuitable objects are not allowed to enter the shredder. Over sized logs to be stacked in the set area for disposal.	3	2	6

Activity hazards:

Activity: Building windrows

Description of activity: From where the shredded waste is deposited by the shredder's conveyor belt it is moved using the front-end loader. Once inside the building it is formed in to windrows to allow the composting process to take place.

Hazard	Description of existing workplace precautions	Severity	Likelihood	Risk
Risk of impact with site personnel	No personnel should be in the area of the front-end loader whilst in operation. Personnel are required to wear high visibility clothing If personnel need to go on to site they should make their presence known to the operator and await acknowledgement.	5	1	5
Risk of impact with site machinery or delivery lorry	All deliveries are required to stop at the site entrance and seek permission to proceed. Tractors are fitted with orange hazard lights to increase visibility. Speed limit of 10 miles per hour on site.	3	1	3
Vehicle movement hazards i.e. tipping over	Qualified and certified operators to be used. Good driving practises to be used. -keep speed low -keep load in loader as low as possible -avoid uneven surfaces if possible	4	1	4

Activity hazards:

Activity: Turning of compost windrows

Description of activity: To ensure aeration of the composting material it is necessary to turn the windrows. This is achieved using a Ménart 4000 SP windrow turner. The turner is normally connected to the to the back of the tractor that has the front-end loader. The turner is driven by the tractor's power take-off shaft. It consists of a large auger, which is driven through the windrow. The turner also has two hydraulically driven wheels that propel the whole tractor/turner assembly. The turner has two positions; travel and working. Between these two [positions there are several operations that need to be performed that involve remotely controlled hydraulic components.

Hazard	Description of existing workplace precautions	Severity	Likelihood	Risk
Connecting turner to tractor including hydraulics and power take off.	When connecting equipment to the power take-off ensure that the tractor's ignition is turned off and the ignition keys are in the position of the operator. When connecting the hydraulic hoses to the tractors hydraulic system ensure that there is no pressure in the system.	5	1	5
Risk of collision with personnel	No personnel should be in the area of the turner whilst in operation. Any personnel on site are to wear high visibility clothing.	5	1	5
Risk of projectile striking equipment or operator	No personnel should be on foot in the area of the turner. Large objects should not be present in the windrow. The deflecting guard behind the auger should be adjusted correctly to ensure that as much material as possible is deflected towards the ground. The turner should only be used with a tractor with an enclosed cab to ensure that no projectiles strike the operator.	5	1	5

Risk of collision with site machinery	No site vehicles should be operating in the area of the turner. Delivery vehicles should stop at the site entrance and await permission to proceed. Speed limit of 10 miles per hour on site.	3	1	3
Inhalation of particles thrown up by turner.	No personnel to be on foot in the area of the turner. Operator to be within closed cab-preferably filtered	4	1	4
Risk of damaged equipment causing an accident and injury.	All large and non-compostable items should already be removed from the mixture at the inspection stage. All machinery is to be serviced at the recommended service intervals. Machinery should be given a cursory check to ensure no obvious defects are present. Whilst inspecting machinery it should be disconnected from the tractor and the keys should be in the operators possession.	5	1	5

Activity hazards:

Activity: Screening of finished compost

Description of activity: Once the compost is judged to be finished, it is screened in order to separate the various size fractions. This is achieved using a ménart screen that is loaded by the front-end loader. The screen consists of a rotating mesh drum that sieves out the required size particles. Oversize material and the fraction that is required are removed by the front-end loader and stored separately.

Hazard	Description of existing workplace precautions	Severity	Likelihood	Risk
Risk of impact with site personnel	No personnel should be in the area of the front-end loader or turner whilst in operation. Personnel are required to wear high visibility clothing If personnel need to go on to site they should make their presence known to the operator and await acknowledgement.	5	1	5
Risk of impact with site machinery or delivery lorry	All deliveries are required to stop at the site entrance and seek permission to proceed. Tractors are fitted with orange hazard lights to increase visibility. Speed limit of 10 miles per hour on site.	3	1	3
Vehicle movement hazards i.e. tipping over	Qualified and certified operators to be used. Good driving practises to be used. -keep speed low -keep load in loader as low as possible -avoid uneven surfaces if possible	4	1	4
Inhalation of particles thrown out by screen	No personnel to be on foot in the area of the screen whilst it is operational. Operator to be within closed cab-preferably filtered.	4	1	4
Risk of accident due to poorly maintained machinery.	Maintenance to be carried out in accordance with manufacturers schedule. Cursory checks to be given to all machinery	4	1	4

	before use to ensure that there are no obvious defects. No personnel to be on foot in the immediate area of the screen whilst it is operating.			
Risk of injury from rotating mesh drum	No operation to be carried out whilst screen is operating. All maintenance to be carried out with engine stopped and keys in operators possession.	5	1	5

Activity hazards:

Activity: Sampling of compost

Description of activity: Due to the research nature of the site and in order to meet compost association standards it is necessary to take samples of the compost.

Hazard	Description of existing workplace precautions	Severity	Likelihood	Risk
Risk of interaction with site machinery	No personnel to be on site in the immediate vicinity of any machinery. All personnel to wear high visibility clothing whilst on site.	5	1	5
Contact with composting material.	Gloves should be worn whilst handling compost. Wash hands after handling compost.	3	1	3
Injuries from hand tools.	Do not apply too much force to prevent slipping. Ensure handles and tools are in good order before using.	2	1	2
Use of oven for drying samples.	Familiarise yourself with the operation of the oven before use. Ensure sufficient insulation between hands and tray before removing from oven.	2	2	4

Activity hazards:

Activity: Maintaining machinery and equipment.

Description of activity: Although an external contractor carries out most of the maintenance, some minor tasks can be performed by site personnel.

Hazard	Description of existing workplace precautions	Severity	Likelihood	Risk
Risk of injury whilst changing mesh on screen.	Ensure that engine is stopped and keys are in operator's possession. Use gloves to avoid damage to hands. Keep screen at lowest height. Inform others of what you are doing.	5	1	5
Injury from maintaining teeth within shredder.	Ensure that shredder is fully disconnected from driving tractor. Keys should be in possession of operator. Use gloves to avoid damage to hands. Inform others of what you are doing.	5	1	5

Physical layout hazards:

Description: As mentioned above there are various storage piles for compost, logs and non compostable materials as well as various processes that can create mess and hazards. Much of this is already covered in the waste management license but a brief description is given below.

Hazard	Description of existing workplace precautions	Severity	Likelihood	Risk
Danger of log pile collapse.	Logs to be disposed of as soon as is practicable. No climbing on the log pile. Logs to be stacked sensibly.	4	1	4
Danger of collapse of storage piles	Avoid climbing on windrows or compost storage piles. Piles should be kept to a manageable size.	4	1	4
Trip hazards due to waste being spread out for inspection, turned and screened.	Concrete surface to be kept clear of obstacles in accordance with waste management license. Any major hazards to be moved as soon as practicable.	2	2	4

Chemical and substance hazards:

Description: Where applicable consult the materials safety data sheet (COSHH sheet) for details, these should be stored on site.

Substance	Description of Substance
Green waste /Compost/ composting material	This is the material that is delivered, is shredded and formed in to windrows. It also has a variety of bacterial species present in it. It may cause a reaction in sensitive receptors. Compost has been related to various illnesses, such as farmers lung. Wear gloves when handling compost. Wash hands after contact. Do not eat. If irritation occurs after contact, seek medical advice.
Compost Leachate	This is fluid that has drained from the composting material. It has a variety of bacterial species present in it. The floor of the composting building is sloped so that leachate can be collected in the leachate tank. It may cause a reaction in sensitive receptors. Avoid contact if possible. Rinse off if contact occurs. Do not drink. If any irritation occurs after contact seek medical advice.
Diesel fuel	As part of the site operation, machinery operators are required to refuel the vehicles. Consult material safety data sheet.
Diesel engine oil	As machinery is maintained by a contractor contact with diesel oil should be minimised-except in the case of spillage. Compost has good absorbent properties and can be used to clear up spills. Engine oil has the ability to be carcinogenic. Consult material safety data sheet.

Hydraulic oil	As machinery is maintained by a contractor contact with hydraulic oil should be minimised-except in the case of spillage. Compost has good absorbent properties and can be used to clear up spills. Consult material safety data sheet.

Appendix F: List of Publications

Commercial Scale Dynamic Respiration Rate as a Process Optimisation Tool. Methods, Results and Analysis from Several Different Composting Systems. 2005. Hewings, G. Notton, D.J. Griffiths, A.J and Williams, K.P. Presented at the 20th International Conference on Solid Waste Technology and Management, Philadelphia, PA. 3rd-6th April 2005.

Dynamic Respiration Rate Measurement &Thermodynamic Modeling to Increase Compost Production Rates. Notton, D.J. Hewings, G. Griffiths, A.J and Williams, K.P. *The Composting Council of Canada's 13th Annual National Composting Conference*, 24th-26th September 2003, London, Canada.

Compost Manufactue for an Emerging Market in the U.K. Hewings, G. Notton, D.J. Griffiths, A.J and Williams, K.P. *The Composting Council of Canada's 13th Annual National Composting Conference*, 24th-26th September 2003, London, Canada.

The standards registration process a practical approach. Hewings, G. Notton, D. J. presented to the Welsh assembly Government and the Waste and Resources Action Programme seminar on Compost quality Assurance and Standards, 25th of Febuary 2002